INFORMATION TO USERS

This material was produced from a microfilm copy of the original document. While the most advanced technological means to photograph and reproduce this document have been used, the quality is heavily dependent upon the quality of the original submitted.

The following explanation of techniques is provided to help you understand markings or patterns which may appear on this reproduction.

1. The sign or "target" for pages apparently lacking from the document photographed is "Missing Page(s)". If it was possible to obtain the missing page(s) or section, they are spliced into the film along with adjacent pages. This may have necessitated cutting thru an image and duplicating adjacent pages to insure you complete continuity.

2. When an image on the film is obliterated with a large round black mark, it is an indication that the photographer suspected that the copy may have moved during exposure and thus cause a blurred image. You will find a good image of the page in the adjacent frame.

3. When a map, drawing or chart, etc., was part of the material being photographed the photographer followed a definite method in "sectioning" the material. It is customary to begin photoing at the upper left hand corner of a large sheet and to continue photoing from left to right in equal sections with a small overlap. If necessary, sectioning is continued again — beginning below the first row and continuing on until complete.

4. The majority of users indicate that the textual content is of greatest value, however, a somewhat higher quality reproduction could be made from "photographs" if essential to the understanding of the dissertation. Silver prints of "photographs" may be ordered at additional charge by writing the Order Department, giving the catalog number, title, author and specific pages you wish reproduced.

5. PLEASE NOTE: Some pages may have indistinct print. Filmed as received.

Xerox University Microfilms

300 North Zeeb Road
Ann Arbor, Michigan 48106

74-7626

JAKOBSEN, Jørgen, 1930-
LUBRICANT RHEOLOGY AT HIGH SHEAR STRESS.

Georgia Institute of Technology, Ph.D., 1973
Engineering, mechanical

University Microfilms, A XEROX Company, Ann Arbor, Michigan

LUBRICANT RHEOLOGY AT HIGH SHEAR STRESS

A THESIS

Presented to

The Faculty of the Division of Graduate

Studies and Research

by

Jørgen Jakobsen

In Partial Fulfillment

of the Requirements for the Degree

Doctor of Philosophy in the

School of Mechanical Engineering

Georgia Institute of Technology

September, 1973

LUBRICANT RHEOLOGY AT HIGH SHEAR STRESS

Approved:

Ward O. Winer, Chairman

Prateen V. Desai

John L. Lundberg

Andrew W. Marris

John D. Muzzy

David M. Sanborn

Date approved by Chairman: 2 November 1973

ACKNOWLEDGMENTS

The author is most grateful to his thesis committee for their time, interest, and suggestions. The advice and assistance from the chairman of the thesis committee, Professor Ward O. Winer is particularly appreciated. The author is thankful for the innovative and inspiring discussions during the thesis work.

The research reported herein was supported in part by the National Science Foundation (NSF GK-31154) and by NASA (NGR-11-002-133). Grant-in-aid assistance was also received from Dow Corning Corporation, the Sun Oil Company and the Monsanto Chemical Company. The NASA-Lewis Research Center, the Dow Corning Corporation and the Rohm and Haas Company have donated the experimental fluids and the corresponding descriptive data.

The study and research were also supported by Statens teknisk-videnskabelige Fond (1959.M-158 and 2097.M-183) and Otto Mønsteds Fond (1972 and 1973) Denmark. The support is greatly appreciated.

The author wants to acknowledge the grant of leave from the Technical University of Denmark, the Department of Machine Design, for this study and research. The support and assistance from the head of the department Professor Eyvind Frederiksen is particularly appreciated.

TABLE OF CONTENTS

Page

ACKNOWLEDGMENTS ii

LIST OF TABLES vii

LIST OF ILLUSTRATIONS ix

SUMMARY xiii

Chapter

I. INTRODUCTION 1

Summary
Previous Research - Literature Survey

II. HIGH SHEAR STRESS BEHAVIOR OF SOME LUBRICANTS 15

Introduction
Modifications of the High Pressure Viscometer
Calibration Procedures
The Differential Pressure Transducers
The Pressure Level Transducer
The Velocity Transducer
Calibration of the Capillaries
Fluid Measurements
Diester
Dimethyl Siloxane DC-200-50
Polyalkyl Aromatic + Additive (DN 600 + Additive)
Synthetic Paraffinic Oils XRM 109 F4 and XRM 177 F4
B3J: Paraffinic Mineral Oil with 11.5%
Polyalkylmethacrylate MW ≈ $.2 \times 10^7$

III. DISSIPATIVE HEATING EFFECTS IN CAPILLARY VISCOMETRY. . 85

Introduction
Review of Solutions
Problem Formulation
Equations
Adiabatic Flow
Flow with Radial Conduction
Nondimensionalizing
Approximate Solution
Calculation of Flow Rate

TABLE OF CONTENTS (Continued)

Chapter		Page
IV.	NONISOTHERMAL STEADY PLANE LAMINAR COUETTE FLOW OF A LUBRICANT BETWEEN PARALLEL BEARING SURFACES . . .	111
	Flow with Constant Viscosity	
	Flow with Temperature Dependent Viscosity	
	Review of Solutions	
	Problem Formulation	
	Equations	
	Nondimensionalization	
	The Shear Stress in the Film	
	The Maximum Temperature in the Film	
	The Adiabatic Wall Condition	
	Graphical Representation of the Statement of the Maximum Film Temperature	
	Determination of the Shear Stress in the Film Via a Graphical Solution	
	Determination of Temperature and Velocity Gradients in the Film	
	The Case of the Nonadiabatic Wall	
V.	APPLICATION OF THE MAXIMUM TEMPERATURE CONCEPT TO ELASTOHYDRODYNAMIC FILMS	139
	Assumptions	
	Parallel Bearing Surfaces	
	The Pressure Gradients	
	The Shear Stress in the Film for an Elastohydrodynamic Point Contact	
	The Ratio Between Shear Stresses Generated by the Pressure Gradient and by the Sliding Motion	
	The Ratio π_α in Actual Lubrication	
	The Pressure Gradient $p_{,2}$	
	The Pressure Gradient $p_{,3}$	
	The Effect of the Temperature Gradients $T_{,1}$ and $T_{,2}$ Incompressible Lubricants	
	Velocity Changes Due to the Convection Term	
VI.	DISCUSSION AND CONCLUSIONS - EXPERIMENTAL WORK	166
	Fluid Measurements	
	Analysis of Heating Effects in Capillary Flow	
	Heat Conduction Absent	
	Heat Conduction Present	
	Evaluation of Boundary and Initial Conditions	
	Evaluation of the Effects of Variations of Capillary Dimensions	

TABLE OF CONTENTS (Continued)

Chapter		Page
	Non-Liquid Behavior Shear Thinning Behavior of the Polymer Blended Mineral Oil Observations of Time Independent Lubricant Behavior Conclusions	
VII.	DISCUSSION AND CONCLUSIONS - THEORETICAL DEVELOPMENTS .	176
	A New Theory for the High Pressure Area of an Elastohydrodynamic Contact Prediction of the Maximum Temperature and the Shear Stress in the Film The Adiabatic Plane in the Film Convection in the Film Applicability of the Theory to Actual Elastohydrodynamic Films An Example of a Film Calculation Shear Stress and Maximum Temperatures Conclusion	
VIII.	RECOMMENDATIONS FOR FURTHER RESEARCH	181
APPENDICES	. . . . .	183
A.	DESCRIPTION OF FLUIDS	184
B.	MANUFACTURER'S SPECIFICATION ON THE VELOCITY TRANSDUCER	192
C.	MEASURED RESULTS FOR THE INVESTIGATED LUBRICANTS . . .	195
D.	CONVERSION FACTORS	264
E.	PROGRAM TO CALCULATE ESTIMATED TEMPERATURES AND APPROXIMATED FLOW CURVES	266
F.	AUXILIARY DIAGRAMS FOR CHAPTER IV	268
G.	EXAMPLE OF FILM CALCULATION OF AN ELASTOHYDRODYNAMIC POINT CONTACT IN PURE SLIDING	274
H.	PROGRAM TO DETERMINE DIMENSIONLESS TEMPERATURES IN THE FILM	297

TABLE OF CONTENTS (Continued)

Appendices Page

I. PROGRAM TO DETERMINE DIMENSIONLESS SHEAR STRESS IN THE FILM 298

J. NOMENCLATURE 301

BIBLIOGRAPHY 309

VITA 315

LIST OF TABLES

Table		Page
1.	Capillary Dimensions and Materials	19
2.	Typical Calibration of Transducer TR1	23
3.	Some Results from Calibrations of Transducer TR1 + Amplifier 1 and Transducer TR2 + Amplifier 2	24
4.	Viscosities (cp) of Calibration Fluids at Atmospheric Pressure	31
5.	Diester, 32°F	38
6.	Pressure Temperature Viscosity Relationship for Diester	47
7.	The Coefficient of Heat Conduction for Some Liquids	51
8.	Paraffinic Mineral Oil with 11.5 Per cent Polyalkylmethacrylate MW = .2 × 10⁷ Viscosities at Atmospheric Pressure	83
9.	Assumptions	94
10.	Assumptions	115
11.	Flow Situations for the Film. $Su = Su(\pi_2,\pi_1,\pi_3)$ π_3,π_4 Constant	123
12.	Assumptions	147
13.	The Ratio π_α between Shear Stress Generated by The Pressure Gradient and the Shear Stress Generated by the Sliding Motion	153
14.	Diester, 32°F	197
15.	Diester, 10°F	206
16.	Dimethyl Siloxane DC-200-50	211
17.	Dimethyl Siloxane DC-200-50, 75°F	216

LIST OF TABLES (Continued)

Table		Page
18.	Dimethyl Siloxane DC-200-50, 75°F, L/D = 1.35	221
19.	Dimethyl Siloxane DC-200-50, 32°F, L/D = 1.35	222
20.	Dimethyl Siloxane DC-200-50, 32°F, L/D = 1.35	225
21.	Dimethyl Siloxane DC-200-50, 100°F	226
22.	Polyalkyl Aromatic + Additive, 10°F	228
23.	XRM 109 F4, Synthetic Paraffinic Oil, Plot, L/D = 297	234
24.	XRM 177 F4, Synthetic Paraffinic Oil, Plot, L/D = 297	237
25.	XRM 177 F4, Synthetic Paraffinic Oil, 100°F	240
26.	B3J: Paraffinic Mineral Oil R-620-12 + 11.5 per cent Polyalkylmethacrylate PL 4523 (MW = .2 + 07), 100°F	250
27.	B3J: Paraffinic Mineral Oil R-620-12 + 11.5 per cent Polyalkylmethacrylate PL 4523 (MW = .2 + 07), 100°F	253
28.	B3J: Paraffinic Mineral Oil R-620-12 + 11.5 per cent Polyalkylmethacrylate PL 4523 (MW = .2 + 07), Plot, L/D = 297	262
29.	The Temperature E as Function of the Viscosity at 100°F (cp) and π_3	273
30.	Hertzian Pressures and Temperatures of the Moving Surface	278
31.	Temperature and Shear Stress Calculation at the Center of a Point Contact. W = 15 lbf. Sliding Velocity = 54.8 inch/sec. Lubricant: Fluid D	289
32.	Comparison of Temperatures T_s Generated by a Constant Heat Flux Source (R_q = 5.7 $\times 10^{-3}$ in) and the Maximum Temperatures of the Stationary Wall $T_{wall}(0)_{max}$	292

LIST OF ILLUSTRATIONS

Figure		Page
1.	The Modified Viscometer	17
2.	Characteristics of Transducer TR1 and Amplifier 1	25
3.	Characteristic of Amplifier 2 and Recorder	27
4.	Linearity Check of a Symmetric Amplifier, No. 1, for No. 1 Pressure Transducer, TR1	28
5.	Capillary 0, Sapphire	33
6.	Shear Stress Obtainable in a Capillary for a Unit Pressure Drop	36
7.	Isothermal Pressure Viscosity Plot for Diester	39
8.	Roelands Plot for Diester	40
9.	Flow Curves for Diester, Calibration, T = 32°F	41
10.	Flow Curves for Diester, High Shear Stress, T = 100°F	44
11.	Temperature Pressure Viscosity Presentation for Diester. (ASTM D-341-43)	45
12.	Typical Flow Curves for Siloxane (S) and Diester (D)	52
13.	Low Shear Pressure Temperature Viscosity Characteristics for Dimethyl Siloxane DC-200-50 (DC-12)	53
14.	Low Shear Pressure Temperature Viscosity Characteristics for Dimethyl Siloxane DC-200-50 (DC-12)	54
15.	Low Shear Temperature Pressure Viscosity Characteristics for Dimethyl Siloxane DC-200-50 (DC-12)	55
16.	Low Shear Pressure Viscosity Characteristic of Dimethyl Siloxane DC-200-50, 32°F	57

LIST OF ILLUSTRATIONS (Continued)

Figure		Page
17.	Low Shear Temperature Pressure Viscosity Characteristics of Dimethyl Siloxane DC-200-50 in the Range 32 - 100°F, (ASTM D 341-43)	58
18.	High Shear Measurements of Dimethyl Siloxane DC-200-50, T = 75°F	59
19.	High Shear Measurements with Partially Blocked Capillary	61
20.	Non-liquid Behavior of Siloxane at 40 kpsi, High Shear Measurements	62
21.	Non-Liquid Behavior of Siloxane at 40 kpsi, High Shear Measurements	64
22.	Low Shear Measurements (Capillary 4) and High Shear Measurements (Capillary 0) for Comparison with Previous Collected Data	65
23.	Range of Possible Non-liquid Behavior of Siloxane, 75°F	67
24.	Flow Curves for Polyalkyl Aromatic + Additive (DN 600 + Additive)	68
25.	Isothermal Pressure Viscosity Plot for XRM 109 F4	70
26.	Roelands Plot for XRM 109 F4	71
27.	Isothermal Pressure Viscosity Plot for XRM 177 F4	72
28.	Roelands Plot for XRM 177 F4	73
29.	Isothermal Pressure Viscosity Plot of Fluid D, XRM 109 F4 and XRM 177 F4	75
30.	High Shear Measurements of XRM 177 F4, 100°F	76
31.	High Shear Measurements of Fluid B3J	79
32.	Isothermal Pressure Viscosity Plot for Fluid B3J	81

LIST OF ILLUSTRATIONS (Continued)

Figure		Page
33.	Roelands Plot for Fluid B3J	82
34.	The Flow Situation, Flow of a Viscous Lubricant through a Cylindrical Capillary	93
35.	Temperature Distribution in Capillaries for the Case of No Heat Conduction in the Fluid	98
36.	Temperature Distribution in Capillary 0, Heat Conduction Present	105
37.	Heat Balance. Capillary 0. Axial Location: $\omega = 1$	107
38.	Calculated Flow Curves for Synthetic Paraffinic Oil and Siloxane	110
39.	The Lubrication Situation, Flow of a Viscous Lubricant Between Parallel Bearing Surfaces	114
40.	Dimensionless Maximum Film Temperature π_1	131
41.	The Dimensionless Shear Stress π_5 in the Film	135
42.	Typical Computer Solution of the Pressure Distribution in an Elastohydrodynamic Contact	141
43.	Typical Examples of Reported Pressure Measurements in Elastohydrodynamic Contacts	143
44.	The Lubrication Situation, Flow of a Viscous Lubricant between Parallel Bearing Surfaces	146
45.	Dimensionless Pressure and Pressure Gradient of a Hertzian Contact	151
46.	The Temperature Viscosity Coefficient π_3	269
47.	The Temperature E (^{o}R)	270
48.	The Temperature E (^{o}R)	271
49.	Determination of π_3	280
50.	Determination of E(^{o}R)	281

LIST OF ILLUSTRATIONS (Continued)

Figure		Page
51.	Determination of π_1	282
52.	Determination of π_5	283
53.	Extrapolation Procedure to Determine T_{max} and the Corresponding Shear Stress	287
54.	Results of a Film Calculation	293
55.	Measured Total Traction Coefficient Compared with Traction Coefficient from the High Pressure Area of the Contact	295

SUMMARY

This thesis reports capillary viscometric measurements at shear stresses up to 700 psi (4.8×10^7 dyn/cm^2) and reports the general observation of constant viscosity of the investigated unblended lubricants in the range of investigation. The thesis also reports the development of a theory to predict the maximum temperature and the shear stress in elastohydrodynamic liquid films. Solutions can be obtained via dimensionless graphs and contain most other lubrication related quantities. Experimental observations are consistent with the theory.

The purpose of the work is to develop a method to determine the viscous properties of lubricants under elastohydrodynamic operating conditions in a laboratory experiment where the parameters of pressure, temperature and shear stress can be independently varied. The use of a short length capillary has been introduced in order to achieve high shear stress. Reliable entrance and exit corrections for highly viscous capillary flow appears to have been found. The upper limit of shear stress attainable in capillary viscometry has been increased approximately 50 times over previously reported values of about 10^6 dyn/cm^2 (~14.5 psi). The increased shear stress limit is only 3 - 5 times less than the average shear stress experienced by the fluid during passage of an elastohydrodynamic contact. A further increase in shear stress limit up to about 1.4×10^8 dyn/cm^2 (~2 kpsi) appears to be possible. This higher predicted level of shear stress is of the same order of magnitude as the average shear stress to which the fluid is subjected during passage of an

elastohydrodynamic contact.

The work has shown that unblended synthetic hydrocarbon oils and a silicone oil tested have constant viscosity as function of shear stress in the investigated range, $\leq$ ~700 psi shear stress, when liquid behavior is displayed. The silicone fluid shows solidification at pressure above 50 kpsi and shear stress above about 10^7 dyn/cm^2, at 75°F. The polymer blended mineral oil shows non-liquid behavior at low stress (above about 10^5 dyn/cm^2, 1.4 psi).

These observations of non-liquid behavior of a silicone oil and a polymer blended mineral oil may possibly provide part of an understanding of the anomalous behavior of these types of lubricants with respect to the ability to create an elastohydrodynamic film. Existing theory for prediction of film thickness assumes implicitly liquid behavior of the lubricants.

No discernible time dependent effects were observed for the liquid lubricants.

The thesis further deals with application of the viscosity measurements to determine liquid film behavior in the high pressure area of a point contact configuration.

The purpose of this part of the work is to develop a general theory which will predict the elastohydrodynamic quantities of interest, particularly shear stress and maximum temperature, under physically reasonable assumptions.

The theory has been developed to a stage where the shear stress and the maximum attainable temperature each can be determined through a

few graphical steps on a dimensionless diagram. Other related elasto-hydrodynamic quantities can be derived from the maximum temperature and the shear stress.

CHAPTER I

INTRODUCTION

Summary

This thesis reports capillary viscometric measurements at shear stresses up to 700 psi (4.8×10^7 dyn/cm^2) and reports the general observation of constant viscosity of the unblended lubricants in the range of investigation. The thesis also reports the development of a theory to predict the maximum temperature and the shear stress in elastohydrodynamic liquid films. Solutions can be obtained via dimensionless graphs and contain most other lubrication related quantities. Experimental observations are consistent with the theory.

The purpose of the work is to develop a method to determine the viscous properties of lubricants, temperature pressure shear stress viscosity relations, under elastohydrodynamic operating conditions in a laboratory experiment where the parameters of pressure, temperature and shear stress can be independently varied. Improved calibration and measurement techniques have been developed. The use of a short length capillary has been introduced in order to achieve high shear stress. Reliable entrance and exit corrections for highly viscous capillary flow appears to have been found. The upper limit of shear stress attainable in capillary viscometry has been increased approximately 50 times over previously reported values (1) of about 10^6 dyn/cm^2 (~14.5 psi). The increased shear stress limit is only 3 - 5 times less than the average shear stress

experienced by the fluid during passage of an elastohydrodynamic contact. A further increase in shear stress limit up to about 1.4×10^8 dyn/cm^2 (~2 kpsi) appears to be possible. This higher level of predicted shear stress is of the same order of magnitude as the average shear stress to which the fluid is subjected during passage of an elastohydrodynamic contact.

The work has shown that unblended synthetic hydrocarbon oils and a silicone oil tested have constant viscosity as function of shear stress in the investigated range, $\leq$ ~700 psi shear stress, when liquid behavior is displayed. The silicone fluid shows solidification at pressures above 50 kpsi and shear stress above about 10^7 dyn/cm^2, at 75°F. The polymer blended mineral oil shows non-liquid behavior at low stress (above about 10^5 dyn/cm^2, 1.4 psi).

These observations of non-liquid behavior of a silicone oil and a polymer blended mineral oil may possibly provide part of an understanding of the anomalous behavior of these types of lubricants with respect to the ability to create an elastohydrodynamic film. Existing theory for prediction of film thickness assumes implicitly liquid behavior of the lubricants.

No discernible time dependent effects were observed for the liquid lubricants.

The thesis further deals with application of the viscosity measurements to determine liquid film behavior in the high pressure area of a point contact configuration. The particular lubrication situation in question is a sliding ball surface loaded against a stationary flat surface.

The purpose of this part of the work is to develop a general theory which will predict the elastohydrodynamic quantities of interest, particularly shear stress and maximum temperature, under physically reasonable assumptions.

The theory has been developed to a stage where prediction of the shear stress and the maximum attainable temperature each can be made pointwise at any location in the high pressure area of the contact through a few graphical steps on a dimensionless diagram. Other related elastohydrodynamic quantities can be derived from the maximum temperature and the shear stress. The approach has been followed up with a computer program which yields convenient print out of most relevant film data. The elastohydrodynamic film of a synthetic paraffinic oil in a point contact has been investigated with the new theory and compared with traction measurements of the lubricant. Measurements at three velocities, 13.7 - 27.4 - 54.8 inch/sec, were available for the comparison. The ratios of measured to calculated traction coefficients are of order of magnitude 1 (.8 - 1 - 1.4 with an estimated accuracy of .1). The results are obtained with viscosity data from extrapolated pressure temperature viscosity characteristics and assume liquid behavior of the lubricant in the total range of elastohydrodynamic operational conditions.

Previous Research - Literature Survey

The viscosity of a liquid lubricant is the major material property which determines its function in a lubrication situation. The measurement of the viscosity of liquid lubricants is of great importance from an engineering point of view and has received much attention.

The ASME Pressure Viscosity Report 1953 (2) is the most extensive experimental work on temperature pressure viscosity relations found in the literature. Measurements reported therein were performed at very low shear stresses, in a falling body viscometer. The report shows pressure temperature viscosity relations and pressure temperature density relations for forty six lubricants. Both mineral oils and synthetic lubricants were investigated. The density relations show isothermal density increases of the order of 10% when the pressure increases from 50 kpsi to 150 kpsi. All investigated lubricants show nearly exponentially increasing viscosities as a function of pressure.

High shear stress investigations at low pressure have been carried out with both capillary and Couette viscometers by several investigators. Both of these measuring methods are sensitive to heating effects which complicate interpretation of results.

High shear stress or high pressure capillary measurements of lubricants have been performed by several investigators. Hersey and Snyder 1932 (3) measured flow rate of greases and of castor oil as a function of pressure drop over a long capillary at temperatures of 20°C and 23°C. The maximum applied pressure drop was about 45 kpsi. The viscosity therefore varies significantly along the length of the capillary. An approach to compute the pressure viscosity relation from measurements was shown. A correction to Poiseuille's equation was presented which determined the reduction in flow rate due to the increased viscosity with pressure. The measured pressure flow rate data shows a distinct upper bound for the flow rate reached at pressure drop of 20 - 40 kpsi. This is consistent with an assumption of an exponential pressure

viscosity relation. The yield point of the greases was calculated to be equivalent to a pressure drop of about .9 kpsi in the capillary. The yield pressure is thus only a small fraction of the total applied pressure drop and the grease behaves nearly as a fluid in most experimental situations. The ratio of capillary length to diameter was about 4170. The average shear stress was therefore relatively low of the order of 2.5 psi. No temperature effect due to dissipation was taken into account. Hersey and Zimmer 1937 (4) report viscosity measurements on three mineral oils. The viscosities at atmospheric pressure and 77°F were 135 cp and 378 cp. The range of the ratio of capillary length to diameter was 86 - 322. The highest shear rate reported was 1.49×10^6 sec^{-1} and the highest shear stress was 4.86×10^5 dyn/cm^2 (about 7 psi). They measured reductions in apparent viscosity at the high shear stresses. They derived an approximate expression for the reduction of the apparent viscosity under the assumption of adiabatic conditions, heat conduction absent, and found smaller reduction of the measurements than predicted. They found that the observed smaller reduction effect could be explained by the heat conduction of the fluid itself and concluded that the observed drop in viscosity can be accounted for by heat effects without assuming any change in viscosity with shear rate at constant temperature. An important conclusion from the consideration of the adiabatic situation is that the flow curves can be expected to be of one general configuration. Norton, et al., 1941 (5), demonstrated a method to overcome the situation of large pressure drop over the capillary. They attempted the use of a throttling valve at the

exit of the long capillary used earlier by Hersey and Zimmer. However steady conditions could not be obtained. A new short test capillary was therefore placed between the pressure source and the long capillary which then had the function only of maintaining a high pressure level at the exit of the test capillary. The flow rate could be changed by the use of variable lengths of the second, pressure reducing, capillary. The pressure drop over the test capillary was measured with two Bourdon pressure gauges. Pressure drop from about 100 psi up to more than 30 kpsi were applied. The flow curves show an appreciable amount of deviation from constant viscosity. No final conclusion was formulated with respect to the behavior of the investigated mineral oil; a medium oil (SAE 30) of 100 cp at atmospheric pressure and 100°F.

Philippoff 1942 (6) developed an approximate thermal theory for the heating effects in capillary flow. The conduction of the lubricant was taken into account in the equations. An exponential pressure viscosity relation was used. A series expression in the variable r^4 was used to obtain an approximate solution for the temperature distribution. The approach gives a more detailed description of the flow. The experimental investigations conducted concurrently are claimed to confirm the theory. Shear stresses of about 5×10^5 dyn/cm^2 and shear rates of about 5×10^5 sec^{-1} was reached. The flow curves show distinct increases of the apparent shear rate when the shear stress is above 10^5 dyn/cm^2 which shows the heating effect. The lengths of the capillaries were 12 to 50 mm. The diameters were .5 to .15 mm. Driving pressure was up to 100 atm, about 1400 psi. The paper summarizes in one figure some of the high shear stress results known then. Deviation from constant

viscosity is significant only above 10^5 dyn/cm^2. The maximum shear stress obtained in the summarized works is in the range 4×10^5 to 8×10^5 dyn/cm^2. The flow curves appear to be of the same general configuration as predicted by Hersey and Zimmer, (4). Fritz and Hennenhöfer 1947 (7) performed experiments similar to Philippoff's investigation, (6). The measurements were corrected for viscosity variations due to the pressure drop over the capillary. An exponential pressure viscosity relation was used. The capillary dimensions were: L = 12.264 cm, D = .08295 cm giving L/D = 148. The three lubricants investigated showed decreasing apparent viscosity with increasing pressure drop. The authors compared their experimental results and the experimental results from the investigations of Hersey and Snyder 1932 (3) and Philippoff 1942 (6) with the theory of Philippoff and with an adiabatic situation. They found that the actual measurements did not confirm the theory of Philippoff in fact most of Philippoff's experimental results tend to follow the characteristic of the adiabatic situation. The investigation did not reach a definite answer to the question of a possible existence of shear thinning effects but concluded cautiously that the presence of such an effect was highly unlikely in the shear stress range investigated. Schnurmann 1962 (8) investigated a series of lubricants, primarily mineral oils, with a capillary which was very short compared to capillary lengths used in earlier works. The ratio of L/D can be estimated from a sketch in the paper to be about 1. The diameter is about 10^{-2} cm, 4×10^{-3} inch. It is stated that the temperature increase is very small and of the order of .05°C at a shear rate of 10^5 sec^{-1}, however, without

specifying the corresponding viscosity. The reported measurements show constant viscosity of all investigated lubricants up to a shear stress of about 4 psi! The measurements with castor oil were reported. The flow curve shows decreasing viscosity as a function of shear rate. Unfortunately the reporting of data is incomplete. Volume flow rates and viscosities are not reported. No conclusion is drawn with respect to the mechanism causing the drop in measured viscosity of castor oil. Heat dissipation seems to contradict the claim of very small temperature increases, 0.05°C, and shear thinning effects seem to contradict the assumption that the castor oil is a Newtonian fluid. The work shows however the feasibility of the use of capillaries with short lengths in high shear stress viscometry. The work shows careful correction for kinetic energy of the flow through the capillary. None of the previously referred works appears to have commented on this important detail. Gerrard and Philippoff 1963 (9) reported measurements on a highly refined petroleum oil of 11.51 Stoke, 10.25 Poise, (77°F) with a series of capillaries with a range of L/D from about 60 to 230. Gerrard, Steidler and Appeldoorn 1964 (10), 1965 (11) conducted an extensive investigation in the capillary flow situation both experimentally and with computer solutions. The work is referred to in Chapter III of this thesis.

A new type high pressure high shear stress capillary viscometer was developed and used to investigate pressure temperature shear stress relations for a series of mineral oils, polymer blended mineral oils and some synthetic lubricants and reported by Novak 1968 (1), Novak and Winer 1968 (12), 1968 (13) and Winer 1972 (14). The parameters of

interest, pressure, temperature, and shear stress, can be independently varied. The viscometer is described in detail in Chapter II. Its primary components are a pressure intensifier (50x) and a traversing piston containing the high pressurized test fluid in two separate chambers, cylinders with the pistons solidly fixed to the frame. The capillary which is immersed in a constant temperature bath connects the two high pressure volumes in the traversing piston. The maximum shear stress reported, Novak, (1), is 1.04×10^6 dyn/cm^2, 15.1 psi, obtained at a pressure drop of about 700 psi over the capillary. The capillary has a ratio of length to diameter of 11.6. Paraffinic and napthenic base oil with 4% and 8% polyalkylmethacrylate as well as unblended synthetic lubricants were investigated. Polymer blended mineral oils are used extensively in many engineering fields and particularly in the automotive industry; therefore these lubricants are of great importance. The measurements showed pressure temperature relations all of the same general characteristics as reported in the pressure viscosity report ASME 1952 (2). The flow curves showed constant viscosity for all unblended lubricants, the base oils and the synthetic lubricants. The polymer blended lubricants showed shear thinning effects above a shear stress of about 10^3 dyn/cm^2. A second constant viscosity level was found for all polymer blended oils, at shear stresses above about 10^5 dyn/cm^2. This constant viscosity at high shear stress is often referred to as a second Newtonian viscosity. This second Newtonian viscosity level is higher than the viscosity of the base oils even for the mixtures with the lowest concentration of polymer. The investigated range of shear stress of the second Newtonian viscosity level is from 10^5 to 10^6 dyn/cm^2 in which the

viscosity appeared to be constant. The ratio of the viscosity at the first Newtonian level, the very low shear stress situation, and the second Newtonian viscosity level is less than 2. Significant dissipation heating was not encountered. The napthenic base oil which has the greatest temperature viscosity coefficient shows a slight deviation from constant viscosity of the flow curve at shear stresses of about 8.6×10^5 dyn/cm^2. However only two data points are available at that shear stress level. Measurements of the paraffinic base oil under comparison do not extend higher than 5.26×10^5 dyn/cm^2 at which shear stress level even the more temperature viscosity sensitive napthenic base oil shows no significant deviation from a constant viscosity level flow curve. The two base oils can therefore hardly be compared. The shear stress level where heating effects are discernible in the new type high pressure viscometer is about five times higher than the shear stress level where heating effects could be detected as reported in earlier works and summarized by Philippoff 1942 (6). It was argued by Novak 1968 (1), that the short time duration required to obtain data was significant in an explanation of the increase of 5 times of the heating limit. While this statement probably can be maintained it seems more likely that the explanation is to be found in the use of a capillary with a considerably smaller ratio of length to diameter than used in previous works. It can be shown that more of the heat generated by viscous dissipation is contained in the efflux from the capillary when the L/D ratio is diminished. The cooling effect from the walls of the capillary decreases therefore with shorter capillaries. This will tend to give greater deviation from a constant viscosity characteristic.

However the gain in increased shear stress per unit pressure drop over the capillary more than compensates for the slight loss in cooling. Schnurmann 1962 (8), might have encountered this effect. The present thesis uses the effect.

In a summary it can be stated that the maximum shear stress was approximately 10^5 dyn/cm^2 for the earlier works increasing to 10^6 dyn/cm^2 with the more recent group of works, Novak and Winer. Heating effects were encountered in most of the works. Shear thinning effects were found only in polymer blended oils.

Theoretical works of Bondi 1946 (15) and Smith 1968 (16) have predicted nonlinear behavior of lubricants under extreme stress. Both works are essentially based on the molecular behavior of the liquids. Bondi finds a viscosity drop to about .6 times the low shear viscosity at shear stresses of 10^6 dyn/cm^2 for a liquid with molecular weight of 600. Smith predicts large rates of viscosity decrease with increase of shear rate. The shear rate where viscosity changes can be observed is highly temperature sensitive. These analyses have not been confirmed experimentally in attained shear stress shear rate ranges in fact some has been shown not to be correct.

The discovery of the elastohydrodynamic lubrication between non-conforming machine element surfaces by Grubin and Vinogradova, 1949 (17) and the advancement of the analysis, notably Dowson and Higginson 1959 (18), 1960 (19), Dowson, Higginson and Whitaker 1962 (20), Cheng and Sternlicht 1965 (21), Dowson and Whitaker 1965-66 (22) and Cheng 1965 (23), 1967 (24) have created interest and need for investigations of lubricant behavior under the extreme conditions the liquid is subjected

to during passage of an elastohydrodynamic contact: pressures of 100 to 300 kpsi, temperatures 100 - 400°F, maximum shear stresses of 1000 - 3000 psi, viscosity increases with a factor of 10^5, resident times 10^3 - 10^4 μsec implying pressure gradients typically 10^7 psi/inch or time rate of pressure changes of the order of 10^9 psi/sec. In the extensive amount of experimental and theoretical work that has been carried out many viscosity functions have been applied: the Newtonian $\eta(p,T)$ relation, shear thinning relations, $\eta(p,T,\tau)$, Rhe-Eyring hyperbolic sin law fluids, $\tau = f(\sinh^{-1}(\dot{\gamma}))$, power law models $\tau = -k, |\dot{\gamma}^n|$ and viscoelastic models, to mention some of the relations used to attempt to explain measurements or to advance theoretical analyses. The elastohydrodynamic contact itself has been used as a viscometer in sliding, rolling or squeeze-film arrangements. Many measurements of total traction, temperature and pressure distributions have been carried out, for the main part in cylindrical contacts. It may have been implicitly assumed that it was impossible to reproduce the elastohydrodynamic conditions in a controlled laboratory experiment outside the elastohydrodynamic contact itself, a point of view which has even been published. Evaluation of data from elastohydrodynamic contacts is difficult particularly when the data are used for evaluation of viscosity relations using the bearing surfaces as a plane parallel viscometer. The main difficulty with the use of an elastohydrodynamic contact as viscometer seems to be that the parameters of primary interest pressure, temperature and shear stress cannot be varied independently of each other.

Some success has been achieved with vibrating crystal viscometers. The technique of measurement with a torsionally vibrating crystal was

described in detail by Mason 1947 (25). The oscillator was a tube formed crystal with plated electrodes near the ends. Three wires in the nodal plane, the middle plane perpendicular to the tube axis, give mechanical support and electric contact. The instrument constants which essentially are electric resistance and mechanical eigenfrequency can be calculated and are checked by measurements with the crystal in vacuum and with the crystal loaded with a known fluid. The viscosity of a series of test fluids (η_o in the range 2 cp up to 660 cp) was measured with both continuous flow methods and with the vibrating crystal method. The results showed good consistency (per cent error + 7.8 to -11.0) of the two methods. Polymerized castor oil showed shear elasticity as well as shear viscosity. The data gave a viscosity of 18 poise, consistent with the value measured by continuous flow methods, and a modulus of elasticity in shearing of 1.26×10^7 dyn/cm^2. O'Neil 1949 (26), described a vibrating crystal arrangement where a plane shear wave is reflected under an oblique incidence from a plane interface between the crystal and the fluid under investigation. Relations between material constants and the reflection coefficient, reflection loss and phase shift, were derived. Barlow and Lamb, et al., (27), (28), (29), (30), have published extensive investigations on viscoelastic behavior of lubricants measured with the methods of cyclic shearing stress. A recent paper 1972 (31) reports the relationship between the modulus of shear elasticity and pressure for two test fluids. Pressures up to 200 kpsi was investigated. The shear modulus was found to increase with pressure. A maximum value of about 6×10^5 psi (4×10^{10} dyn/cm^2) was found for one of the test fluids at 200 kpsi. Appeldoorn, Okrent and Philippoff 1962

(32) used the torsionally vibrating crystal viscometer in investigations of straight mineral oils under pressure up to 15 kpsi. The lubricants showed shear independent viscosity up to a maximum value of calculated shear stress of about 150 psi (10^7 dyn/cm^2). The shear stress is calculated under the assumption that the angular frequency is equivalent with the shear rate in steady shear. Applied frequencies were 20 kHz and 60 kHz.

Rotational viscometers of cone and plate type or of cylindrical type seem not to have been used in high pressure high shear stress viscometry until very recently (33).

CHAPTER II

HIGH SHEAR STRESS BEHAVIOR OF SOME LUBRICANTS

Introduction

Investigations have been carried out in the high pressure viscometer to determine lubricant behavior at high shear stress. The operating temperatures, pressures and shear stresses for a lubricant in an elastohydrodynamic contact can be approached in the viscometer. Furthermore, all these operational parameters can be varied independently of each other.

Five lubricants were investigated: a diester, a polyalkyl aromatic plus additive (DN 600 plus Additive), a synthetic paraffinic oil (XRM 177 F4), a silicone oil (Dimethyl Siloxane DC-200-50) and a mixture (B3J) of paraffinic, mineral oil with 11.5% polyalkylmethacrylate (PL 4523) with an average molecular weight of 2×10^6. A detailed description of each fluid is found in Appendix A.

Apparent Newtonian behavior has been found for all fluids except B3J (the polymer blend) up to a shear stress of approximately 700 psi ($\sim 4.8 \times 10^7$ dyn/cm^2), which is the present upper limit of shear stress for the high pressure viscometer. Viscous dissipation heating alone seems to dominate up to the maximum stress in causing an apparent shear thinning effect. The data for the mixture (B3J) of paraffinic mineral oil and 11.5% polymer (PL 4523) show a significant amount of scatter when the apparent viscosity is plotted against calculated capillary wall shear

stress. The scatter of the data is pronounced at shear stresses above 1 - 2 psi ($\sim 10^5$ dyn/cm^2) making interpretation difficult in terms of liquid behavior alone.

Distinct non-liquid behavior was observed at extreme pressures and temperatures for the lubricant DN 600 plus Additive. Similar behavior was observed for the siloxane but at high shear stresses, 150-600 psi ($1 - 4 \times 10^7$ dyn/cm^2).

Modifications of the High Pressure Viscometer

The measurements were carried out in a high pressure viscometer. The design and operation of the viscometer is described in detail in (1) and (12). The pressure level p_3 of the test section and the volumes R1 and R2 is controlled by the pressure of the cylindrical volume I, Figure 1. An area ratio of fifty-to-one between the pistons of volume I and volume R1 allows the use of low operational pressures of the pressurizing hydraulic system for cylinder I. The maximum pressure is 3 kpsi which gives a maximum pressure of 150 kpsi in the volume for the test fluid. The pressure level p_3 is recorded with the pressure transducer TR3. Displacement of the translating piston generates flow through the capillary in the test section. Displacement is achieved hydraulically with low pressure oil supplied to the volumes III or IV. The volume flow rate through the capillary was previously determined by the measurements of time and displacement. The volume flow rate is now measured with a velocity transducer. The pressure drop over the capillary is measured with the pressure transducers TR1 and TR2.

The viscometer has been modified and the operational procedures

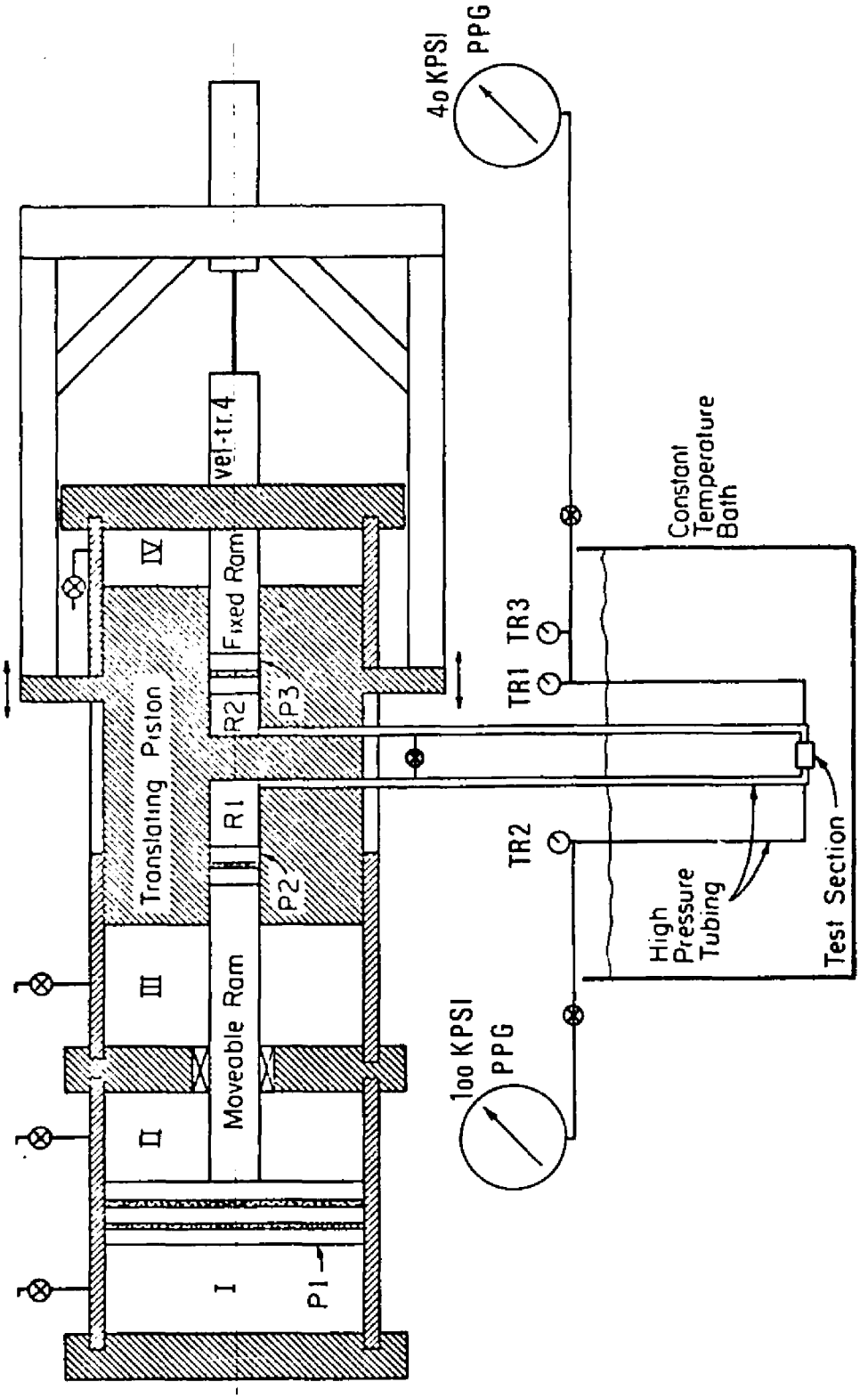

Schematic Drawing of Viscometer.

Figure 1. The Modified Viscometer.

have been changed. An analog-to-digital converter and a multichannel tape recorder have been added to the equipment. The transducer signals are recorded on magnetic tape. The raw data are processed with the aid of a computer program.

Figure 1 shows a schematic of the viscometer including some of the most recent modifications. The displacement transducer, which was used for flow rate measurement, has been replaced with a velocity transducer, Hewlett-Packard L6VI, and a high gain amplifier. The change was motivated by the addition of the analog-to-digital data recorder, which made a direct signal preferable to a differentiated signal. Interest in the possibility of measurements of transient phenomena also motivated the change. Two high precision pressure gauges (Heise Bourdon Tube Co., 40 kpsi and 100 kpsi) have been added in order to improve accuracy of the calibration procedure. An infinitely variable drive has been provided for displacing the translating piston (Figure 1) at constant velocities. The piston is moved hydraulically as before by charging volume III or IV with a low pressure fluid. The flow rate of this fluid is, however, kept constant by direct coupling of the drive unit to the piston of the charging pump. The drive unit gives good reproducibility of the measurements. The displacement of the pump piston is, however, not big enough to obtain a satisfactory flow rate for measurements at the highest attainable shear stresses. Manual drive (hand pull) is therefore used for these measurements. Satisfactory reproducibility can be obtained for these higher speed displacements of the translating piston of the viscometer.

Capillaries with a low L/D ratio have been used. The smallest

ratio applied has been L/D = .1 (L = 0.001 inch and D = .01 inch) this ratio, however, was used only for exploratory purposes. The correction was found to be excessive for the L/D ratio of .1. Measurements were therefore not carried out with this capillary. The lowest ratio used so far is L/D = 1.35 and the smallest diameter used is .0035 inch.

The measurements were carried out with capillaries of L/D = 297, L/D = 14.9 and L/D = 1.35. Corrections for kinetic energy were incorporated as described in detail in (1), Novak, 1968.

Table 1. Capillary Dimensions and Materials

	L/D	D Inch	L Inch
Stainless Steel Capillary No. 4	297	.01009	2.996
Stainless Steel Capillary No. 1	14.9	.00785	.117
Sapphire Capillary No. 0	1.35	.0035	.0047

Calibration Procedures

The viscosity measurements are carried out essentially as measurements of pressure drop and flow rate in the capillary. Shear stress is derived from the pressure drop measured with the differential pressure transducers TR1 and TR2 (Figure 1). Shear rate is determined from measurements of flow rate indicated by the velocity transducer TR4. Pressure transducer TR3 measures the pressure level.

The Differential Pressure Transducers

The differential pressure transducer consists essentially of a strain gauge Wheatstone bridge which is accentuated by a diaphragm. The transducers have been calibrated with an approach involving summation

of small increments of pressure in the test section of the viscometer. Pressure readings from the Heise precision gauges are recorded simultaneously with the amplifier outputs from TR1 and TR2. Only one transducer is calibrated at a time. The pressure increments are applied with a pressurizing hand pump with a small piston diameter and controlled through measurements of the transducer-amplifier output. The output is measured with a DC-Differential Voltmeter (Hewlett-Packard 3420B) which has a precision of 10 μvolts. The voltmeter is used as a null meter. The steps are accurately controlled and measured to 6.0 volts, from an output of -3.0 volts to +3.0 volts from the symmetric transducer amplifier. The estimated accuracy of the setting of a pressure increment is equivalent to .02 volt. The precision range (10 μV) of the differential voltmeter is, therefore, completely sufficient.

The amplifier output is changed from +3.0 volts to -3.0 volts after each pressure measurement by balancing the input potentiometers of the amplifier, (1). This change is a preparation for the next pressure increase. The accuracy of the change in potentiometer setting is estimated to be .01 volt. Total estimated accuracy of a measurement of a pressure increment is therefore .03 volt, on a deflection of 6.0 volts, which is equivalent to .5%. This error estimate is also valid for the voltage sum of the steps. Each increment of 6.0 volts is equivalent to approximately 440 psi for 6 volts excitation of the transducers. The accuracy of the high pressure gauges is better than .1% of full scale deflection (40 psi or 100 psi). This is about 10% to 25% of a single pressure increment. This high inaccuracy will, however, diminish rapidly with increasing numbers of steps. The gauge accuracy of .1% of

full scale deflection is constant. A typical calibration of a transducer-amplifier involves nearly 100 pressure increments. The pressure gauge error will, therefore, typically be of the order of .1% - .2%. The estimated accuracy of .5% for the voltage sum and the pressure gauge accuracy of .1% - .2% may safely imply that the calibration procedure is correct within considerably less than 1% of the full range of calibration.

It is essential for the accuracy of the calibration procedure that the system pressure remains constant during the change of potentiometer setting of amplifier output from +3.0 volts to -3.0 volts. The constancy of system pressure is assured by steady state conditions. These are obtained when temperature transients, possible relaxation of seals, etc., have faded away after each pressure increment. The change of potentiometer setting can be carried out in about 10 seconds. The constancy of system pressure during this period can be verified and measured with the transducer-amplifier, which is not undergoing calibration. Changes as small as 30 millivolts (~2.0 psi) can be detected with this channel when it is used as null indicator. System pressure constancy is assumed to be achieved when no pressure variation is detected for a period of about 100 seconds.

The exitation voltage for the transducers was measured continuously during the calibration procedure. Changes in the voltage were, however, insignificant and about .1 millivolts. The average value was applied in calculations. Standard excitation voltage level is 6 volts. Some high shear stress measurements, however, were carried out with 1.5 volt excitation. The transducer sensitivity is directly proportional to the

excitation voltage. Measurement accuracy is, therefore, not impaired by changes in excitation voltage. A series of control measurements confirmed this assumption.

Table 2 shows a typical set of pressure gauge readings from a transducer calibration and Figure 2 shows the characteristic of a transducer-amplifier combination. The slope of the characteristic of Figure 2 is incorporated in the computer program which is used to process the raw data. It was found that the characteristic could be superseded satisfactorily with a continuous curve consisting of straight line segments for pressure levels above 8 kpsi.

Amplifier linearity is demonstrated in Figure 3, which shows amplifier output in terms of galvanometer deflection on a Honeywell Visicorder 906c recorder as function of micro-volt level input. The amplifiers 1 and 2 are the same type amplifiers and are assumed to have the same general properties. Amplifier 2 is, therefore, chosen to demonstrate the linearity. The graph shows deflection to only one side, but the amplifier is assumed to be symmetric. The graph includes a possible minor recorder nonlinearity (~2% of the deflection) and possible errors in the graphical procedure of measuring the deflection from the recording paper. Figure 4 shows a linearity check of output from 5.0 volts to saturation. It can be concluded from Figure 3 and Figure 4 that the amplifier linearity is satisfactory.

Table 3 shows some results of two calibrations of the differential pressure channels. The viscometer had been in use between the times of calibrations. However, the consistency of the numbers indicates the degree of reproducibility of the calibration. The total inaccuracy of the

Table 2. Typical Calibration of Transducer TR1.

Each pressure increment is equal to 6.00 ± .015 Volt amplifier output.
Pressure readings (units kpsi) from a HEISE 40 kpsi precision gauge.

0.0	8.44	15.24	21.80	28.40	34.94
1.06	8.92	15.68	22.26	28.84	35.38
1.78	9.38	16.11	22.70	29.26	35.82
2.38	9.85	16.54	23.14	29.68	36.26
3.00	10.28	16.98	23.58	30.12	36.68
3.54	10.74	17.42	24.02	30.56	37.12
4.08	11.18	17.86	24.44	31.00	37.56
4.60	11.62	18.30	24.88	31.44	37.98
5.10	12.06	18.74	25.32	31.88	38.42
5.60	12.52	19.18	25.74	32.32	38.86
6.08	12.98	19.60	26.18	32.76	39.30
6.56	13.44	20.02	26.62	33.20	39.76
7.05	13.89	20.48	27.08	33.62	
7.52	14.34	20.92	27.50	34.06	
7.98	14.78	21.38	27.96	34.48	

Remark to Table 2

At pressure (kpsi)	Excitation Voltage	Time Nov. 27, 1972
0.0	6.05480	16:36
7.05	6.05504	17:15
19.18	6.05522	18:16
39.76	6.05536	19:34

Average excitation voltage 6.05508 Volt. 86 pressure increments of 6 Volts = 516 Volts.

Remark to Table 2 (Continued)

The characteristic is essentially a straight line from 14 kpsi to 40 kpsi. A pressure difference of 26.32 kpsi corresponds to 360 Volts. The slope of the characteristic is therefore:

13.678 mV/psi re 6.05508 Volts

or

13.55 mV/psi re 6.0 Volts

Slopes at	10 kpsi	5 kpsi
	13.05 mV/psi	11.72 mV/psi
	re 6.0 Volts	

Table 3. Some Results from Calibrations of Transducer TR1 + Amplifier 1 and Transducer TR2 + Amplifier 2.

Time of calibration	June 1972	November 1972
Transducer TR1 + amplifier 1 (14 kpsi, 40 kpsi)	13.55 mV/psi	13.55 mV/psi
Transducer TR2 + amplifier 2 (14 kpsi, 30 kpsi)	13.3 mV/psi	13.37 mV/psi
(30 kpsi, 40 kpsi)	13.64 mV/psi	13.64 mV/psi

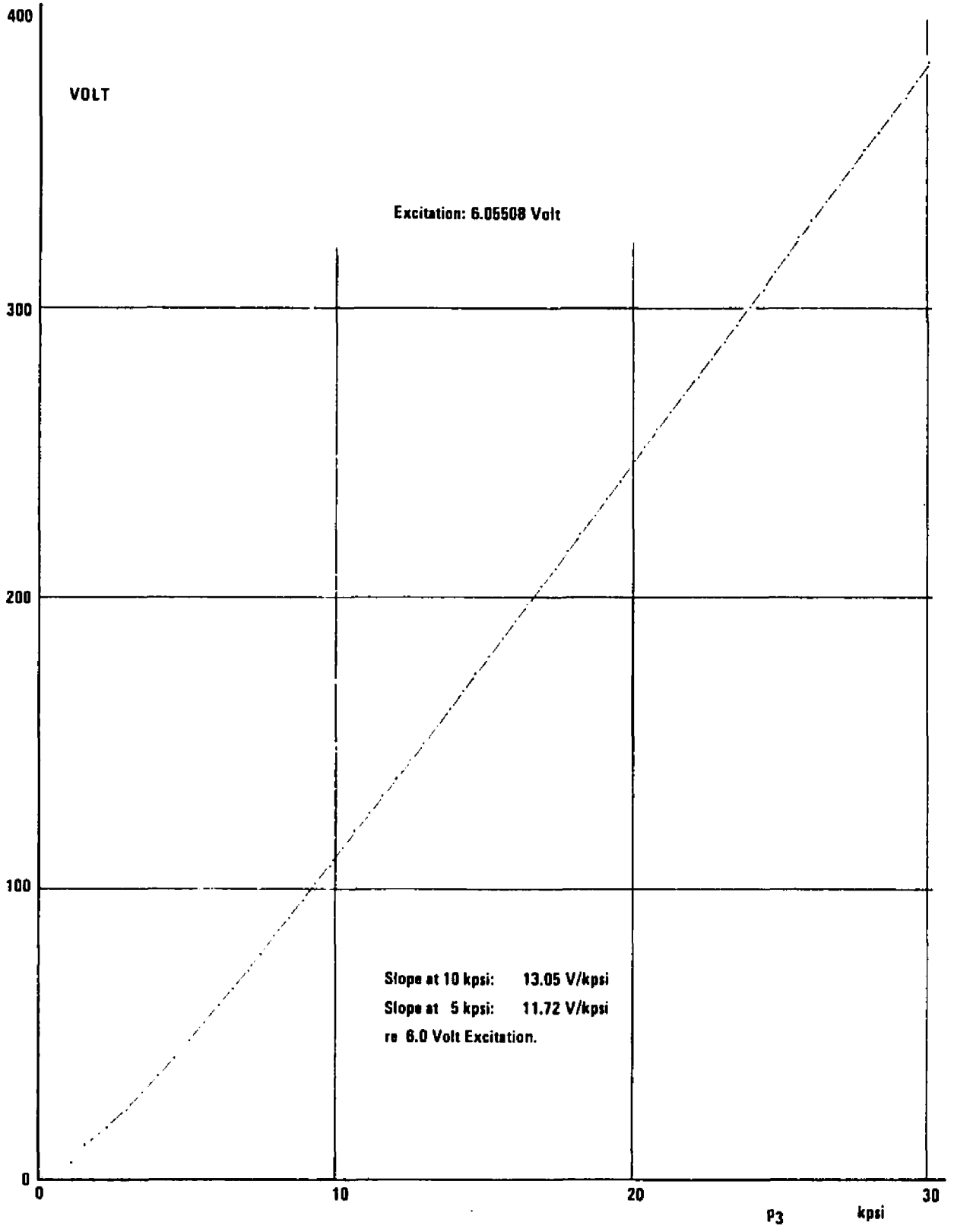

Figure 2. Characteristics of Transducer TR1 and Amplifier 1.

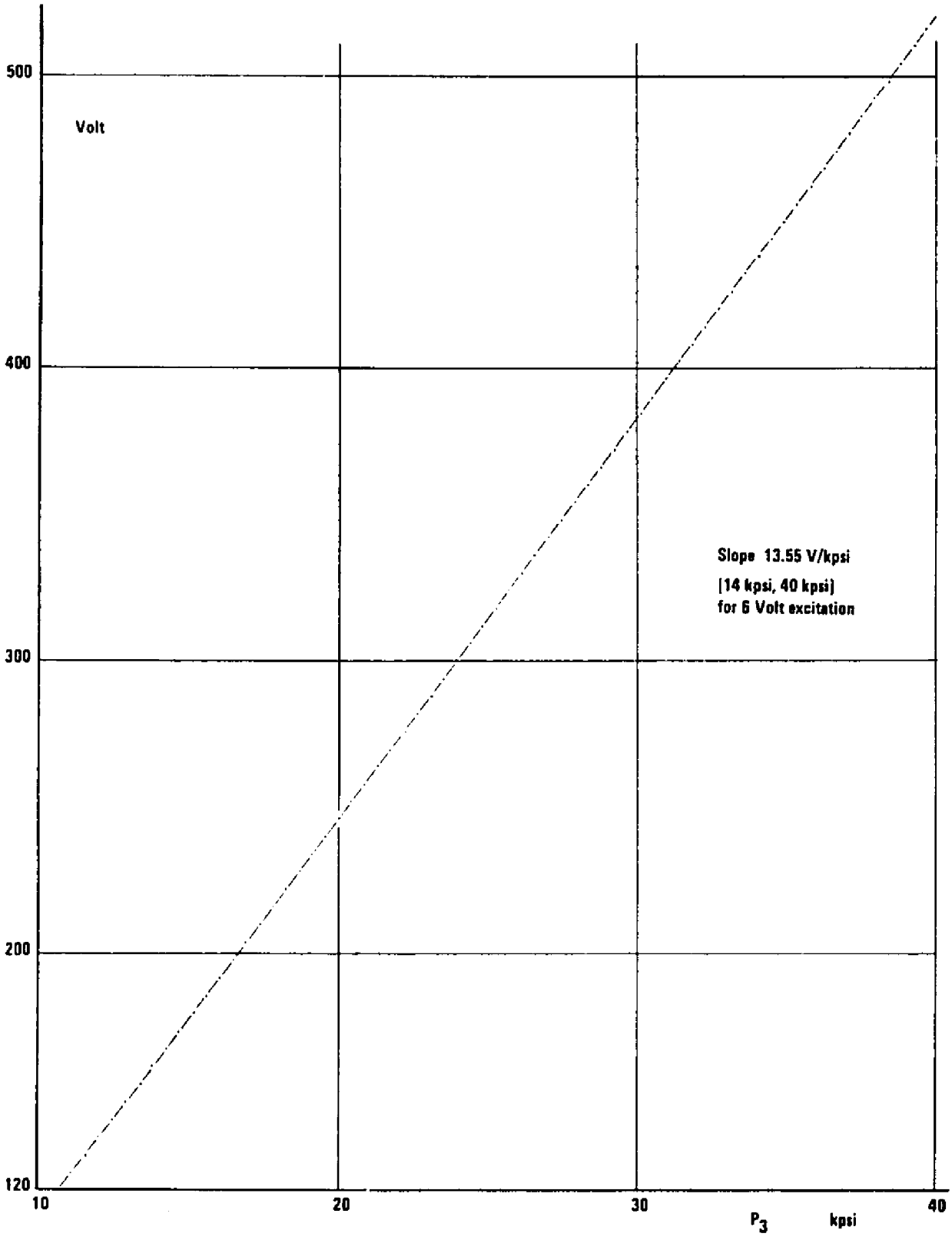

Figure 2. (Continued)

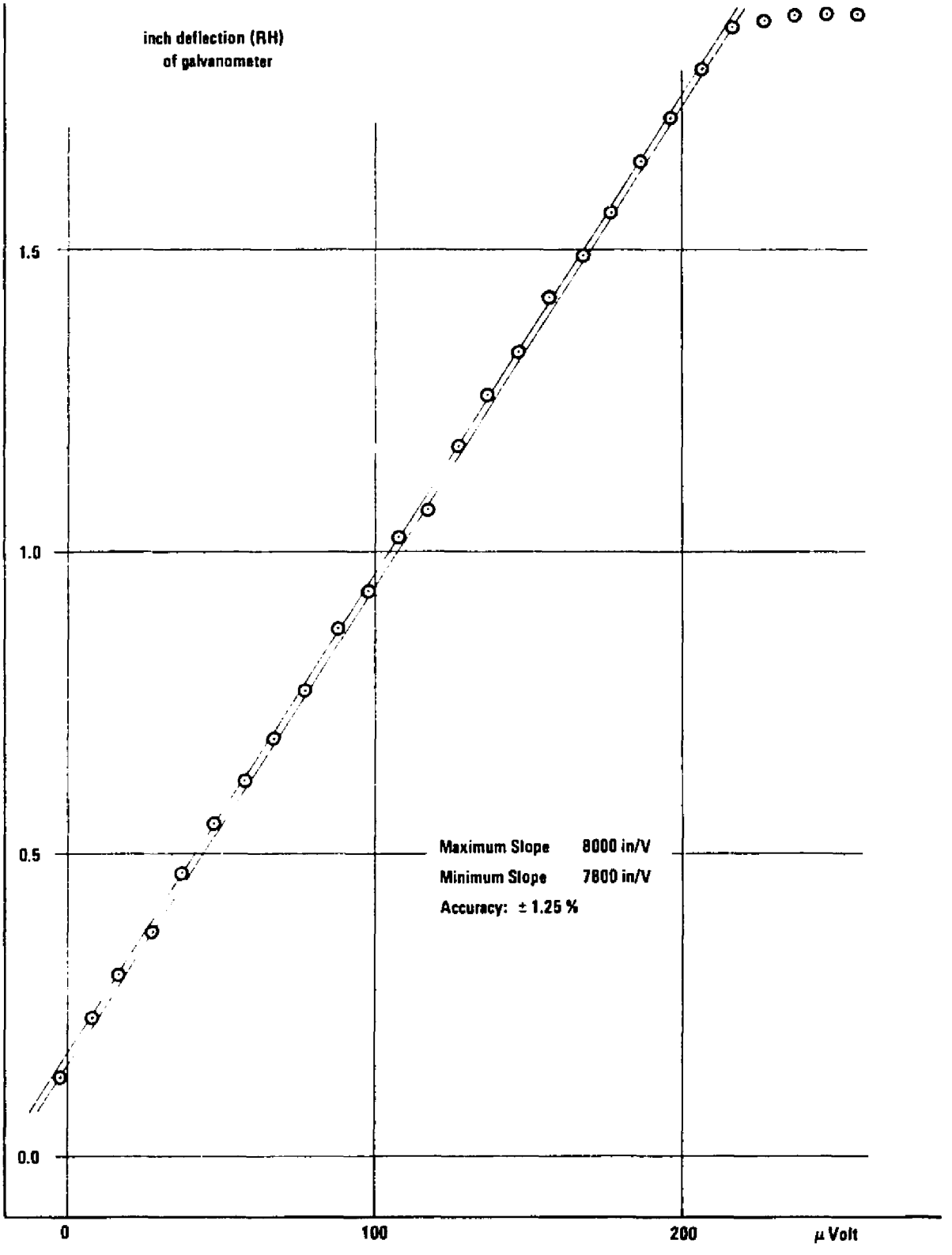

Figure 3. Characteristic of Amplifier 2 and Recorder.

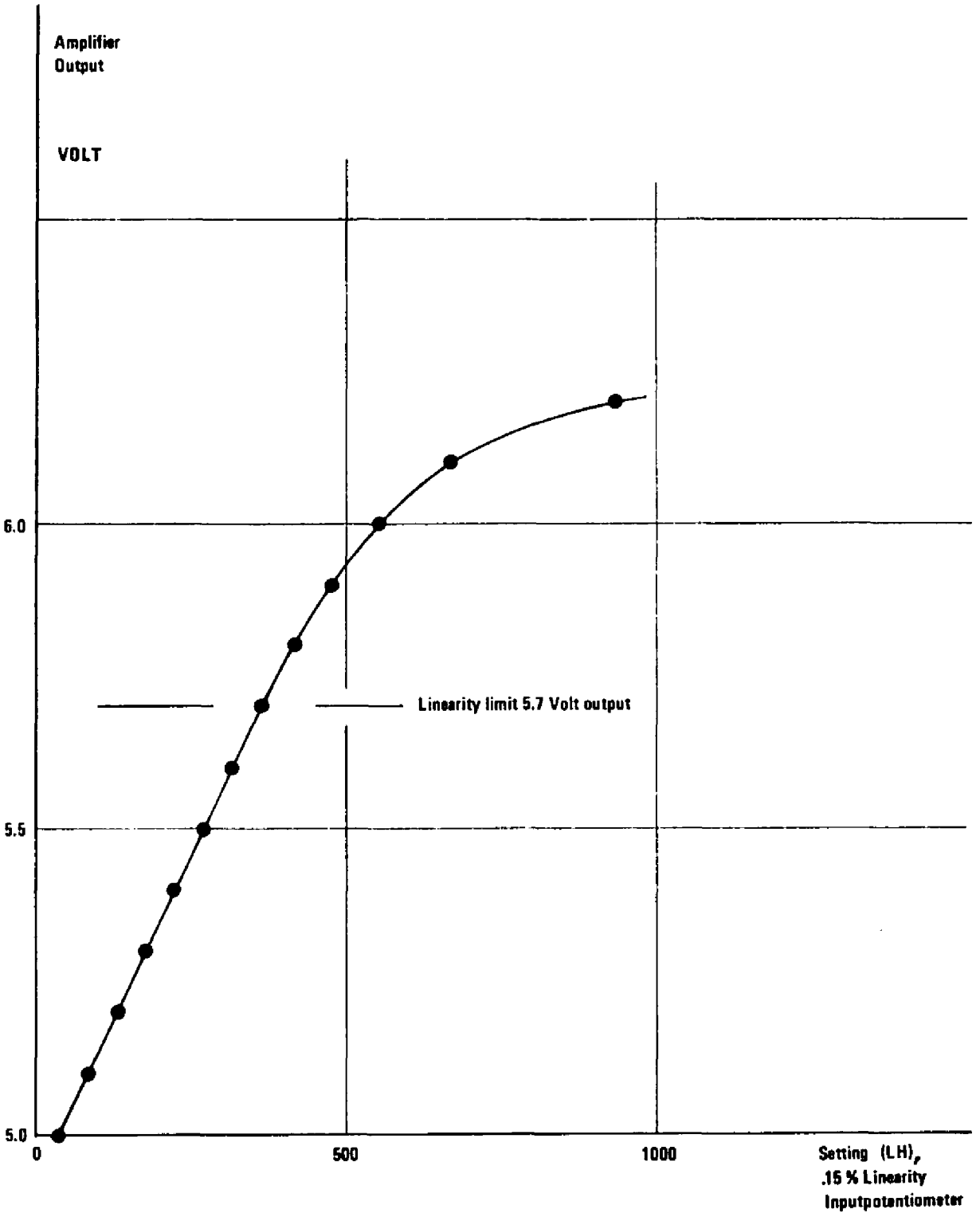

Figure 4. Linearity Check of a Symmetric Amplifier, No. 1, for No. 1 Pressure Transducer, TR1. (The transducer is subjected to a constant pressure (atm). Output is generated by changes of the input balance of the amplifier. Only output above 5 volt is shown.)

numbers is assumed to be less than 1%. The calibration procedure can be interrupted as well as initiated at any desired pressure level.

The Pressure Level Transducer

The pressure level transducer (TR3, Figure 1) was calibrated by recording transducer output and pressure readings from the high precision gaugds. An interval of 5 kpsi was used. The transducer characteristic was linear above 5 kpsi within calibration accuracy.

The Velocity Transducer

The velocity transducer measures linear, straight line velocity. It consists of a shielded coil and an axially located, cylindrical core. The core is a high coercitive force permanent magnet. Motion of the core generates a voltage in the coil proportional to linear velocity with an output of 545 millivolts/ips. The working range is 1.0 inch. Manufacturer's specifications (see Appendix B) show a linearity of better than 1% and output variations between 95% and 100% of nominal output over the total working range.

Considerations of the function of the transducer suggest considerably increased accuracy above the mentioned magnitude of ± 2.5%, however, for a reduced working range. A working range of about 0.5 inch was, therefore, maintained during the experiment.

The transducer and amplifier calibration were carried out as measurements of displacement and corresponding time duration. The velocity of the traversing piston was maintained constant with the above mentioned drive unit during the calibration. The amplifier output was sampled by the appropriate channel on the analog-to-digital recorder. A typical calibration speed was 0.001 in/sec.

Time was measured between the consecutive openings of two micro-switches. A bracket on the traversing piston activated the switches. These switches were connected electrically over the inputs of two dummy channels on the analog-to-digital converter. The opening times can, therefore, easily be assessed from a computer printout.

The travelled distance between activation of the switches was measured with a precision dial indicator and was typically 0.01 - 0.02 inch. The accuracy of the indicator is guaranteed to be better than 0.0001 inch. This was confirmed in a series of measurements performed with parallel gauge blocks (Grade L).

The amplifier gain was approximately 890. The transfer function for the transducer and amplifier was therefore 485 V/ips. The input to the analog-to-digital recorder will be 485 millivolts for a calibrating speed of 0.001 in/sec. This output level of about 500 mv is appropriate for accurate recording by the analog-to-digital converter, which has a threshold of distinction of 4.85 millivolts. This 1% ratio between threshold and signal magnitude is however lowered considerably by the great amount of sampled data and the following averaging process in the computer treatment.

Calibration of the Capillaries

Two calibration fluids were used, a viscosity standard, S-60 from Cannon Instrument Company, and diester (bis 2-ethylhexylsebacate) from Rohm and Haas Company. Table 4 summarizes the viscosities of the fluids. The fluid S-60 was used only at low shear stress calibrations. The diester was used over the total range of shear stress. Both fluids are assumed to be Newtonian liquids in the sense that the ratio between meas-

Table 4. Viscosities (cp) of Calibration Fluids at Atmospheric Pressure

	100°F	210°F	300°F
S-60	51.06 cp	5.899 cp	—
Diester	11.41 cp	2.86 cp	1.46 cp

Viscosities for S-60 are from the manufacturer's specifications.

ured shear stress and shear rate is constant.

The viscosity of the diester was determined at 100°F, 210°F and 300°F with a Cannon-Fenske Routine Glass viscometer 150-E707. This viscometer was calibrated with the S-60 fluid. Capillary 4 (Table 1) was used as the standard capillary for high pressure measurements. Calibration of capillary 4 was carried out at atmospheric pressure with diester and checked with the S-60 fluid. The diameter of capillary 4 was found to be 0.01009 inch. Later calibrations confirmed this measurement within 5 μinch.

These statements about the diameter of capillary 4 assume the physical length of the capillary tube to be 2.996 ± .001 inch as measured with a micrometer screw. Therefore, the diameter 0.01009 inch contains all possible corrections originating outside the capillary cavity, however, only for Newtonian liquids.

Calibration of the capillary 1 was carried out as a comparison of low shear stress measurements with capillary 4 measurements. The diester was used as calibration fluid. The pressure range applied was 10 - 40 kpsi. Calibration temperature was 31.9°F ± 0.1°F. This temperature was selected because the viscosity of the calibrating fluid for the applied

pressures is then about 10^3 cp, well within the expected viscosity range in the elastohydrodynamic lubrication film. The selected calibration temperature is also appropriate for comparison with previous work, notably ASME 1953 (2).

The diameter of capillary 1 was found to be 0.00785 inch for a measured physical length of 0.117 inch. This diameter statement includes all possible corrections originating outside the capillary cavity, however, only for Newtonian liquids.

The capillary with L/D = 1.35, capillary 0, is a sapphire ring (Figure 5) embedded in stainless steel high pressure seals of a similar type as employed by AMINCO*(AMINCO is the manufacturer of the utilized standard high pressure tubes and fittings). The seals are of local design and manufacture.

Calibration of capillary 0 was carried out as a comparison of low shear stress measurements with capillary 1 and capillary 4 measurements. The calibration fluid was the diester. The applied pressure range was 10 - 40 kpsi. The calibration was carried out at 31.9°F ± 0.1°F. The diameter of the sapphire capillary was determined with a high power microscope (200X and 500X) to be 0.0035 inch with an estimated accuracy of 3%. The magnitude 0.00348 inch was actually used in the computer program because this number was believed to be the most nearly accurate.

The comparison with capillary 1 and capillary 4 measurements showed the effective capillary length to be 0.0047 inch. This calibration also takes into account all possible corrections originating outside the cylindrical part of the capillary cavity. It will, therefore, also give a correct shear stress determination, according to the expression

*AMINCO is an abbreviation for American Instrument Company.

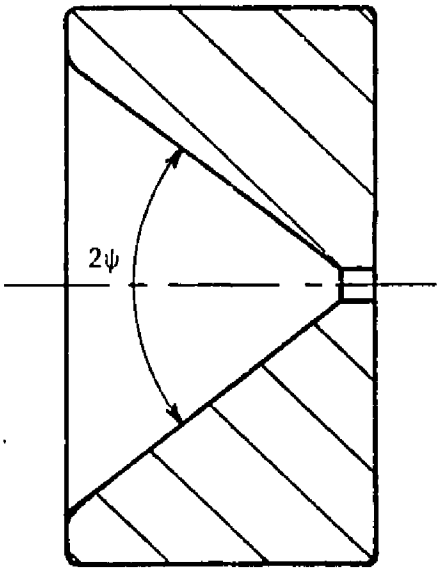

Figure 5. Capillary 0, Sapphire. (Outside diameter .055 inch. Thickness .030 inch. Cone angle $2\Psi \simeq 80^{o}$. Capillary diameter .0035 inch. Capillary length $\simeq$ .0047 inch.)

$\tau = \Delta pD/4L.$

One known correction originating outside the capillary is the pressure drop due to flow contraction before the inlet and to flow dispersion after the capillary exit. Wurst 1954 (34) estimates the pressure drop over an orifice, L/D ~ 0, to:

$$\Delta p_o = (50.4/\pi)(\bar{Q}/D^3) \qquad (1)$$

for small Reynolds numbers. Equation (1) can be written as

$$\Delta p_o = (50.4/128)(D/L)(128/\pi)(\eta L\bar{Q}/D^4) \qquad (2)$$

or

$$\Delta p_o = .394(D/L)\Delta p \qquad (3)$$

where Δp is the pressure drop $(128/\pi)(L\bar{Q}\eta/D^4)$ due to wall shear stress in the capillary cavity itself. The total pressure drop Δp_t over capillary 0 is the sum of Δp_o and Δp:

$$\Delta p_t = (1 + .394(D/L))\Delta p \tag{4}$$

or

$$\tau = \Delta p/4(L/D) = \Delta p_t/(4(L/D) + 1.572) \tag{5}$$

The manufacturers specification for the ratio length to diameter, L/D, of the capillary 0 is 1. A calibration of the capillary with a Newtonian fluid will therefore give a ratio L/D = 1.394, L = .00485 inch, D = .00348 inch. This calculated length deviates only about 3% from the length, L = .0047 inch, which was found during calibration with a Newtonian fluid, diester. The calibrated equivalent length .0047 was assumed to be the correct length and the most nearly accurate measure of the capillary length. This length was used during evaluation of the measurements. The length .0047 is equivalent with a ratio L/D = 1.35.

No directional effect was found for the capillaries during the calibration measurements. Reversal of flow direction for all capillaries gave consistently identical results within the measuring accuracy. This observation is consistent with the symmetry of the equations for the flow problem (35), (36), and with the approximate solution (34).

The distance in the capillary from the entrance to the point of fully developed parabolic velocity profile is called the entrance length. The calibration of capillary 0 was carried out for entrance length from 2% down to 0.06% of the total length. The corresponding Reynolds numbers for the low shear stress measurements were 0.2 to 0.006. Entrance lengths

as great as 8% of the total length did not produce significant deviations in apparent viscosity. It should be added that calibration for capillary 1 was carried out for equally small Reynolds numbers.

It is an assumption for the concept of the entrance length that the velocity is taken to be constant at the entrance. The velocity profile for the flow at the entrance of the capillary does not satisfy this assumption of constant velocity when the flow is highly viscous. The velocity profile can be estimated to be nearly a parabolic distribution at the entrance. The approximately parabolic profile is created by the viscous pressure drop outside the capillary cavity. This is consistent with the observation of the indifference of the viscosity measurements to the variation from about 0% to 4% of the calculated entrance length.

The concept of entrance length appears thus not to be applicable to flow at small Reynolds numbers, $Re \leq \sim 1$, into a capillary.

Capillaries with ratio D/L of 6.52 and 10 have been used in the initial stage of the work. The preliminary results are consistent with equations (1), (2) and (4). The necessary corrections are however greater (up to 400%) than the pressure drop over the capillary. This great correction suggests that an undesirably high inaccuracy of the experimental results might be expected. These capillaries were not used in the reported investigation.

Figure 6 shows the shear stress at the wall created by a unit total pressure drop impressed on a flow through a capillary for the conditions of low Reynolds number, $Re \leq \sim 1$. It is seen that the shear stress is about 50% of the impressed pressure drop when the capillary has a ratio D/L of 10.

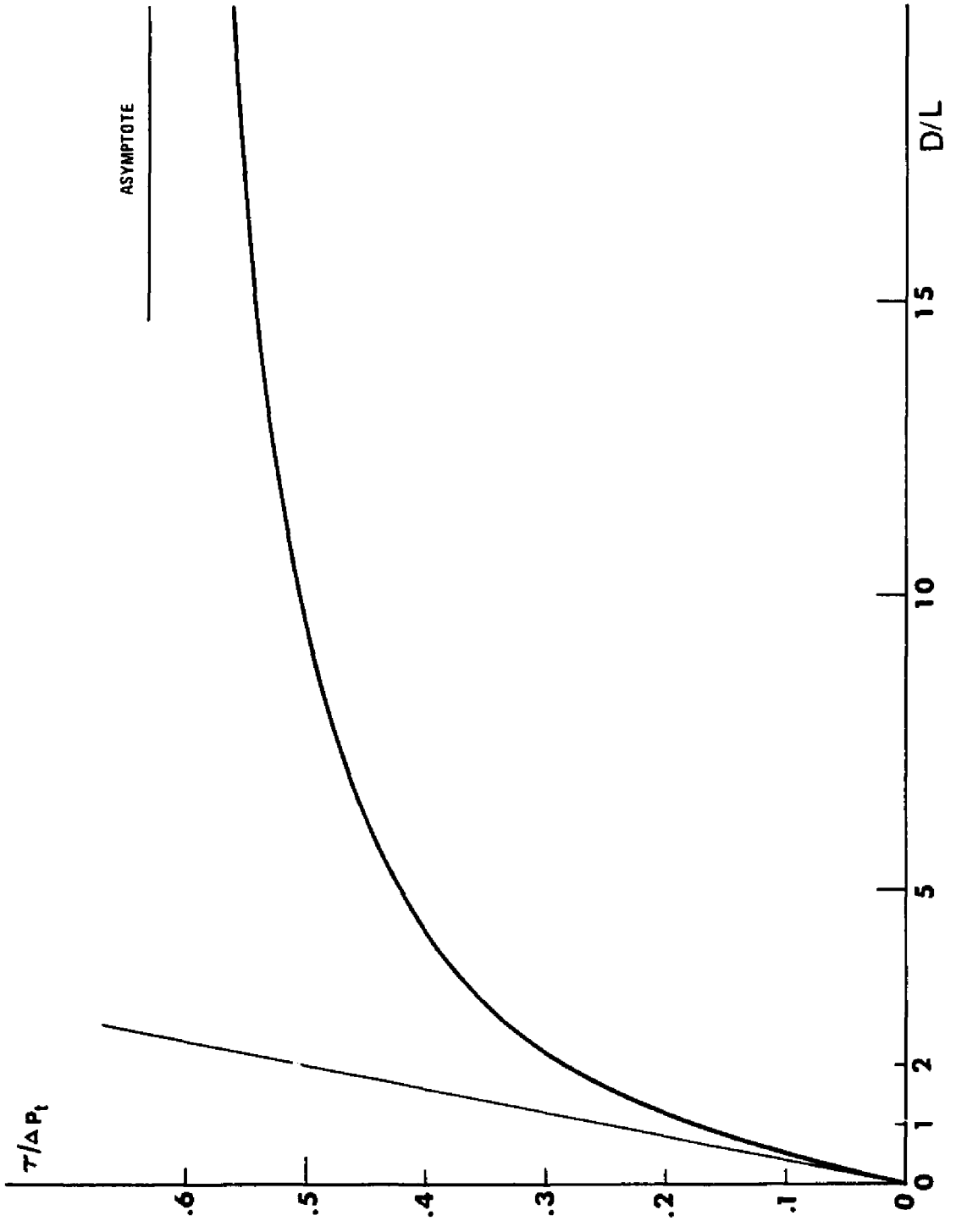

Figure 6. Shear Stress Obtainable in a Capillary for a Unit Pressure Drop.

The calibration measurements for capillary 0 are found in Table 14 - Diester, 32°F. The measurements with the standard high pressure capillary, capillary 4, are plotted in Figures 7 and 8. Table 5 gives a comparison of the averaged data of Table 14 with data for a diester reported as sample A1 in the ASME Pressure Viscosity Report of 1953 (2).

The data summarized in Table 5 are taken from two different charges. The dates of the measurements are separated by about 20 years. The viscosity values in columns 1973 and 1953 are interpolated graphically. This process also incorporates inaccuracies in the data of corresponding pressure levels (5 - 40 kpsi) aside from graphically generated inaccuracies in the viscosity values. The viscosity values are furthermore obtained in two basically different ways of calibration and measurement approaches.

Table 5 shows that the 1973 data deviate less than ±2% from the 1953 data. This small magnitude of deviation can be interpreted as a verification and a support of the previous stated measurement inaccuracy of ±1%, when all prepositioned conditions for the data of Table 5 are taken into consideration.

The data of Table 5 indicate also that a search for further increase of measuring accuracy will not be of value. An accuracy of ±1% seems to be satisfactory for general investigations of high pressure properties of lubricants as long as the lubricants are no more well defined. The conclusions of the work are not at all impaired by a ±1% accuracy of the measurements. A greater accuracy would only have contributed insignificantly to refinements of the results.

Table 5. Diester, 32°F

Pressure Viscosity Relation (Diesters)			
32°F	Data 1973 Capillary 4	ASME 1953 A1	Deviation of 1973 Data from ASME 1953 Data
0 kpsi	57.5 cp	56.8 cp	+1.2%
5	109 cp	108 cp	+ .9%
10	196 cp	194 cp	+1.0%
20	546 cp	547 cp	- .2%
30	1400 cp	1420 cp	-1.4%
40	3365 cp	3310 cp	+1.7%

All viscosities are interpolated graphically on expanded semilog diagrams.

For the column: DATA 1973 - Capillary 4:

Measurements at pressure levels 5 kpsi to 40 kpsi are performed in the high pressure viscometer. Measurements at atmospheric pressure are extrapolated from straight line pressure viscosity characteristics mapped on a rectifying diagram (lnlnη-lnT) of type ASTM D 341-43.

Figure 9 shows the viscosity measurements plotted as function of shear stress. The figure illustrates the high degree of correspondence of the low shear stress measurements for capillary 0 and capillary 1 with those of capillary 4. The high shear stress measurements of Figure 9 (Table 14) show for both capillary 0 and capillary 1 an apparent shear thinning behavior of the diester. This calibration liquid, which is

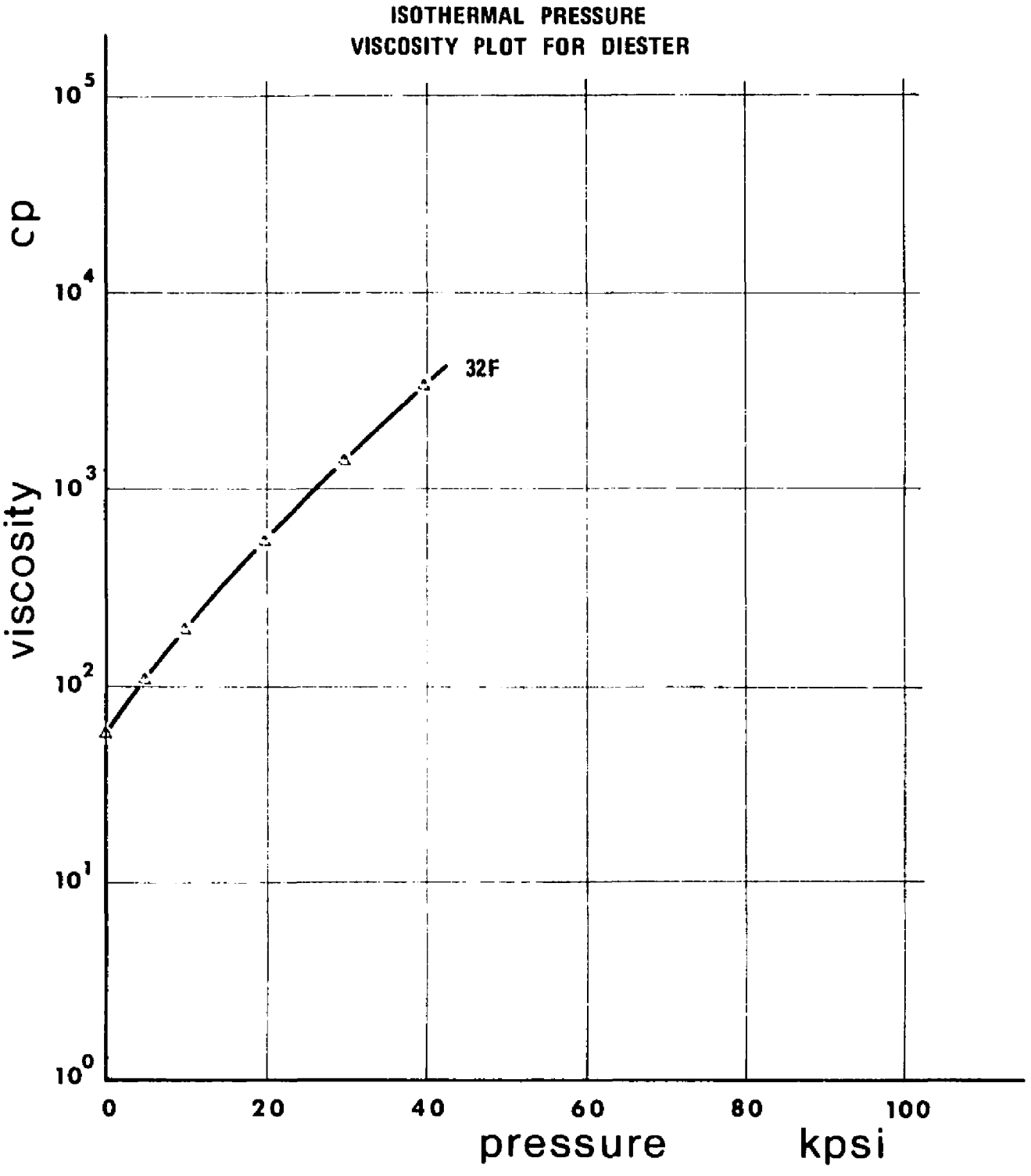

Figure 7. Isothermal Pressure Viscosity Plot for Diester. (Semilog Presentation.)

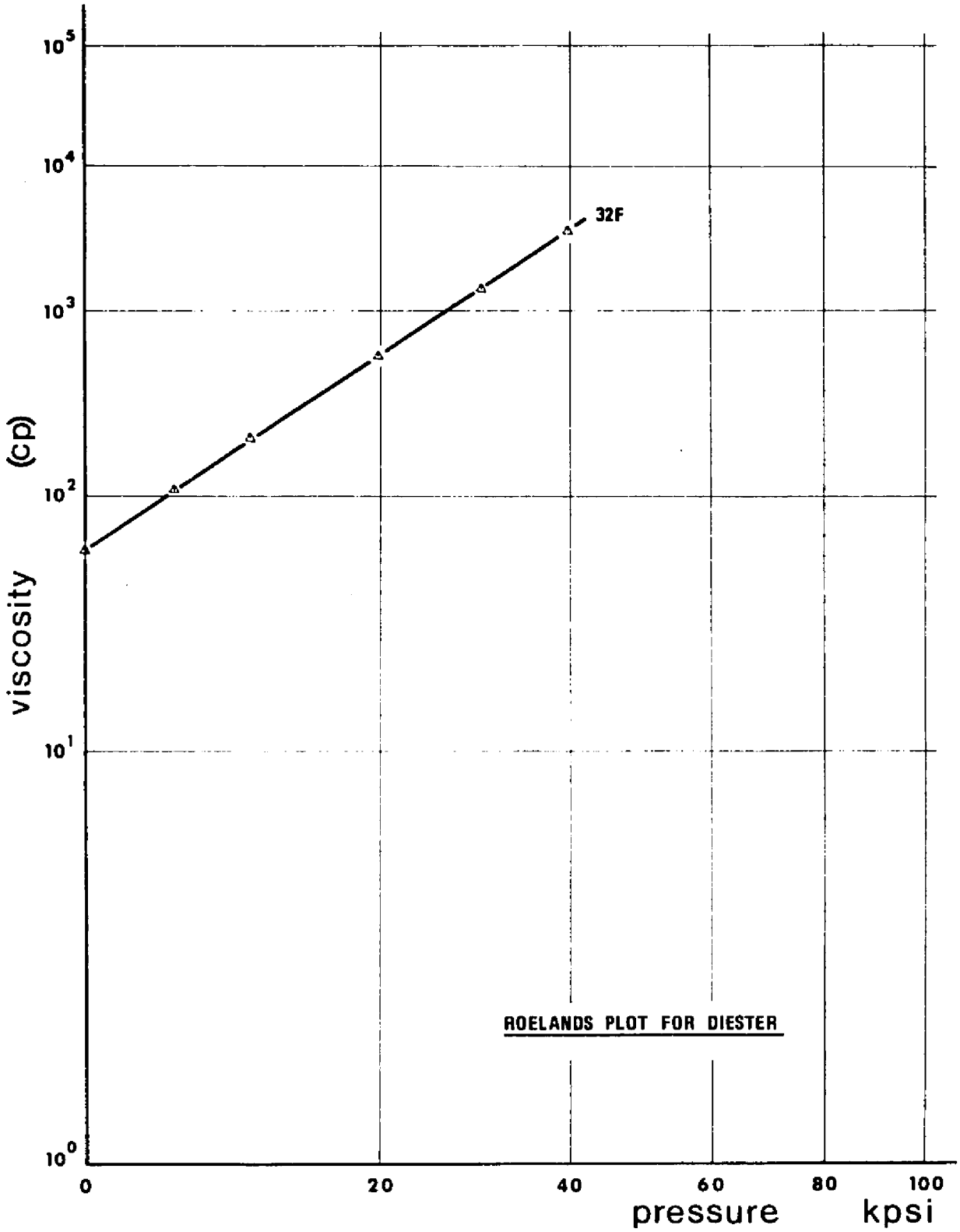

Figure 8. Roelands Plot for Diester.

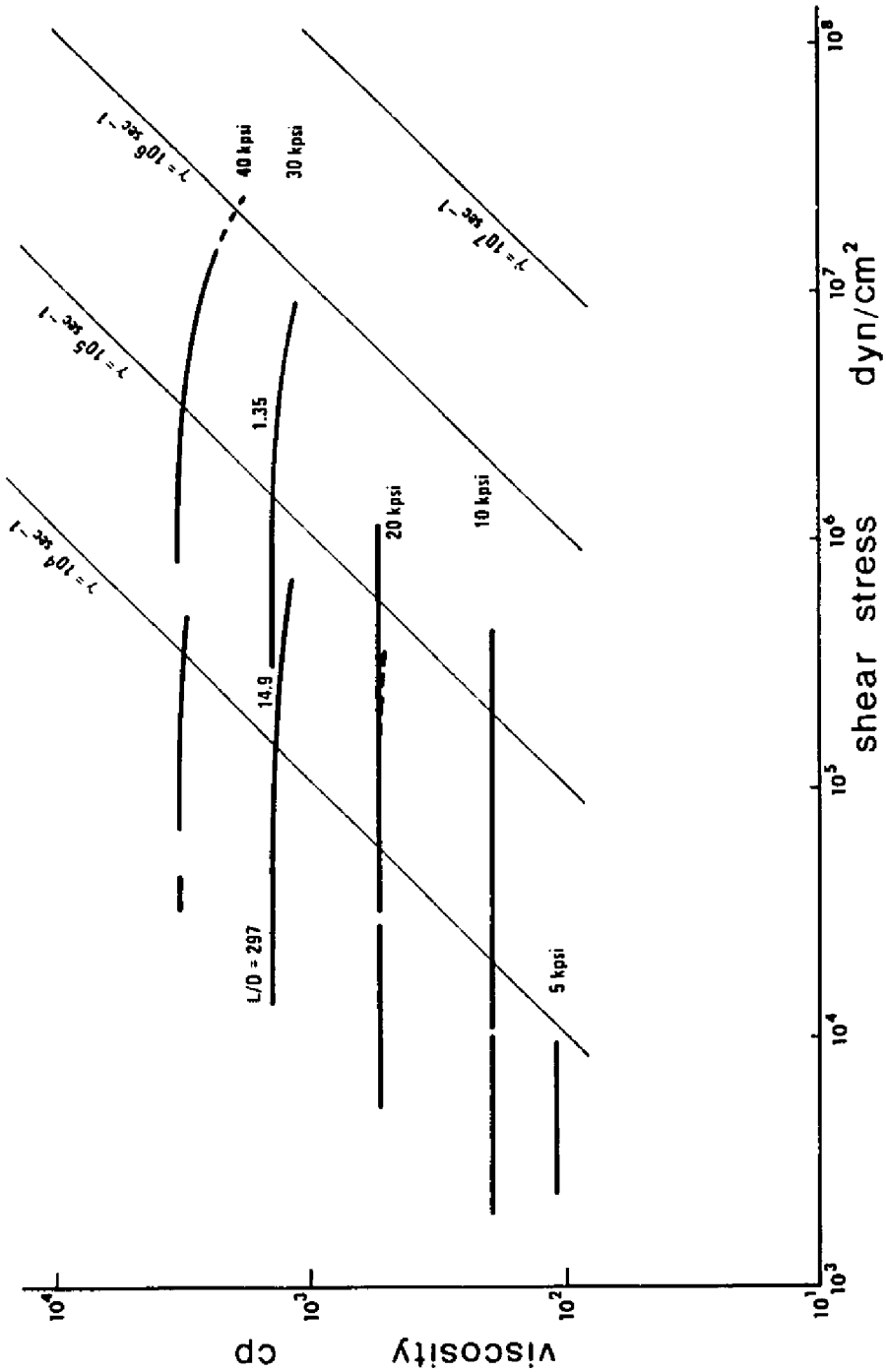

Figure 9. Flow Curves for Diester, Calibration, T = 32°F.

assumed to have completely Newtonian properties, is presumably then subject to dissipation heating in the capillary cavity. A series of measurements with only one capillary cannot easily discern shear thinning effects from dissipation. Comparison between measurements with different L/D ratios will allow a differentiation of these effects.

The measurements plotted in Figure 9 for capillary 0 (L/D = 1.35) and capillary 1 (L/D = 14.9) show for the same fluid at each pressure level consistently lower measured viscosity values for capillary 1 in the overlap zone of the shear stress ranges of the capillaries. This holds true whatever shear stress or shear rate is used as a basis of comparison.

The general form of the characteristics of Figure 9 at 20 - 30 - 40 kpsi and particularly the comparison between capillary 0 and capillary 1 measurements at the overlap zone ($\sim 5 \times 10^5$ dyn/cm^2) where capillary 1 results deviate from the Newtonian characteristic, indicates strongly that shear thinning effects cannot explain the high shear stress behavior of the diester as it is measured with capillary 1, L/D = 14.9.

The diester behaves, therefore, as a Newtonian liquid up to about 10^6 dyn/cm^2 which is the upper limit for capillary 1 measurements in this series of experiments. The common form of the characteristic leads furthermore to the supposition that the diester behaves as a Newtonian fluid up to about 2×10^7 dyn/cm^2 (about 300 psi) shear stress.

Fluid Measurements

Diester

The high shear stress behavior of diester was investigated at

somewhat greater viscosity levels than the calibration measurements. Higher viscosities were achieved by applying a low temperature of 10°F and maintaining the pressure levels 10 - 20 - 30 - 40 kpsi. Table 15 contains the results of the measurements. Figure 10 shows a graphical presentation. Measurements with capillary 4 were not performed because the low shear stress viscosities measured with capillary 0 and capillary 1 showed consistency with previously obtained data for the diester when interpreted through mapping on an ASTM Standard Viscosity-Temperature Chart. The mapping is illustrated in Figure 11.

The presentation of Figure 10 shows the same values of limiting low shear stress viscosity for capillary 0 and for capillary 1 at every pressure level. These viscosities are within procedural accuracy of the viscosities predicted by straight line characteristics as applied in Figure 11.

Comparison with Figure 9 shows that the high shear stress characteristics have the same general form of constant shear stress. The measurements with capillary 1 also show deviation at the same shear stress or the same shear rate downward from the Newtonian characteristic measured with capillary 0 in the same way as found in Figure 9. This confirms the statement that the deviation of capillary 1 measurements at high shear cannot be explained by a shear thinning effect.

The flow curves of Figure 10 (Diester, 10°F) are similar to the flow curves for the diester at 32°F (Figure 9). A translation along the viscosity axis (shear stress constant) will allow one flow curve to be superimposed on another flow curve. This holds also for flow curves measured at the same temperature. These observations suggest that the

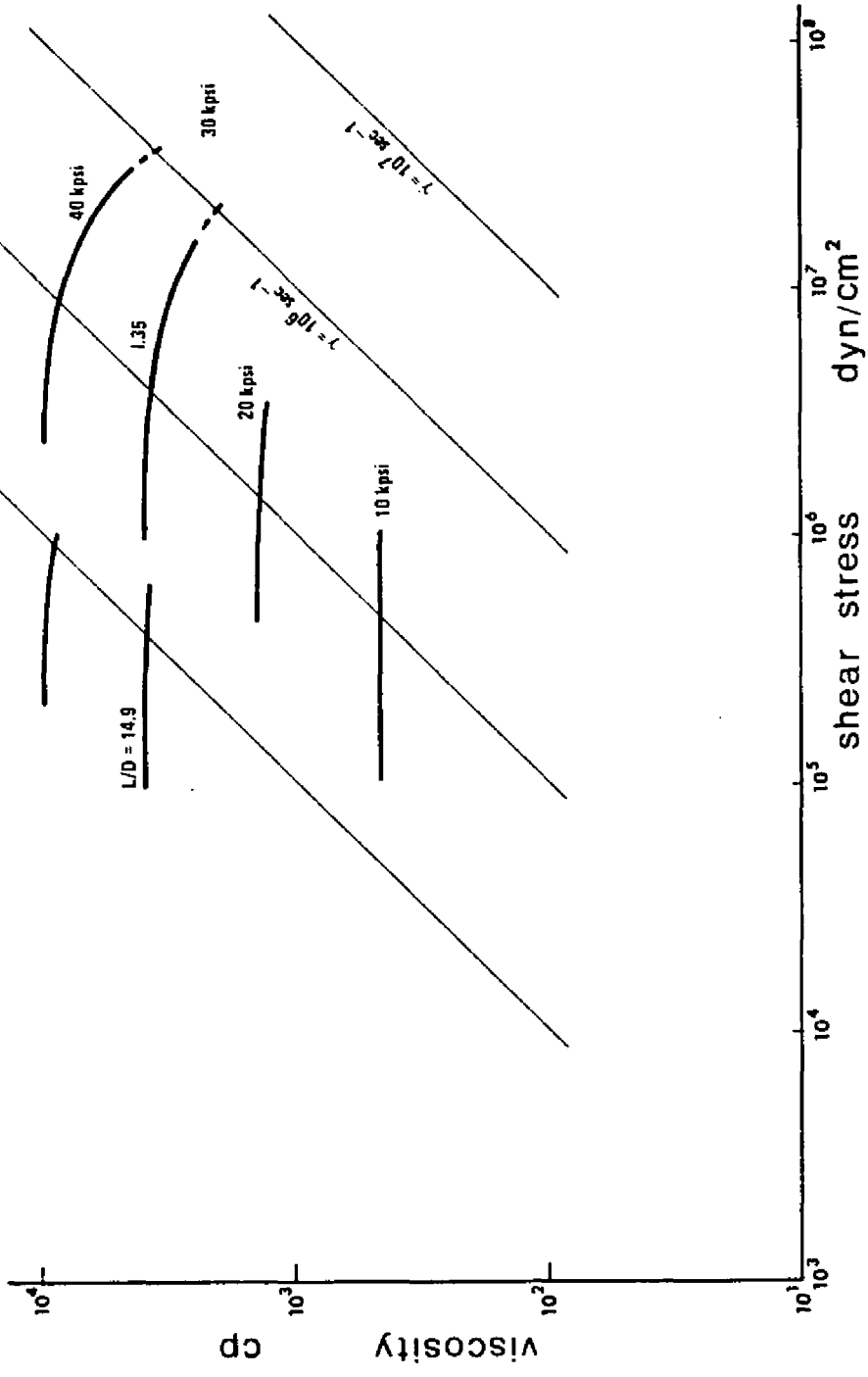

Figure 10. Flow Curves for Diester, High Shear Stress, T = 10°F.

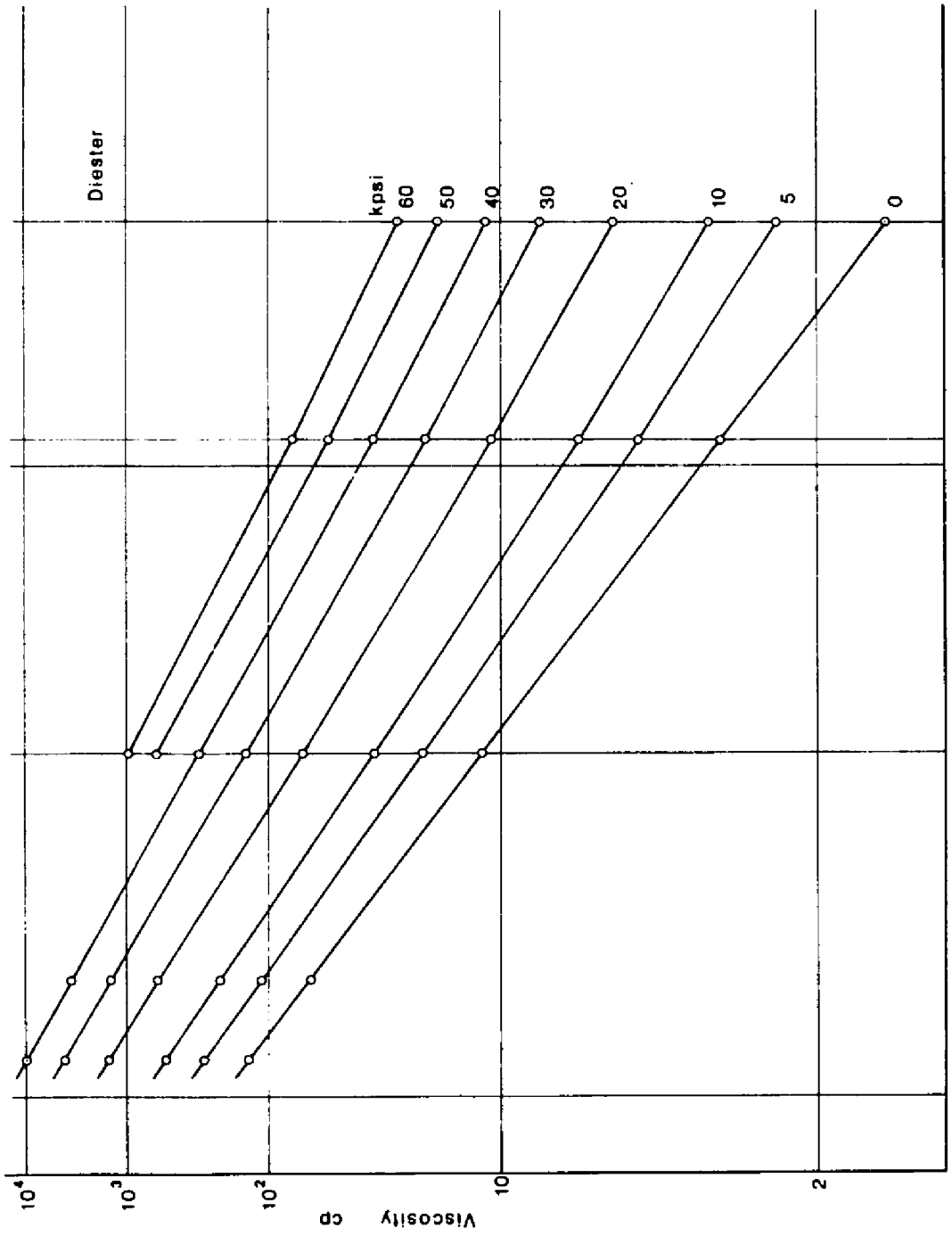

Figure 11. Temperature Pressure Viscosity Presentation for Diester. (ASTM D-341-43).

mechanism responsible for the flow curve deviation from constant viscosity is dependent on the pressure drop over the capillary, capillary geometry (L and D), and possibly some fluid properties; but it is not dependent on viscosity level nor on shear rate. It can be shown that dissipation heating satisfies these requirements.

The highest shear stress shown in Figure 10 is about 3×10^7 dyn/cm^2 ($\simeq$435 psi). Slightly higher stresses were applied. However, amplifier saturation of the velocity signal prevented proper measurements from being taken. Similar conditions had also arisen for the diester, 32°F, 40 kpsi (Figure 9). These measurements are not incorporated in Tables 14 and 15. An extrapolated flow curve signature has been used in Figure 9 and 10 to show an estimated behavior of the fluid.

Figure 11 shows the low shear stress behavior of diester over the temperature range covered. Table 6 gives the numerical values of the pressure temperature viscosity characteristics of the diester plotted in Figure 11.

The rectifying diagrammatic presentation of Figure 11 is essentially that of the ASTM Standard Viscosity-Temperature Charts (D 341 - 43). The generating formula for the chart is $\ln\ln(\nu + c_o) = \ln A - Q \ln T$, (37), where ν is the kinematic viscosity in centistokes at the absolute temperature T (°R) and c_o, A, Q are constants (c_o = .6 cs for ν < 2cs). A and Q are material describing constants. The usefulness of these rectifying charts is based on the observation that mineral oils plot as straight lines presumably, however, only at atmospheric pressure. Hersey (37) states that fair results can be obtained by plotting the values of dynamic viscosity directly using the scale of kinematic viscosities.

Table 6. Pressure Temperature Viscosity Relationship for Diester

	Temperature				
kpsi	10	32	100	210	300°F
			units centipoise		
0	(130)	(57.5)	11.41	2.86	1.46
5	250	109	18.6	4.3	2.28
10	472	196	28.95	6.0	3.05
20	1420	546	64.2	10.7	4.92
30	3900	1400	134.5	18.0	7.52
40	9900	3365	268	79.1	11.1
50	-	-	510	46.7	16.2
60	-	-	940	72.0	23.2
70	-	-	-	-	-

The table values above 0 kpsi are interpolated graphically on expanded semilog diagrams.

(): Extrapolated from straight line pressure viscosity characteristics mapped on a rectifying diagram lnlnη-lnT of type ASTM D 341-43.

Figure 11 is generated with such a simplified plotting method.

The error that arises from the simplified use of the rectifying charts is not significant for use in traction investigations of elastohydrodynamic lubrication. The density of the lubricant varies at most from about 0.9 g/cm^3 to 1.1 g/cm^3 (2) in the pressure and temperature ranges of interest. This is a change in density of $\pm$10%.

The equivalent plotted error is totally about ±0.7% at 1000cp, ±1.4% at 100 cp and ±5% at 10 cp. The relative error between consecutive points is certainly smaller. A somewhat greater error may be expected because the characteristics for many fluids tend to show a slight curvature above atmospheric pressure and for large temperature ranges. The lower bound for the viscosity range of interest in traction investigations is 100 cp to 1000 cp. The maximum error due to simplifications of the generating formula is then about 1%. It will in most cases be considerably smaller. The simplified plotting method may, therefore, safely be applied without any appreciable loss of accuracy.

The constant c_o (0.6cs) can also be discarded for traction investigations. The magnitude of this change is about 0.1% at 100 cp and diminishes rapidly for higher viscosities. The generating formula can therefore be regarded as having the form: $\ln\ln\eta = \ln A - Q\ln T$ which conveniently is a formula with two constants. The constant A stands for some defined base viscosity. The constant Q expresses the change of viscosity with temperature such that a large Q represents great changes in viscosity for a given temperature change.

Figure 11 shows that diester has straight line characteristics in the lnln - ln rectifying diagram for viscosities above 100 cp. It is also seen that the characteristics are straight lines for the ranges 0 - 40 kpsi and 10°F to 100°F as well as for atmospheric pressure and 10°F to 300°F. There is a minor curvature at all the reported pressure levels above atmospheric pressure and above 100°F, when the viscosity is less than 100 cp. The curvature is, however, equivalent to deviations less than about 5% of predicted viscosities. These deviations are

furthermore found at viscosity levels, less than 100 cp, which is outside the range of interest for the high pressure range in elastohydrodynamic lubrication.

The high shear stress measurements of the calibration liquid, diester, show that dissipation heating most likely is the cause of the well observed deviation of flow curves of many lubricants from the Newtonian characteristics toward smaller apparent viscosities for high shear stress conditions. It was further shown that the diester has a constant viscosity in the shear stress range up to about 14 psi ($\sim 10^6$ dyn/cm^2) measured with capillary 1. This indicates that the diester is a Newtonian liquid up to 14 psi. Non-Newtonian effects thus do not participate in the generation of the deviating flow curves for diester measured with capillary 1.

Heat generation per unit volume and unit time is equal to the product of shear stress and shear rate. The measurements of the diester showed that the flow curves, Figures 9 and 10, for both capillary 1 and 0 were influenced by changes in shear stress, but hardly influenced by changes in viscosity, or changes in shear rate. Decreasing shear rates, or lower flow velocities, give equally longer resident times for the liquid in the same capillary. The heat generation per unit volume in a capillary is, therefore, independent of the shear rate and depends alone on the shear stress, or on the pressure drop experienced by the fluid. The temperature changes depend on the amount of heat generated, on capillary geometry (location in the capillary cavity) and on fluid properties. Possible important fluid parameters are specific heat and density.

The specific heat per unit mass and the density are both very nearly constant for many lubricants. The values are in the range c_v: 0.3 to 0.5 Btu/lbm^{o}F (0.3 to 0.5 cal/g^{o}C) and ρ:0.03 to 0.036 lbm/in^3 (0.83 to 1.0 g/cm^3) giving a specific heat c per unit volume of 85 - 170 lbf/in^{2o}F. The thermal conductivity and the previously mentioned material constant Q are other possible important parameters.

The thermal conductivity does not vary drastically for mineral oil lubricants and for many of the synthetic lubricants. The operational values are in the range 0.015 - 0.017 lbf/sec^{o}F (.7 -.8 Btu/hr^{o}F ft) with lower and upper extremes at 0.013 and 0.020 lbf/sec^{o}F. The conductivity decreases about 3% per 100°F temperature increase and decreases about 1% per percent increase in density (37). Deviations from these levels of thermal conductivities are few. Table 7 gives some examples of deviations.

Dimethyl Siloxane DC-200-50

One outstanding property of silicone oils is the relatively small decrease of viscosity with increasing temperature. The Q-exponent is a factor of 2 to 4 less than the Q-exponent of the diester. The flow curves for siloxane will show considerably less deviation from the Newtonian characteristic than the diester flow curve for the same shear stress. Typical flow curves for the siloxane and for the diester is plotted in Figure 12. The figure shows the much smaller loss of apparent viscosity for the siloxane, thus supporting the hypothesis of heat dissipation as an important mechanism in generating the deviating flow curves for the capillary 0 measurements.

Figures 13, 14, and 15 show the low shear behavior of the siloxane

Table 7. The Coefficient of Heat Conduction for Some Liquids

	k_t (lb_f/°F sec)
Clorofluorcarbon	.0087
Fluorinated polyether	.0117
Most hydrocarbon and methyl siloxane lubricants	.0150 to .0170
Methylalcohol	.024
Fluorsilicones	.034
Glycerin	.036
Water-Glycol mixtures	.05 to .06
Water 32°F	.073
Water 140°F	.082

Values from reference (38).

as a function of pressure at 100°F, 210°F and 300°F. The characteristics of Figure 13 are S-shaped and have inflection points at 20 - 60 kpsi This is similar to the shape of the characteristic of a 550 silicone oil reported in (2) as sample 53-H.

Figure 15 shows the considerably smaller slope of the characteristics as compared to the curves of Figure 11 - Diester. Table 16 gives the results of the measurements plotted in Figures 13, 14, and 15. These measurements were carried out before the modifications to the high pressure viscometer were made. A second series of measurements of the

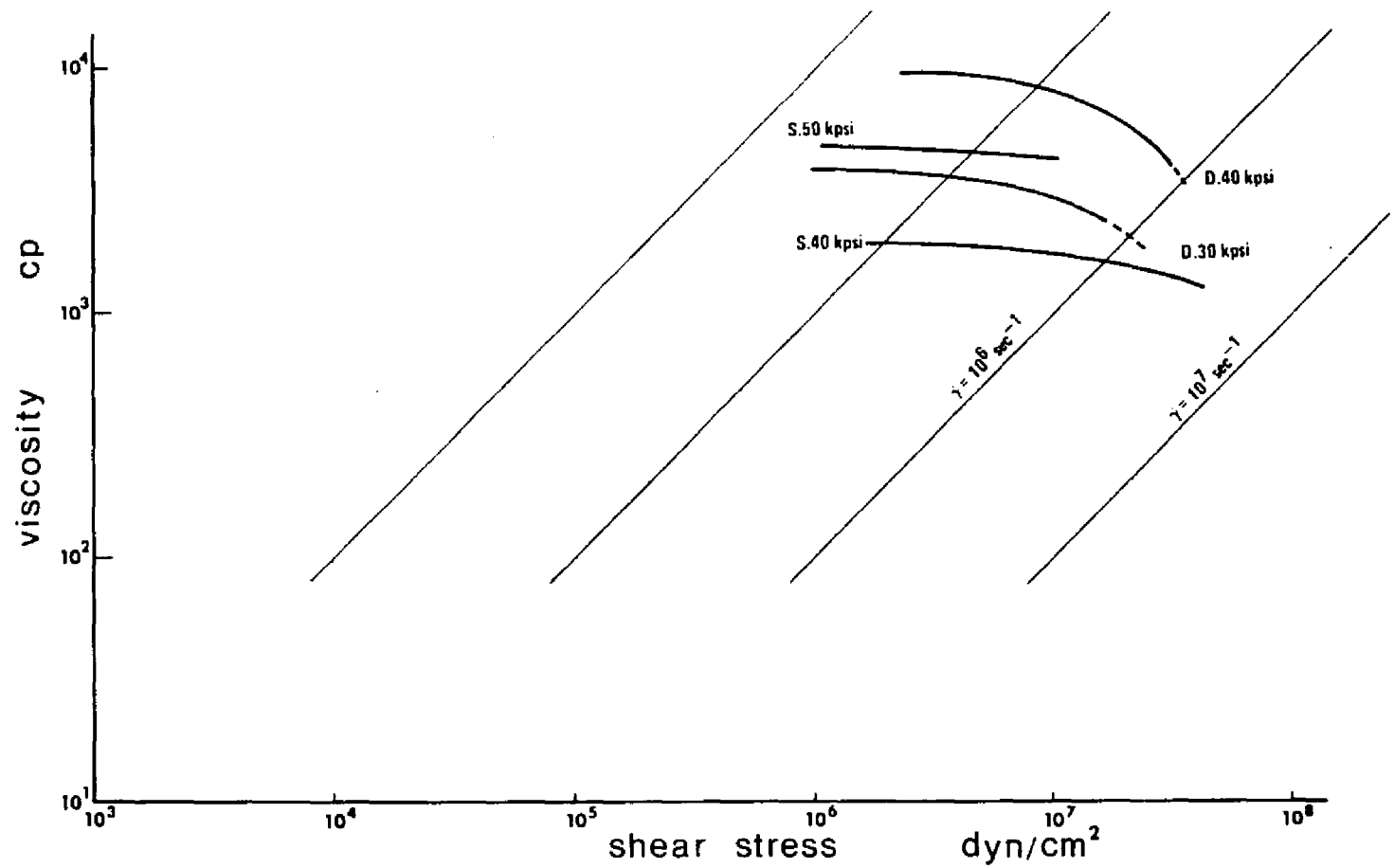

Figure 12. Typical Flow Curves for Siloxane (S) and Diester (D). (Deviation from Newtonian behavior is more pronounced for the diester, which has a greater Q-exponent, than for the Siloxane. Data from Figure 10 (Table 15) and Figure 18 (Table 17).)

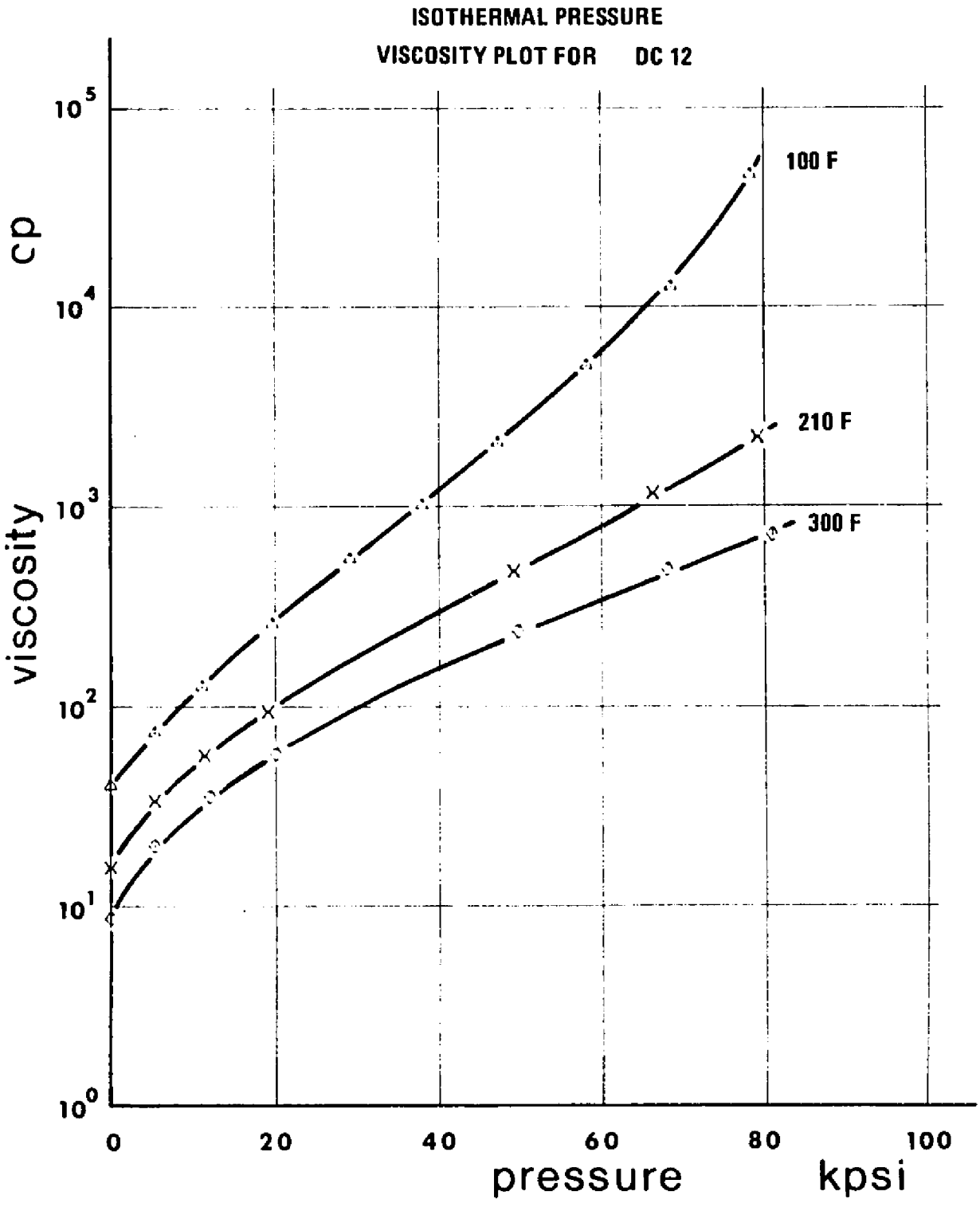

Figure 13. Low Shear Pressure Temperature Viscosity Characteristics for Dimethyl Siloxane DC-200-50 (DC-12). (Semilog representation.)

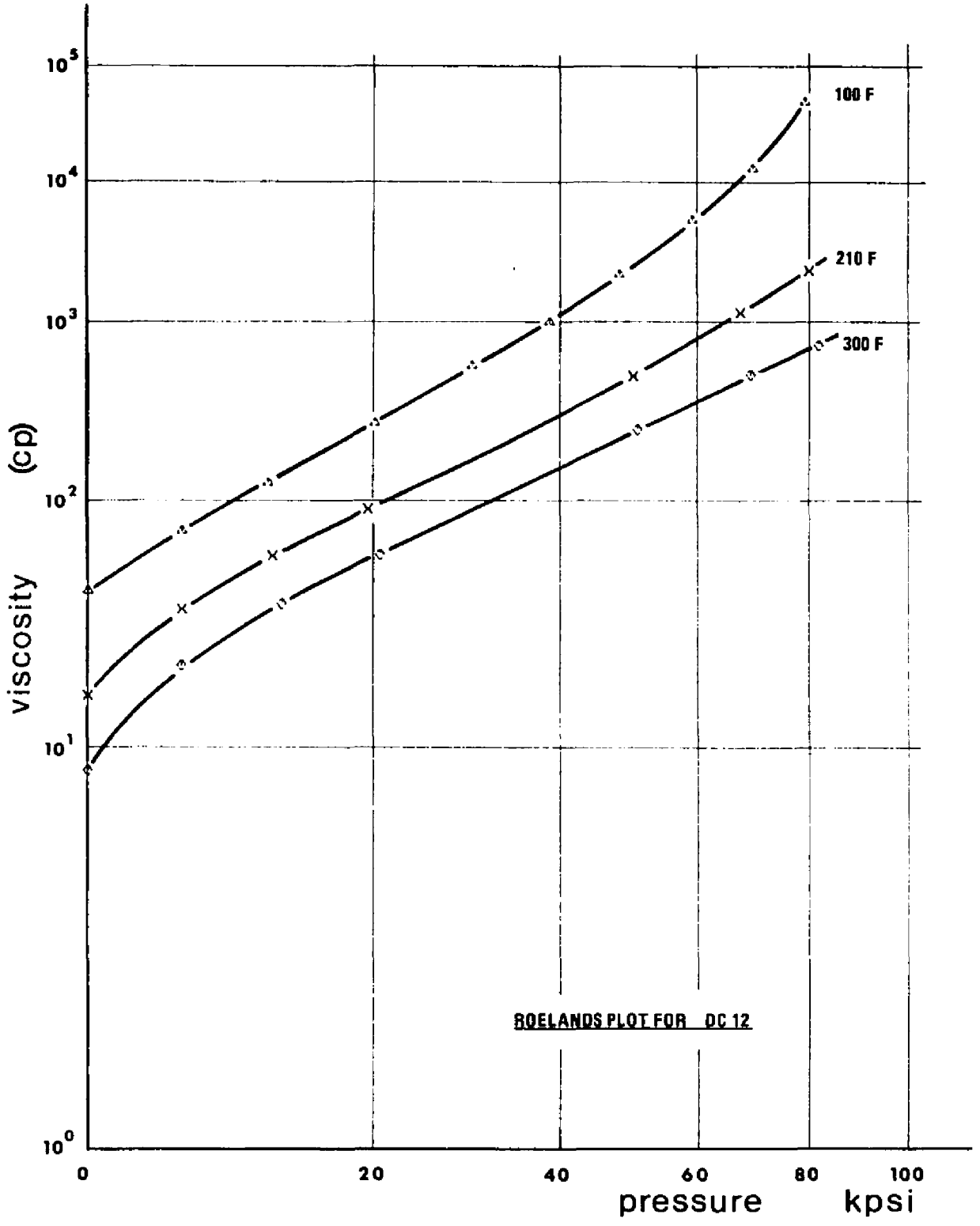

Figure 14. Low Shear Pressure Temperature Viscosity Characteristics for Dimethyl Siloxane DC-200-50. (DC-12.)

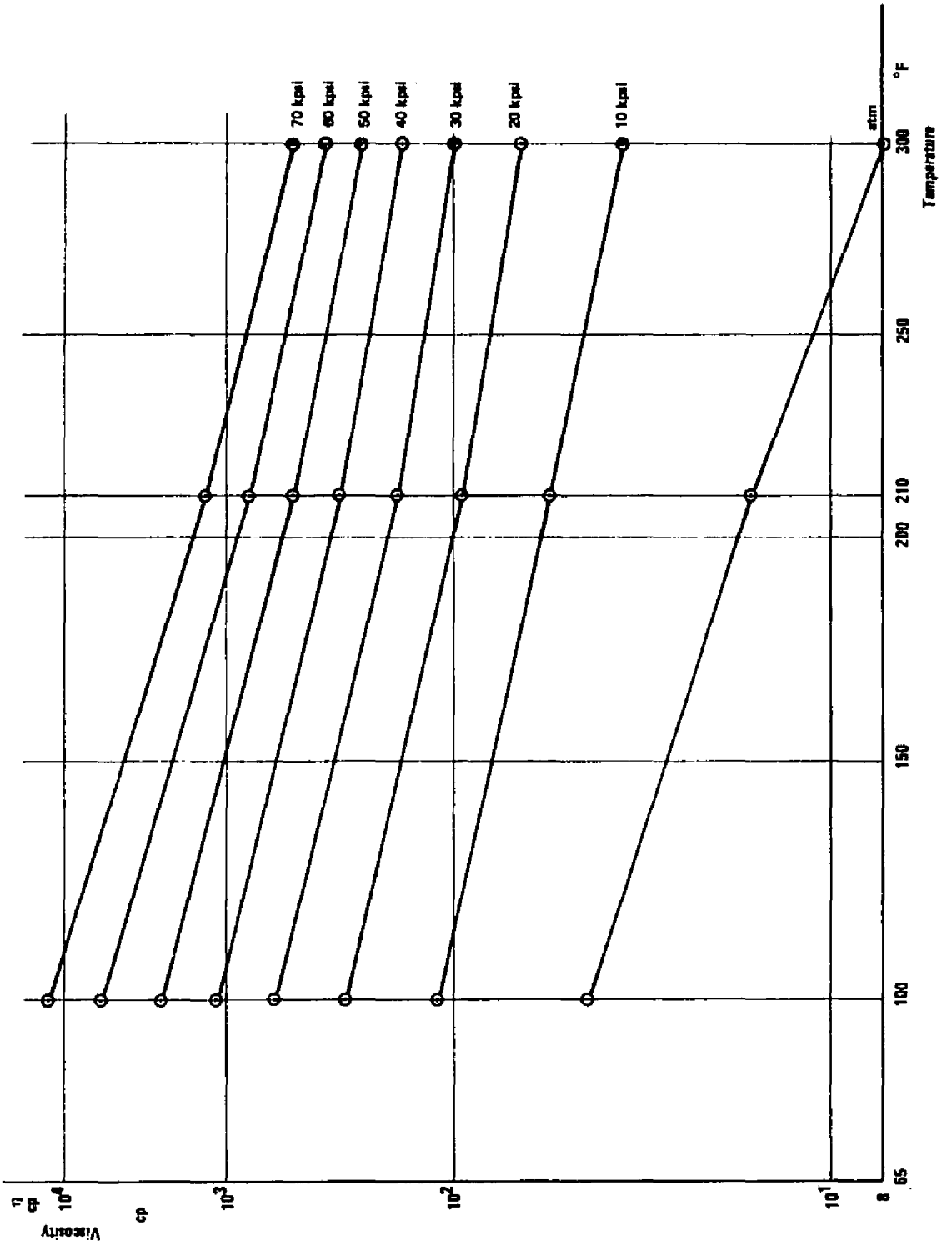

Figure 15. Low Shear Temperature Pressure Viscosity Characteristics for Dimethyl Siloxane DC-200-50. (DC-12).

siloxane were carried out at low temperatures 32°F, 75°F and 100°F after the modifications were performed. Figures 16 and 17 summarize these measurements. The same general characteristics of the siloxane were found in the low temperature range. The pressure viscosity curve at 32°F, Figure 16, is S-shaped; however, the inflection point is located as low as 15 kpsi. The temperature viscosity characteristics, Figure 17, at low temperatures are straight lines with slopes of the same magnitude as the slopes in the temperature range 100-210°F, Figure 15.

High shear stress measurements of the siloxane fluid were carried out at 75°F. The results are shown in Table 17 and Figure 18. The flow curves, Figure 18, for capillary 1 measurements also deviate downward from the curves of capillary 0 at the same shear stress of the same shear rate in the shear stress range covered by both capillaries. Therefore, shear thinning is not present for dimethyl siloxane for stresses up to at least 4×10^6 dyn/cm^2 (57 psi). This is shown by the flow curves at 30 kpsi where the overlap zone is more than a decade wide, $10^5 - 10^6$ dyn/cm^2, Figure 18. The flow curves for the siloxane fluid for both capillaries are seen to be similar in form. A translation along the viscosity axis will allow one flow to be superimposed on another curve. This indicates that dissipation heating is the cause of the observed deviation from Newtonian behavior for both capillary 1 and capillary 0 as was the case for the diester and suggests further that the range where shear thinning effects are absent can be extended to the highest stress reported in Figure 18, which is 4×10^7 dyn/cm^2 (570 psi).

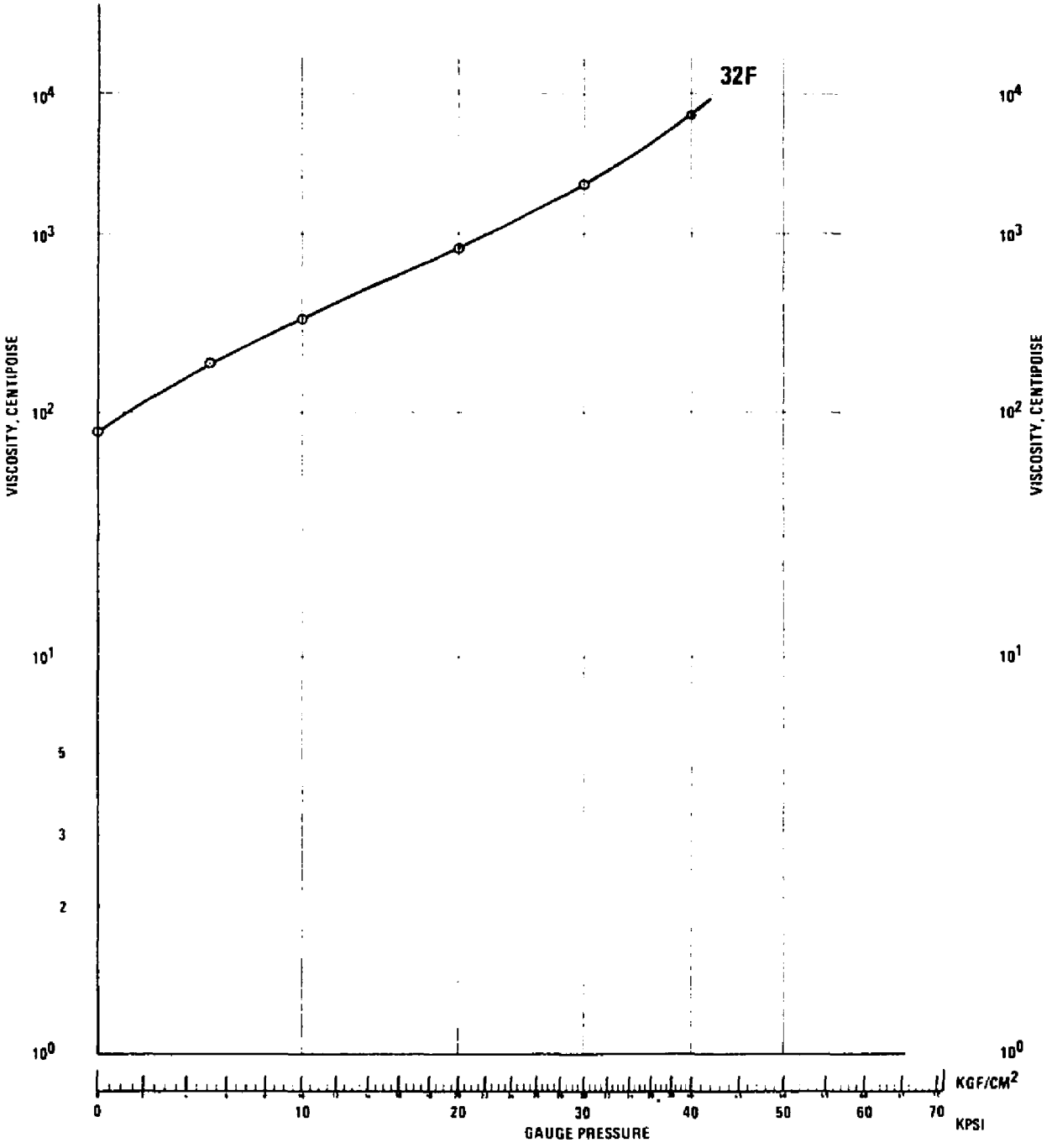

Figure 16. Low Shear Pressure Viscosity Characteristic of Dimethyl Siloxane DC-200-50, 32°F.

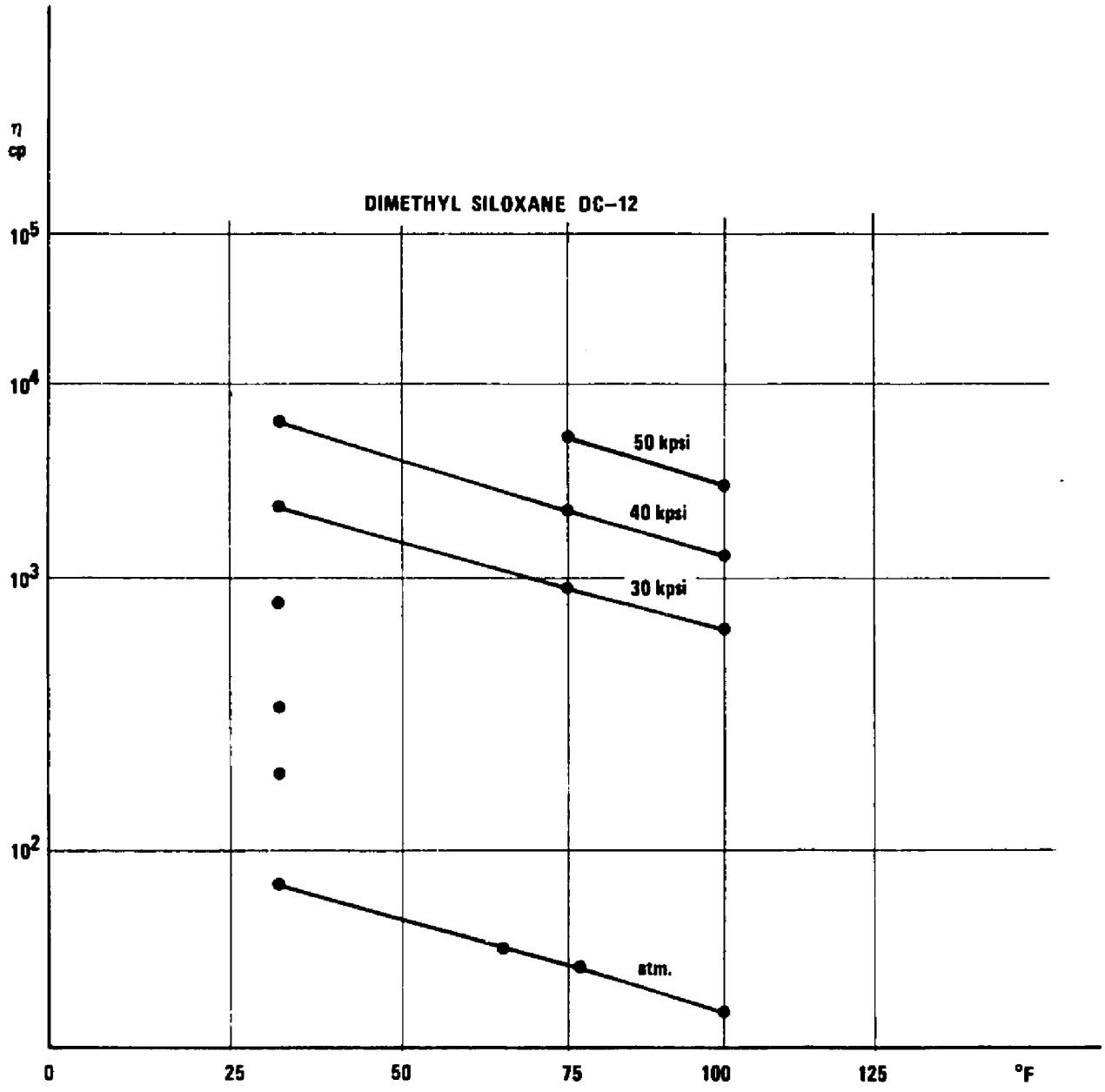

Figure 17. Low Shear Temperature Pressure Viscosity Characteristics of Dimethyl Siloxane DC-200-50 in the Range 32 - 100°F, (ASTM D 341-43).

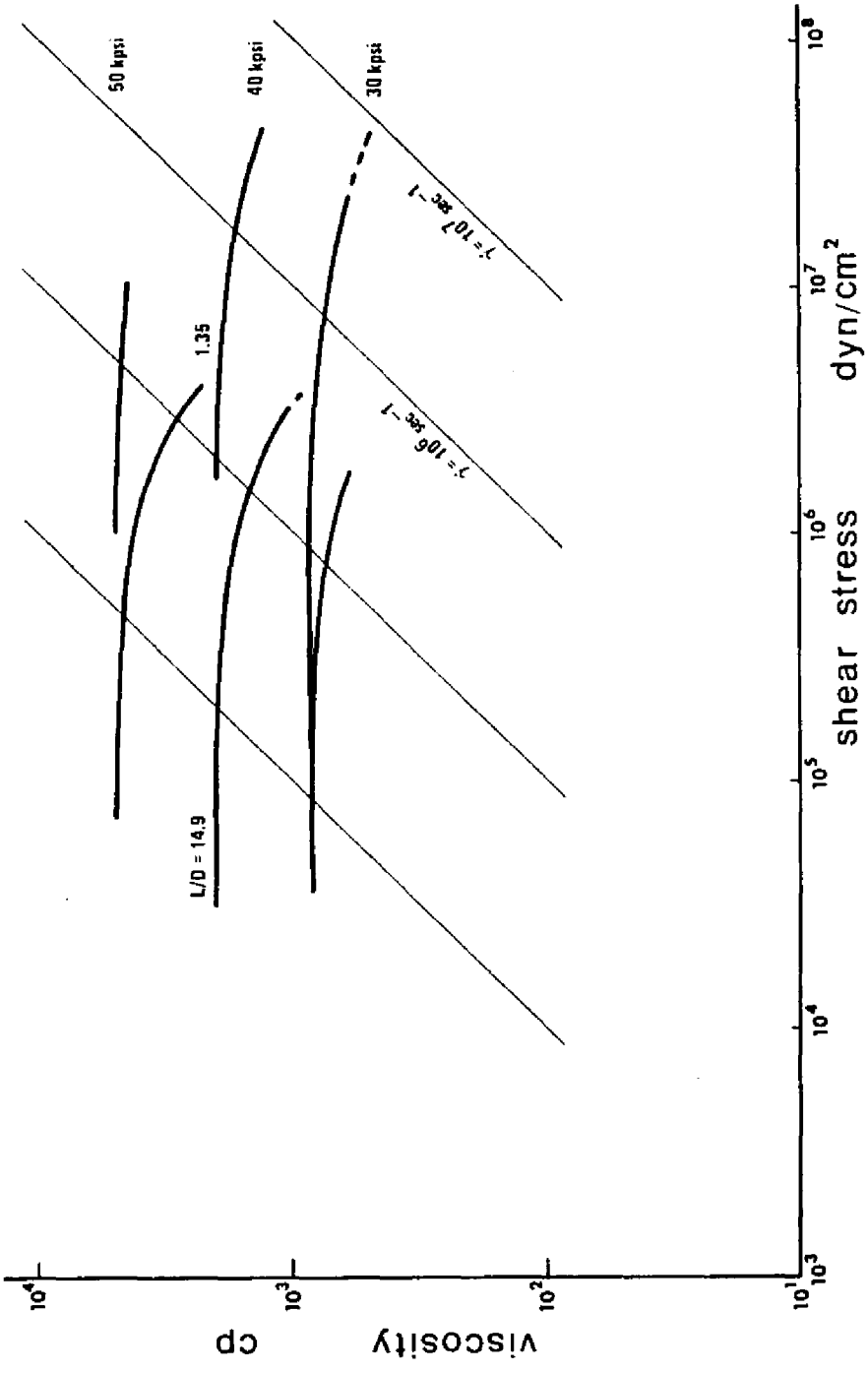

Figure 18. High Shear Measurements of Dimethyl Siloxane DC-200-50, T = 75°F.

Partial blockage of the capillary occurred occasionally during the high shear experiment with capillary 0. Figure 19 shows the results from measurements at 30 and 40 kpsi with such partially blocked capillary and tubing. The results are plotted with Figure 18 as the background. Table 18 gives the measured values. The plotted results are grouped in a meaningless pattern in terms of liquid behavior. All apparent viscosities are higher than what would be expected for liquid behavior. These higher values of apparent viscosities possibly indicate partial solidification of the siloxane.

The values of Table 18 show the chronologic order of the execution of the measurements. The results of the first measurements follow the previously measured flow curve for 40 kpsi - 75°F conditions. The applied shear stress was below 2×10^7 dyn/cm^2 (285 psi). The latter part of the 40 kpsi series yields meaningless results. Applied shear stresses were above 2×10^7 dyn/cm^2. High shear stress measurement was attempted at 50 kpsi with capillary 0 without giving meaningful results. This explains the missing high shear stress in Figure 12 of the flow curve for capillary 0 at 50 kpsi. The sapphire capillary, capillary 0, was taken out and inspected in the microscope after such experiments. No damage to the sapphire or its seals was ever observed.

The siloxane was investigated also at 32°F. Figure 20 and Table 19 contain the results. In order to investigate high shear stress behavior, only capillary 0 experiments were performed.

Measurements at 50 kpsi could not be carried out. A partial solidification was observed at 40 kpsi above shear stresses of about

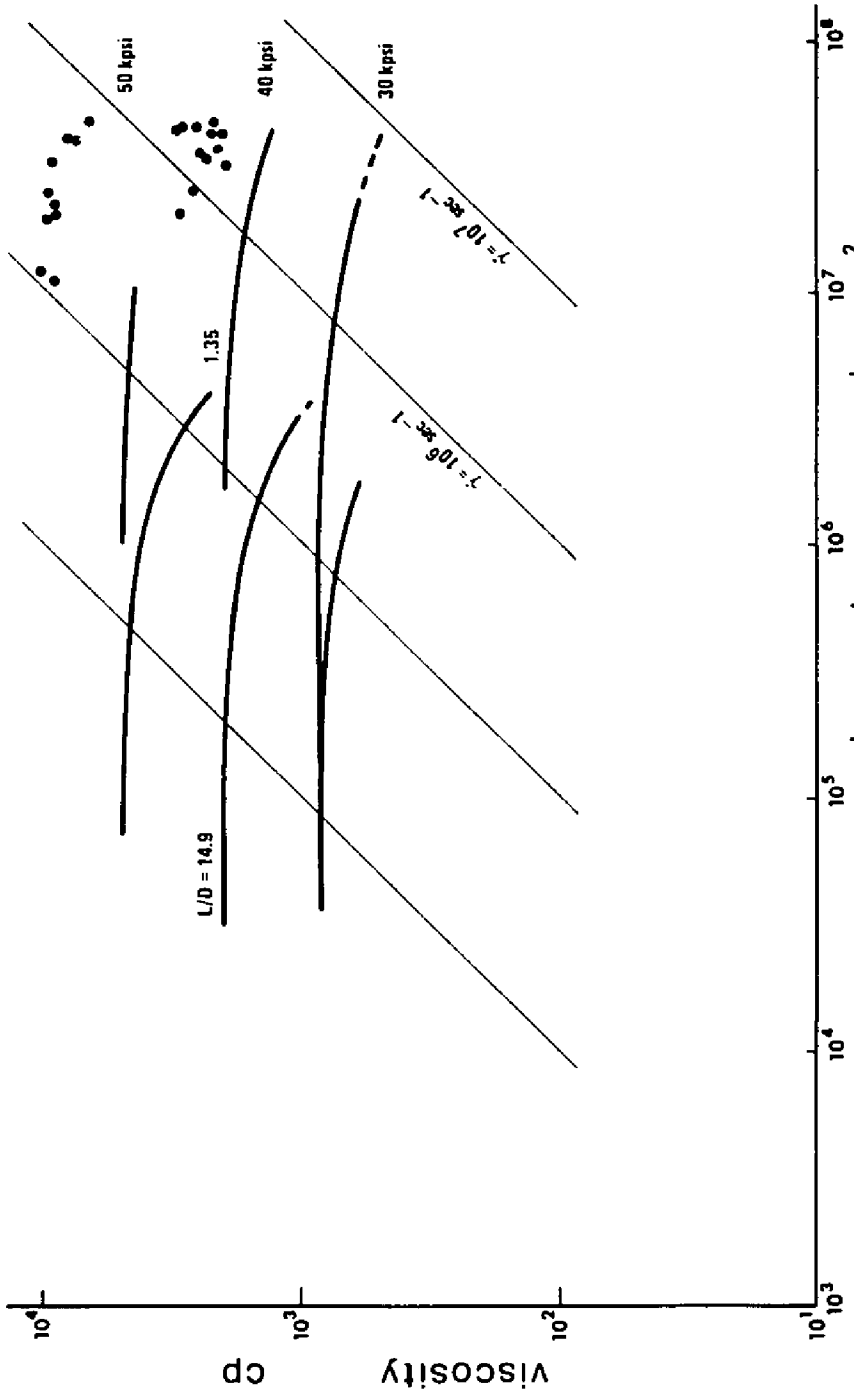

Figure 19. High Shear Measurements with Partially Blocked Capillary. (Dimethyl Siloxane DC-200-50. T = 75°F. The results are plotted with Figure 18 as the background.)

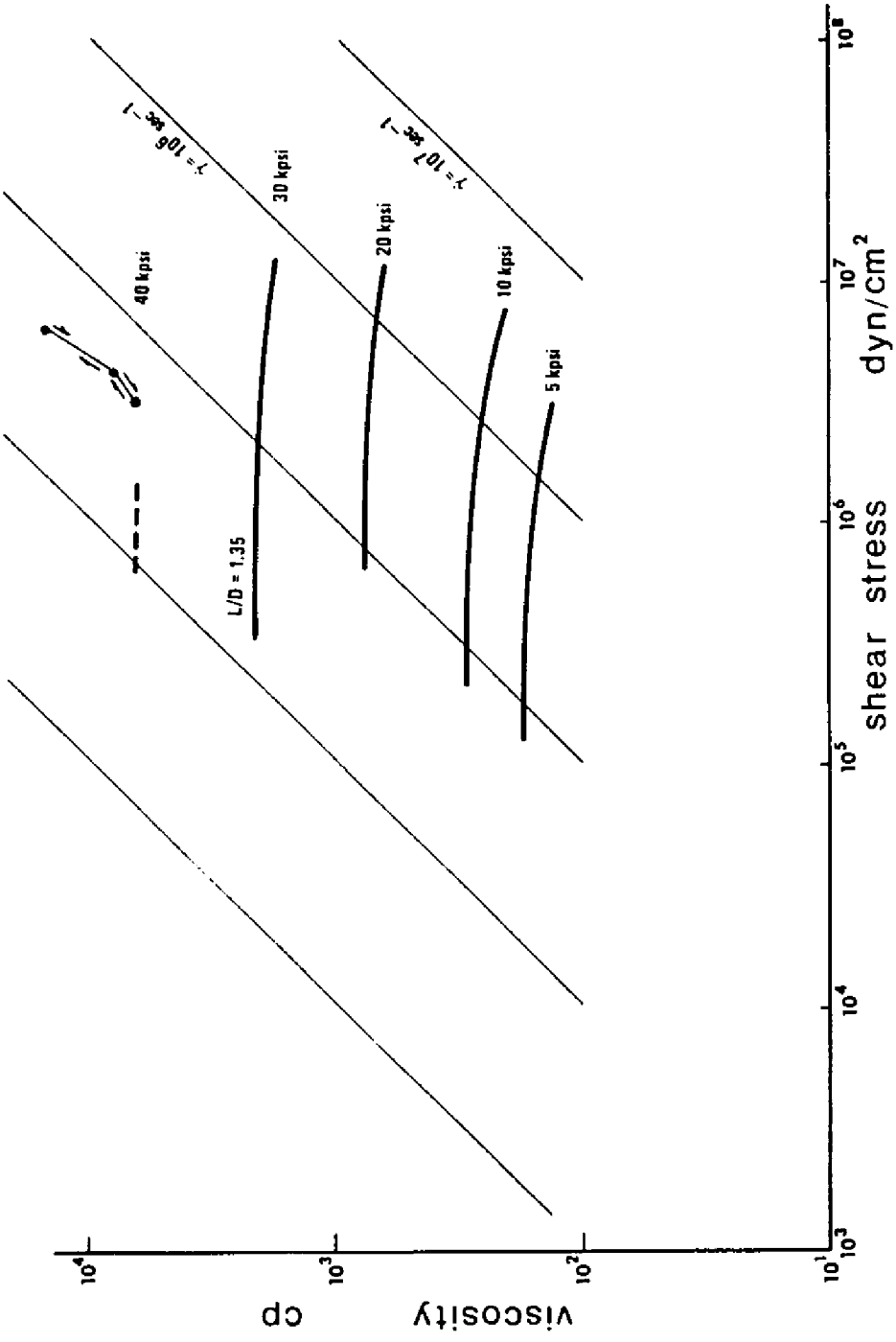

Figure 20. Non-Liquid Behavior of Siloxane at 40 kpsi, High Shear Measurements. (Apparent reversible behavior T = 32°F.)

3×10^6 dyn/cm^2 (43 psi). The siloxane seemed to be in a stable condition in that lower shear stresses applied after a high stress situation gave results consistent with earlier results within the same series, Table 19, 40 kpsi.

The flow curves of Figure 20 at 5 and 10 kpsi show greater deviation from the Newtonian characteristic than previously observed. This greater deviation is consistent with a slightly greater slope (greater Q) in the temperature region 32° - 75° as seen from Figure 17 compared with Figure 15.

The experiment was repeated under identical conditions as the previous measurements, 32°F capillary 0 only. The results are found in Figure 21 and Table 20. Non-liquid behavior was again observed at 40 kpsi and shear stresses above 3×10^6 dyn/cm^2. A gradual process toward complete solidification seemed to prevail, however. No definite explanation was found of this slightly altered behavior under otherwise identical conditions.

The siloxane was measured at 100°F with capillary 4 in order to establish a connection with low shear stress data previously measured. The results are plotted in Figure 22 from Table 21. The results of capillary 4 measurements were found to be of slightly larger magnitude than expected (Figure 17 and Figure 15). The reason for this deviation was not pursued further because the discrepancy was considered insignificant for the general conclusions of the work.

Several investigations were performed into the solidification of the siloxane. The more rugged capillary 1 was mounted in the system during these investigations. The temperatures were 75°F and 32°F.

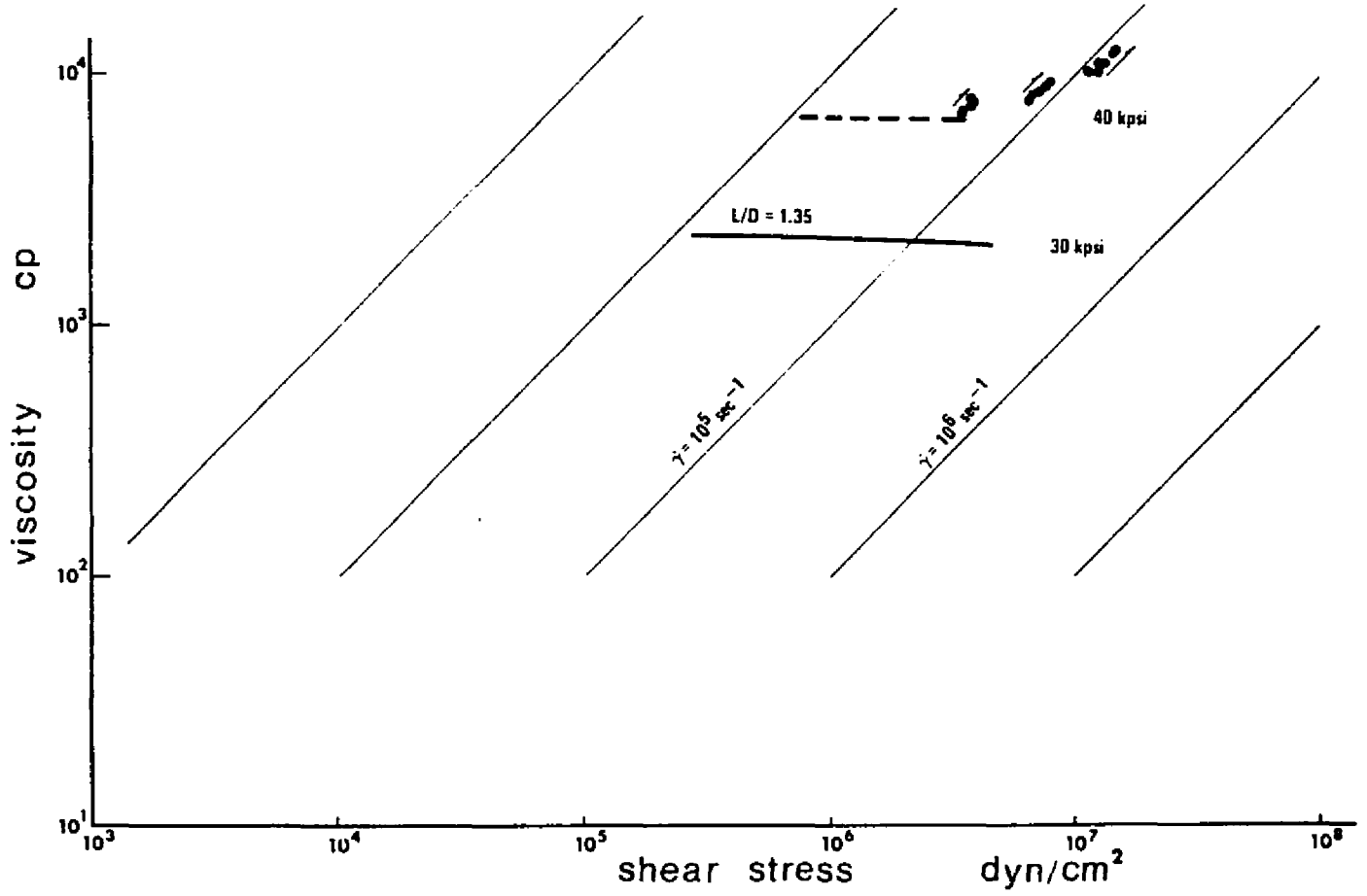

Figure 21. Non-Liquid Behavior of Siloxane at 40 kpsi, High Shear Measurements. (Apparent irreversible behavior T = 32°F.)

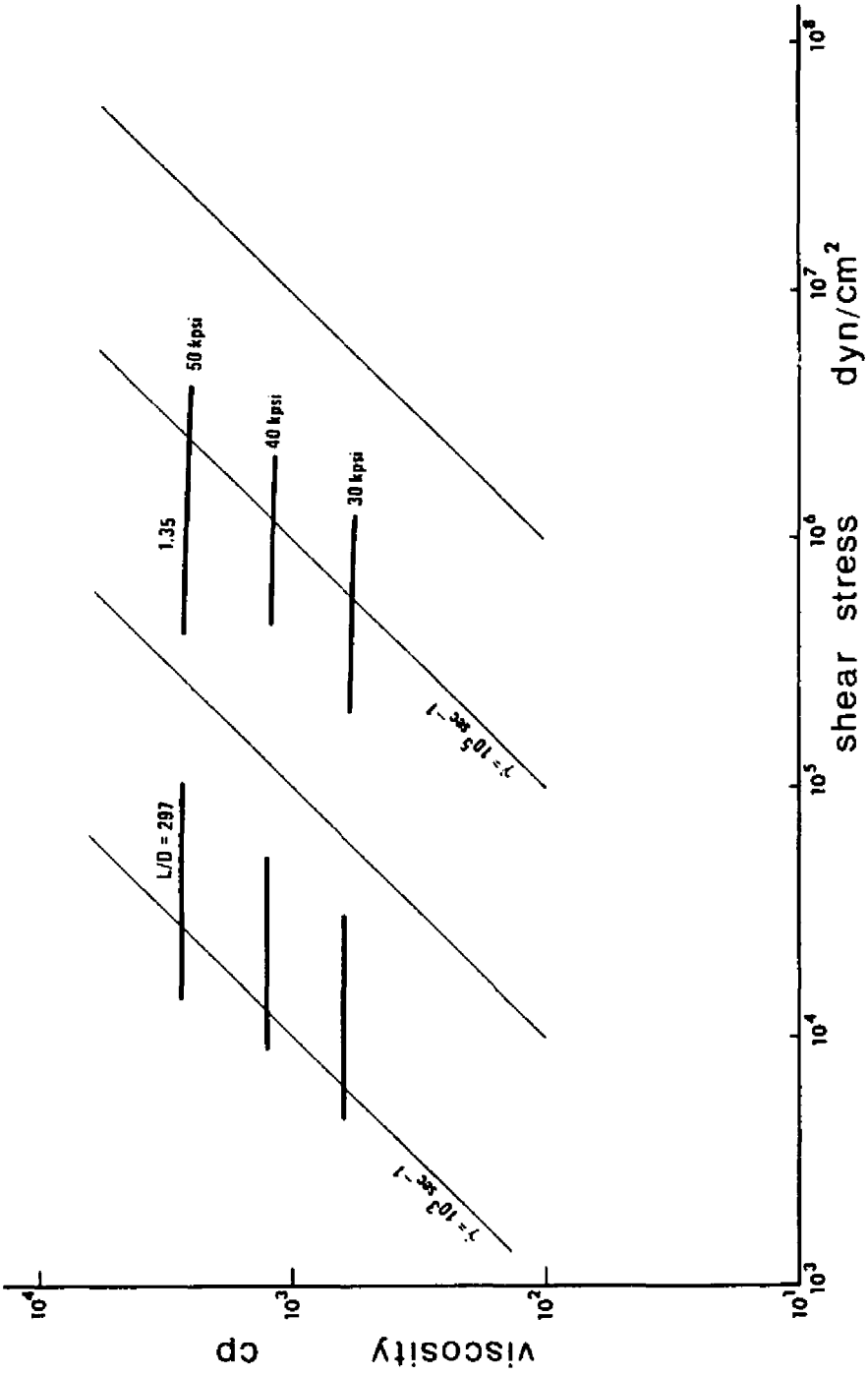

Figure 22. Low Shear Measurements (Capillary 4) and High Shear Measurements (Capillary 0) for Comparison with Previous Collected Data.

Pressure was increased in steps of 10 kpsi with a waiting period of several minutes between increments. Shear stress shocks were applied at each pressure level to provoke a possible solidification. Shear stress peaks are estimated to have of about 5×10^5 dyn/cm^2. Complete blockage of some of the tube of the test systems was observed at 60 kpsi for 75° and at 50 kpsi for 32°F. These observations were reproducible. A large hysteresis in reversal to complete liquid state was found. A return to the liquid state started first after the system pressure - in the still liquid branches - was lowered 25 to 35 kpsi below the blockage generating pressure. This return to the liquid state was accompanied by a slight volume increase observed as a slight pressure increase in the liquid branches. The observations of blockage pressures and the solidifications experienced at lower pressures and viscosities seem to justify a tentative viscosity - shear stress diagram (Figure 23) which predicts ranges where non-liquid behavior can be anticipated. These observations are interesting and may provide a key to a possible explanation for the anomalous behavior of some silicone oils in their ability to create an elastohydrodynamic lubrication film. Figure 23 is plotted with Figure 19 as background.

Polyalkyl Aromatic + Additive (DN 600 + Additive)

High shear stress measurements of the synthetic lubricant DN600 + Additive are found in Figure 24 and Table 22. The flow curves show Newtonian behavior at least up to 3×10^6 dyn/cm^2 (~44 psi). The general form of the flow curves suggests that Newtonian behavior persists up to the maximum employed stress of 4.2×10^7 dyn/cm^2 (610 psi). Partially non-liquid behavior was possibly encountered at 30 kpsi and certainly at 40 kpsi.

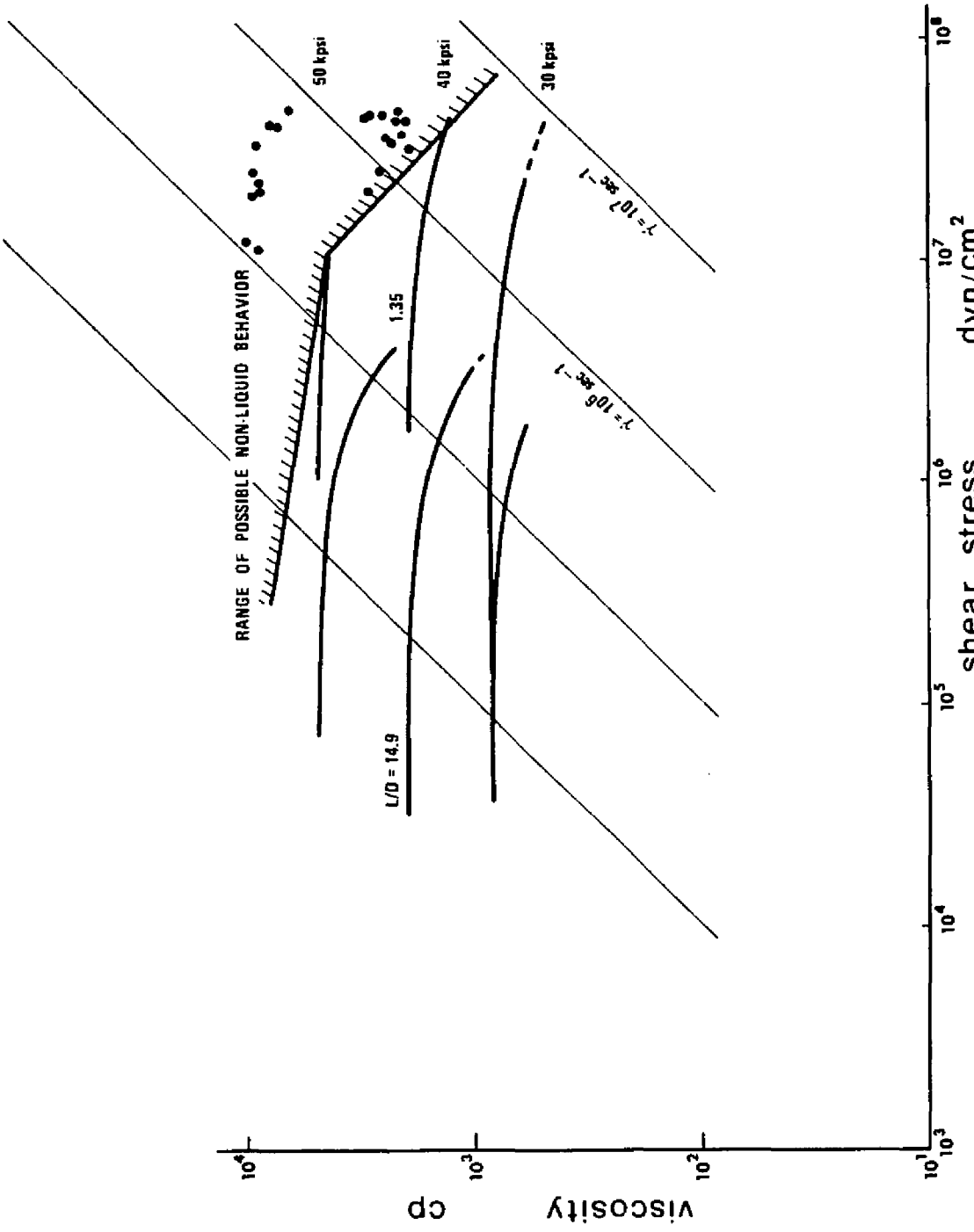

Figure 23. Range of Possible Non-liquid Behavior of Siloxane, 75°F. (This figure is plotted with Figure 19 as the background.)

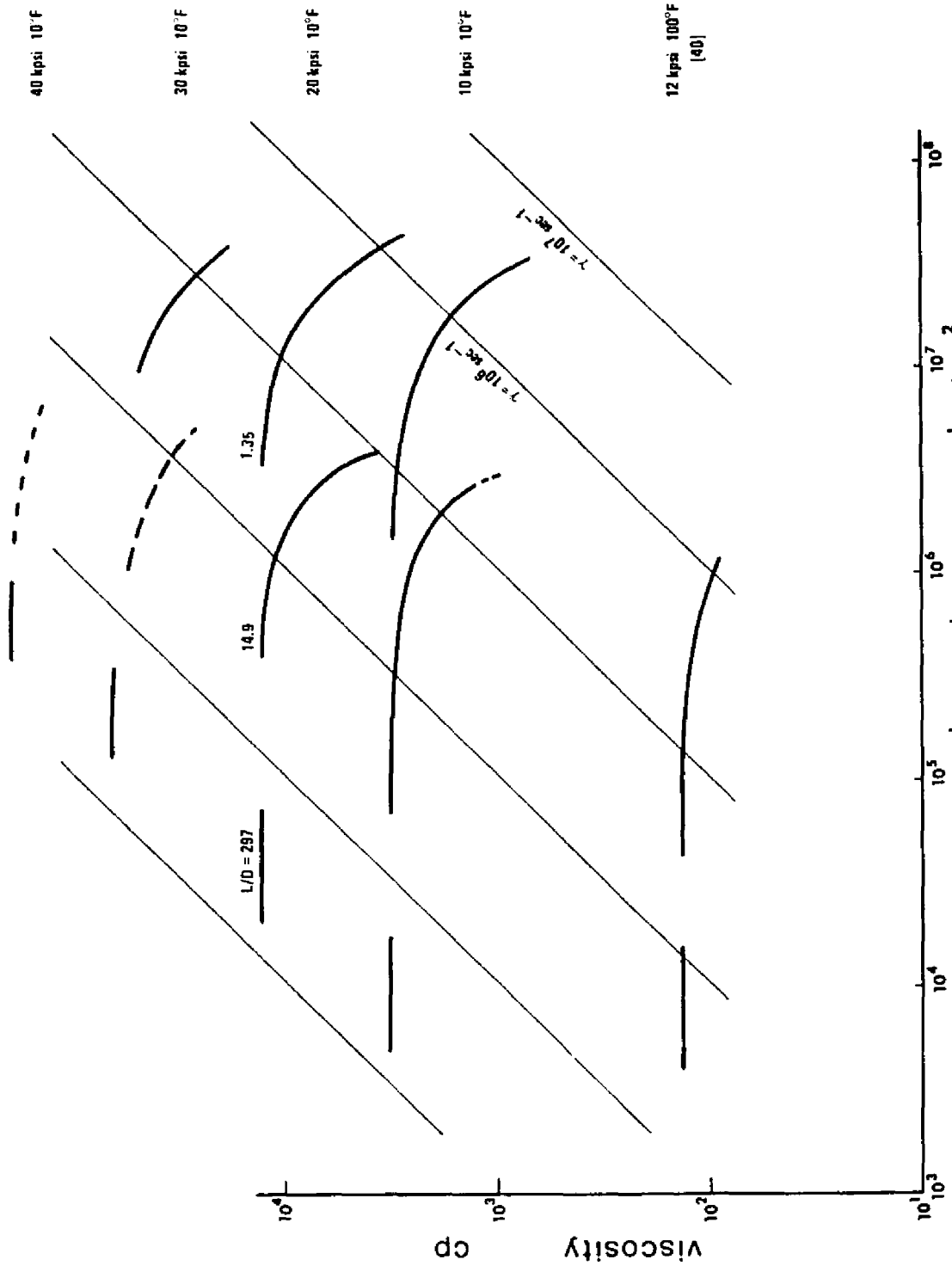

Figure 24. Flow Curves for Polyalkyl Aromatic + Additive (DN 600 + Additive). 10°F and 100°F.

The table values of capillary 1 at 20 kpsi show some scatter around 10^6 dyn/cm^2. These data were taken with a manual traverse of the viscometer. Difficulties in maintaining steady conditions at very low speed may explain the scatter. Some low speed data points created with the constant speed drive are found at 3 x 10^5, 6.6 x 10^5, and 9.6 x 10^5 dyn/cm^2. Scatter for these groups is very small.

Previous measurements of DN600 + Additive were carried out up to 1.65 x 10^5 cp. Conditions were 100 kpsi and 100°F. Non-liquid behavior was not experienced, presumably due to the higher temperature. The scatter at 1 - 2 x 10^5 cp (40 kpsi, 10°F) as reported in Table 22 may therefore be explained as a partial solidification caused by low temperatures but not necessarily due to high shear stress.

Synthetic Paraffinic Oils XRM 109 F4 and XRM 177 F4

The lubricants XRM 109 F4 and XRM 177 F4 are essentially the same, except that XRM 177 F4 is blended with an anti-wear additive. This additive is not expected to cause significant changes in the viscosity of the blend. The base lubricant in XRM 109 F4 and XRM 177 F4 is a synthetic paraffinic oil similar to Fluid D, the synthetic paraffinic oil reported in (39), (40) and to fluid XRM 109 reported in (41).

Figures 25, 26, 27, and 28 and Tables 23 and 24 show the low shear stress data. Viscosities at atmospheric pressure are equal for the two lubricants. The pressure viscosity relations at 100°F are also very nearly identical. There is a trend for XRM 109 F4 to show slightly higher viscosities than XRM 177 F4 at higher pressures and temperatures. The greatest deviation is found at 50 kpsi and 300°F. XRM 109 F4 has a viscosity which is about 8% higher than the corresponding viscosity of

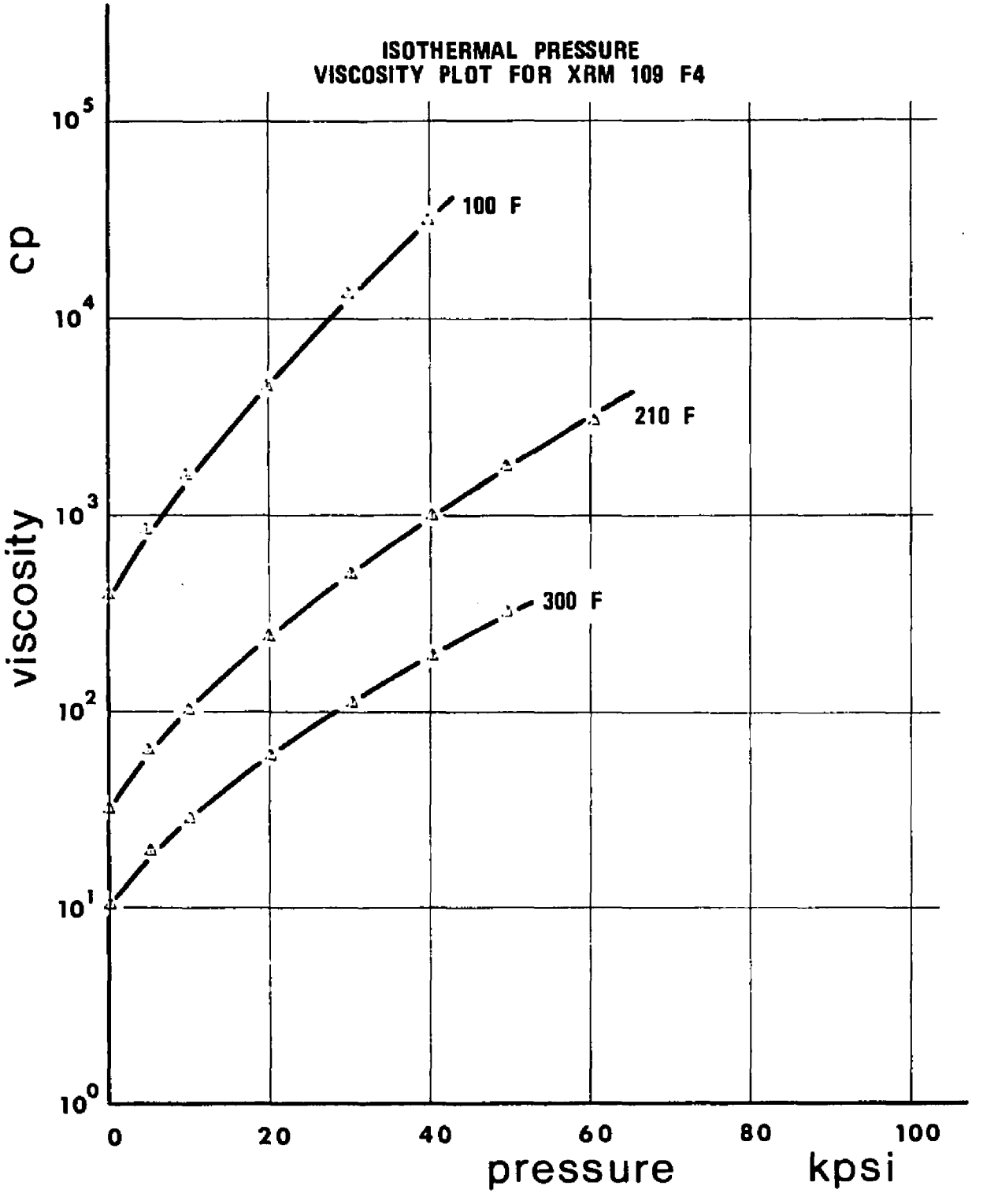

Figure 25. Isothermal Pressure Viscosity Plot for XRM 109 F4. (Semilog Presentation.)

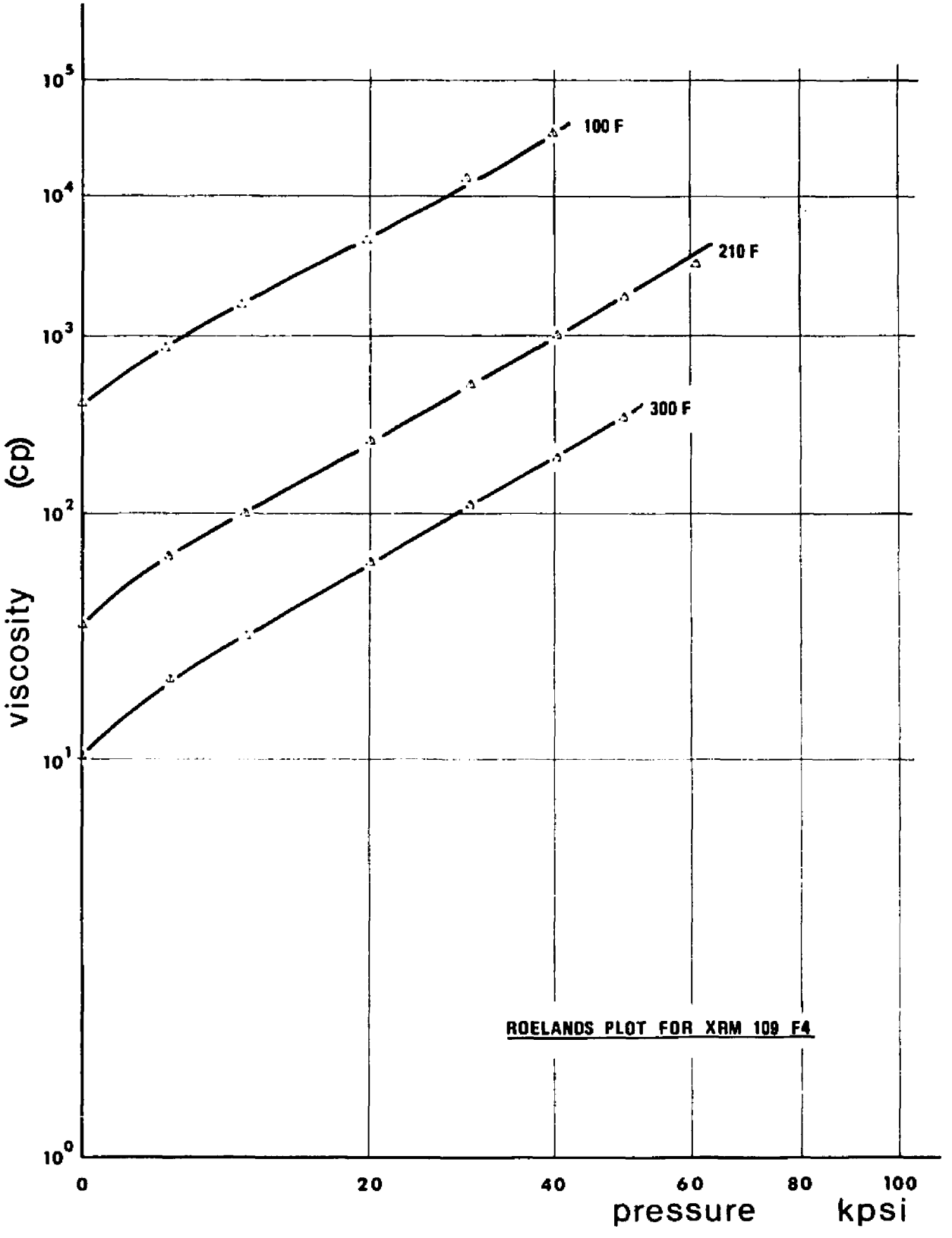

Figure 26. Roelands Plot for XRM 109 F4.

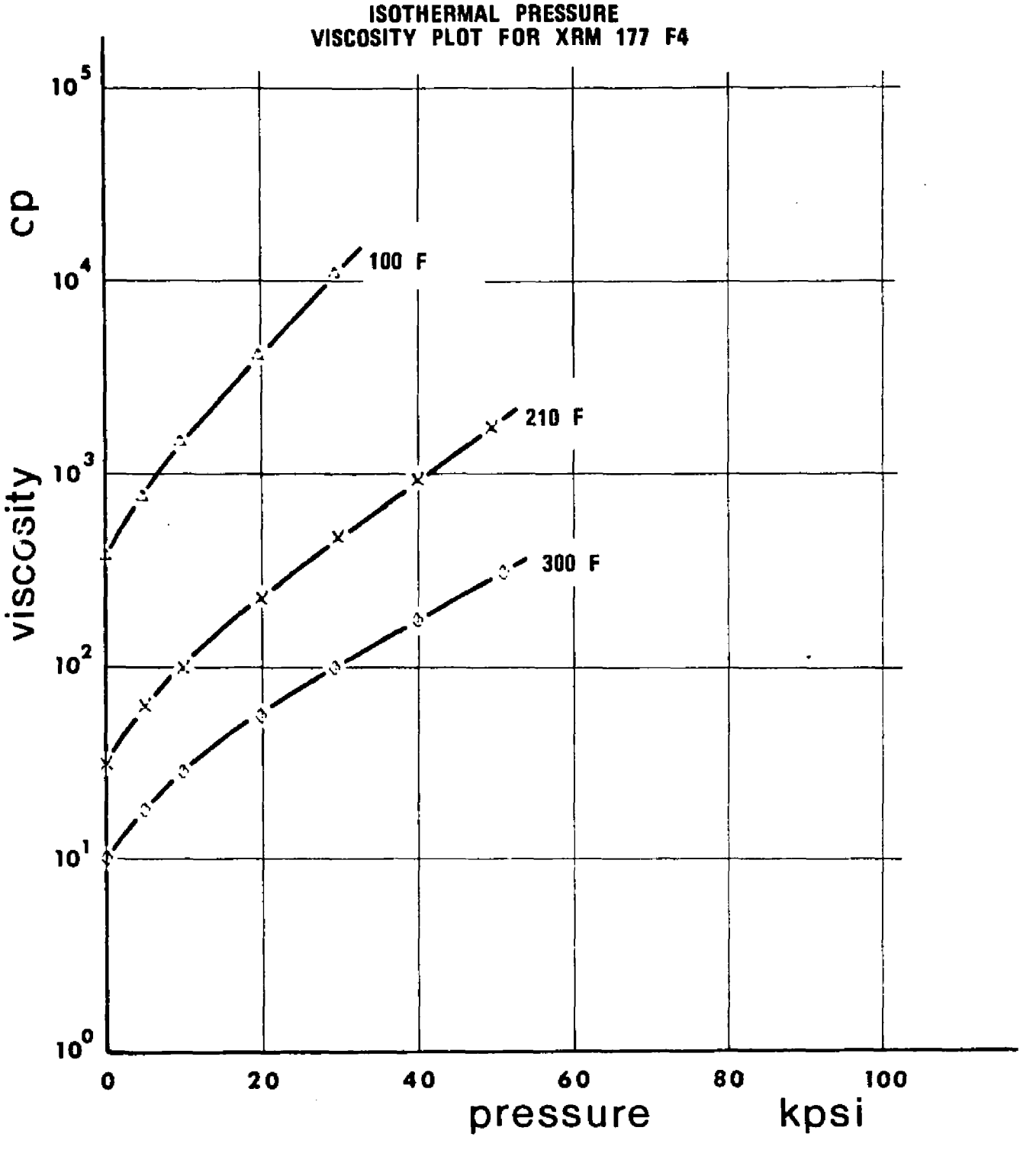

Figure 27. Isothermal Pressure Viscosity Plot for XRM 177 F4. (Semilog Presentation.)

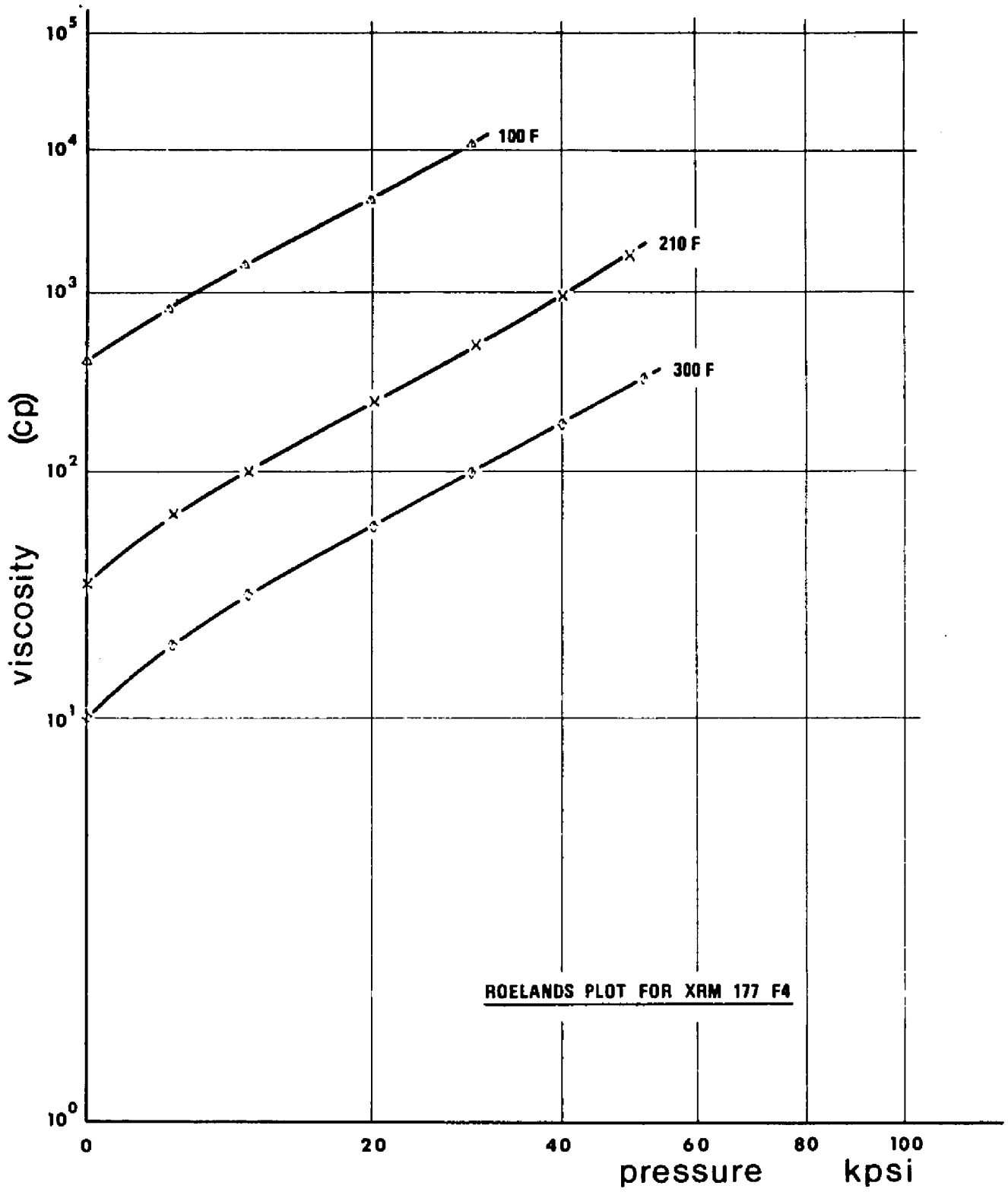

Figure 28. Roelands Plot for XRM 177 F4.

XRM 177 F4.

Figure 29 shows a pressure-viscosity plot of XRM 109 F4, XRM 177 F4 and Fluid D. The figure illustrates the difference between samples which are not from the same lot. The viscosity of Fluid D is consistently lower than the viscosities of the XRM fluids. The figure also shows the slightly increased viscosities for XRM 109 F4 compared with XRM 177 F4. The trend is particularly visible at 300°F. The anti-wear additive reduces the viscosity slightly compared with that of the base fluid.

Figure 30 and Table 25 show the high shear stress measurements of XRM 177 F4. The two fluids XRM 177 F4 and XRM 109 F4 were found previously during the low shear stress investigation to be very nearly identical. Shear stress investigations of XRM 109 F4 would expectedly not yield significant new information and were therefore not carried out.

Some of the flow curves for a capillary cover more than two decades of shear stress. The Newtonian parts of the curves are particularly far extended into the low shear region showing good agreement with measured low shear data. The overlap zone is more than a decade wide. The heating effect of the curves of capillary 1 is distinctly seen. The general form of the flow curves suggests that the apparent non-Newtonian behavior measured with capillary 0 is caused by heating alone. The highest shear stress measured was 4.78×10^7 dyn/cm^2 (695 psi).

The operating characteristic for the lubricant in an elastohydrodynamic contact is also shown in Figure 30. The vertical line is estimated working conditions for the lubricant at a load of 15 lbf at 54.8 in/sec sliding speed in a steel ball and sapphire disc contact. The position is in the center of the contact (Appendix G, Table 31 and Figure 54).

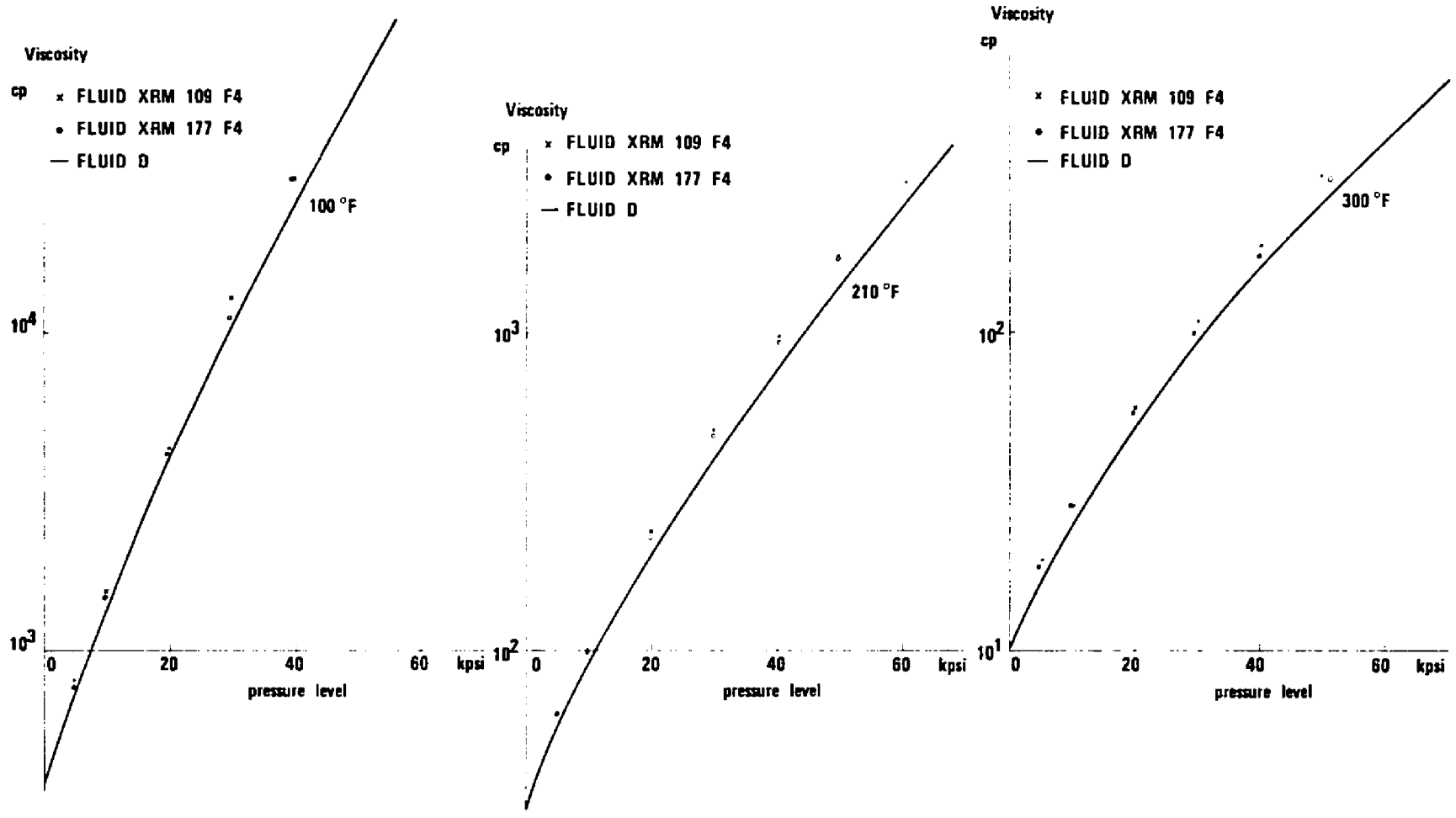

Figure 29. Isothermal Pressure Viscosity Plot of Fluid D, XRM 109 F4 and XRM 177 F4. (The effect of the antiwear additive, XRM 109 and XRM 177, and the difference in properties when the fluids are not from the same lot, fluid D and fluids XRM, are shown.)

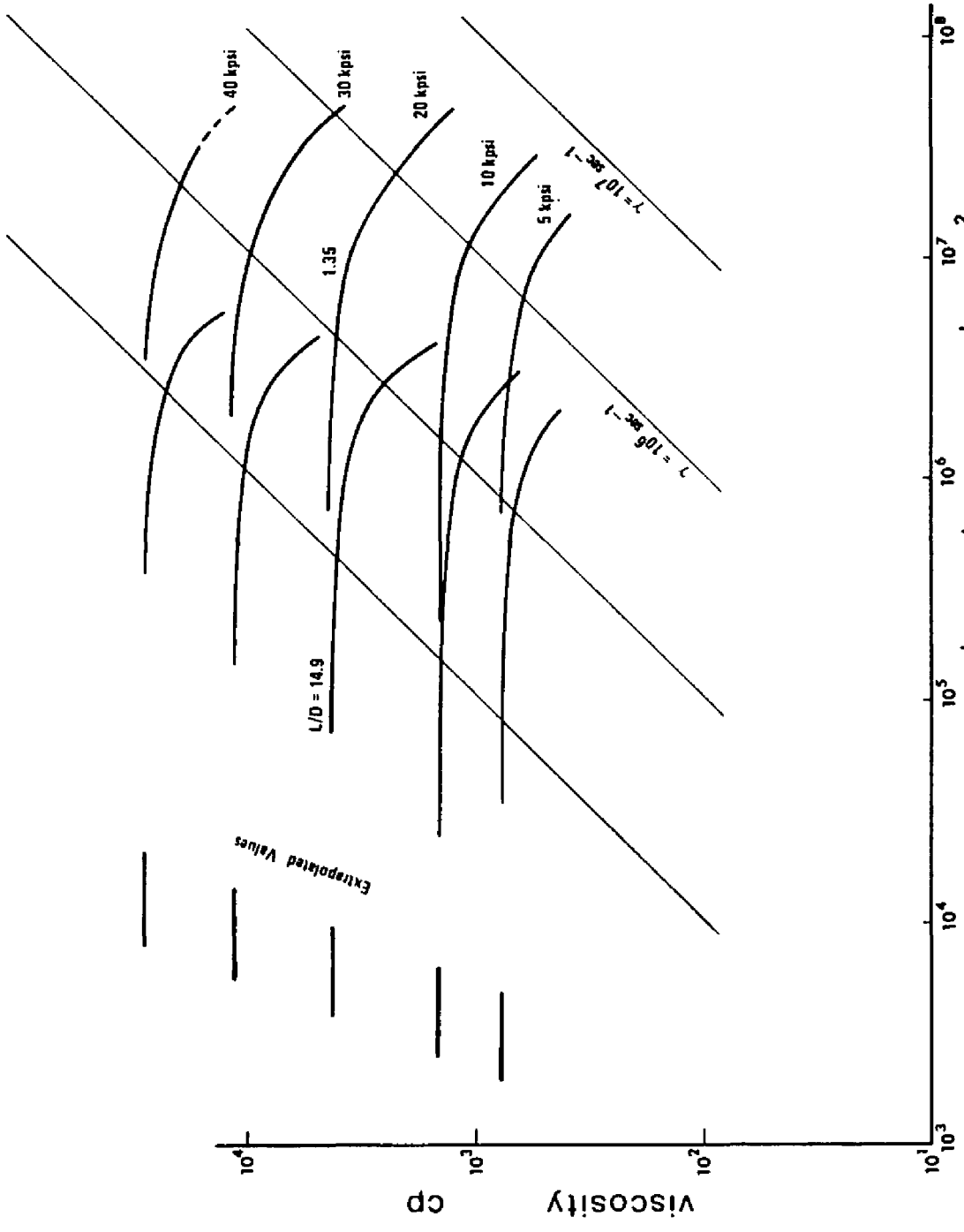

Figure 30. High Shear Measurements of XRM 177 F4, 100°F. (A maximum shear stress of about 700 psi is obtained. The figure shows the operational characteristic for the lubricant in an elastohydrodynamic contact with a maximum Hertzian pressure of 150 kpsi.)

Figure 30 shows clearly that capillary viscometry is not very far from the situation where elastohydrodynamic conditions for a lubricant can be created in a laboratory experiment in which the parameters of interest can be varied independently of each other.

An investigation of all the reported flow curves of the four lubricants has shown that all characteristics do fit to one general standard curve, regardless of the fluid type and for both capillary 1 and capillary 0 measurements. Deviations from this master curve are of the same magnitude as the experimental error. This observation of generality strongly indicates that the same mechanism is responsible for deviation from a Newtonian characteristic. Further work on the hypothesis of dissipation heating particularly with respect to the influence of the coefficients of temperature viscosity and heat conduction is reported in the following chapter.

B3J: Paraffinic Mineral Oil with 11.5% Polyalkylmethacrylate MW=.2 x 10^7

Polymer blended lubricants have long been used extensively in various engineering fields, particularly the automotive industry. High shear stress investigations of a polymer mixed lubricant are therefore of interest. It was decided to select a high molecular weight polymer in a relatively high concentration with a straight paraffinic mineral base oil for such an investigation.

The base oil as well as mixtures with a lower molecular weight polymer (MW - .56 x 10^6) have been investigated before (1), however, only up to about 10^6 dyn/cm^2. The base oil was then found to have completely Newtonian characteristics in the range investigated. The mixtures showed liquid response and some shear thinning effects.

The same base oil (R-620-12) was selected in this investigation. A polymer (Rohm and Haas PL 4523) with considerably greater molecular weight (MW ~ $.2 \times 10^7$) than used before, was used in order to produce extreme properties of the mixture. The polymer was delivered in solution with a paraffinic oil similar to the base oil. A viscosity increase of 20 times the base oil viscosity was desired. The appropriate percentage polymer, 11.5%, was predicted from (1). A blend with this concentration was prepared and mixed vigorously for 48 hours at room temperature. The mixing was carried out by bubbling dry, filtered air through the charge from the bottom of the container.

Table 26 shows the results of capillary 4 and capillary 1 measurements with this blend. Lack of expected consistancy of the data led to a suspicion of incomplete mixing. The viscometer was then purged. The remaining blend was agitated vigorously for another 24 hours at 160°F. Measurements with the more thoroughly mixed charge were carried out with all three capillaries at 100°F and at 5, 10, and 20 kpsi. Table 27 reports the results. It was found that the extra mixing operation did not improve the consistancy of the newly collected data. The contents of both Table 26 and Table 27 are, therefore, considered representative for the behavior of the mixture. Figure 31 summarizes the tabulated data.

It is seen from the figure that non-liquid response sets in for a relatively low magnitude of shear stress of about 3×10^5 dyn/cm^2 (4 psi). A pronounced directional effect is found for capillary 1 measurement at 20 kpsi. Apparent viscosities differ by a factor 2-3 for capillary 0 measurements at 10 kpsi and for the same shear stress or the

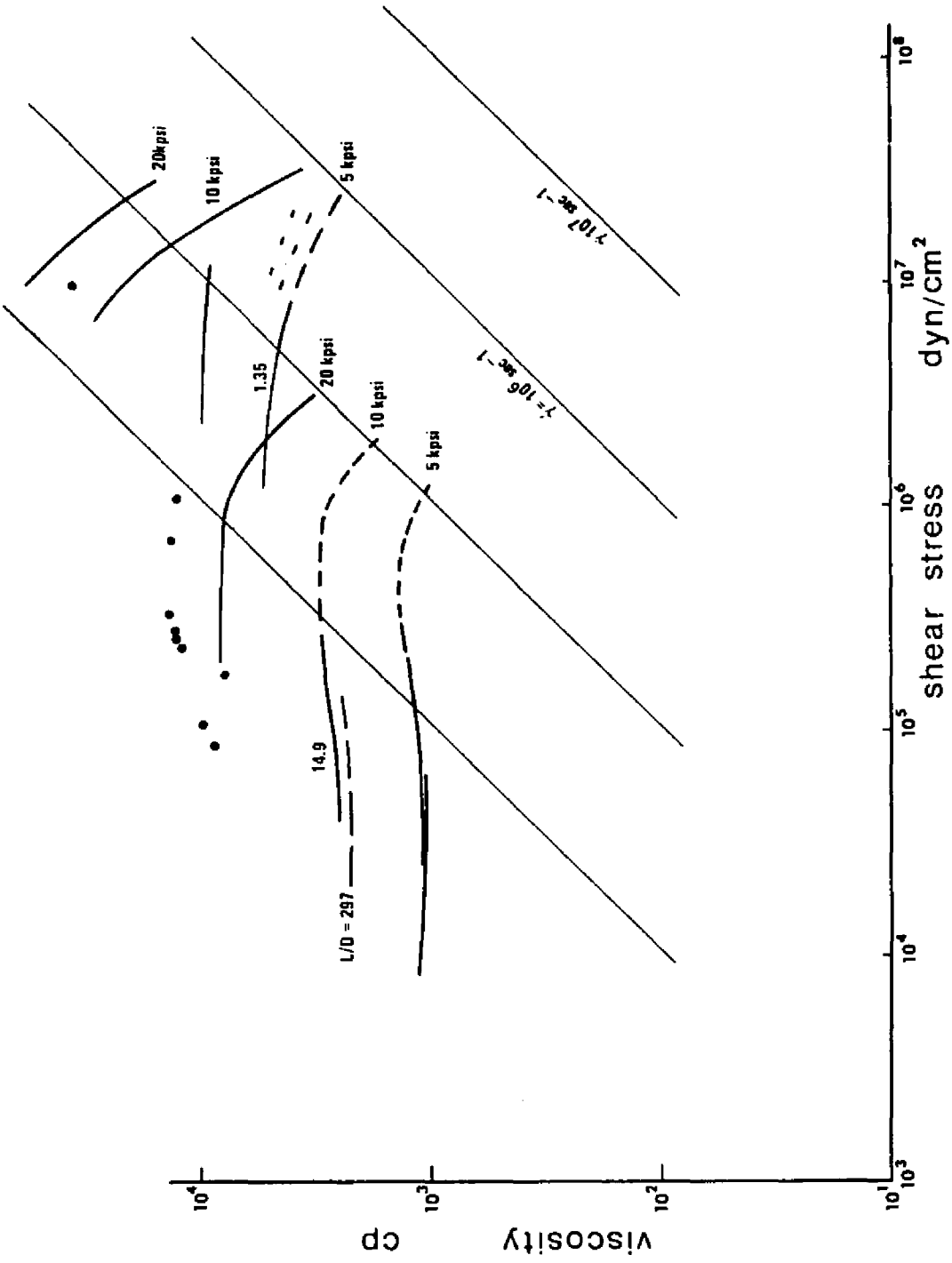

Figure 31. High Shear Measurements of Fluid B3J. (Paraffinic mineral oil with 11.5 per cent polyalkylmethacrylate ($\overline{MW} = 2 \times 10^6$).)

same shear rate. The method of generating the data was different, however. The 10 kpsi series at 2 x 10^6 dyn/cm^2 was produced with the constant speed unit. The 10 kpsi data from 7 x 10^6 to 3 x 10^7 dyn/cm^2 were produced manually.

The data from capillary 4 may be regarded as second Newtonian viscosities. A pronounced viscosity increase (~30%) occurs for increasing shear stresses before apparent non-liquid response sets in at about 3 x 10^5 dyn/cm^2. Such viscosity increases as well as the non-liquid behavior were not observed in previous measurements (1) in the same shear stress range. The concentration of polymer and the molecular weight were, however, significantly lower.

Figures 32 and 33 and Table 28 show the pressure temperature viscosity relations at shear stresses believed to correspond to the second Newtonian viscosities. The temperature pressure viscosity characteristics plotted on an ASTM D 341-43 chart show a pronounced curvature. Viscosities at atmospheric pressure (in Table 8) are estimated from an ASTM type rectifying chart. The viscosities at atmospheric pressure were measured with a Cannon Fenske Routine Glass Viscometer No. 400. The applied shear stress is about 60 dyn/cm^2 for ρ~0.85, whereas the lowest shear stresses reported in Tables 26, 27 and 28 are of order 10^4 dyn/cm^2. The measured viscosities at the very low level of shear stress were about 2.5 times greater than the viscosities at 10^4 dyn/cm^2. Table 8 summarizes these viscosities at atmospheric pressure. The tabular values are believed to represent the first Newtonian state (column 1) and the second Newtonian viscosity level (column 2).

Fluid B3J shows the expected shear thinning flow curve character-

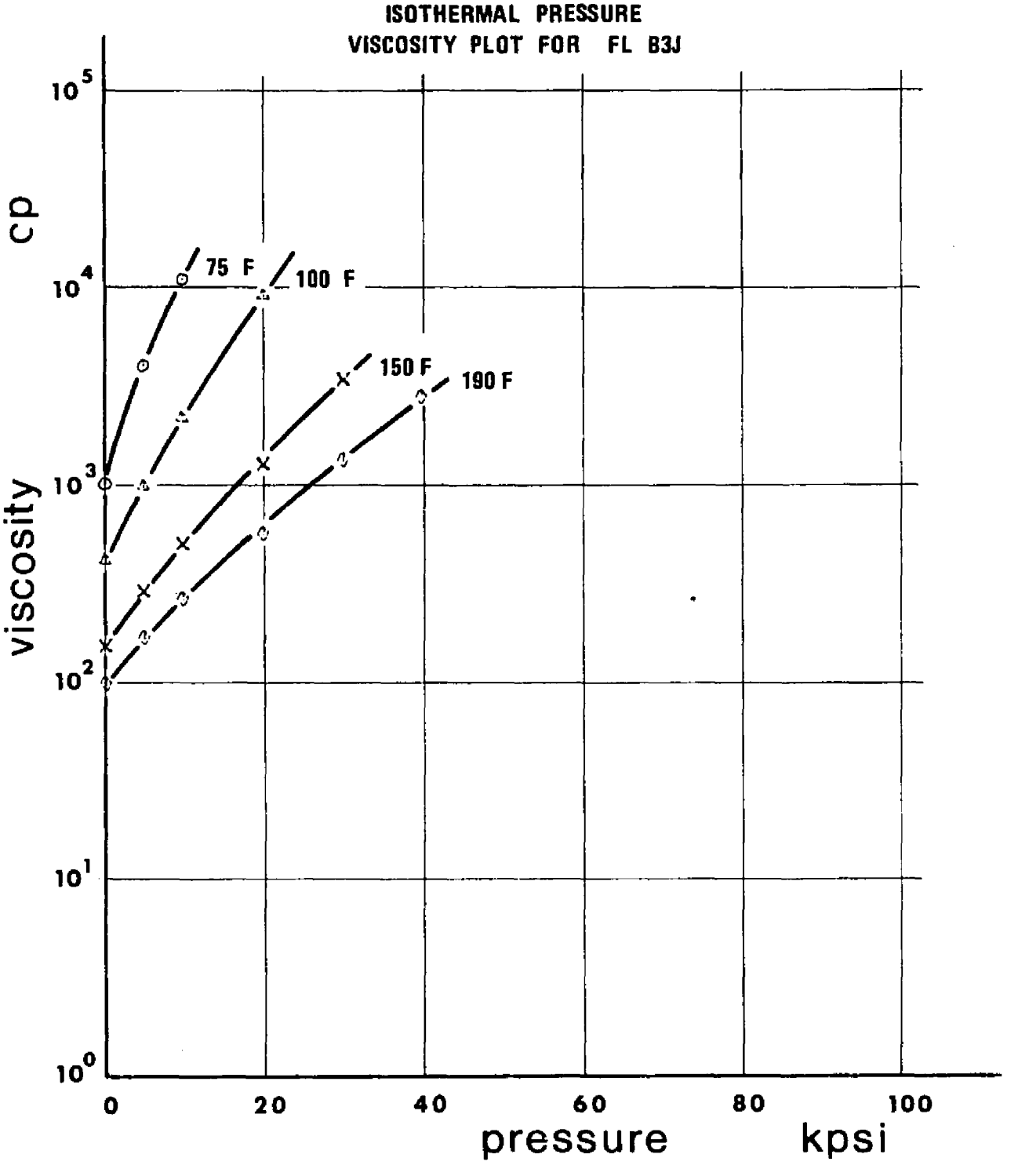

Figure 32. Isothermal Pressure Viscosity Plot for Fluid B3J. (Paraffinic mineral oil with 11.5 per cent polyalkylmethacrylate (MW = 2 x 10^6). Measurements with capillary 4. Semilog presentation.)

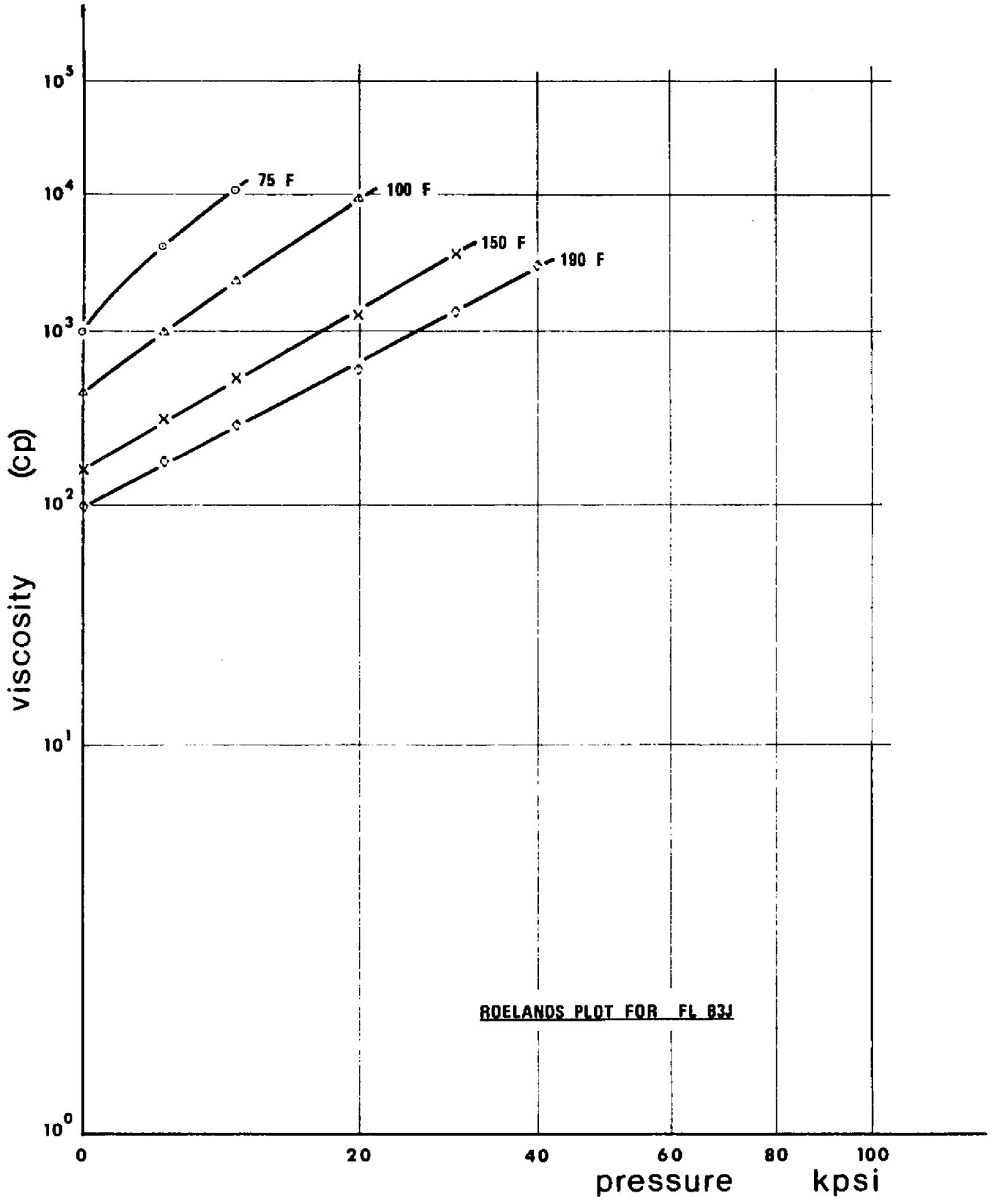

Figure 33. Roelands Plot for Fluid B3J. (Paraffinic mineral oil with 11.5 per cent polyalkylmethacrylate (MW = 2 x 10^6). Measurements with Capillary 4.)

Table 8. Paraffinic Mineral Oil with 11.5 Per cent Polyalkylmethacrylate MW = .2 x 10^7 Viscosities at Atmospheric Pressure

	1 ≃ 60 dyn/cm^2 Capillary No. 400	2 10^4 - 10^5 dyn/cm^2 Cap 4 + Cap 1 *
75°F	-	1000 cp
100°F	1010 cp	420 cp
150°F	384 cp	155 cp
190°F	221 cp	100 cp

*Table values are estimated from extrapolated characteristics on ASTM D 341-43 type charts.

ized by a first Newtonian viscosity η_1 at low shear stress (~10^2 dyn/cm^2) and a second Newtonian viscosity η_2 at a shear stress of about 10^4 dyn/cm^2. The ratio η_1/η_2 is approximately 2.5. The second Newtonian viscosity η_2 never approaches the viscosity η_b of the base liquid. The ratio η_2/η_b is of the order of 10. The second Newtonian viscosity level extends only to about 4 x 10^4 dyn/cm^2 where the apparent viscosity increases again. The increase in viscosity amounts to about 30%. Distinct non-liquid behavior appears shortly above 10^5 dyn/cm^2 (1.4 psi) and continues to the highest shear stress ~3.5 x 10^7 dyn/cm^2 (500 psi). It is significant that non-liquid behavior sets in at stresses (1.4 psi) which are more than 10^3 times smaller than the average shear stress in a moderately loaded elastohydrodynamic point or line contact. These shear stresses (~1.4 psi), where transition to non-liquid behavior appears for the

material B3J, are found far out in the inlet zone of an elastohydrodynamic contact. At this location, the pressures are low, film thicknesses are many times the centerline film thickness and temperatures are very nearly equal to ambient temperatures.

CHAPTER III

DISSIPATIVE HEATING EFFECTS IN CAPILLARY VISCOMETRY

Introduction

The flow of a fluid through a cylindrical capillary generates a temperature increase and a corresponding viscosity decrease in the fluid. This change of viscosity represents a possible source of error in the measurements.

The temperature increase is given by the ratio of the driving pressure drop to the specific heat capacity when the generated dissipation heat is uniformly distributed in the liquid and heat conduction is absent. The specific heat capacity of the liquid is the product of specific heat and density. These quantities are near the values .5 Btu/lbm^{o}F and .03 lbm/in^{3} respectively for many lubricants. The uniformly distributed temperature rise is of the order of 1°F per 140 psi pressure drop (5-6°C per 100 kp/cm^{2}), when the specific heat capacity for the fluid is .015 Btu/in^{3}^{o}F. The situation of uniformly distributed heat and no heat conduction from the liquid is seldom achieved in high shear stress capillary viscometry. The shear stress and the shear rate are both maxima at the wall. The temperature distribution immediately after the inlet is therefore characterized by increasing temperatures in the neighborhood of the wall and nearly unchanged temperatures at the center. The fluid temperatures at the wall remain low due to the relatively high heat conductivity of the wall material compared with the heat

conductivity of the fluid. The temperature distribution is thus an annular maximum a short distance from the wall and low temperatures at the wall and at the center of the capillary. These considerations assume that the liquid has a uniform temperature when it enters the inlet. The temperature distribution further downstream of the inlet is assumed to be a steady state configuration with maximum at the capillary axis.

The dissipation heating and other sources of uneven temperature distributions cause distortion of the measurements in capillary viscometry. The viscosity of the liquid decreases due to the temperatures at some locations which results in an overall increase in volume flow. The measurements will thus show an apparent decrease in viscosity and an apparent increase in shear rate for well defined pressure drop, or shear stress.

Review of Solutions

The problem of viscous dissipation heating is of importance for capillary viscometry and has attracted the attention of many investigators. Many of the contributions are achieved in entirely theoretical works. Some simplifying assumptions have been necessary in order to reach results. The assumption of a non-convective situation and the assumption of constant viscosity have been applied. Most of the previous works assume implicitly that other material parameters, density, heat conductivity, etc. are constant, that the flow is telescopic (tangential and radial velocity components are zero), that the pressure gradient is constant and that the temperature of the liquid is constant at the entry. Compression heating (expansion cooling) is in general not

discussed. The viscosity is often assumed to be dependent on temperature alone when viscosity is variable in the problem treatment. Only situations far downstream from the entry or situations immediately after the entry are discussed. The boundary conditions when r = R are typically the adiabatic or the isothermal walls. Schlichting 1951 (44) has shown that the steady state temperature distribution is described by a 4th order polynomial expression in h for laminar Couette flow between parallel plates. The corresponding solution for pipe flow is shown by Hersey 1936 (42) and Grigull 1955 (43) to be the same functional expression in r however with smaller constants. All three workers assumed constant viscosity and disregarded thermal expansion effects.

Hersey 1936 (42) derived an expression for the temperature distribution in the capillary assuming that the heat stays in the fluid volume where it was generated, which is equal to the situation where heat conduction is absent. He integrated the heat flux at the exit and found it consistent with the case of uniformly distributed heat in the efflux. An approximate expression was derived by Hersey 1936 (42) and Hersey and Zimmer 1937 (4) for the reduction in apparent viscosity due to heating effect in the capillary flow situation under adiabatic conditions.

Philippoff 1942 (6) developed equations and series expressions of the solution; he apparently deleted one term of the equations. He obtained temperature distributions and velocity profiles. Hausenblas 1950 (46) showed solutions to the capillary flow situation in terms of temperature and velocity profiles for variable viscosity but

at locations far downstream the inlet. His temperature viscosity function was $\eta = (k_o + k_1 T)^{-1}$. The temperature profiles obtained are similar to the fourth order profiles obtained with constant viscosity, Schlichting 1951 (44), Hersey 1936 (42) and Grigull 1955 (43). His velocity profiles show significant deviations from the parabolic velocity profiles of the constant viscosity case. The velocity at the axis increases relatively much more than the velocities near the wall, apparently because the viscosity is higher near the wall. The velocity profiles becomes more slender with pronounced maximum at the center and an inflection point at about half radius when the pressure drop increases. The shear rate at the wall is thus a weak function of the pressure drop which suggests a maximum of the volume flow at some pressure gradient. This point was later discussed briefly by Kearsley 1962 (52). Brinkman 1951 (47) gave the solution for the flow immediately downstream of the inlet however for constant viscosity. He incorporated convection in axial direction and assumed that the pressure gradient was constant. His solution shows the annular temperature profiles with the peak increasing in the flow direction and moving to the center at locations downstream from the inlet. Grigull 1955 (43) reported solutions for the temperature profiles both near the inlet and far downstream. He incorporated axial convection but the solutions are based on parabolic velocity profiles and constant viscosity. The closed form expression for the solution was obtained by assuming that the temperature is a linear combination of the axial coordinate itself and an arbitrary function of the radius coordinate. The solution does not in general satisfy the initial condition $T = 0$ at the inlet.

Millsaps and Pohlhausen 1953 (48) gave thermal solutions for steady laminar flow between non-parallel plane walls with small opening angles. Analytic solutions exist for this flow situation of the velocity profiles when the viscosity is assumed to be constant. The known velocity solutions are used in the energy equation. The temperature profiles are reported in the form of a dimensionless function G which contains the viscosity. G is a function of angular position in the wedge. The solutions represent steady conditions far from the inlet. The work is of interest for flow through slender conical diameter reduction tubes anticipating an analogy similar to the analogy of temperature and velocity profiles for flow between plane parallel walls and flow in cylindrical capillaries, Hersey 1936 (42), Grigull 1950 (43), and Schlichting 1951 (44), or Hausenblas 1950 (46). The thermal profiles reported by Millsaps and Pohlhausen for converging flow are remarkably alike in the investigated Reynolds number range from about 1 to 5000. The annular thermal peaks stay consistently near the wall in contradiction to the behavior in the cylindrical capillary where the peaks move to the center position in equilibrium. The profiles in a diverging section show significantly different behavior than the profiles in a convergent section. The analytic solution for the diverging section shows strong oscillations with negative values of the thermal function G over significant angular distance even for the lowest Reynolds number. This suggests thermal instabilities. Similar analytic solutions do not apparently exist for velocity and temperature profiles for flow through axisymmetric sections.

Toor 1956 (49), 1957 (50) treated the case of flow of a compressible non-Newtonian power law liquid. He showed that the temperature at the center of the capillary initially will decrease due to expansion cooling. The resulting temperature and velocity profiles are similar to the profiles in the Newtonian case. Gee and Lyon 1957 (51) reported solutions to the same problem formulation however with a semi empirical stress strain relationship that fits the behavior of plastic melts. The isothermal wall case was treated. The wall temperature was a parameter. The obtained temperature and velocity profiles are similar in character to the solutions of Grigull, Brinkman and Hausenblas, and later of Kearsley, when the wall temperature is lower than the initial melt temperature. The temperature profiles become highly distorted from the parabolic profiles when the melt and the wall have about the same temperature but show only relatively small deviations from an average temperature equal to the wall temperature.

Kearsley 1962 (52) gave closed form solutions for temperatures and velocities when the viscosity is an exponential function of temperature. The location is far from the inlet. A conclusion from the results is that there exists an upper limiting pressure gradient for the flow situation and a corresponding upper volume flow rate. The velocity profiles deviate from the profiles of the case of constant viscosity. They become more slender with inflection point at about half radius when the pressure drop increases. The flow situation is similar to the case described by Hausenblas however with a more physically realistic viscosity function for temperature differences of up to about $50^{o}F$. Both Kearsley

and Hausenblas describe situations where the temperature gradient in axial direction is zero.

Gerrard and Philippoff 1963 (9) investigated the adiabatic wall case and developed a thermal correction to the shear stress, shear rate flow curves very similar to the Rabinowitz correction to flow curves for non-Newtonian liquids. They pointed out that application of the correction was not justified for isothermal wall cases. Gerrard, Steidler and Appeldoorn 1964 (10), 1965 (11) conducted an extensive investigation in the capillary flow situation both experimentally and with computed solutions. The computations incorporated equations and boundary conditions with more realistic assumptions than the assumptions made in earlier work. The viscosity function was a hyperbolic dependency of viscosity on temperature to the power - 3.55. A pressure viscosity relation was also incorporated. Both the adiabatic and the isothermal case was treated. Good agreement was found between calculations and measurements in the adiabatic wall case. It was found difficult to conduct the dissipated heat completely away in the isothermal wall case and the flow curves show deviation in direction of lower apparent viscosity when the shear stress is above about 10^5 dyn/cm^2. Radial temperature profiles were measured at the exit. The applied capillary diameter was of the order of .017 in, .43 mm. The profiles showed a strong annular peak near the wall and very nearly zero temperature change at the center. This very uneven temperature distribution for a long capillary, ~10 cm, is remarkable and shows that convection in axial direction is significant even for the small diameters of .017 inch as applied in this work.

Problem Formulation

The distribution of increased temperatures in a short capillary for high shear stress measurements are estimated along with the increase of flow rate due to the distribution of increased temperatures.

The configuration of the flow is shown in Figure 34. A viscous lubricant enters a short length cylindrical capillary. The volume flow rate and the pressure drop over the capillary are measured. Cylindrical coordinates are applicable for the physical configuration. The presentation for the remainder of the chapter comprise flow with radial conduction and axial convection.

The temperature distribution in the capillary due to dissipation is estimated for the case of axial convection and constant viscosity. The deviation of the flow curves will be evaluated assuming the estimated temperature distribution but using a temperature dependent viscosity function in the calculations of velocities and flow rates.

The procedure is repeated incorporating radial conduction. The temperature distribution is estimated assuming axial convection, radial conduction and constant viscosity. The flow curves are evaluated using the estimated temperatures (for axial convection - radial conduction - constant viscosity) but assuming temperature dependent viscosity in the calculations of velocities and flow rates.

Equations

The equation of mass conservation is

$$r\rho_{,t} + (\rho r u_r)_{,r} + (\rho u_\theta)_{,\theta} + r(\rho u_z)_{,z} = 0 \qquad (1)$$

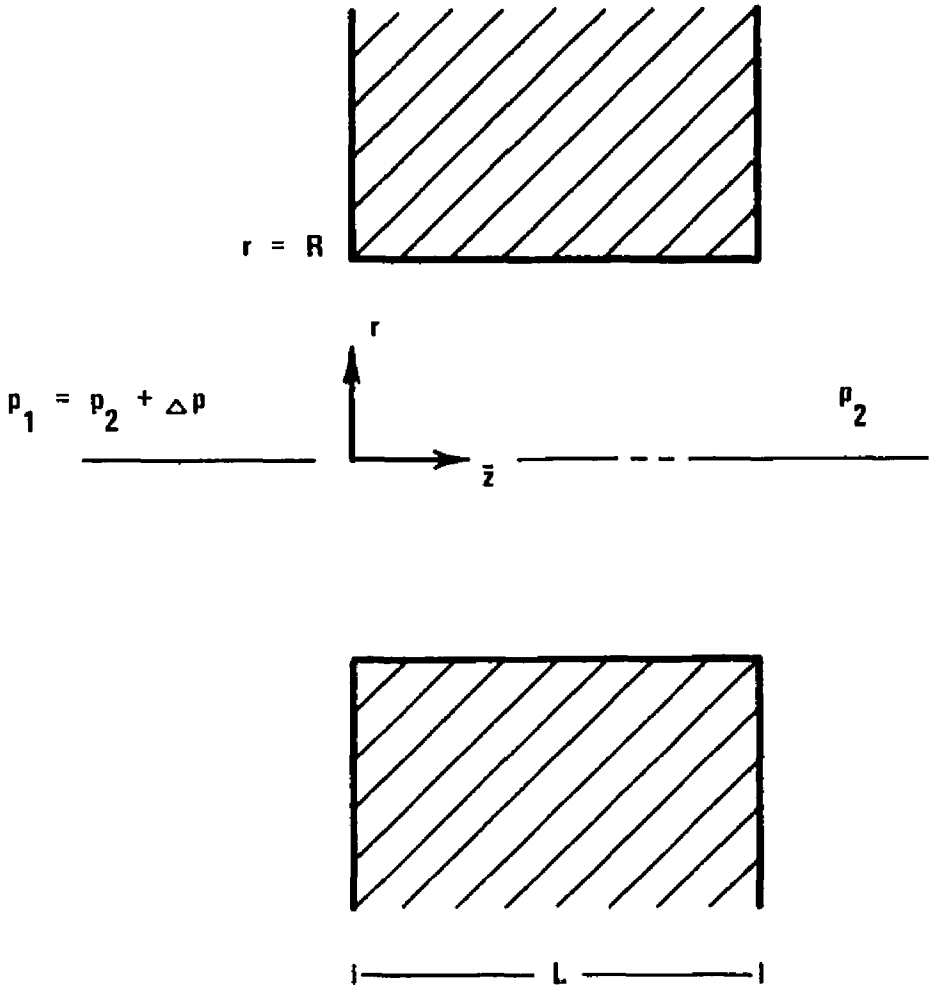

Figure 34. The Flow Situation, Flow of a Viscous Lubricant through a Cylindrical Capillary.

Table 9. Assumptions

1. Steady state conditions. Laminar flow.
2. $u_{\bar{z}} = u(r)$ only $u_r = 0$ $u_{\bar{\theta}} = 0$ $u_{\bar{z}}(R) = 0$ $u_{\bar{z}},_r(0) = 0$.
3. $p,_{\bar{z}} =$ constant $p,_r = 0$ $p,_{\bar{\theta}} = 0$.
4. Body forces and inertial forces are zero.
5. $T = T(r,\bar{z})$ only $T(R,\bar{z}) = T(r,0) = 0$.
6. The material parameters η, ρ, c_v, k_t are constant.
7. Re << 1
8. Heat conduction in axial direction is zero.

The equation is satisfied by the assumptions 1 and 2.

The equations of motion are for ρ = constant.

$$\rho\left(\frac{Du_r}{Dt} - \frac{u_{\bar{\theta}}^2}{r}\right) = R_o - p,_r + \eta(\nabla^2 u_r - (u_r + 2u_{\bar{\theta}},_{\bar{\theta}})/r^2) \tag{2}$$

$$\rho\left(\frac{D\bar{\theta}}{Dt} + \frac{u_r u_{\bar{\theta}}}{r}\right) = \Theta_o - (p,_{\bar{\theta}})/r + \eta(\nabla^2 u_{\bar{\theta}} + (2u_r,_{\bar{\theta}} - u_{\bar{\theta}})r^2) \tag{3}$$

$$\rho\ \frac{Du_{\bar{z}}}{Dt} = Z_o - p,_{\bar{z}} + \eta\nabla^2 u_{\bar{z}} \tag{4}$$

where $\frac{D}{Dt}$ and ∇^2, shown for example for u_r, is:

$$\frac{Du_r}{Dt} = u_r,_t + u_r(u_r,_r) + (u_{\bar{\theta}}/r)(u_r,_{\bar{\theta}}) + u_{\bar{z}}\ (u_r,_z) \tag{5}$$

and

$$\nabla^2 u_r = u_{r,r,r} + (1/r)(u_{r,r}) + (u_{r,\theta,\theta})(1/r^2) + u_{r,z,z} \qquad (6)$$

Assumptions 1, 2, 3, and 4 reduce the equations to

$$p_{,z} = \eta(u_{z,r,r} + (u_{z,r})/r) \qquad (7)$$

or

$$rp_{,z} = (\eta r u_{z,r})_{,r} \qquad (8)$$

Integrations and the assumptions 2 give

$$u_{z,r} = rp_{,z}/2\eta \qquad (9)$$

and

$$u_z = ((r/R)^2 - 1)(R^2 p_{,z}/4\eta) = -(R^2 p_{,z}/4\eta)(1 - (r/R)^2) \qquad (10)$$

The energy equation is

$$\rho c_v \frac{DT}{Dt} = k_t(T_{,r,r} + (1/r)T_{,r} + (1/r^2)T_{,\theta,\theta} + T_{,z,z}) + \Phi_c \qquad (11)$$

Assumptions 1, 2, 5 and 8 reduce equation (11) to

$$\rho c_v u_z T_{,z} = k_t(T_{,r,r} + (1/r)T_{,r}) + \eta(u_{z,r})^2 \qquad (12)$$

Equations (9), (10) and (12) give

$$-((\rho c_v)(-p_{,z})R^2/4\eta)(1 - r^2/R^2)T_{,z} + k_t(T_{,r,r} + (1/r)T_{,r}) \qquad (13)$$

$$+ r^2 p_{,z}^2/4\eta = 0$$

The first term in equation (13) represents axial convection. The second

term is radial conduction, in a cylinder, and the last term is the heat generation by dissipation. The assumption of constant viscosity allows an uncoupling of equations (7) and (11) integration of equation (7) to equation (10) and application of equation (9) and (10) into equation (12). Other shear stress-shear rate relations than the Newtonian, $\tau = \eta u,_z$, can be applied; particularly straightforward is the use of power law fluids. Temperature dependency in the shear stress-shear rate relation would require simultaneous solution of equations (7) and (12).

Adiabatic Flow

The special case of complete adiabatic conditions in the liquid (no heat conduction in the fluid) is of interest because it gives an approximate description of the expected temperature profiles immediately after the inlet. The adiabatic case also gives a particularly good description of the temperatures of the fluid following streamlines near the capillary axis. When heat conduction is absent equation (13) reduces, $\bar{\rho} = r/R$, to:

$$T,_{\bar{z}} = (\bar{\rho}^2/(1 - \bar{\rho}^2))((-p,_{\bar{z}})/c_v\rho) \tag{14}$$

with the solution

$$\Delta T = \bar{z}(\bar{\rho}^2/(1 - \bar{\rho}^2))((-p,_{\bar{z}})/(c_v\rho)) \tag{15}$$

satisfying the condition $\Delta T(\bar{\rho}, 0) = 0$. The isothermal condition $\Delta T(R,\bar{z}) = 0$ cannot be expected to be satisfied in an adiabatic situation.

The temperature in the capillary increases linearly with the axial coordinate. It is zero along the axis and increases without bound when $\bar{\rho} = 1$. The temperature profile as a function of relative radius is shown in Figure 35. The temperatures depend only on the pressure gradient, the specific heat per unit volume and on the location on the radius. Fluid viscosity and capillary diameter does not participate in the determination of the temperatures. For a typical pressure drop of 500 psi over the length $\bar{z}$ the equation (15) gives the following temperature profile at $\bar{z}$:

$$\Delta T = (500/140)(\bar{\rho}^2/(1 - \bar{\rho}^2)) \quad {}^{o}F \tag{16}$$

or

$$\Delta T \simeq 3(\bar{\rho}^2/(1 - \bar{\rho}^2)) \quad {}^{o}F \tag{17}$$

Equations (15) and (16) are obtained with the assumption of constant viscosity. The shear rate is proportional to $\bar{\rho}$ and the velocity is proportional to $(1 - \bar{\rho}^2)$ in this situation.

A temperature dependent viscosity can be introduced in order to estimate the increase in volume flow, and thereby the decrease in apparent viscosity, due to heat dissipation. Shear rates and fluid velocities can be determined when the temperatures as described by equation (15) are assumed. An increased flow rate can then be found direct by integration of the velocities. The decrease in apparent viscosity are thereafter found by the ratio between pressure drop and increased flow rate. The assumption of an unchanged temperature profile represents an approximation which can be justified only within a certain interval of applied pressure drop.

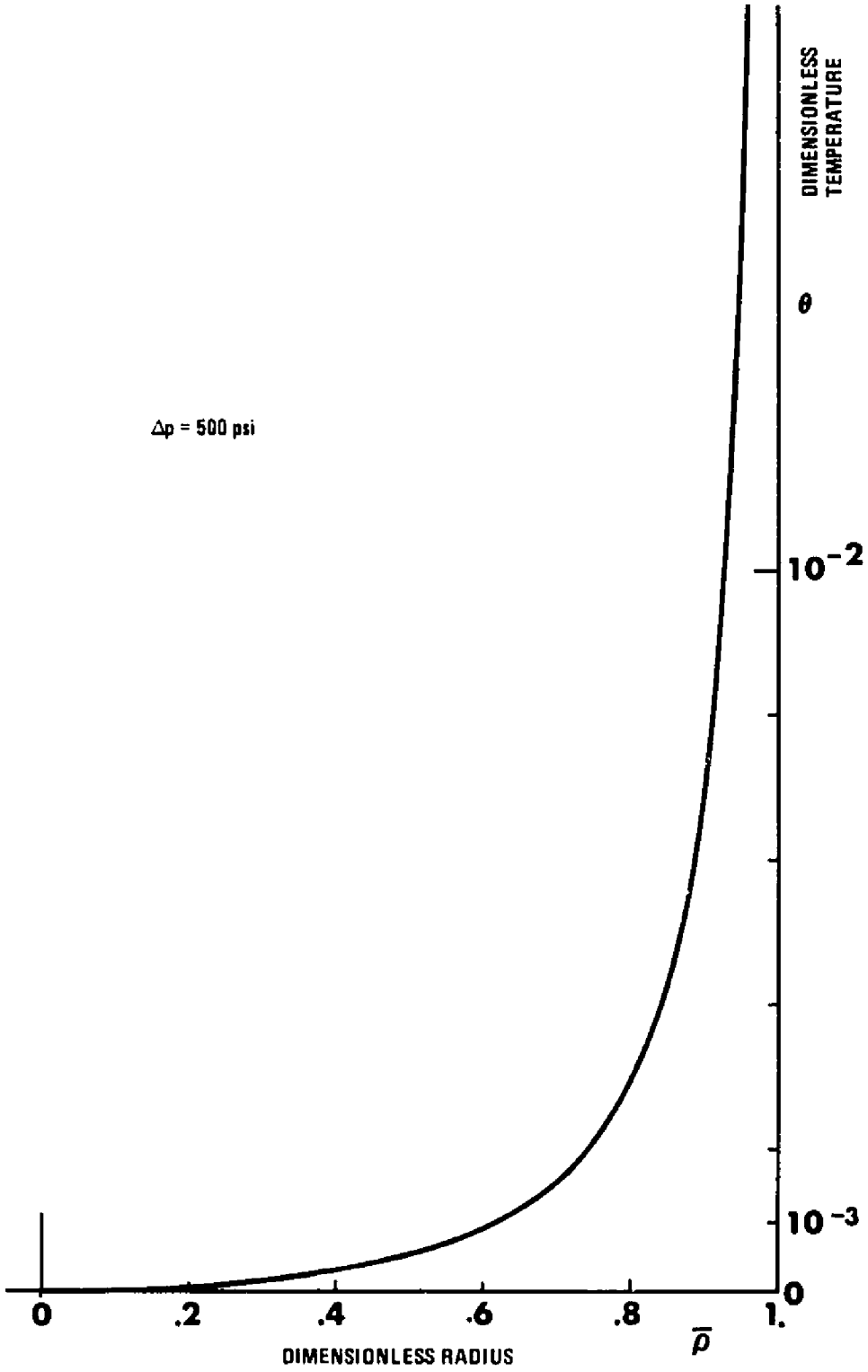

Figure 35. Temperature Distribution in Capillaries for the Case of No Heat Conduction in the Fluid.

The dimensionless velocity profile thus determined, by assuming the temperatures of equation (15) and assuming an arbitrary temperature viscosity relation, does not depend on capillary dimensions or materials, (Equation (15)). The relative change in flow rate through different capillaries of the same liquid will therefore depend on pressure drop alone over the capillaries. The flow curves, measured apparent viscosity, proportional to $\Delta p/\bar{Q}$, as function of shear stress, will consequently have the same configuration but will be displaced in the direction of the shear stress axis according to the actual length over diameter ratio for the capillary in question.

Equation (15) shows that the temperature profiles are independent of the viscosity of the fluid. Distortion of the velocity profiles from the parabolic form, change in volume flow rate and the change in measured apparent viscosity are therefore also independent of viscosity level but depend on pressure drop alone. The flow curves for different viscosity levels are of the same congruent form displaced through a translation along the viscosity axis alone. This result that the flow curves for a fluid are of the same form independent of capillary configuration and viscosity level was obtained as experimental observations individually for each fluid during the measurements on four fluids of widely different properties, described in the preceding chapter.

In a comparison between two fluids different temperature viscosity relations must be assumed. An exponential temperature viscosity relation of the form

$$(\eta = \eta_o \exp(-\beta \Delta T))\Big|_p \qquad (18)$$

is of sufficient generality to describe properly the viscosity behavior of fluids for a range of ΔT of 10 - 20°F, which is the order of magnitude of the temperature increase of interest. The fluid under comparison which is the least temperature sensitive with respect to viscosity changes, with the smallest temperature viscosity coefficient β, will show the smallest deviation in measured apparent viscosity for a given pressure drop. It will show the same temperature profile as the temperature profile of the more temperature viscosity sensitive fluid under comparison however at a greater pressure drop corresponding to a greater temperature increase, in accordance with equation (15). The pressure drop necessary to give the same reduction in measured apparent viscosity (measured total flow rate) can thus be determined from the expression

$$\beta\Delta p = \text{constant} \tag{19}$$

valid for both fluids under comparison. The ratio of pressure drop applied for the two fluids are inversely proportional to their temperature viscosity coefficients and therefore constant. Flow curves with this property will be plotted in a $\ln\tau$, shear stress, $\ln\eta$, viscosity, presentation, which are used both in the preceding chapter and in this chapter for plotting of flow curves, in the same configuration however located at different positions along the τ-axis. This result that the flow curves of different fluids were congruous with a common standard form of flow curve was also an observation done during the evaluation of the measurements.

The temperature viscosity relation

$$(\ln\eta = A/T^{Q})\Big|_{p} \tag{20}$$

yields a more nearly accurate description of the viscosity behavior with a validity range of 100-200°F for many fluids. It can be shown that the flow curves will be congruent with the general standard curve even for this greatly extended range of temperature changes. Assume that the two fluids under comparison in the extended range of temperature changes are described by

$$\ln \eta_1^* = A_1^*/T_1^{*Q_1^*} \qquad \text{for fluid 1} \tag{21}$$

$$\ln \eta_2^* = A_2^*/T_2^{*Q_2^*} \qquad \text{for fluid 2} \tag{22}$$

and

$$\eta_1^* = \eta_2^* \ (>> 1) \tag{23}$$

therefore

$$\frac{A_1^*}{A_2^*} = \frac{T_1^{*Q_1^*}}{T_2^{*Q_2^*}} \tag{24}$$

A_1^* A_2^* Q_1^* Q_2^* T_1^* T_2^* are presumed known. A constant a_c can then be determined such that $T_2^* = a_c T_1^*$. Changes in viscosity $\Delta\eta_1^*$ and $\Delta\eta_2^*$ for the two fluids 1 and 2 will yield

$$\frac{A_1^*}{A_2^*} = \frac{(T_1^* + \Delta T_1^*)^{Q_1^*}}{(T_2^* + \Delta T_2^*)^{Q_2^*}} \tag{25}$$

when

$$\Delta\eta_1^* = \Delta\eta_2^* \tag{26}$$

The condition $\Delta\eta_1^* = \Delta\eta_2^*$ implies however the same change of flow rate for the two fluids in the same capillary. Equations (24) and (25) imply $\Delta T_2^* = a_c \Delta T_1^*$. Equation (15) then yields $\Delta p_1^* = a_c \Delta p_2^*$. The flow curves for the two fluids will therefore be plotted in an identical form in a $\ln\tau - \ln\eta$ diagram however at different locations along the τ axis. The conformity of the flow curves are thus not limited to temperature changes of about $20^{\circ}F$ but can be expected over much greater temperature increases.

It has been shown that the flow curves will be of identical form irrespective of fluid type, viscosity level and capillary configuration in a capillary experiment. The assumptions for the approach were the assumptions of Table 1 with $k_t = 0$. The temperature profile was determined with constant viscosity. The total flow rate was determined relaxing the assumption of constant viscosity in calculations of velocity gradients and velocities. No thermal feedback as correction to the temperature calculation was assumed. Liquid behavior of the fluid was assumed. The general characteristics thus derived are consistent with the experimental results.

Flow with Radial Conduction

The general form of the flow curve will be modified to some extent when heat conduction is present. The temperature profiles can be achieved through solution of equation (13) with an approximate method.

Nondimensionalizing

Introducing the variable

$$\theta = T/E \quad \bar{z} = L\omega \tag{27}$$

where $E = A^{(1/Q)}$

and the parameters

$$R1 = (-p,_{\bar{z}})\ R^4/4L\eta\kappa \qquad R2 = (-p,_{\bar{z}})L/c_v\rho\ E \tag{28}$$

one obtains for the derivatives

$$\theta,_{\omega} = T,_{\bar{z}}L/E \quad \theta,_{\bar{\rho}} = T,_r R/E \quad \theta,_{\bar{\rho},\bar{\rho}} = T,_r,_r R^2/E \tag{29}$$

in that $\bar{\rho} = r/R$

Equation (13) then becomes

$$(-R1)\ \theta,_{\omega}(1 - \bar{\rho}^2) + \theta,_{\bar{\rho},\bar{\rho}} + (1/\bar{\rho})\theta,_{\bar{\rho}} + (R1)(R2)\bar{\rho}^2 = 0 \tag{30}$$

with $\theta(1,\omega) = 0$ and $\theta(\bar{\rho},0) = 0$

Approximate Solution

Temperature Distribution. The term containing $\theta,_{\omega}$ suggests solutions with an exponential expression, $e^{s\omega}$. The range of interest for the solution is the locations immediately downstream of the inlet where $s\omega$ is expected to be small ($s\omega << 1$). The factor $e^{s\omega}$ can therefore be approximated with $1 + s\omega$. The condition $\theta(\bar{\rho},0) = 0$ leads however to the product type expression

$$\theta = s\omega \sum_{0}^{\bar{n}} \Omega\ (\bar{\rho}^{2\bar{n}})\ a_{\bar{n}} \tag{31}$$

as the assumed dimensionless temperatures, a series expansion, as a possible approximate solution. The temperature of the fluid along the

capillary axis will not increase discernibly during passage at a relatively short capillary. The centerline temperature is therefore assumed to remain constant in the solution. Terms of the form $(1 - \bar{\rho}^{2\bar{n}})$ will give a dimensionless temperature at the center equal to the sum of the coefficients $a_{\bar{n}}$ and also satisfy the condition $(1,\omega) = 0$. The series expression for the approximate solution was therefore selected as

$$\theta \simeq \omega \sum_{1}^{\bar{n}} a_{\bar{n}}(1 - \bar{\rho}^{2\bar{n}}) \qquad (32)$$

Determination of the constants of equation (32) was carried out by the collocation method. The calculations were performed on a computer. A program which would accept up to eight collocation points, $\bar{\rho}$, was created. The program finds the coefficients $a_{\bar{n}}$ for $\omega = 1$, at the exit, calculates the temperatures at the eight radially displaced collocation points, and determines the deviation from zero when θ is inserted in equation (30). The program is found in Appendix E. Execution time is about 250 msec. A typical flow situation for the sapphire capillary is Δp = 500 psi, η = 3000 cp and E = 2000°R which gives R1 ~ 1140 and R2 ~ 1.585×10^{-3}. The temperature profile is shown in Figure 36. The maximum temperature is located at $\bar{\rho}$ ~ .9. The magnitude of the maximum is 8.8°F at the exit which gives approximately 4.4°F average temperature increase at that radial location. The figure shows also the temperature profile at ω = .5. The maximum temperature is 5.7°F at $\bar{\rho}$ = .93. The selected expression for equation (32) gives thus the correct trend in the solutions obtained via collocation. It can also be seen that the magnitude of the temperature peak is not proportional with axial position

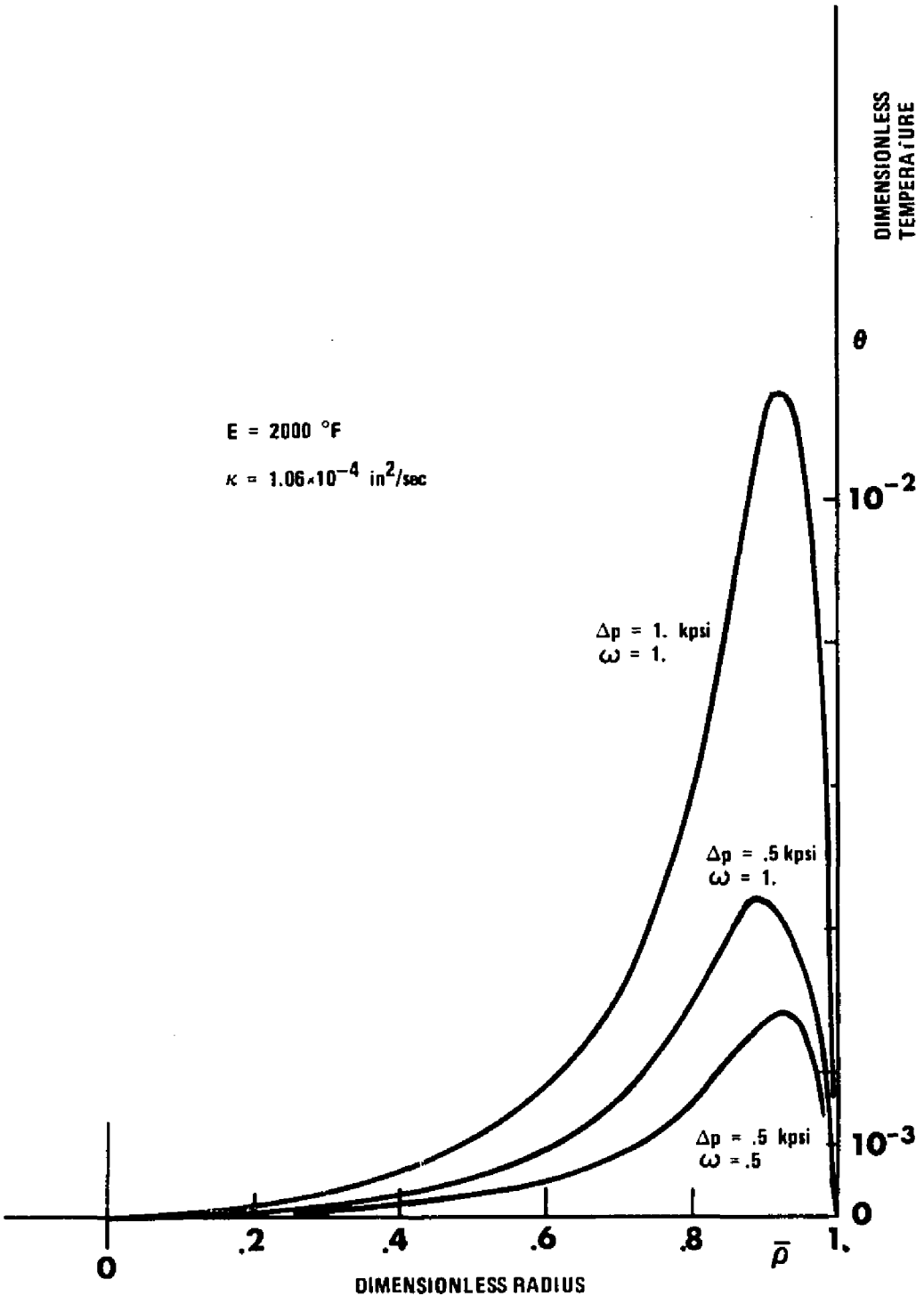

Figure 36. Temperature Distribution in Capillary 0, Heat Conduction Present.

ω. This is in general true at all positions, for $\bar{\rho}$ greater than about .7, where heat conduction is significant. Heat conduction is not significant in a center core, $\bar{\rho} < \sim.7$, and temperature increases are seen to be proportional to axial displacement in this region. The figure shows also the temperature profile for a pressure drop of 1000 psi over the sapphire capillary. Temperatures in the center core region is doubled compared to the temperatures when the pressure drop was 500 psi. The temperature peak at $\Delta p = 1000$ psi is however much more pronounced with a maximum of approximately $23^{o}F$ at $\bar{\rho} \sim .92$.

Figure 37 shows the contributions from convection, conduction and dissipation from equation (30). The pressure drop is 1000 psi. The profiles are calculated at $\omega = 1$. The dissipation profile is the same when $\omega = 0$ as for $\omega = 1$. The convection profile is a mirror picture about the $\bar{\rho}$-axis of the dissipation profile when $\omega = 0$. Convection removes therefore the total amount of generated heat when $\omega = 0$. The generated heat is seen to be removed primarily also by convection even when $\omega = 1$. Conduction, in radial direction, sends an estimated 15% of the total dissipation heat to the capillary wall when $\omega = 1$. This happens in the region $\bar{\rho} > .86$. The total amount of heat conducted away to the walls can be estimated to be of the order of 7.5% for the total capillary length assuming as an approximation that the conduction contribution increases linearly with ω position. It is seen, at $\omega = 1$, that a small amount of heat is conducted inwards when $\bar{\rho} < .86$. The heat conducted away to the walls is a relatively small proportion of the total generated heat. The generality of the flow curves when heat conduction is absent

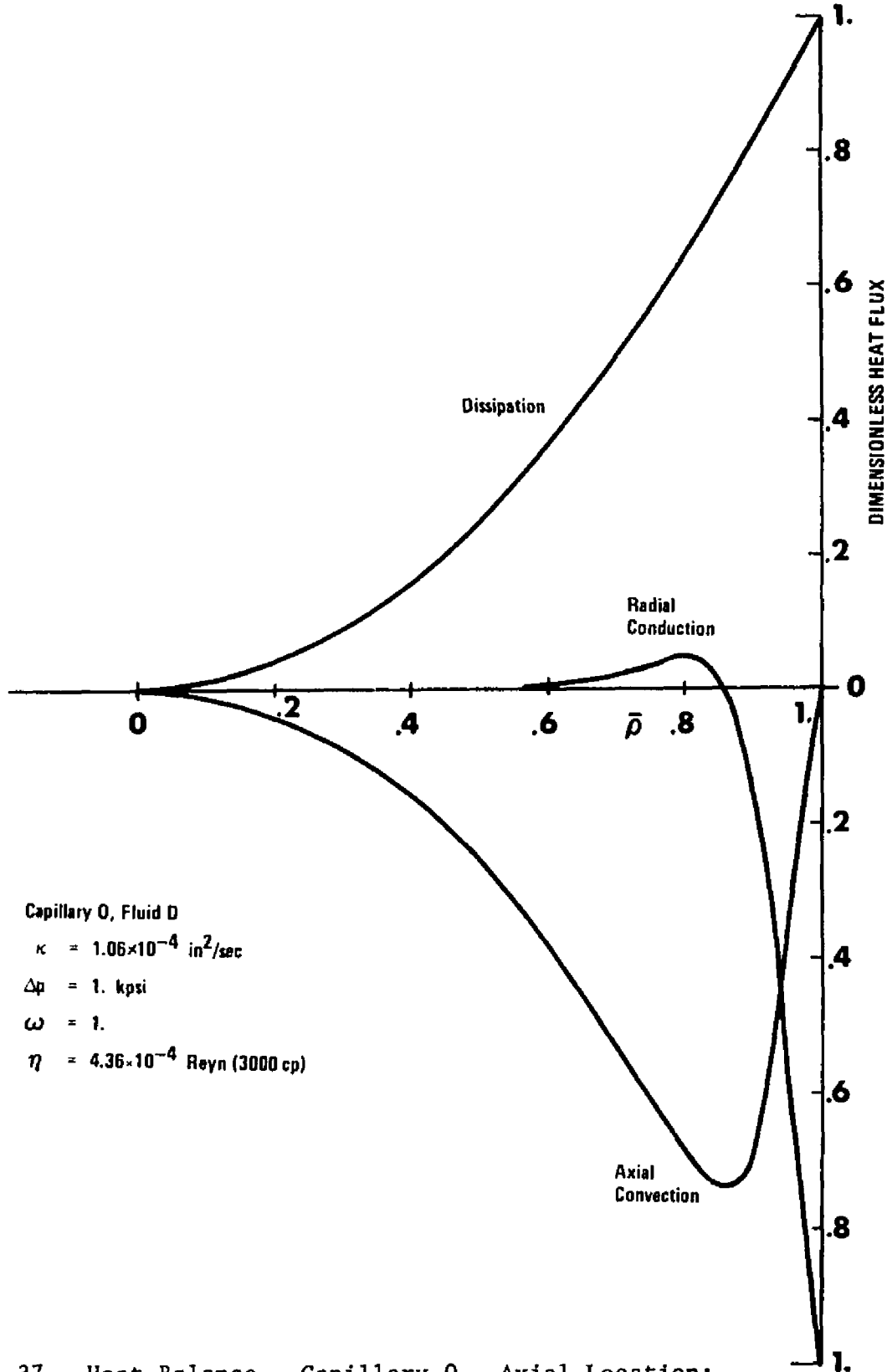

Figure 37. Heat Balance. Capillary O. Axial Location: ω = 1. (The Heat Flux' are nondimensionalized with respect to the dissipation at $\bar{\rho}$ = 1.)

will, therefore, expectedly transfer to the case when heat conduction is present with some slight modifications. The small amount of heat conducted away suggests also that the capillary measurements are strongly insensitive to the degree to which the desired condition of isothermal wall is satisfied. This insensitivity is consistent with observation during the measurements.

Calculation of Flow Rate

The program which determines the temperatures at the collocation points calculates further a velocity profile and a flow rate at $\omega = 1$ under the assumption that the shear rate is modified by exp ($\beta\Delta T$) where β is the temperature viscosity coefficient for an exponential viscosity dependency of the fluid temperature and T is the temperature increase as calculated through the preceding steps assuming constant viscosity. The temperature increase ΔT is

$$\Delta T = \theta \times E \tag{33}$$

A short series of calculations of volume flow rates was performed with the program. Exponential temperature viscosity coefficients β in the range corresponding to the coefficients for fluid D and for the dimethyl siloxane were selected. For fluid D which has a Q exponent of about 2.2 in a $\ln\ln\eta$-$\ln T$ presentation an exponential coefficient of .03 was selected. A coefficient of .015 was selected for the siloxane which is less temperature viscosity sensitive. The temperature E was assumed to be 2000°R common for both cases. ΔT was thus

$$\Delta T = 60 \times \theta \quad \text{for fluid D} \tag{34}$$

and

$$\Delta T = 30 \times \theta \quad \text{for siloxane} \tag{35}$$

Calculations were performed with the pressure drop increasing with a factor of 2 for each step and beginning with 250 psi. The series ended at Δp = 3-4000 psi in that higher pressure drop were considered to cause unacceptable deviations in the assumptions made for the calculation. An apparent viscosity defined as Δp/calculated total flow rate was determined. Figure 38 shows a plot of the calculated flow curves for the two model fluids, representing fluid D and siloxane, as generated in situations equivalent with flow through capillary 0 and capillary 1. The flow curves follow accurately the standard flow curve which was found to be a common configuration for all the experimental measured flow curves. The calculated flow curves are furthermore located very near the actual position along the τ-axis of the measured flow curves for fluid D and siloxane.

While the agreement between measurements and a calculation is remarkable it does not rigorously determine that viscous heating is the only mechanism generating the apparent non-Newtonian flow curves. The calculation procedure approximates the actual flow situation in the capillary. However, the example, together with the evidence collected during measurements and evaluation, shows that the investigated fluids probably are Newtonian in flow properties up to the highest shear stress applied.

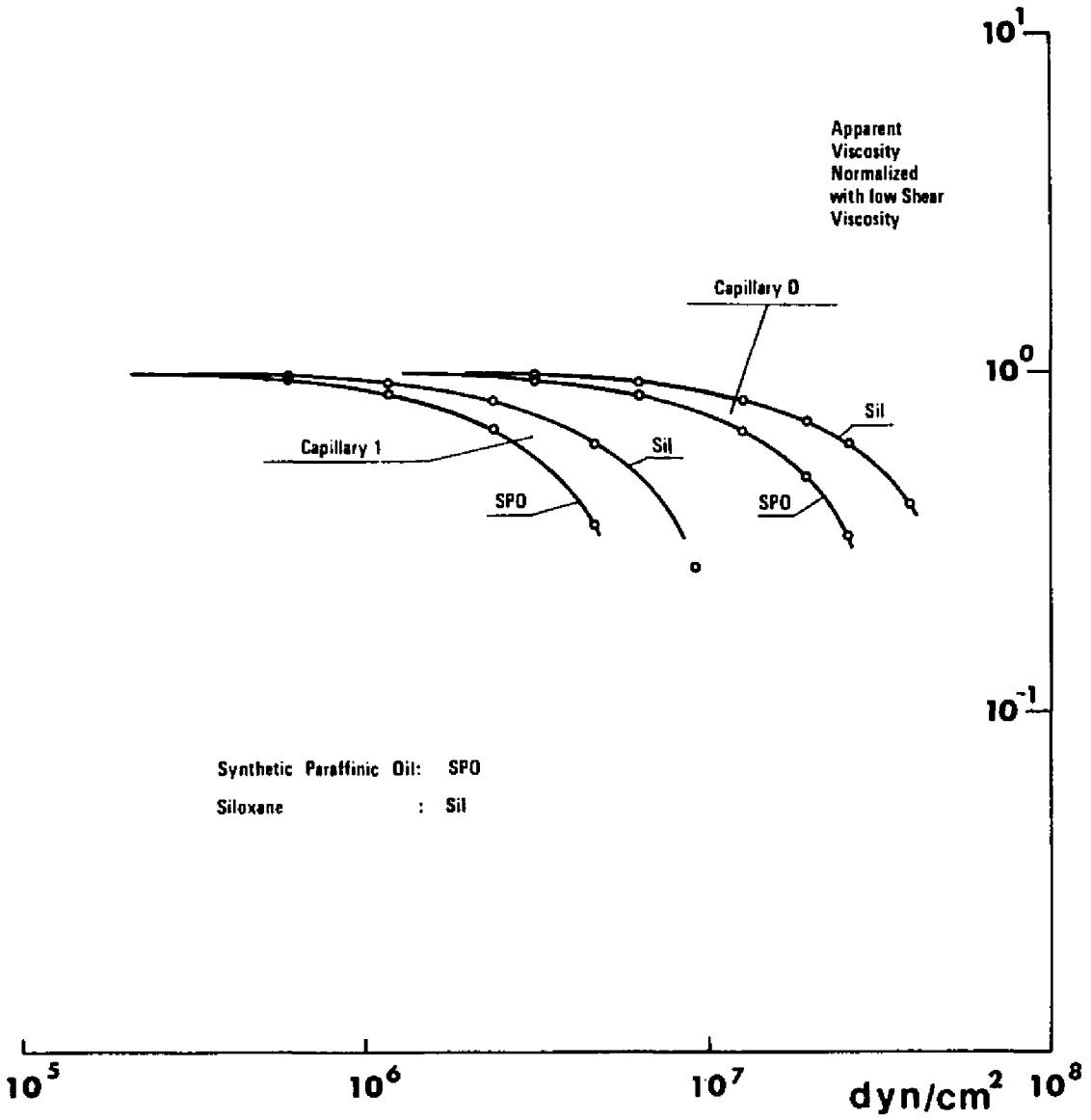

Figure 38. Calculated Flow Curves for Synthetic Paraffinic Oil and Siloxane. (Apparent viscosities are normalized with the low shear viscosities. Both capillary 1 and capillary 0 situations are shown.)

CHAPTER IV

NONISOTHERMAL STEADY PLANE LAMINAR COUETTE FLOW OF A LUBRICANT BETWEEN PARALLEL BEARING SURFACES

Flow with Constant Viscosity

The steady plane Couette flow with constant viscosity is thoroughly described in the literature. Textbooks, Pai (53), give the case as one of the exact solutions to the Navier-Stokes equations. The energy dissipation is constant throughout the film as both shear rate and shear stress are constant. The temperature profile is a linear combination of two conduction terms. One is due to a temperature difference between the walls, and one is generated by the energy dissipation in the film.

The assumption of constant viscosity is justified for only relatively small temperature differences due to the strong temperature dependency of the viscosity of most liquids.

Flow with Temperature Dependent Viscosity

Review of Solutions

The literature has several solutions where the temperature dependency of the viscosity of the lubricant is taken into account. The solutions are, in most cases, only for specific temperature viscosity relations, which furthermore give incomplete accuracy of the viscosity prediction for the relatively large temperature differences encountered in an elastohydrodynamic film. Usually the solutions are intended to be

applied to thick film lubrication. They give better accuracy for thick film situations because the temperature difference is smaller than in an elastohydrodynamic film.

Kingsbury 1933 (54) used a hyperbolic temperature viscosity relation for a thick film, low pressure situation. His method of solution is graphic and can accommodate any viscosity function, whether given as an analytic expression or as experimental data in table form. Hagg 1944 (55) performed a similar investigation of low pressure films. The temperature viscosity relation was limited to the exponential case, and the method of solution was analytic. His results are presented primarily in terms of shear stresses. Temperature differences in the experimental part of these two reports are of the order of $50^{o}F$. Shear rates are about 10^{5} sec^{-1}. Shear stresses are less than 1 psi; that is, approximately 10^{3} times lower than the shear stress in a typical elastohydrodynamic film.

Regirer 1958 (56) treated the case of an arbitrary dependence of the viscosity on temperature. This analytical work is profound and thorough. The investigation is concentrated on determining the shear stresses and the velocities of the lubricant. One important result is the derivation of expressions for the shear stress and particular expressions for the limit of the stress when the maximum film temperature increases beyond bound.

Crook 1961 (57) and Bostandzhyan et al., 1965 (58) studied the exponential temperature viscosity relation and gave results in terms of viscosities and temperatures through the film. Crook worked primarily with elastohydrodynamic films. He limited the investigation to the

situation of the same temperature for both walls. Hunter, et al. (59) used the exponential relation, but in the case of a wedge-shaped low pressure film.

None of the investigations discussed the physics of the problem. The inherent limitations of the analytical approach imposed by the assumptions are not mentioned. Only Bostandzhyan (58) remarked that the equation to be solved does not admit arbitrary parameter variations.

Problem Formulation

The lubrication situation considered is the flow of a viscous liquid between two parallel bearing surfaces as shown in Figure 39.

One surface 2 is moving with a constant velocity $u_1 = UN$ in the x_1 direction. The other velocity components u_2 and u_3 of the surface 2 in the x_2 and x_3 direction are assumed to be zero. Surface 1 is stationary. The temperatures of the surfaces are constant T_1 and T_2. The pressure is constant. The temperature viscosity relation assumed is the formulation $\ln\ln\eta = \ln A - Q \ln T$ described in Chapter II. The temperature viscosity relation contains two material constants: a characteristic temperature (E) and a characteristic pressure (q) besides the two variables, temperature and viscosity. $E = A^{1/Q}$ and $p/q = Q$ where p is the pressure. The equation is

$$\eta = c_1 e^{(E/T)^{p/q}} \tag{1}$$

where c_1 is a dimensioned constant $c_1 = \eta/|\eta|$. E has the dimension of ^{o}Rankine and q has the dimension of lbf/in^2. E and q are functions of the pressure p.

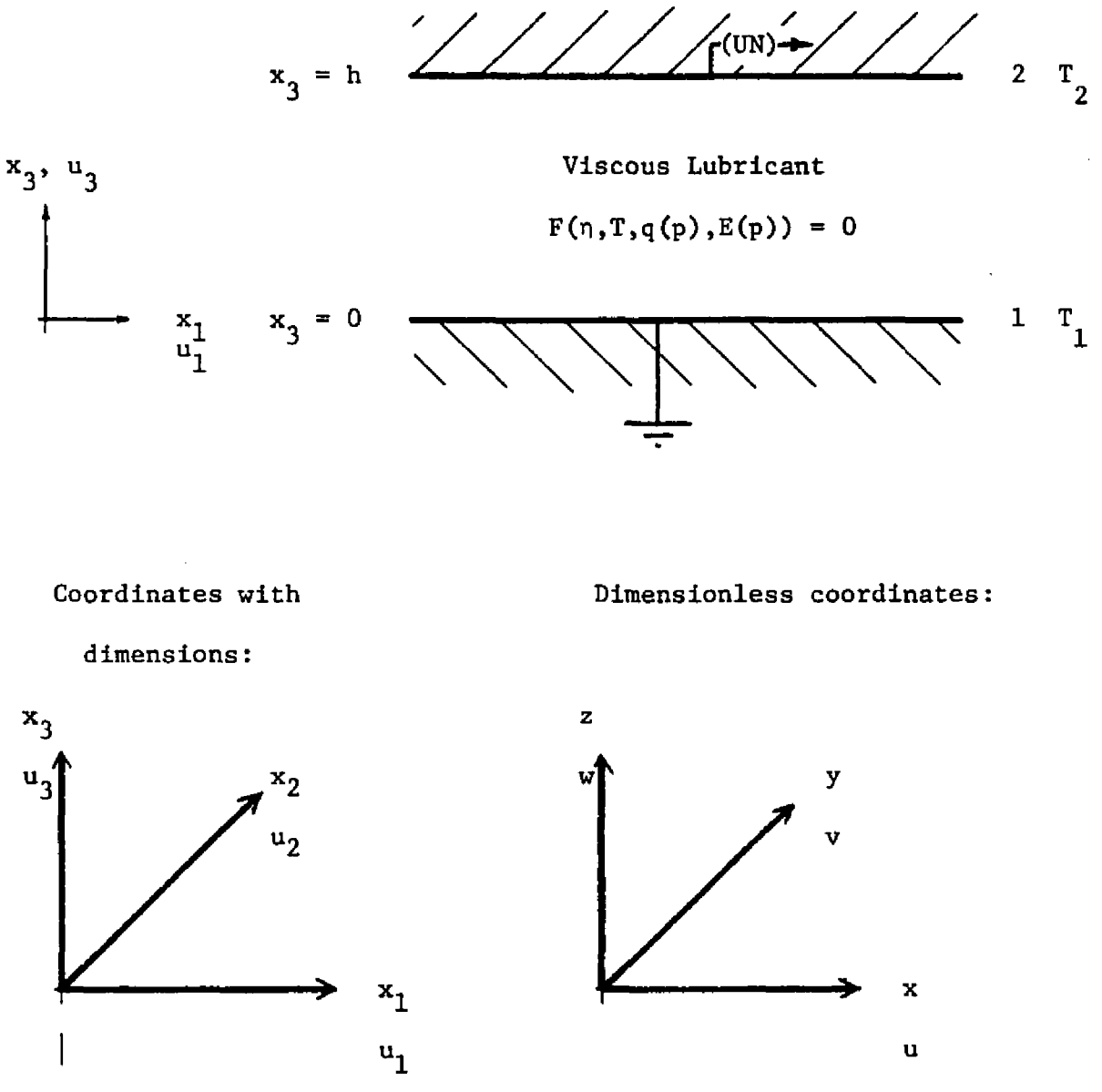

Figure 39. The Lubrication Situation, Flow of a Viscous Lubricant Between Parallel Bearing Surfaces.

Steady state conditions and laminar flow are assumed. The assumptions are summarized in Table 10.

Table 10. Assumptions

1.	Steady state conditions. Laminar flow.
2.	$u_1 = u_1(x_3)$ only; $u_2 = 0$; $u_3 = 0$; $u_1(0) = 0$; $u_1(h) = (UN)$.
3.	p = constant
4.	Body forces are zero.
5.	$T = T(x_3)$ only; $T(0) = T_1$ = constant; $T(h) = T_2$ = constant.
6.	$\rho = \rho(x_2, x_3)$
7.	$c_v = c_v(x_2, x_3)$
8.	$k_t = k_t(x_1, x_2)$

Equations

Cartesian coordinates are applicable for the physical configuration. The equation of mass conservation is

$$\rho_{,t} + (\rho u_i)_{,i} = 0 \qquad i = 1,2,3 \tag{2}$$

The equations of motion are

$$\rho \frac{Du_i}{Dt} = X_i + (\tau_{ij})_{,j} \qquad \begin{matrix} i = 1,2,3 \\ j = 1,2,3 \end{matrix} \tag{3}$$

where

$$\tau_{ij} = (\lambda u_{k,k} - p)\delta_{ij} + \eta(u_{i,j} + u_{j,i}) \qquad i,j,k = 1,2,3 \tag{4}$$

and

$$\lambda = -2\eta/3 \tag{5}$$

The energy equation is

$$\rho \frac{D(En)}{Dt} + p\rho\frac{D(1/\rho)}{Dt} = (k_t T,_i),_i + \Phi \quad i = 1,2,3 \tag{6}$$

where the dissipation function is

$$\Phi = 2\eta\left(u_1^2,_1 + u_2^2,_2 + u_3^2,_3 - \frac{1}{3}(u_1,_1 + u_2,_2 + u_3,_3)^2\right)$$

$$+ \eta\left((u_1,_2 + u_2,_1)^2 + (u_2,_3 + u_3,_2)^2\right.$$

$$\left. + (u_3,_1 + u_1,_3)^2\right) \tag{7}$$

The temperature viscosity relation is

$$\eta = c_1 e^{(E(p)/T)^{(p/q(p))}} \tag{8}$$

The assumptions 1, 2, and 6 satisfy the equation of mass conservation (2). The assumptions 1, 2, 3, and 4 reduce the equation of motion to

$$\eta u_1,_3 = \text{constant} \tag{9}$$

The stresses reduce through assumptions 2 and 3 to

$$\tau_{ii} = -p \qquad i=1,2,3 \tag{10}$$

and

$$\tau_{13} = \tau_{31} = \eta u_{1,3} \tag{11}$$

Equations (9) and (11) show that the shear stress is constant in the film.

The energy equation reduces through assumptions 1, 2, 5, 6, and 7 to

$$(k_t T_{,3})_{,3} + \eta u_{1,3}^2 = 0 \tag{12}$$

The viscosity function is conveniently rewritten in the form:

$$\eta = c_1 |\eta(T,q,E)| \tag{13}$$

such that the constant c_1 has the units of the viscosity. The numerical value of c_1 is unconstrained except, of course: $c_1 \neq 0$. The equations are thus reduced to the following set:

$$\eta = c_1 \mu(T,q,p) \tag{14}$$

$$\eta u_{1,3} = \text{const} = \tau_{31} = \tau_{13} (=\tau) \tag{15}$$

$$(k_t T_{,3})_{,3} + \eta u_{1,3}^2 = 0 \tag{16}$$

Nondimensionalization

Introducing the variables

$$\theta = T/E \qquad u = u_1/(UN) \qquad z = x_3/h \tag{17}$$

and the parameters

$$\pi_1 = T_1/E \qquad \pi_2 = T_2/E \qquad \pi_3 = p/q \tag{18}$$

$$\pi_4 = c_1(UN)^2/2k_tE \qquad \pi_5 = \tau h/c_1(UN) \tag{19}$$

one obtains for the derivatives

$$\theta_{,z} = T_{,3}h/E \qquad \theta_{,zz} = T_{,33}h^2/E \tag{20}$$

$$u_{,z} = u_{1},_{3}h/(UN) \tag{21}$$

The equations (14), (15), and (16) then become in non-dimensional form:

$$n/c_1 = \mu(\theta,\pi_3) = e^{\theta-\pi_3} \tag{22}$$

$$\mu u_{,z} = \pi_5 \tag{23}$$

and

$$\theta_{,zz} + 2\pi_4\pi_5 u_{,z} = 0 \tag{24}$$

The boundary conditions for (24) become:

$$\begin{aligned} u(0) &= 0 \qquad \theta(0) = \pi_1 \\ u(1) &= 1 \qquad \theta(1) = \pi_2 \end{aligned} \tag{25}$$

The Shear Stress in the Film

Integration of equation (24) yields:

$$\theta_{,z} + 2\pi_4\pi_5 u = c_2 \tag{26}$$

The boundary conditions give:

$$\theta_{,z}(0) = c_2 \qquad \theta_{,z}(1) = c_2 - 2\pi_4\pi_5 \tag{27}$$

If one defines the auxiliary parameter Γ to be

$$\Gamma = \theta_{,z}(1)/2\pi_4\pi_5 \tag{28}$$

then the constant c_2 is:

$$c_2 = 2\pi_4\pi_5(1+\Gamma) \tag{29}$$

and the equation (26) is

$$\theta_{,z} + 2\pi_4\pi_5\left(u-(1+\Gamma)\right) = 0 \tag{30}$$

or

$$\theta_{,z}/\mu\pi_4 + 2u_{,z}\left(u-(1+\Gamma)\right) = 0 \tag{31}$$

Integrating equation (31) once yields:

$$\left(1/\pi_4 \int_{\pi_1}^{\theta} \frac{d\xi}{\mu(\xi,\pi_3)} + \int_0^{u^2} d(\zeta^2) - 2(1+\Gamma) \int_0^{u} d\zeta\right)\Big|_{\pi_3} = 0 \tag{32}$$

as $\theta = \theta(z)$ only and $u = u(z)$ only. π_3, π_4, π_5 are constants in the following derivation. Equation (32) gives:

$$Su(\theta,\pi_1,\pi_3) + u^2 - 2(1+\Gamma)u = 0 \tag{33}$$

or

$$u = (1+\Gamma) \pm \left((1+\Gamma)^2 - Su(\theta,\pi_1,\pi_3)\right)^{1/2} \tag{34}$$

where

$$Su(\theta,\pi_1,\pi) = 1/\pi_4 \int_{\pi_1}^{\theta} \frac{d\xi}{\mu(\xi,\pi_3)} \tag{35}$$

Equations (30) and (34) show

$$u - (1+\Gamma) = \pm \left((1+\Gamma)^2 - Su(\theta,\pi_1,\pi_3)\right)^{1/2} = - \theta,_z/2\pi_4\pi_5 \tag{36}$$

furthermore $\pi_4 > 0$ and $\pi_5 > 0$.

The signs of equation (34) are therefore applied as + when $\theta,_z < 0$ and - when $\theta,_z > 0$. When $\theta,_z = 0$, the square root expression is zero and $u = 1 + \Gamma$. From (33) it is seen that:

$$Su(\pi_2,\pi_1,\pi_3) = 2\Gamma + 1 \quad \text{or} \quad \Gamma = \frac{1}{2}\left(Su(\pi_2,\pi_1,\pi_3) - 1\right) \tag{37}$$

So far in the derivation, only π_1 through π_4 have been involved. The local lubricant velocity in the film is expressed as function of temperatures and material constants (equation 34). This leads directly to a statement of the maximum temperature attainable in the film.

It may be added that equations (33), (34) and (35) could be derived directly from equation (31) by integration after elimination of z as variable.

In order to obtain expressions for the shear stress in the film, an integration of equation (30) is carried out, giving:

$$\int_{\pi_1}^{\theta} d\xi + \pi_4 \int_0^{u^2} \mu d(\xi^2) - 2\pi_4\pi_5(1+\Gamma) \int_0^z d\xi = 0 \tag{38}$$

By squaring and differentiating equation (34)

$$d(u^2) = (-1/\pi_4\mu)(1 \pm (1+\Gamma)((1+\Gamma)^2 - Su(\theta,\pi_1,\pi_3))^{-1/2})d\theta \qquad (39)$$

and equation (38) reduces to

$$\pm 2\pi_4\pi_5 z = \int_{\pi_1}^{\theta} ((1+\Gamma)^2 - Su(\xi,\pi_1,\pi_3))^{-1/2}\, d\theta \qquad (40)$$

from which in the limit of $z = 1$ and $\theta = \pi_2$ one gets

$$\pi_5 = \pm(-\tfrac{1}{2})\int_{\pi_1}^{\pi_2}(((1/4)\int_{\pi_1}^{\pi_2}\mu(\xi,\pi_3)^{-1}d\xi + \pi_4)^2$$

$$- \pi_4\int_{\pi_1}^{\theta}\mu(\xi,\pi_3)^{-1}d\xi)^{-1/2}\, d\theta \qquad (41)$$

The sign convention for equation (41) is that of equation (34): + for $\theta_{,z} < 0$ and - for $\theta_{,z} > 0$.

The transformation (39) is not defined when $Su(\theta,\pi_1,\pi_3) = (1+\Gamma)^2$ which happens for $\theta_{,z} = 0$ ($d\theta$ is zero here). The integral (41) is therefore improper if the maximum temperature in the film is located in the interval $0 < z < 1$ (or if $\theta_{,z} = 0$, for $z = 0$ or $z = 1$). A comparison with equation (38) which essentially is the same as equation (41) will verify that the integral of (41) is bounded. The integration may appropriately be carried out, if $T_{max}(\theta_{,z} = 0)$ is located in $0 < z < 1$, as separate operations in each of the two subintervals using the correct sign.

It may be added that equations (40) or (41) could be derived directly from equation (30) substituting equation (33) and integrating.

The Maximum Temperature in the Film

The maximum temperature is located at one of the boundaries ($z = 0$ or $z = 1$) if $\theta_{,z}(0)$ and $\theta_{,z}(1)$ both have the same sign or if one of the gradients are zero. The maximum temperature is located within the film in all other cases.

Equation (30) shows that if $\theta_{,z} = 0$ then

$$u\big|_{\theta_{,z}=0} = 1 + \Gamma \tag{42}$$

It is presupposed that the range of interest does not contain:

$\pi_4 = 0 = \pi_5$. ($\pi_4 = 0 \Rightarrow (UN) = 0$ or $k_t = \infty$ or $E = \infty$.

$\pi_5 = 0 \Rightarrow h = 0$ or $\tau = 0$ or $(UN) = \infty$).

Table 11 shows temperature and velocity profiles for selected values of Γ. It is seen that

$$\theta_{,z} = 0 \quad \text{only when} \quad -1 \le \Gamma \le 0 \tag{43}$$

Equation (34) and equation (42) imply:

$$(1+\Gamma)^2 = Su(\theta, \pi_1, \pi_3)\big|_{\theta=\theta_{max}} \tag{44}$$

or with equation (35) and (37) equation (44) becomes

$$\left(\frac{1}{2}\left(Su(\pi_2, \pi_1, \pi_3) + 1\right)\right)^2 = Su(\theta, \pi_1, \pi_3)\Big|_{\theta = \theta_{max}} \tag{45}$$

Table 11. Flow Situations for the Film. $Su = Su(\pi_2,\pi_1,\pi_3)$ π_3, π_4 Constant

	u	θ		
1	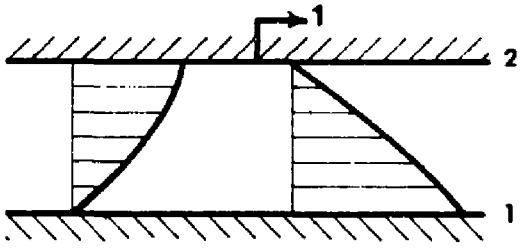	$\Gamma < -1$ $Su < -1$	$c_2 < 0$ $\theta_{max} > \pi_2$ $\theta_{max} = \pi_1$	at 2: $\hat{Q}\uparrow$ and $\theta_{,z} < 0$ at 1: $\hat{Q}\uparrow$ and $\theta_{,z} < 0$
2	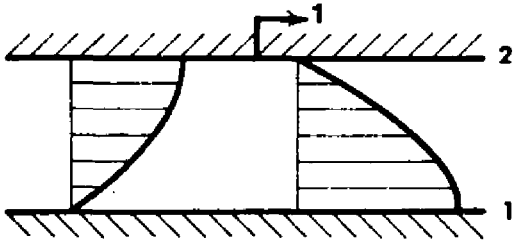	$\Gamma = -1$ $Su = -1$	$c_2 = 0$ $\theta_{max} > \pi_2$ $\theta_{max} = \pi_1$	at 2: $\hat{Q}\uparrow$ and $\theta_{,z} < 0$ at 1: $\hat{Q}=0$ and $\theta_{,z} = 0$
3	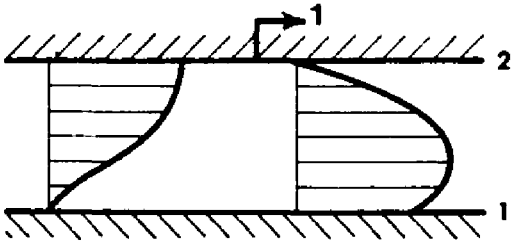	$-1 < \Gamma < -\frac{1}{2}$ $-1 < Su < 0$	$c_2 > 0$ $\theta_{max} > \pi_2$ $\theta_{max} > \pi_1$	at 2: $\hat{Q}\uparrow$ and $\theta_{,z} < 0$ at 1: $\hat{Q}\downarrow$ and $\theta_{,z} > 0$

-continued-

Table 11. Flow Situations for the Film. $Su = Su(\pi_2,\pi_1,\pi_3)$ π_3, π_4 Constant (Continued)

	u θ			
4	Symmetry 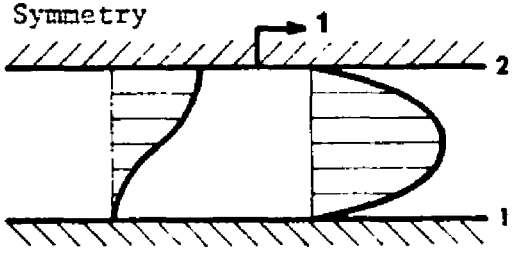	$\Gamma = -\frac{1}{2}$ $Su = 0$	$c_2 = \pi_4\pi_5 > 0$ $\theta_{max} > \pi_2$ $\theta_{max} > \pi_1$	at 2: $\hat{Q}\uparrow$ and $\theta_{,z} < 0$ at 1: $\hat{Q}\downarrow$ and $\theta_{,z} > 0$
5	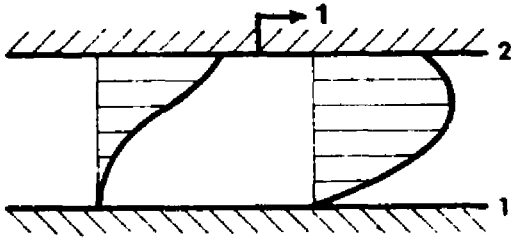	$-\frac{1}{2} < \Gamma < 0$ $0 < Su < 1$	$c_2 > 0$ $\theta_{max} > \pi_2$ $\theta_{max} > \pi_1$	at 2: $\hat{Q}\uparrow$ and $\theta_{,z} < 0$ at 1: $\hat{Q}\downarrow$ and $\theta_{,z} > 0$
6	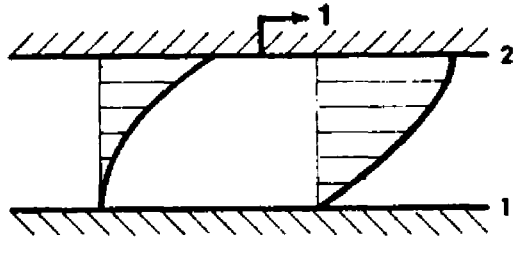	$\Gamma = 0$ $Su = 1$	$c_2 > 0$ $\theta_{max} = \pi_2$ $\theta_{max} > \pi_1$	at 2: $\hat{Q}=0$ and $\theta_{,z} = 0$ at 1: $\hat{Q}\downarrow$ and $\theta_{,z} > 0$

-continued-

Table 11. Flow Situations for the Film. Su = Su(π_2,π_1,π_3) π_3, π_4 Constant (Concluded)

u	θ			
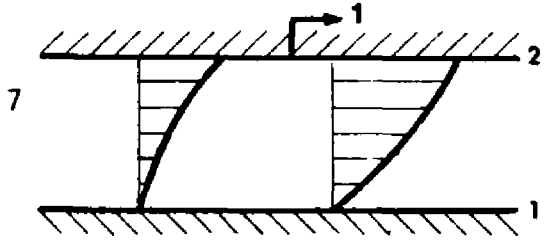	$\Gamma > 0$	$c_2 > 0$	at 2: $\hat{Q}\downarrow$ and $\theta_{,z} > 0$
	Su = 1	$\theta_{max} = \pi_2$	at 1: $\hat{Q}\downarrow$ and $\theta_{,z} > 0$
		$\theta_{max} > \pi_1$	

which can be written as

$$H_1(\pi_1,\pi_2,\pi_3,\theta_{max}) = 0 \tag{46}$$

The behavior of $\theta_{max}(\pi_2,\pi_1)$ is illustrated also in Table 11.

Table 11 shows that heat sources must be present outside the film if $\Gamma < -1$ or $\Gamma > 0$. The situation of viscous heat dissipation in the film without external heat sources is found when Γ is in the interval $-1 \leq \Gamma \leq 0$. These conclusions can also be deduced directly from equations (27), (28), and (29). It is seen from Table 11 that

$$\pi_2 < \theta_{max} \quad \text{and} \quad \pi_1 < \theta_{max} \quad \text{when} \quad -1 < \Gamma < 0 \tag{47}$$

$$\theta_{max} = \pi_2 \quad \text{when } \Gamma = 0$$

$$\theta_{max} = \pi_1 \quad \text{when } \Gamma = -1$$

Equation (45) yields, as $(\theta_{max})_{,\pi_1} = - H_{1,\pi_1}/H_{1,\theta_{max}}$

$$(\theta_{max})_{,\pi_1} = (1 - Su(\pi_2,\pi_1,\pi_3)) \times \mu(\theta_{max})/2\mu(\pi_1) \tag{48}$$

or

$$(\theta_{max})_{,\pi_1} > 0 \quad \text{when} \quad -1 \leq \Gamma < 0 \tag{49}$$

because $Su(\pi_2,\pi_1,\pi_3) < 1$ when $-1 \leq \Gamma < 0$, Table 11, and $\mu(\theta_{max}/2\mu(\pi_1) > 0$. Consequently:

$$\theta_{max}\big|_{\substack{\Gamma=-1 \\ \Gamma=0}} > \theta_{max}\big|_{-1<\Gamma<0} \tag{50}$$

also:

$$\theta_{max} = \pi_2 \quad \text{when } \Gamma \geq 0$$
$$\theta_{max} = \pi_1 \quad \text{when } \Gamma \leq -1 \tag{51}$$

Equations (50) and (51) state that the highest attainable film temperature is located at one of the bearing surfaces. A temperature extremum which is found within the film will be of smaller magnitude than the highest attainable temperature although it in itself is a temperature maximum in the particular lubrication situation.

The parameter Γ is equal to -1 when the maximum film temperature is located at the stationary surface. This case is significant because all other flow situations can be derived directly from it.

When $\Gamma = -1$, adiabatic conditions exist in the plane $z = 0$. When $\Gamma \neq -1$, in $[-1,0]$, there exists a plane at some $z = z_1$, $z_1[0,1]$ where adiabatic conditions and symmetry exist with respect to temperatures, heat fluxes, and velocity gradients. The velocity at z_1 is easily found (equation (30)) as

$$u(z_1) = 1 + \Gamma \tag{52}$$

Also the velocity difference $u(z) - u(z_1)$ is seen to be symmetric about the plane $z = z_1$.

The case of adiabatic conditions at one of the bearing surfaces is also important because many lubricant films operate physically under conditions where the major part of the heat generated by the energy dissipation is conducted away through only one of the surfaces. The other

surface can therefore be approximated with an adiabatic wall situation.

The Adiabatic Wall Condition

The condition of no heat flux at wall number 1 is equivalent to $\Gamma = -1$ or $Su(\pi_2,\pi_1,\pi_3) = -1$. There exists a symmetry of the flow situations with respect to the parameter Γ about the value $\Gamma = -1/2$. No heat flux is found at wall number 2 (the moving bearing surface) for $Su(\pi_2,\pi_1,\pi_3) = 1$. This situation is physically the same as $Su(\pi_2,\pi_1,\pi_3) = -1$ if the dimensionless unit velocity is subtracted from the arrangement.

The condition of no heat flux at one wall or bearing surface can therefore be obtained from the definition of Su, equation (35)

$$\int_{\pi_1}^{\pi_2} \mu(\theta,\pi_3)^{-1} d\theta = \pm \pi_4 \qquad (53)$$

The sign $\pm$ correspond to $\pi_2 \gtrless \pi_1$.

The temperature at the adiabatic bearing surface is the maximum temperature that can exist in the film under the assumptions of Tables 10 and 11 and the extra assumption that no external heat sources influence the film temperatures.

Only four parameters $\pi_1 - \pi_4$ are involved in its determination. Film thickness is not an element in the parameters $\pi_1 - \pi_4$ and therefore does not influence the highest temperature that can be maintained in a film.

The upper limit for the temperature in any lubricant film can be determined if the following properties are known: the bearing

surface velocity (UN), the coefficient of heat conduction k_t of the lubricant, the temperature T_2 of the moving bearing surface and the viscosity as function of pressure and temperature.

The solutions are usually not found to be sensitive to the accuracy of π_2 (T_2). The integrand $1/\mu$ of equation (53) decreases rapidly with decreasing $\pi_2(T_2)$. The contribution from the low temperature region becomes therefore insignificant below some temperature T_2.

A diagram has been prepared which will let the solution of equation (53) be carried out in a few graphical operations.

Graphical Representation of the Statement of the Maximum Film Temperature

The temperature viscosity relation equation (1)

$$\eta = c_1 e^{(E/T)^{p/q}} \tag{1}$$

is used for the graphical presentation. It predicts lubricant viscosities under elastohydrodynamic conditions with a satisfactory accuracy as discussed in Chapter II. The relation can be written as

$$\eta = c_1 e^{(E/T)^{\pi_3}} = c_1 e^{(\theta)^{-\pi_3}} = c_1 \mu(\theta, \pi_3) \tag{54}$$

which for constant pressure become

$$\eta = c_1 \mu(\theta) \tag{55}$$

E is the temperature (^{o}R) at which the viscosity is equal to e centipoise, π_3 is the slope of the straight line characteristic on the rectifying

double ln single ln diagram, c_1 is a unit carrying constant (=1 centipoise),T is in ^{o}Rankine and η is in centipoise. Calculations are usually carried out with Reyn as viscosity units and the constant c_1 thus becomes $(6.895 \times 10^6)^{-1}$. The actual value of $\mu(\theta,\pi_3)$ is the numerical value of the viscosity as measured in centipoise. The equation (53) is expressed for the graphical, approximate, general method of solution as

$$\int_{\pi_1}^{\pi_2} e^{-(\theta)^{-\pi_3}} d\theta = \pm \pi_4 \qquad \begin{matrix} \pi_2 < \pi_1 \Rightarrow - \\ \pi_2 > \pi_1 \Rightarrow + \end{matrix} \tag{56}$$

The integral term is plotted in Figure40 for π_3 = 1, 1.5, 2, 2.5, 3 and 4. The entrance to the diagram is through π_2. Intersection of the vertical line π_2 with the appropriate, interpolated π_3 value gives the value of the term:

$$I_2 = \int_{\pi_0}^{\pi_2} \mu(\theta)^{-1} d\theta \quad (\pi_0 << \pi_1) \tag{57}$$

The value of the parameter π_4 is added to I_2 giving I_1

$$I_1 = \int_{\pi_0}^{\pi_1} \mu(\theta)^{-1} d\theta \quad (\pi_0 << \pi_1) \tag{58}$$

Intersection of the horizontal line I_1 with the appropriate, interpolated π_3 value gives the desired π_1 value.

The maximum temperature in the film is therefore thus found as

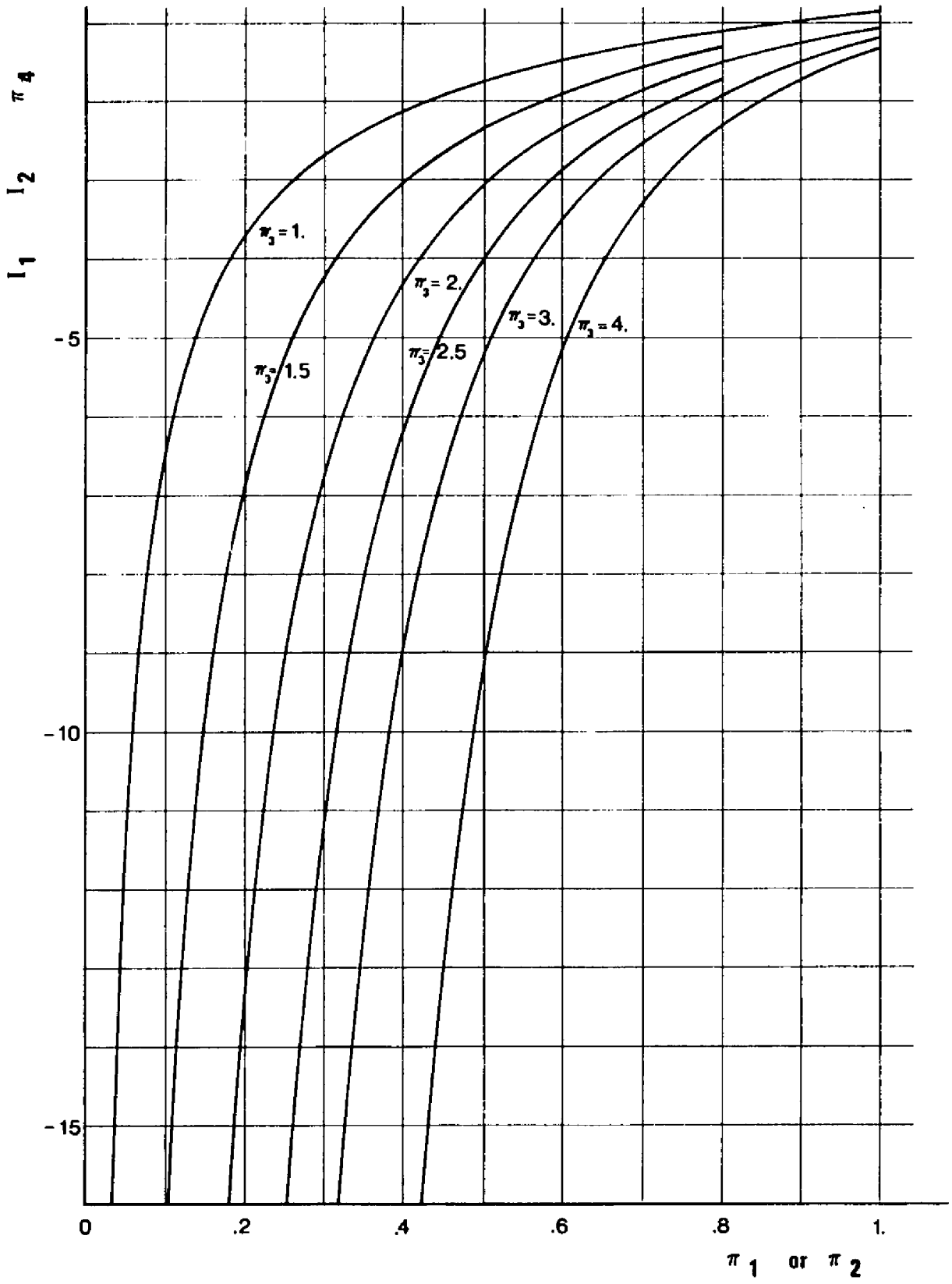

Figure 40. Dimensionless Maximum Film temperature π_1.

$$T_{max} = \pi_1 \times E \tag{59}$$

This is the maximum temperature that can be maintained by viscous dissipation in the film itself. It is reached only under adiabatic conditions at one wall. This is a situation where the generated heat is conducted away to one side alone through the total film thickness. The temperatures in the film are lower under non-adiabatic wall conditions, equation (49) when the generated heat is conducted a shorter distance than the film thickness away to both walls.

The condition for the maximum attainable film temperature, equation (53), is obtained directly from the integrated energy equation (31) and the result of a further integration, the expression for film velocities equation (34) by applying the adiabatic condition at one wall. This condition implies $c_2 = 0 \quad \Gamma = -1$ $\theta,_z(1) = -2\pi_4\pi_5$ and thereby direct $Su(\pi_2, \pi_1, \pi_3) = -1$ which then in itself is the condition for maximum temperature, equation (53). Equation (49) shows that this is the absolute maximum film generated temperature.

Auxiliary diagrams to determine the actual properties π_3 and E of the lubricant might be necessary. Appendix F describes such graphs and the use. Appendix G describes approaches to determine the temperature of the moving surface. Appendix H shows the program used in calculation of equations (57) and (58) in Figure 40. The program consists mainly of a simple summation and requires about 600 msec (on a UNIVAC 1108) for each π_3 value. Similar procedures can easily be prepared for any desired viscosity temperature function.

Determination of the Shear Stress in the Film Via a Graphical Solution

Equation (41) gives the general expression for the dimensionless shear stress as

$$\pi_5 = H_2(\pi_1, \pi_2, \pi_3, \pi_4) \tag{60}$$

The integral is improper in the range of interest $-1 \leq \Gamma \leq 0$ which makes it slightly cumbersome to work with.

The parameter π_5 depends also on four parameters. It is difficult to present this solution in a two-dimensional graph. Two parameters are in most cases the limit for such a presentation.

A somewhat simpler approach is to determine and graphically present the shear stress in the film for the case of the adiabatic wall. Symmetry considerations as illustrated in Table 11 can thereafter be applied.

For this situation, of the adiabatic plane located at the stationary wall (wall number 1) at $z = 0$, the expression for the dimensionless shear stress (equation (41)) reduces to

$$\pi_5 = -\frac{1}{2} \int_{\pi_1}^{\pi_2} \left(-\pi_4 \int_{\pi_1}^{\hat{\theta}} \mu(\xi, \pi_3)^{-1} d\xi \right)^{-1/2} d\hat{\theta} \qquad \pi_2 < \pi_1 \tag{61}$$

because in this case

$$\pi_4 = -\int_{\pi_1}^{\pi_2} \mu(\xi, \pi_3)^{-1} \, d\xi \tag{62}$$

and therefore equation (61) is

$$\pi_5 = H_3(\pi_1, \pi_2, \pi_3) \tag{63}$$

π_5 depends in this case on three parameters only of which the dependency on parameter π_2 in most cases is relatively weak.

Figure 41 shows a graph of equation (63) for π_3 = 1.0, 1.5, 2.0, 2.5, 3 and 4, and for appropriate π_2 values. The range of π_5 in Figure 41 covers primarily the expected operation of elastohydrodynamic films. The program used to determine π_5 (Figure 41) is found in Appendix I.

The interpolation procedure to determine π_5 can be carried out as two π_5 determinations for the two π_3's nearest to the actual π_3-value of the lubricant. A straight line between these two π_5 values will intersect with the actual π_3 curve of the lubricant giving an approximation to the desired actual dimensionless shear stress π_5.

The shear stress in the film is therefore found as

$$\tau = \pi_5 c_1 (UN)/h \tag{64}$$

π_5 c_1 and (UN) are known. Information about film thickness must be available, from measurements or from calculations, in order to determine the shear stress.

The procedure to determine the maximum temperature and the shear stress has been simplified to solutions via two dimensionless graphs and straightforward calculations. The procedure has assumed Newtonian behavior, constant ratio between measured shear stress and shear rate, of the lubricants as the behavior was found in the investigated shear

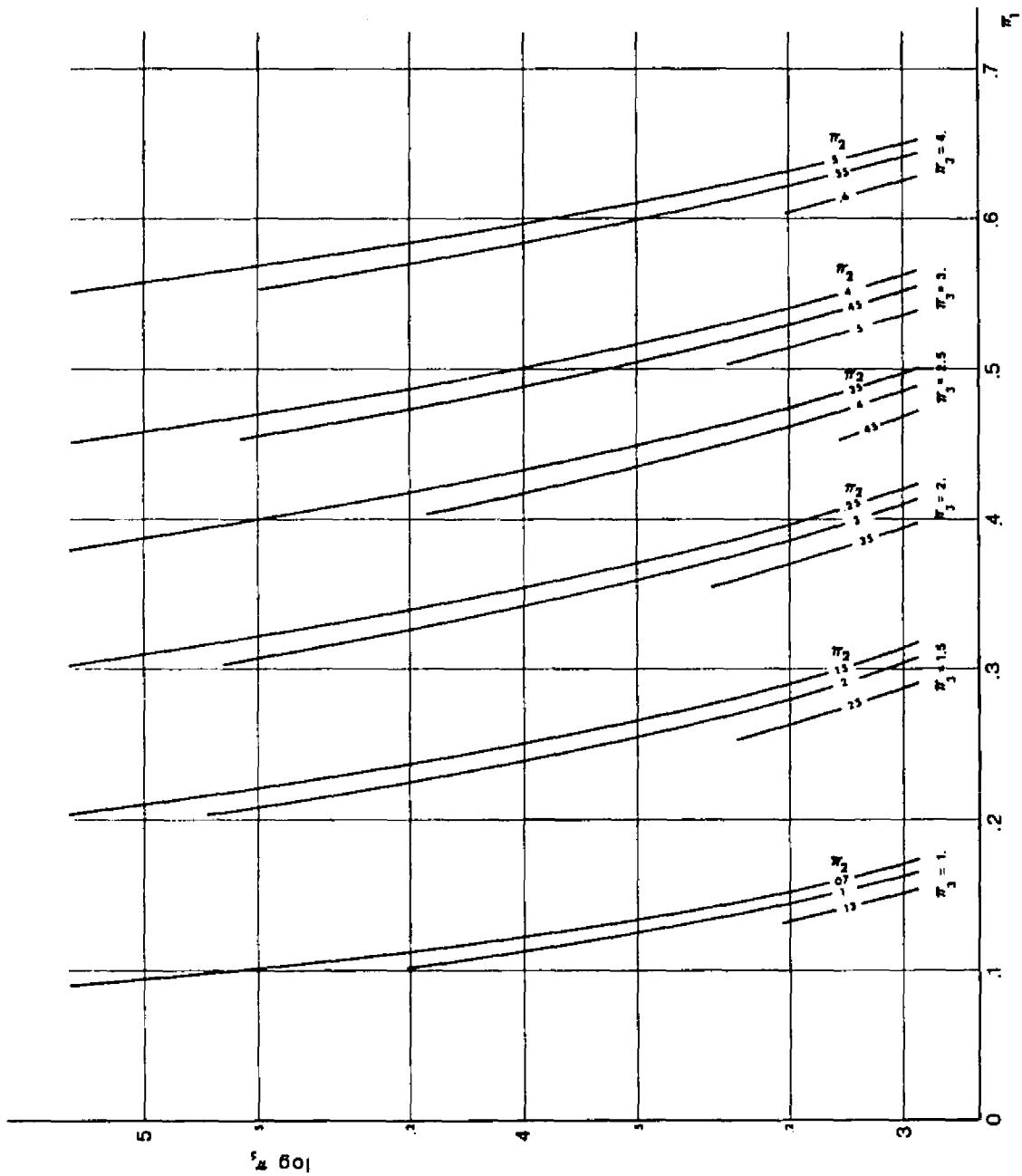

Figure 41. The Dimensionless Shear Stress π_5 in the Film.

stress ranges for diester, polyalkyl aromatic plus additive, dimethyl siloxane and synthetic paraffinic oil in Chapters II and III. The procedure can be used also for some cases when the lubricant exhibits non-Newtonian behavior, changes of the ratio between shear stress and shear rate, particularly when the measured viscosity is dependent on shear stress. The temperature pressure shear stress viscosity relation must be known. One approach is to use a T - p - η relation corresponding to an estimated shear stress. One or two iterations with the diagrams, Figures 40 and 41 are sufficient to obtain interpolated results with satisfactory small inaccuracy.

The procedure assumes liquid behavior of the lubricant as it was found in most of the measurements of the test fluids. The test fluid B3J which showed distinct non-liquid behavior at relatively low shear stresses can not be expected to follow response as predicted by equations (35), (53) and (40), (41), or by Figures 40 and 41. Application of existing theory to predict film thickness might possibly also be questionable for a fluid as B3J in as much as the theory assumes liquid behavior of the lubricant both in the inlet and in the contact area itself. The capillary measurements showed non-liquid response at shear stresses 10^3 less than the average shear stress in the contact. The pressure was 5 - 20 kpsi which corresponds to conditions far out in the inlet region to the elastohydrodynamic contact.

Determination of Temperature and Velocity Gradients in the Film

The description of the flow situation may be completed by determination of the gradients of temperatures and velocities and finally

determination of the location in the film.

The shear rate is found from equation (22)

$$\pi_5 = \mu u_{,z} \tag{22}$$

which is

$$u_{,z} = \pi_5/\mu(\theta) = H_4(\theta,\pi_1,\pi_2,\pi_3,\pi_4,\pi_5) \tag{65}$$

The temperature gradients can be determined from equation (30), which rewritten for the adiabatic wall case is

$$\theta_{,z} = -2\pi_4\pi_5(-Su(\theta,\pi_1,\pi_3))^{1/2} \tag{66}$$

or

$$\theta_{,z} = -2\pi_4^{1/2}\pi_5\left(-\int_{\pi_1}^{\theta} \mu(\xi,\pi_3)^{-1}\ d\xi\right)^{1/2} \tag{67}$$

Determination of the z coordinates of the film is desirable for the purpose of a graphical presentation of profiles of velocity, temperature, and the gradients of these. The z coordinate can be determined through equation (40) which rewritten for the adiabatic wall case is

$$z = 1/(2\pi_4^{1/2}\pi_5)\int_{\theta}^{\pi_1}\left(\int_{\theta^*}^{\pi_1} \mu(\xi,\pi_3)^{-1}d\xi\right)^{-1/2} d\theta^* \tag{68}$$

The Case of the Nonadiabatic Wall

The results from the adiabatic wall can be easily generalized applying the symmetry considerations of Table 11. Assumptions about the wall temperatures must be made in this more general case. Equation (37) yields the Γ value for the film, and equation (45) yields θ_{max}. Equation (I1) will give the π_5 value valid for the part of the film from θ_{max} to π_2 in that θ_{max} supersedes π_1 in (I1). The result of the preceding chapter can be applied directly to the part of the film going from θ_{max} to π_2, in that the velocity of the wall number 2 must be reduced as shown in equation (52).

The z values of the film from θ_{max} to π_2 may be found from equation (40) which simplifies to

$$2\pi_4^{1/2}\pi_5 z = -\int_{\theta_{max}}^{\theta} \left(- \int_{\theta_{max}}^{\theta^*} \mu(\xi,\pi_3)^{-1} d\xi \right)^{-1/2} d\theta^* \qquad \pi_2 \leq \theta \leq \theta_{max} \quad (69)$$

The expression (69) is valid only for the part of the film from θ_{max} to π_2.

Integration from θ_{max} to π_1 of equation (69) will give the z value (the thickness) of the film from π_1 to θ_{max} and thereby both the total dimensionless film thickness and the fraction of the actual film thickness that must be applied in equation (19): $\pi_5 = \tau h/c_1(UN)$ to determine the shear stress τ. (UN) is the above-mentioned reduced velocity. Symmetry about the plane where $u = 1 + \Gamma$ for the temperature range $\pi_1 - \theta_{max} - \pi_1$ completes the profiles of velocity, temperature, and gradients of these.

CHAPTER V

APPLICATION OF THE MAXIMUM TEMPERATURE CONCEPT TO ELASTOHYDRODYNAMIC FILMS

Assumptions

The lubrication situation in an elastohydrodynamic contact deviates in several respects from the assumptions stated in Chapter IV for the derivation of maximum temperature and the shear stress of a liquid lubricant film. The pressure and temperature gradients of the elastohydrodynamic film seem to interfere with the application of the obtained results. Deviations from liquid behavior, one-dimensional velocity situations, and parallelism of the bearing surfaces may, however, also influence the applications to elastohydrodynamic films. This chapter will attempt an evaluation of the effects of the actual deviations from the assumptions.

Parallel Bearing Surfaces

The elastohydrodynamic lubrication of a moderate-to-heavily loaded elastohydrodynamic contact is characterized by a large ratio of film length to film thickness. Although the situation is shown in most of the literature with steep slopes of the bearing surfaces, the actual situation is parallel surfaces over most of the contact area. Both analyses and experiments confirm this (18), (27), (60), (61), (62). Detectable deviations from parallel configuration are usually found only in areas near the exit. The maximum deviation is here angles of the

order of 10^{-3} radians. The average size of the slope over these limited areas is even smaller. The contribution to the traction from these parts of the contact area can, to a first and relatively accurate approximation, be estimated as if the surfaces were completely parallel and of the same film thickness as the main part of the contact area. A more accurate determination of the total traction of the contact can be achieved by adding small correction terms to the stress summation based on an average film thickness in this area. The corrections will expectedly not add significantly to the understanding of the traction mechanism in the contact, but adds only to some increase in accuracy. These corrections can be disregarded in this first treatment without severe loss of accuracy. Measurements of film thickness can be performed with an accuracy of the magnitude of ± 1 μinch. The general range of filmthickness in elastohydrodynamic lubrication goes from about 5 μinch to about 50 μinch. The relative accuracy is thus ± 20% to ± 2%. The comments on parallel configuration are therefore modified with inaccuracies of magnitude 5 - 10% in most cases.

The Pressure Gradients

The pressure distribution in a contact has been investigated, particularly through computer solutions. Figure 42 shows a typical graph of the film pressures.

The computed film pressure shows only minor deviations from the Hertzian pressures over a major part of the high pressure region of the contact area where the greatest contributions to the traction expectedly are generated. The important maximum pressures are the same for the two

curves. The viscosity and traction are therefore not widely different in the high pressure region for the two pressure distributions.

The solutions show a spike of high pressure before the exit region for certain ranges of parameters, Figure 42. The spike has only a small extension in the film direction and will therefore contribute only with an amount equivalent to the hatched area of Figure 42. The spike has furthermore not been demonstrated experimentally in such exaggerated form as shown in Figure 42.

As such it might be regarded to some degree as a computer generated phenomenon only and not a physical reality. Its influence on the total traction may therefore be disregarded without severe loss of accuracy.

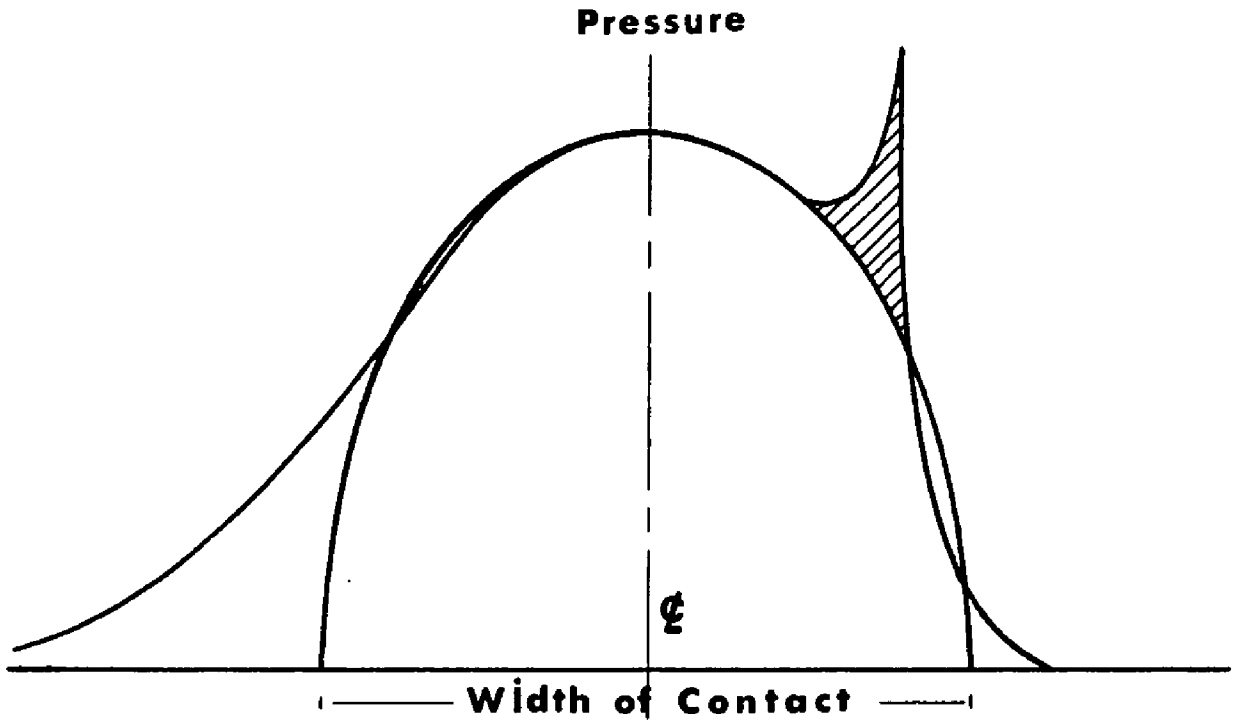

Figure 42. Typical Computer Solution of the Pressure Distribution in an Elastohydrodynamic Contact. (The Hertzian pressure distribution is shown for comparison.)

The pressure rise ahead of the contact often represents a significant contribution to the generated normal load. The viscosities in this area are low due to the near exponential pressure viscosity relation for the lubricants. The film thickness increases furthermore rapidly outside the contact area so that the net contribution to the total traction force will probably be considerably smaller than the contribution from the contact area itself.

Experimental investigations of pressure distribution for rolling contacts have been conducted. Figure 43 shows typical examples of reported measurements.

The measurement technique and the lubricants vary widely. The pressure profiles characteristically do not have many details in common. The maximum pressures measured are, however, of the same magnitude as the Hertzian maximum pressure.

The pressure transducers and the applied data reduction technique in these investigations can be evaluated to possess sufficient accuracy and selectivity to record the actual pressures. Unreported quantities, such as lubricant characteristics, solidification, etc., can, however, influence the recordings, particularly with respect to a diminishing of maximum pressures.

It will be shown in the following that the influence of pressure gradients on the shear stress is very small for the contact region with high pressures, high viscosities, and high shear stresses. It is assumed that actual pressure gradients are of the same magnitude or smaller than the gradients of the Hertzian pressure as experienced and shown in Figures 42 and 43. The Hertzian pressure distribution is therefore chosen

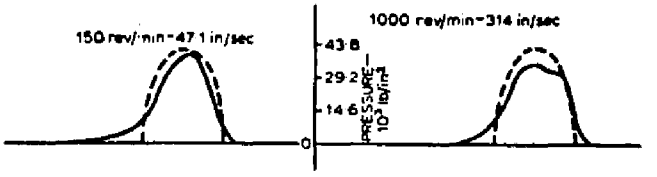

Broken lines are Hertzian contact pressure distributions according to calibration. The pressure profiles are corrected for temperature effects. Load 1000 lb/in, Acme H oil.

Effect of rolling speed on pressure - 50 and 1000 rev/min

From Cheng, H. S. and Orcutt, F.K. 'A correlation between the theoretical and experimental results on the elastohydrodynamic lubrication of rolling and sliding contacts', Proc Instn Mech Engrs 1965-66, Vol 180 Pt 3B, page 164.

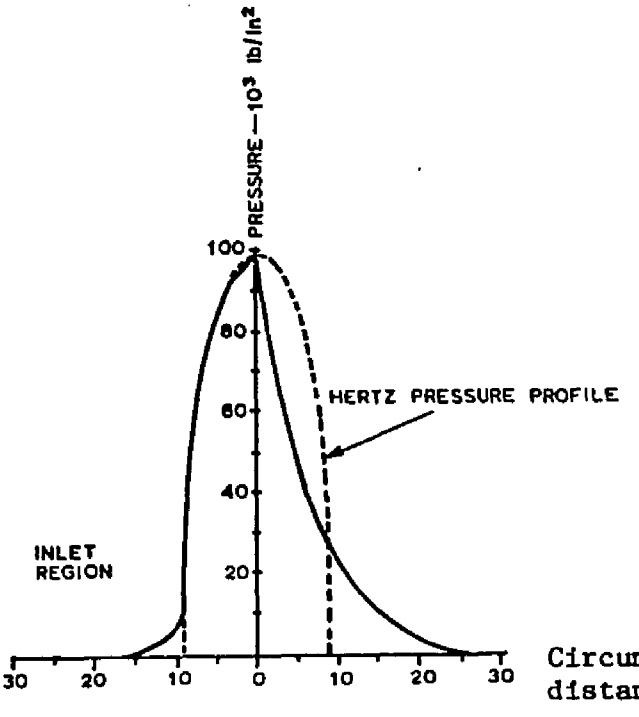

Preliminary film-pressure profile obtained using averaging process. P_h = 100 000 lb/in^2. T = 175 °F. RS = 2520 ft/min. Lubricant: polyphenyl-ether.

From Kannel, J.W. 'Measurements of pressures in rolling contact', Proc Instn Mech Engrs 1965-66, Vol 180 Pt 3B, page 137.

Figure 43. Typical Examples of Reported Pressure Measurements in Elastohydrodynamic Contacts.

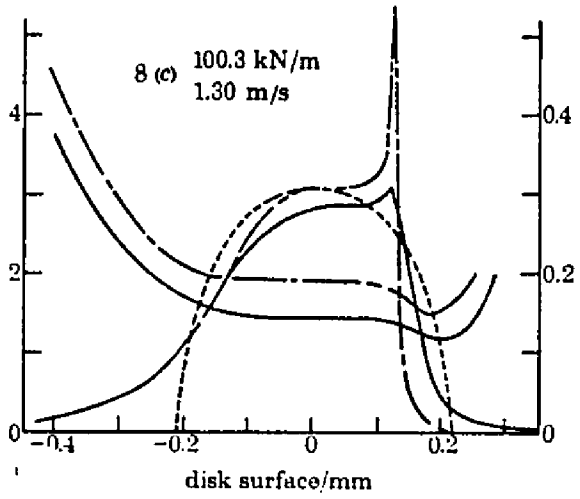

From Hamilton, G. M. and Moore, S. L., Deformation and pressure in an elastohydrodynamic contact. Proc. Roy. Soc. Lond. A. 322, 313-330 (1971).

Rolling disks. 26.9°C 184 cp.

Figure 43. (Continued)

as a representative case for the elastohydrodynamic film in the evaluation of the influence of pressure gradients on the shear stress. It is assumed that the Hertzian pressure distribution is representative both for line contacts, with a symmetric pressure distribution about a plane, and for point contacts, with an axisymmetric pressure distribution.

The Shear Stress in the Film for an Elastohydrodynamic Point Contact

The assumptions of Table 10 Chapter IV, are assumed, except assumption 3 which is changed to $p = p(x_1)$. The lubrication situation is the same as the situation of the preceeding Chapter IV. The Figure 39 of Chapter IV, which shows configuration and coordinate orientation, is reproduced here. The Table 10 of Chapter IV, Assumptions, is also reproduced however with assumption 3 changed to $p = p(x_1)$.

The reduction of the equation of mass conservation and the energy equation of the previous chapter are not changed by the change to $p = p(x_1)$. The equations of motion are reduced to

$$p_{,1} = \left(\eta(u_{1,3})\right)_{,3} \tag{1}$$

Integration of equation (1) gives

$$p_{,1}x_3 = \eta u_{1,3} - c_5\left((UN),p_{,1}\right) \tag{2}$$

If one assumes that the constant c_5 can be written as

$$c_5 = -p_{,1}\, h/2 + \tau(UN) \tag{3}$$

where $\tau(UN)\big|_{UN=0} = 0$ then equation (2) converts to

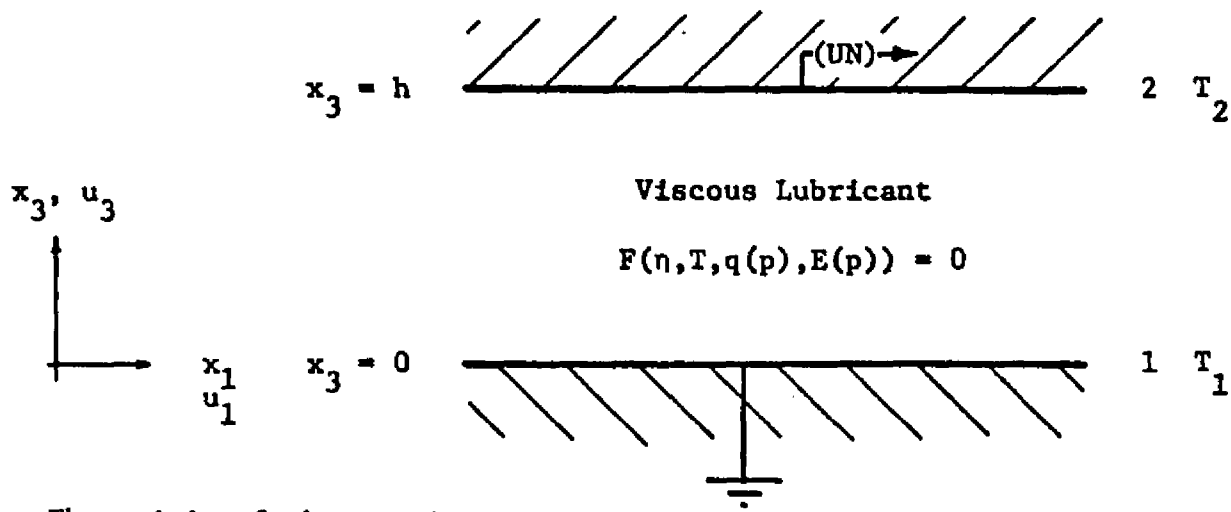

The origin of the coordinate system is located at the center of the elastohydrodynamic contact.

Coordinates with dimensions:

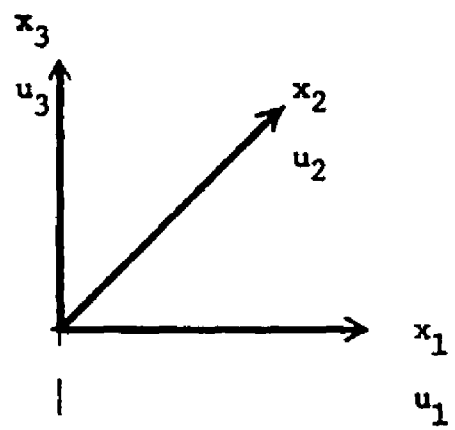

Dimensionless coordinates:

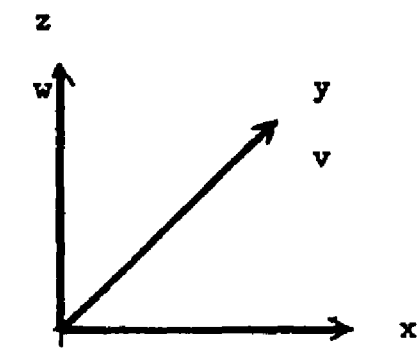

Figure 44. The Lubrication Situation, Flow of a Viscous Lubricant between Parallel Bearing Surfaces.

Table 12. Assumptions.

1.	Steady state conditions. Laminar flow
2.	$u_1 = u_1(x_3)$ only; $u_2 = 0$; $u_3 = 0$; $u_1(0) = 0$; $u_1(h) = (UN)$
3.	$p = p(x_1)$
4.	Body forces are zero.
5.	$T = T(x_3)$ only; $T(0) = T_1$ = constant; $T(h) = T_2$ = constant.
6.	$\rho = \rho(x_2,x_3)$
7.	$c_v = c_v(x_2,x_3)$
8.	$k_t = k_t(x_1,x_2)$

$$\tau = p_{,1}(x_3-h/2) + \tau(UN) \tag{4}$$

which satisfies equation (1).

Equation (4) shows that the local shear stress is a linear combination of a term dependent only on the pressure gradient and a term dependently only on the velocity (UN) of the sliding bearing surface.

An integration of equation (4) with respect to x_1 from inlet to outlet shows that the contribution from the pressure gradients to the total traction is zero in a parallel plate configuration. The effect of the presence of pressure gradients is therefore primarily an influence on the assumed condition $u_{1,1} = 0$.

An investigation of the relative magnitude of the two shear stress terms of equation (4) over the major part of the contact area shows that the term dependent on the pressure gradient is very small compared to the term dependent on the velocity of the sliding wall.

The chosen Hertzian pressure distribution, which is selected as a representative case for the elastohydrodynamic film over the major part of the contact area, is described by

$$(p/p_m)^2 + (r/a)^2 = 1 \tag{5}$$

where $r = x_1$ or by

$$p/p_m = \bar{p} = (1-\bar{\rho}^2)^{1/2} \tag{6}$$

where p_m is the maximum Hertzian pressure, a is the radius of the point contact, $\bar{\rho} = r/a$ and $\bar{p} = p/p_m$. The pressure gradient is

$$p_{,r} = -(p_m/a)\bar{\rho}(1-\bar{\rho}^2)^{-1/2} \quad \text{or} \quad \bar{p}_{,\bar{\rho}} = -\bar{\rho}(1-\bar{\rho}^2)^{-1/2} \tag{7}$$

A typical value of the gradient of $p_{,r}$ is $p_{,r} \simeq 10^7$ psi/inch obtained for the conditions $p_m \simeq 150$ kpsi, $a = 7 \times 10^{-3}$ inch and $\bar{\rho} = r/a = 1/2$. (The more accurate value of $p_{,r}$ for this example is 1.24×10^7 psi/inch.) In that

$$W = p_m a^2 \, 2\pi/3 \qquad a = (WR_b\Delta 3/4)^{1/3} \tag{8}$$

where W is the bearing load, R_b is the equivalent radius of the contacting surfaces ($R_b^{-1} = R_1^{-1} + R_2^{-1}$) and

$$\Delta = (1-\sigma_i^2)/E_i \qquad i=1,2 \tag{9}$$

then

$$p_m/a = 2/\pi R_b \Delta \tag{10}$$

The ratio between the Hertzian normal stress and the radius of the contact depends thus on the effective radius R_b and material constants σ_i, E_i only, but not on the bearing load.

If one defines

$$H = h/R_b \quad \text{and} \quad U = c_1(UN)/R_b E' \tag{11}$$

where

$$E' = 2/\Delta \tag{12}$$

then the ratio π_α between the two shear stress terms of equation (4)

$$\pi_\alpha = p_{,1}\ (x_3 - h/2)/\tau(UN) \tag{13}$$

becomes

$$\pi_\alpha = (H^2/\pi_5 U)(\bar{p}_{,\bar{\rho}})(z - 1/2)/\pi \tag{14}$$

The Ratio Between Shear Stresses Generated by the Pressure Gradient and by the Sliding Motion

Equation (14) shows that the magnitude of the ratio π_α between the two stress components is determined primarily by the dimensionless numbers H, U, and π_5 over the major part of the contact area.

Figure 45 shows that the magnitude of the dimensionless pressure gradient is limited to a factor of about 2 for $\bar{\rho}$ less than approximately .9. The pressure curve shows that the Hertzian pressure at this location is only about 40 per cent of the maximum pressure. The pressure decreases rapidly and the deviation of the actual pressure (Figures 42 and 43) from the Hertzian pressures increases with further increase in $\bar{\rho}$. The viscosity decreases very rapidly in the region $\bar{\rho} > .9$ due to the near exponential pressure viscosity dependency of the lubricant. The value of π_α will therefore expectedly increase rapidly for $\bar{\rho} > .9$.

The pressure gradient $\bar{p}_{\bar{\rho}}$ (part of equation (14)) is less than 2.06 if $\bar{\rho}$ is less than the selected value .9. The numerical value of the term $(z - 1/2)$ of equation (14) is furthermore less than or equal to 1/2.

The numerical value of the ratio π_α is therefore

$$|\pi_\alpha|_{\bar{\rho}\leq.9} = \pi_{\alpha.9} \leq .328(H^2/\pi_5 U) \tag{15}$$

where the factor .328 is $(2.06/2\pi)$.

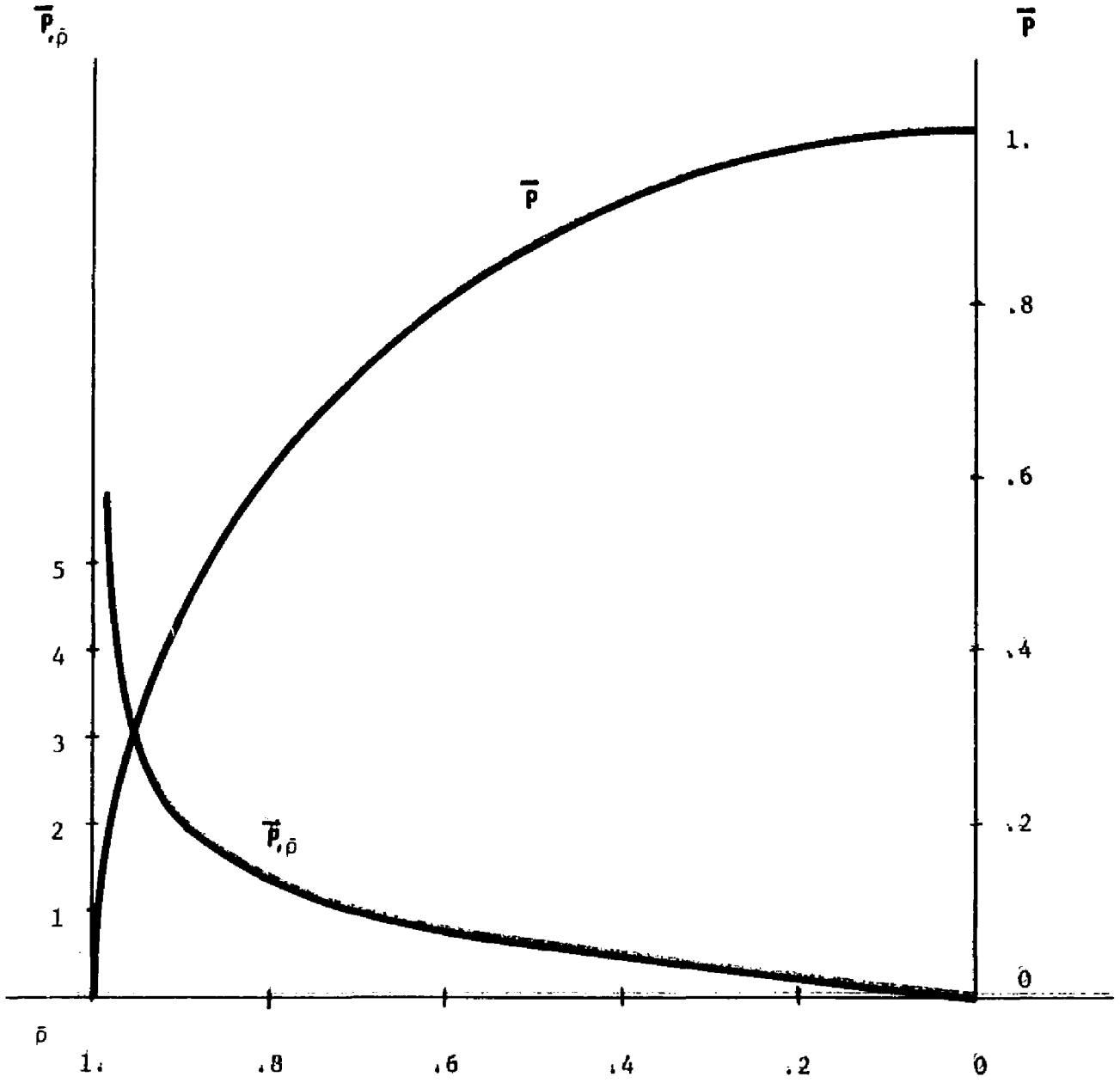

Figure 45. Dimensionless Pressure and Pressure Gradient of a Hertzian Contact.

The Ratio π_α in Actual Lubrication

The ranges of H_1 π_5 and U are

$$H: \quad 5 \times 10^{-6} - 50 \times 10^{-6} \text{ inches}$$

$$\pi_5: \quad 5 \times 10^{3} - 10^{5}$$

$$U: \quad 10^{-13} - 10^{-14}$$

when the range of u is 10-100 ips. The range of $\pi_{\alpha.9}$ is $1 \times 10^{-2} - 1 \times 10^{-1}$.

The results of the traction measurements (39), (66), (67), for 23 synthetic and non-synthetic unmixed lubricants have been used to investigate the range of π_α in actual experiments. Table 13 shows the range of the upper limit for $\pi_{\alpha.9}$. The values of $\pi_{\alpha.9}$ are seen to be generally only a minor fraction of 1. When $\pi_\alpha << 1$, then

$$p,_1(x_3-h/2) = (\eta u_{1,3})_{p,} << \tau(UN) = (\eta u_{1,3})_{sl} \tag{16}$$

where p, symbolizes pressure gradient and sl symbolizes sliding. Equation (4) rewritten is

$$u_{1,3} = (1/\eta)(\eta u_{1,3})_{p,} + (u_{1,3})_{sl} \tag{17}$$

which states that velocity changes due to the pressure gradient are << velocity changes due to the sliding velocity (UN) at any x_3 location when $\pi_\alpha << 1$. Equation (17) states furthermore that velocity changes are independent of x_1 or x_2 location in the film when $x_3 = h/2$.

Therefore it can be seen that the pressure term has only a very limited influence on the film behavior in the circular parallel plate

Table 13. The Ratio π_α between Shear Stress Generated by The Pressure Gradient and The Shear Stress Generated by The Sliding Motion.

Fluid	13.7	27.4	54.8 ips
		Per cent	
FN 2961	2.4	3.3	5.7
MCS 460	.9	1.4	2.5
MCS 418	.8	1.4	2.6
DN 600	.9	1.8	3.5
Adv. Ester	.4	1.2	3.0
Form. Adv. Ester	.4	1.2	2.9
Naph. Min. Oil	2.1	3.2	6.9
Synth. Para. Oil	4.5	9.0	15.0
DN 600 + Add.	1.0	1.4	3.3
Siloxane 1	.4	.5	-
- 2	5.7	10.6	-
- 3	1.2	2.5	-
- 4	3.3	5.5	-
- 6	4.2	7.8	-
- 7	5.2	9.1	-
- 8	3.0	5.7	-
- 9	4.0	5.7	-
- 10	2.7	4.6	-
- 12	.5	.9	-
- 13	4.3	7.3	-
- 14	2.3	3.5	-
- I	.3	.6	-
- J	1.6	2.6	-

configuration for radius $\bar{\rho}$ less than approximately .9. Equations (1) and (2) may thus be approximated with

$$0 = \left(\eta(u_{1,3})\right)_{,3} \tag{18}$$

and

$$\tau = \tau(UN) \tag{19}$$

to the extent that $p_{,1}$ can be disregarded (when $\pi_\alpha << 1$). Equations (18) and (19) are identical to equations (9) and (11) of Chapter IV. The results from that chapter may thus be used as approximations for elastohydrodynamic films described in Figure 42 or Figure 43 with $p_{,1} \neq 0$ wherever the condition $\pi_\alpha << 1$ is satisfied.

The pressure Gradient $p_{,2}$

The assumption 3 of Table 10 can be expanded to $p = p(x_1, x_2)$. The gradients $p_{,1}$ and $p_{,2}$ are equal in the selected referential Hertzian pressure distribution. The corresponding gradients in the actual circular contact are also of the same order of magnitude in the high pressure-high traction center area due to the containment effect of the restrictions at the exit and at the sides. The velocity changes due to the gradient $p_{,2}$ is thus of the same order of magnitude as the velocity changes due to the gradient $p_{,1}$ and can also be neglected when $\pi_\alpha << 1$. This implies that the velocity u_2 can be approximated with zero.

The Pressure Gradient $p_{,3}$

The assumption 3 can be expanded further to $p = p(x_1,x_2,x_3)$. The equation of motion in the 3 - direction is then reduced to

$$p_{,3} = (\eta(u_{1,3}))_{,1} \tag{20}$$

or

$$p_{,3} = \eta_{,1} u_{1,3} \tag{21}$$

The expansion to $p = p(x_1,x_2,x_3)$ implies that $p_{,1} = p_{,1}(x_3)$. The pressure gradient $p_{,1}$ is however only a weak function of x_3 in an actual film. The expression $p_{,1} \neq p_{,1}(x_3)$ can therefore be assumed to be a realistic approximation. Equation (1) can thus be integrated to equation (2) also when $p = p(x_1,x_2,x_3)$ assuming $p_{,1} \neq p_{,1}(x_3)$.

The viscosity changes several orders of 10-magnitude during the passage in the x_1 direction of the lubricant through the contact. Typical values are 1 Reyn/inch near the stationary wall to 10^3 Reyn/inch near the moving wall. The corresponding shear rates are typically 10^7 sec^{-1} to 10^4 sec^{-1}. The pressure gradient $p_{,3}$ is thus of the same magnitude as $p_{,1}$ (10^7 psi/inch). The gradient $p_{,3}$ does not vary greatly in the x_3 direction as the example of typical values of viscosity changes and shear rates indicates. Its effect is to create slightly different pressures on the moving wall from those on the opposite stationary wall. The pressure difference is of a magnitude of 10-100 psi. The difference has the same sign as the sign of $p_{,1}$. The net effect on the load carrying is therefore zero for a Hertzian pressure

distribution. The pressure gradient $p_{,3}$ does not influence the velocities.

It can be summarized that the pressure gradients $p_{,1}$ $p_{,2}$ $p_{,3}$ do not influence the simple flow situation that was assumed in Chapter IV provided the condition $\pi_\alpha << 1$ is satisfied. This implies that the velocities can be approximated with $u_2 = u_3 = 0$ and $u_1 = u_1(x_3)$.

The Effect of the Temperature Gradients $T_{,1}$ and $T_{,2}$ Incompressible Lubricants

The assumptions for correct determination of shear stress and maximum temperatures are that temperature is a function of the x_3 coordinate only, and that the wall temperatures are constant. The temperatures in an actual elastohydrodynamic film are also functions of the x_1 and x_2 ordinates. The degree to which the condition: $(T=T(x_3))$ is fulfilled is investigated in the following:

The density of the lubricant varies less than approximately 5 per cent during the passage through the high pressure part of the contact. The case of incompressible liquid will therefore be considered first as a relevant approximation.

The energy equation written out in its terms is

$$c_v\rho(T_{,t}+u_iT_{,i})= (k_tT_{,i})_{,i} + \Phi \qquad i = 1,2,3 \qquad (22)$$

The condition of steady state eliminates the term $T_{,t}$. Measurements of film temperatures in elastohydrodynamic point contacts (68), (69), have shown that the temperature differences (ΔT) found in the x_1-direction at any given x_3 level are of the same order of magnitude

as the temperature differences over the film. This therefore states that

$$0(T,_3) = (a/h)\left(0(T,_1)\right) \tag{23}$$

where 0( ) symbolizes: The order of magnitude of ( ).

Further $$\left\{\left(k_t(T,_3)\right),_3\right\} = (a/h)^2\left\{0\left(k_t(T,_1)\right),_1\right\} \tag{24}$$

Axisymmetry of elastohydrodynamic point contacts justifies the further statements

$$0(T,_1) = 0(T,_2) \qquad 0\left((T,_1),_1\right) = 0\left((T,_2),_2\right) \tag{25}$$

The increase in temperature T is typically in the range 100 - 200°F.

The condition $\pi_\alpha << 1$ may be interpreted as

$$0(u_2) = (h/a)\left(0(u_1)\right) \tag{26}$$

For non-sliding conditions:

$$0(u_3) = (h/a)\left(0(u_2)\right) \tag{27}$$

Equation (27) is however justified also for sliding conditions.

Application of the principle of superposition for sliding condition, validated, for example, at equation (4), then leads to

$$0(u_3) = (h/a)^2\left(0(u_1)\right) \tag{28}$$

Equation (22) can thus be rewritten as

$$(1/\kappa)\ \left(O(u_1)\right)\left(O(T,_1)\right)(1+2h/a) = O(T,_{33})\left(1+2(h/a)^2\right) + \Phi/k_t \qquad (29)$$

where $\kappa = k_t/\rho c_v$ and k_t is constant.

The ratio h/a is of a magnitude of 10^{-3}. The equation (22) can therefore be approximated with

$$(1/\kappa)u_1T,_1 = T,_{33} + \Phi/k_t \qquad (30)$$

without significant loss of accuracy.

$$\Phi = \eta(u_1,_3)^2 \qquad (31)$$

Nondimensionalization of equation (30) gives

$$\pi_\beta u\theta,_x = \theta,_{zz} + 2\pi_4\pi_5 u,_z \qquad (32)$$

where

$$\pi_\beta = h^2(UN)/\kappa a \quad \text{and} \quad \theta,_x = T,_1 a/E \qquad (33)$$

The boundary conditions are

$$\begin{aligned} u(0) &= 0 \qquad \theta(0) = \pi_1 \\ u(1) &= 1 \qquad \theta(1) = \pi_2 \end{aligned} \qquad (34)$$

as before.

The convection term of equation (32) can at some locations in the film be considerable compared to the terms $|\theta,_{zz}|$ or $2\pi_4\pi_5 u,_z$. An evaluation of the influence of the convective term on the velocities in

the film can therefore not be performed easily. A lower and upper bound for changes of film temperatures and velocities can, however, be established in terms of the relative magnitude of the convection element of equation (32).

π_β and u of the convective term are positive. The temperature gradient $\theta_{,x}$ has extremum approximately for $\bar{\rho} \pm 1/2$. $\theta_{,x}$ is positive ahead of the center of the contact and negative after the center. It does not vary considerably in the direction perpendicular to the film. $\pi_4\pi_5$ and $u_{,z}$ are positive and $\theta_{,zz}$ is in general negative. The numerical values of the terms $\theta_{,zz}$ and $u_{,z}$ are both great near the stationary hot surface and small at the sliding cold surface.

The velocity u is the only factor in the convection term which varies considerably. The velocity u is zero at the stationary wall where $\theta_{,zz}$ and $u_{,z}$ are of great magnitude. The convection term is therefore not significant near the stationary wall ($0 \leq z << 1$). The value of u is at its maximum for z = 1 at the moving wall, where the terms $\theta_{,zz}$ and $u_{,z}$ have their smallest numerical values. It is therefore likely that the convection term of equation (32) may have significant influence on the film behavior, at least in the neighborhood of locations where both conditions u = 1 and $\theta_{,xx} = 0$ are fulfilled.

Integration of equation (32) yields

$$\theta_{,\zeta}\Big|_0^z + 2\pi_4\pi_5 u = \pi_\beta \int_0^z \theta_{,x} u \, d\zeta \tag{35}$$

when $\pi_\alpha << 1$.

The case of adiabatic conditions at the stationary wall is a particularly important and simplified situation. This situation alone will be considered. The gradient $\theta,_x$ does not vary considerably over the film thickness. It can therefore be approximated with the maximum value $\theta,_{xM}$ without appreciable loss of closeness of the upper and lower bounds. These two considerations change equation (35) into

$$\theta,_z + 2\pi_4\pi_5 u = \pi_\beta \theta,_{xM} \lambda(z) \tag{36}$$

where

$$\lambda(z) = \int_0^z u(\zeta)d\zeta \ . \tag{37}$$

Reorganization and integration from 0 to z yield

$$\int_0^z \left[\frac{\theta,_\zeta}{\mu\pi_4} + 2u,_\zeta \left(u - \frac{\pi_\beta}{2\pi_4} \frac{\theta,_{xM}}{\pi_5} \lambda(\zeta) \right) \right] d\zeta = 0 \tag{38}$$

or

$$Su(\theta,\pi_{10}) + u^2 - 2\bar{D} \int_0^z u,_\zeta \lambda(\zeta)d\zeta = 0 \tag{39}$$

where

$$\bar{D} = \frac{\pi_\beta \theta,_{xM}}{\pi_4 \pi_5{}^2} \tag{40}$$

and π_{10} is the temperature at the stationary wall when $\bar{D} \neq 0$. A quantity $\lambda_m(z)$ can be defined such that

$$\lambda_m(z) = 1/u(z) \int_0^z u,_\zeta \lambda(\zeta) d\zeta \tag{41}$$

Equation (39) converts therefore to:

$$Su(\theta,\pi_{10}) + u^2 - 2\bar{D}\lambda_m(z)u = 0 \tag{42}$$

from which:

$$u = \bar{D}\lambda_m(z) + \left(\bar{D}^2\lambda_m^2(z) - Su(\theta,\pi_{10})\right)^{1/2} \tag{43}$$

as $\theta,_z < 0$ in $z[0,1]$. Equation (43) yields (when z=1)

$$1 = \bar{D}\lambda_m(1) + \left(\bar{D}^2\lambda_m^2(1) - Su(\pi_2,\pi_{10})\right)^{1/2} \tag{44}$$

The corresponding expressions are

$$u_H = \left(-Su(\theta,\pi_1)\right)^{1/2} \tag{45}$$

$$1 = \left(-Su(\pi_2,\pi_1)\right)^{1/2} \tag{46}$$

when convection is disregarded. Equations (44) and (46) show that

$$\pi_1 > \pi_{10} \qquad \text{when } \bar{D} > 0 \tag{47}$$

$$\pi_1 < \pi_{10} \qquad \text{when } \bar{D} < 0 \tag{48}$$

and

$$2\bar{D}\lambda_m(1) = Su(\pi_1,\pi_{10}) \tag{49}$$

neglecting terms of $O(\bar{D}^2)$. $O(\lambda_m(1)) = 1$

From equation (49) it can be seen that

$$4\pi_4\bar{D}\lambda_m(1) \simeq \left[\left(1/\mu(\pi_{10})\right) + \left(1/\mu(\pi_1)\right)\right](\pi_1-\pi_{10}) \tag{50}$$

This equation determines the approximate temperature difference $(\pi_1-\pi_{10})$ from the case, when convection is disregarded, expressed in terms of $\bar{D}$ and an easily evaluated upper bound of $\lambda_m(1)$.

$$\lambda_m(z)u(z) = \int_0^z u,_\zeta \lambda(\zeta)d\zeta = \left(u(\zeta)\int u(\zeta)d\zeta\right)\Big|_0^z - \int_0^z u^2(\zeta)d\zeta \tag{51}$$

A typical maximum value of the temperature difference $\pi_1 - \pi_{10} = \Delta\pi_1$ can be evaluated by assuming that $\lambda_m(1)_{max} = 1$. The orders of magnitude of π_4, $\bar{D}$, and $\mu(\pi_1)$ are in the case of a relatively thick elastohydrodynamic film (h ~ 30 μ inch, u ~ 50 ips) where the possible distortion effect from the convection term on the velocities is greatest:

$$0(\pi_4) = 10^{-5}$$

$$0(\bar{D}) = 10^{-2}$$

$$0\left(\mu(\pi_1)\right) = 10^{3}$$

The order of $\Delta\pi_1$ thus becomes

$$0(\Delta\pi_1) = 10^{-4}$$

The order of the temperature difference ΔT_1 therefore becomes $10^{-4} \times E$ or about .08 ^oF (E = 800 ^oR) to 1. ^oF (E = 10000 ^oR)

The influence from the convection term on the temperature at the

stationary wall is thus not significant.

Velocity Changes Due to the Convection Term

A velocity u_L can be defined as

$$u_L = \left(-Su(\theta,\pi_{10})\right)^{1/2} = \left((-1/\pi_4)\int_{\pi_{10}}^{\theta} \mu(\zeta)^{-1}d\zeta\right)^{1/2} \tag{52}$$

Equations (43) and (45) then give ($\theta_{,x} > 0$)

$$u_L + \bar{D}\lambda_m(z) < u < \bar{D}\lambda_m(z) + \left(\bar{D}^2\lambda_m^2(z) + u_H^2\right)^{1/2} \tag{53}$$

When z = 1, then from equation (49), (45) and (52)

$$u_H^2(1) - u_L^2(1) = 2\bar{D}\lambda_m(1) \tag{54}$$

or

$$1 - u_L^2(1) = 2\bar{D}\lambda_m(1) \tag{55}$$

$u_L(1)$ can be approximated with $1 - D\lambda_m(1)$ which then gives

$$u_H(1) - u_L(1) = \bar{D}\lambda_m(1) \tag{56}$$

When $z \neq 1$

$$u_H - u_L < \bar{D}\lambda_m(1) \tag{57}$$

which gives (from equation (53))

$$\bar{D}\lambda_m(z) - \bar{D}\lambda_m(1) < u - u_H \leq 2\bar{D}\lambda_m(z) \tag{58}$$

in that

$$\bar{D}\lambda_m(z) + u_H \geq \left(\bar{D}^2\lambda_m^2(z) + u_H^2\right)^{1/2} \tag{59}$$

The velocity difference $u - u_H$ is therefore

$$-\bar{D}\lambda_m(1) < u - u_H < 2\bar{D}\lambda_m(1) \tag{60}$$

A maximum value of $\lambda_m(1)$ may be estimated considering the maximum velocity profile $u = 1$. This profile can be described by $u = \lim z^n$ $(n \to 0)$. λ_m is then $\lambda_m(z,n)$. and

$$\lambda_m(1,n) = n/(n+1)(2n+1) \tag{61}$$

$$\lim_{n \to 0} \lambda_m(1,n) = 0 \tag{62}$$

The maximum velocity profile does thus not give the upper bound for $\lambda_m(1)$. This result can be obtained also from equation (42).

The minimum velocity profile $u = 0$ described by $u = \lim z^n$ $(n \to \infty)$ gives

$$\lim_{n \to \infty} \lambda_m(1,n) = 0 \tag{63}$$

An estimate of the order of magnitude of the maximum value of $\lambda_m(1)$ can be obtained under the assumption that the expression $u = z^n$ describes the actual velocity profile adequately. With this assumption

$$\lambda_m(1,n)_{max} = .173 \tag{64}$$

obtained for $n = 2^{-(1/2)}$. The velocity difference $u - u_H$ is therefore bound by the inequalities

$$-.18\ \bar{D} < u - u_H < .35\ \bar{D} \tag{65}$$

The factor $\bar{D}$ is typically about 10^{-2} in a moderate loaded elastohydrodynamic contact. Distortion of the flow is insignificant and can be disregarded in an approximate treatment of the traction in the high pressure area of the contact. Then $u_1 = u(x_3)$; $u_2 = 0$; $u_3 = 0$; provided the condition $0(\bar{D}) \leq 10^{-2}$ is satisfied.

CHAPTER VI

DISCUSSION AND CONCLUSIONS - EXPERIMENTAL WORK

Fluid Measurements

The high shear stress characteristics as well as low shear stress characteristics have been investigated for five well defined representative lubricants comprising synthetic hydrocarbons, a silicone oil and a high concentration blend of a high molecular weight viscosity index improving polymer in a straight mineral oil. The range of applied pressure levels was typically from 20 kpsi to 100 kpsi. The applied temperature range was from 10°F to 300°F, however, temperatures as low as -50°F have been used for the purpose of exploration. All investigated lubricants show liquid behavior at low shear stress measurements within the individually applied ranges of pressure level and temperatures.

The low shear pressure temperature viscosity characteristics for the investigated hydrocarbon lubricants all show decreasing pressure viscosity exponent α as function of pressure and temperature, where α is defined as the slope $(\ln\eta)_p$ (in a $\ln\eta$-p presentation) of the viscosity pressure characteristic at any p,T. Presentation in $\ln\ln\eta$-lnT diagrammatic form shows characteristics tending to approach a straight line configuration with nearly constant slope for each hydrocarbon lubricant.

The siloxane also shows decreasing pressure viscosity exponent with increasing temperature. The exponent α decreases with increasing

pressure however only in the range up to 20-60 kpsi. The exponent for siloxane increases thereafter with further increases in pressure level and at an accelerating rate. This behavior is similar to the behavior of the silicone oil investigated earlier, Dow Corning "550 Silicone," Sample 53-H of the Pressure Viscosity Report ASME 1953 (2).

The viscosity level of the lubricants is of the order of 20 cp at atmospheric pressure and room temperature except the level for one synthetic hydrocarbon which has a base viscosity of about 700 cp and the viscosity level for the polymer blend which has a base viscosity of about 1000 cp.

The high shear stress investigation was conducted with capillaries of length to diameter ratios 14.9 and 1.35, capillary 1 and capillary 0 respectively. The viscosity level during the measurements was 10^3 - 10^4 cp which was achieved by adjusting the operational temperature for each lubricant in question and applying pressure levels in the range up to 50 kpsi. The maximum obtained shear stress, at the capillary wall, was in the range 500 - 700 psi (3.5×10^7 - 4.8×10^7 dyn/cm^2). The applied pressure drop was in the range about 10 psi to above 10^3 psi. The flow curves, viscosity as function of shear stress plotted in a $\ln\tau$-$\ln\eta$ presentation, show constant viscosity independent of shear stress for small applied pressure drop, less than approximately 250 psi, for all the unblended lubricants. The viscosities measured at low pressure drop are consistent with the results of the low shear stress measurements. The flow curves show an apparent viscosity decrease with greater pressure drop than about 250 psi. The measured apparent viscosities deviate from the low shear stress constant viscosity at an

accelerating rate with increase in pressure drop. The flow curves for all the unblended lubricants, measured with both capillary 1 and capillary 0, can be shown to be mutually congruent within a margin of estimated experimental error. The measurements can thus be described with one and only one standard flow curve displaced at locations along the shear stress axis, corresponding to the L/D of the capillary, and along the viscosity axis, corresponding to variations in viscosity level. The flow curves obtained with capillary 1 show a deviation from constant viscosity characteristics in shear stress ranges and shear rate ranges where capillary 0 measurements show constant viscosity. This observation excludes shear thinning effects as an explanation of the deviation from constant viscosity characteristics measured with capillary 1 (the viscosity is measured to be constant in the range of capillary 1) and emphasizes dissipation heating as a primary mechanism in the formation of the deviating flow curves. The identical configuration for flow curves obtained with capillary 0 and capillary 1 suggests that shear thinning effects can be excluded and that dissipation heating can be assumed as explanation of the deviation from constant viscosity also for capillary 0 measurements.

Analysis of Heating Effects in Capillary Flow

Heat Conduction Absent

Analysis of dissipation heating of the flow shows that the local temperatures in the lubricant depend on pressure drop and specific heat capacity per unit volume of the fluid alone in the case of no heat conductivity in the fluid. The temperature distribution is a function of

position in the capillary cavity and is proportional to $zr^2/(R^2 - r^2)$, where z is axial position, r the radial coordinate and R radius of the circular cross section of the capillary.

A decrease in apparent viscosity as measured with the capillary, can be evaluated based on increases of volume flow rate when a temperature dependent viscosity is assumed. It has been shown that the decrease in apparent viscosity thus evaluated will follow one and the same flow curve configuration, in a $\ln\tau$-$\ln\eta$ presentation, independent of capillary dimensions and material parameters except $c_v\rho$, the specific heat capacity per unit volume, and the temperature viscosity coefficient. This is consistent with the experimental observations.

Heat Conduction Present

Calculation of temperature distribution when heat conductivity of the fluid is present shows an annular temperature peak near the wall and unchanged temperatures at the center and at the wall. The value of the temperature peak is of the order of $10^{\circ}F$ at the exit for a pressure drop of 500 psi. The temperature peak at the entrance is located at the wall, $r = R$. The peak moves inward at downstream locations and increases with distance from the entrance. The increase is however not proportional with axial position. A heat balance shows that an appreciable part of the dissipation heat is removed by convection. A numerical example shows that less than 10% of the generated heat is conducted away to the walls. The remaining part of the heat is thus found in the fluid at the exit. An attempted estimate of the configuration of the deviating flow curve based on the calculated temperature distribution for heat conduction present resulted in a configuration very nearly congruent with

the experimentally obtained standard configuration for the flow curves. The calculated flow curves for two model fluids similar to a hydrocarbon and a silicone oil from the investigated test fluids were found to be positioned in nearly the same location as the measured flow curves. The relatively insignificant amount of heat conducted away explain the mutual consistency of the experimentally obtained flow curves and also the consistency with the calculated flow curves. It can be concluded that dissipation heating is the only mechanism active in establishing the observed deviations of the flow curves from constant viscosity in the investigated range of parameters. The ratio between pressure drop and flowrate which is proportional to the viscosity will thus remain constant up to the investigated limit of 700 psi when the lubricant operates under conditions of constant temperature.

Evaluation of Boundary and Initial Conditions

The relatively small amount of heat removed by conduction in the short capillaries suggests that the wall condition whether isothermal or adiabatic can not, expectedly, influence the high shear stress measurements significantly. Maintenance of an isothermal wall is thus of less importance for short capillaries than for long capillaries, Gerrard, Steidler and Appeldoorn 1965 (11). A well defined uniform temperature at the inlet is however of great importance. Both conclusions are consistent with experimental observations.

Evaluation of the Effects of Variations of Capillary Dimensions

The small conduction effect makes it unlikely that further improvement of high shear stress viscometry in direction of substantially

higher shear stress can be obtained by reducing the capillary diameter without using capillary diameters 5-10 times smaller than the present diameter 3.5×10^{-3} inch. Furthermore smaller L/D ratios which are desirable in order to obtain higher shear stresses for a given pressure will then imply a capillary length less than $.5 \times 10^{-3}$ inch. Such a capillary, when built, would have to sustain a pressure drop of more than 10^3 psi and would possibly exhibit questionable durability. The shorter capillary length will furthermore imply substantially shorter resident times for the fluid in the capillary which will tend to counteract the improvement in the conduction effect gained by decreasing the capillary diameter.

Increase of the ratio of capillary diameter to capillary length seems to be the most promising and direct method which can be used to obtain a higher shear stress limit in capillary viscometry. The obtainable shear stress is proportional to the ratio D/L and to the pressure drop Δp over the capillary. Heating effects limit the order of the magnitude of the pressure drop to 2 - 4 kpsi as demonstrated in the present thesis. But a higher limit of obtainable shear stress can possibly be achieved by using capillaries with greater D/L ratios (smaller L/D ratios) than the present D/L ratio of .74 (L/D = 1.35) used in capillary 0. The pressure drop outside the capillary will however prevent unlimited shear stress increases. The pressure drop outside the capillary is proportional to the product of the ratio D/L of the capillary and the pressure drop over the capillary itself (34). The constant of proportionality is about .39. The highest shear stress that can be obtained in a capillary is an asymptotic value of about 63.5% of the total applied pressure drop.

This value is achieved when the capillary, in the limit (when $L/D \to 0$), converts to an orifice configuration. The asymptotic value is relatively high compared to previously used capillary arrangements.

An orifice configuration, characterized by $L/D \to 0$, is not realistic but a sturdy capillary can be built with the ratio D/L in the range 5 - 10. Shear stresses at the wall will then be about 40% to about 50% of the total applied pressure drop. The possibility to obtain a shear stress of about 2 kpsi at the capillary wall seems thus to be present.

Non-Liquid Behavior

The non-blended lubricants showed liquid behavior in most of the measurements. Non-liquid behavior is perceptible as a significant degree of scatter of the data points and a grouping of the data points in an apparent meaningless pattern positioned at higher viscosities than the corresponding flow curve. The position of the data points deviates generally less than 1 - 2% of the viscosity values of the flow curves when liquid conditions are present.

The siloxane investigated showed non-liquid behavior in the form of solidification. The conditions were pressures above 50 kpsi and room temperature, 75°F. Solidification could be generated by initiating flow in the tubes and the capillary. Traces of possible non-liquid behavior were observed also at lower pressure, 40 kpsi, in the shear stress range above approximately 1.5×10^7 dyn/cm^2 (~220 psi). Silicone oils do not readily create elastohydrodynamic film thickness sufficiently great according to existing theory. The observation of a non-liquid behavior,

possibly shear induced, is of some interest in this respect.

Shear Thinning Behavior of the Polymer Blended Mineral Oil

The fluid consisting of a blend of polymer and mineral oil shows pronounced non-Newtonian behavior. A shear thinning effect reduces the viscosity approximately 2.5 times when the shear stress increases from about 10^2 dyn/cm^2 to 10^4 dyn/cm^2. The two viscosity levels can probably be characterized as the first and the second Newtonian viscosity level respectively. The reduction of viscosity is nearly constant in the investigated temperature range 75 - 190°F. The flow curves show however increasing viscosity again with further increase of applied shear stress. The viscosity increase is of the order of 30% above the second Newtonian viscosity level when the applied shear stress is about 3×10^5 dyn/cm^2 (4 psi). Apparent non-liquid behavior sets in above this shear stress. This observation seems to be significant for applications of polymer blended oils in elastohydrodynamic lubrication. The non-liquid state of the lubricant is present under conditions equivalent with a situation far before the inlet to the elastohydrodynamic contact area. Existing theory for prediction of film thickness and other related elastohydrodynamic quantities presumes implicitly liquid behavior of the lubricant. Adjustments to the theory seem to be necessary before it can be applied with polymer blended lubricants which must be expected to show similar non-liquid behavior although expectedly at higher shear stresses. Both concentration and molecular weight are considerably lower for most of the available blended oils than for the polymer blended test fluid. This suggests greater range of pressure and shear stress before

non-liquid behavior sets in for the lower concentration polymer blends.

Observations of Time Independent Lubricant Behavior

The average resident time in a capillary for the fluid in a typical series of measurements is in the range from about 4 μ sec to about 10^5 μ sec. The relaxation time for a lubricant with a viscosity of 10^3 - 10^4 cp is of the order 3×10^{-3} to 3×10^{-2} μ sec respectively (30). The relaxation time at this viscosity level is thus 10^2 to 10^3 times smaller than the lowest resident time. Time dependent phenomena in the fluid behavior cannot be expected to appear with any significance. The consistency of the measured flow curves with one common standard flow curve irrespective of viscosity level or capillary type confirms this conclusion. The average resident time in an elastohydrodynamic contact is considerably larger than the smallest resident time of about 4 μ sec in a capillary. The speed of the sliding surface is a nearly accurate measure of the resident time in the high pressure zone for most of the fluid because the shearing occurs primarily near the hotter stationary surface. The diameter of the contact is of the order of 10^{-2} inch. A speed of 10 inch/sec yields thus a resident-time of 10^3 μ sec as a speed of 10^2 inch/sec yields 10^2 μ sec. These times are well within the range of 4 - 10^5 μ sec for the capillary resident times in high shear viscometry as presented in this work. The viscosities in an elastohydrodynamic film can reach a level of 10^6 cp in lamina near the colder sliding surface. The relaxation time is about 3 μ sec under these conditions. This time is however also relatively small compared to a resident time of 10^2 to 10^3 μ sec. Therefore time dependent

phenomena do not appear as mechanisms of major importance in explanation of traction, pressure distribution or film thickness.

Conclusions

The experimental investigation has shown that the pure hydrocarbon test lubricants display Newtonian behavior up to a shear stress of 700 psi. A shear stress of 700 psi is only a factor of 3 to 5 below the actual average shear stress the lubricant experiences during passage of the high pressure zone of an elastohydrodynamic contact, Figure 30, Chapter II. High shear stress capillary viscometry is thus not far from the possibility to create elastohydrodynamic lubrication conditions in a laboratory experiment where the parameters of interest can be varied independent of each other. Capillaries with a smaller length to diameter ratio, of the order of .2 to .1, seem to be a realistic means of increasing the upper limit of attainable shear stress in capillary viscometry from the present level of about 700 psi to possibly 2 kpsi.

CHAPTER VII

DISCUSSION AND CONCLUSIONS - THEORETICAL DEVELOPMENTS

A New Theory for the High Pressure Area of an Elastohydrodynamic Contact

Prediction of the Maximum Temperature and the Shear Stress in the Film

A theory has been developed for an elastohydrodynamic film in a plane parallel bearing surface configuration for prediction of the maximum temperature and the shear stress. The development is based on the energy equation for the film reduced such that only the major contributing terms of viscous dissipation and conduction perpendicular to the film-plane are considered. The velocity in the film is assumed to be one directional, in the direction of sliding only. The velocity is assumed to be constant for each fluid part during the passage of the contact. A Hertzian pressure distribution for a point contact is assumed.

The theory yields criteria to evaluate the maximum attainable temperature in the film. This maximum temperature depends on sliding speed, fluid properties, temperature viscosity coefficient and a base viscosity. Film thickness does not participate in determination of the maximum temperature. The theory yields a dimensionless film stress proportional to the product of the actual stress, the film thickness and the reciprocal of the sliding speed. Film thickness and sliding speed must thus be known before the stress can be evaluated. Information about film thickness must be obtained from other sources, measurements or independent calculation according to existing experience and

theory. The temperature T_2 of the moving surface is an input parameter primarily for the determination of shear stress and must as such be known. Information about the temperature T_2 must be obtained from other sources. The temperature may be calculated from the shear stress distribution. It is as such a step in an iteration procedure to achieve increased accuracy in the calculation of film related quantities.

The Adiabatic Plane in the Film

It is shown that there exists a plane parallel to the film plane where adiabatic conditions and symmetry exist with respect to temperatures, heat fluxes, velocity gradients and fluid velocity relative to the adiabatic plane. Dimensionless diagrams have been prepared which can be used to obtain the solutions for any point in the elastohydrodynamic film in a few graphical steps.

Convection in the Film

A comparison between the neglected term for convection in the direction of sliding $c_v \rho\ u\ T_{,x}$ and the dissipation term $\eta u_{,z}^2$ shows that the ratio of convection to dissipation with actual bearing quantities is of the order of 1% or less in an elastohydrodynamic film even for a sliding speed as high as 50 in/sec. The ratio depends on the specific heat per unit volume of the lubricant, c, the temperature difference between the two bearing surfaces, the square ratio of the film thickness to radius, $(h/r)^2$, and is inversely proportional to the angular velocity of the rotating (sliding) machine element and to the viscosity. The angular velocity and the temperature difference over the film are in many cases of the same magnitude for both elastohydrodynamic lubrication

and thick film lubrication. The ratio h/r is of the order of 10^{-5} in elastohydrodynamic lubrication whereas it is of the order of 10^{-3} in thick film lubrication. The convection term is thus many times greater in thick film lubrication than in elastohydrodynamic lubrication. The developed concepts of maximum film temperature, shear stress and symmetry about an adiabatic plane is therefore not applicable to a thick film evaluation.

Applicability of the Theory to Actual Elastohydrodynamic Films

An investigation has been carried out to determine the extent to which the conditions in an actual elastohydrodynamic situation satisfies the assumption for the developed theory. It is assumed that most of the traction force is generated in the high pressure zone of the contact. It is shown that the actual pressure gradients, temperature gradients in the direction of the film plane and the density variations in the film each causes only insignificant distortion of the assumed one directional velocity within a radius of the high pressure zone of approximately 90% of the radius of the Hertzian contact. The distortions can be a change of magnitude of the velocity or the addition of a small deviation velocity perpendicular to the direction of sliding. It is shown that the magnitude of each distortion is less than 2% to 5% of the sliding velocity for locations within 90% of the Hertzian radius from the center of the contact. The greatest bound for distortions, 5%, originates from estimated inaccuracies in determination of the actual film thickness. The maximum value of the distortion occurs at different locations in the film thus tending not to amplify each other. The level of deviations of the order of 5% or less from the assumptions is considered to possess a sufficiently small inaccuracy for estimating calculations.

An Example of a Film Calculation Shear Stress and Maximum Temperatures

An example of a film calculation is shown in Appendix G. The use of the dimensionless graphs is demonstrated. A dimensioned computer program is applied which yields detailed print-out for the bearing film parameters of interest. The local shear stress and temperature distribution is calculated at a series of representative locations in the high shear, high pressure area of the contact. The total traction from that area is found by integration of the shear stress distribution. The result is plotted, in Figure 54 of Appendix G. The traction is calculated for a series of sliding speed but for constant normal load.

The temperatures of the bearing surfaces and the film temperatures decrease with lower speed, equation (34), Chapter IV. The viscosities increase and the dimensionless shear stress, equation (30), Chapter IV, increases with lower speed. The film thickness decreases with speed. The net effect is that the shear stress varies inversely proportional with sliding speed. Figure 55 of Appendix G shows the calculated traction coefficient. The inverse proportional relation between traction coefficient and sliding speed is seen. The measured traction coefficient is also shown. The ratio between measured and calculated traction coefficients are of order 1 (.8 - 1.1 - 1.4 in the three available data points). These preliminary results can be regarded as a satisfactory check of the developed theory when it is considered that the viscosity values used are estimated from an extrapolation. The pressure viscosity relation is determined experimentally in the range up to 60 kpsi. The viscosities used in the calculation are extrapolated from the

experimental data. The extrapolated viscosities employed are from the pressure range 100 kpsi to 150 kpsi. Some inaccuracy in the estimate of viscosity and thereby in local shear stress may be anticipated. The extrapolation assumes furthermore that the lubricant is a liquid in all locations of the film. It has been found that several types of lubricants will solidify or at least show non-liquid behavior when exposed to pressures of the order of 100 kpsi, however, for a relatively long time, > 1 sec. Solidification of lubricants exposed to high pressures for short time durations, of the order of 10^2 to 10^3 μsec, is not investigated to the same extent yet. There exists therefore a need for viscometric measurements of lubricants at the maximum pressures and the time durations attained in an elastohydrodynamic contact to assess the nature of possible solidification.

Conclusion

It can be concluded that the developed theory with the existing viscometric experience and data predicts the traction of the high pressure area of the Hertzian contact with realistic accuracy.

CHAPTER VIII

RECOMMENDATIONS FOR FURTHER RESEARCH

This report has shown that further investigations in the pressure distribution immediately outside the capillary cavity is desirable for flow situations where Re << 1. A solution will give information about the upper shear stress limit that can be achieved in direct high shear capillary viscometry. It is likely that the present upper limit of about 700 psi can be extended up to above 2000 psi which is the order of magnitude of average shear stress experienced by a moderately high viscosity fluid, Appendix G, during passage through an elastohydrodynamic contact. A logical extension of the topic is the complete description in terms of pressures, fluid velocities and temperature distribution of the flow through a small L/D arrangement, Re << 1. The designation of this project would be: Viscous flow through an orifice.

The thermal solution of the flow of a viscous fluid, Re << 1, through a conical tube section would be of great value in comparing with solutions to the above mentioned proposal, "The Viscous Flow through an Orifice." Millsap's and Pohlhausen (48) have reported work on thermal flow in a wedge, with 1 < Re < 5000.

There is need for a simple solution to the determination of the traction force contribution from the inlet of an elastohydrodynamic contact to supplement the present investigation of traction force generated in the high pressure area of the contact.

An investigation of a possible non-liquid behavior of lubricants is needed. This will involve increase with a factor of 2 to 3 of the present limit of pressure level of high shear viscometry. It is logical to investigate also the influence of possible non-liquid behavior on the ability of the lubricant to create a sufficient elastohydrodynamic film thickness.

Possibly the most important work that should be carried out in order to properly understand traction force generation at low sliding speeds is an investigation into the minimum film thickness areas of the elastohydrodynamic contact. Temperatures higher than predicted by liquid behavior and load carrying capacity are being created in this area although optical film thickness measurements shows positive film thickness. The work could be based extensively on film temperature measurements. The work is important because reduction of the localized high temperature effect is expected to allow a substantial increase in the traction force which can be transmitted through a thin elastohydrodynamic liquid film.

A P P E N D I C E S

APPENDIX A

DESCRIPTION OF FLUIDS

The table summarizes the investigated fluids and gives characteristic data for each fluid.

Experimental Fluids

Diester-Plexol 201 bis-2-ethyl hexyl sebacate

Dimethyl Siloxane DC-200-50

Polyalkyl Aromatic plus additive

Synthetic Paraffinic Hydrocarbon plus antiwear additive

Paraffinic Base Oil R-620-12 plus 11.5% Polyalkylmethacrylate (MW = $.2 \times 10^6$).

Characterization

Diester

Source - Rohm and Haas Company

Data supplied with the sample

Viscosity at 210°F	3.32 cs
Viscosity at 100°F	12.75 cs
Viscosity at -65°F	7988 cs
Viscosity Index (D-2270)	150
Neutralization number (D-974)	0.02
Cloud Point (D-2500)°F	below -65

Data transferred from literature sources

Heat conductivity at 100°F		.087 Btu/h ft °F (38)
37.8°C		
		.0188 lbf/°F sec
		.0154 kp/°C sec
Specific Heat per unit mass		0.46 Btu/lbm °F (38)
at 100°F		0.46 cal/gramm °C
37.8°C		4295 lbf in/lbm °F
Density at 77°F		.0328 lbm/in^3
25°C		
		.91 $gramm/cm^3$ (38)
Specific Heat per unit volume		.01303 Btu/°F in^3
		.416 cal/°C cm^3
		139.5 lbf/in^2 °F
Heat diffusivity		1.35×10^{-4} in^2/sec
		8.69×10^{-4} cm^2/sec

Data measured

Kinematic viscosity at	at 100°F	12.65 cs
	37.8°C	
	at 210°F	3.33 cs
	98.9°C	
	at 300°F	1.775 cs
	148.9°C	
Density	at 100°F	.903 $gramm/cm^3$
	37.8°C	

	at 210°F	.86 gramm/cm^3
	98.9°C	
	at 300°F	.825 gramm/cm^3
	148.9°C	
Viscosity	at 100°F	11.41 cp
	37.8°C	
	at 210°F	2.86 cp
	98.9°C	
	at 300°F	1.46 cp
	148.9°C	
	at 32°F	57.5 cp
	0°C	
	at 10°F	130 cp
	-12.2°C	
Pressure viscosity	at 32°F	Z = .51
Coefficient (Roelands)	0°C	

Elastohydrodynamic film thickness and traction data taken at 15 lbf load (150 kpsi peak Hertzian pressure) 1 1/4 inch diameter steel ball loaded against a sapphire anvil

Sliding speed	13.7 ips	27.4 ips	54.8 ips	92.1 ips
h_c(μ-inch)	.4	.8	2.1	3.3
h_m(μ-inch)	.4	.8	1.3	1.3
TC	.046	.032	-	.025

Dimethyl Siloxane DC-200-50

Source Dow Corning Corporation, Midland, Michigan,

Data supplied with the sample

Degree of polymerization 43

Data measured

Viscosity	at 77°F	25°C	50 cs	48 cp
	at 100°F	37.8°C	41.5 cs	39.1 cp
	at 210°F	98.9°C	17 cs	15.7 cp
	at 300°F	148.9°C	8.6 cs	7.3 cp
Density	at 77°F	25°C	.954 gramm/cm^3	
	at 100°F	37.8°C	.943 gramm/cm^3	
	at 210°F	98.9°C	.894 gramm/cm^3	
	at 300°F	148.9°C	.850 gramm/cm^3	

Pressure viscosity characteristics

			α_{0T} psi^{-1}	α^* psi^{-1}	Z
at	75°F	23.9°C	1.28×10^{-4}	$.98 \times 10^{-4}$	.52
at	100°F	37.8°C	1.36×10^{-4}	$.96 \times 10^{-6}$	.51
at	210°F	98.9°C	1.53×10^{-6}	$.96 \times 10^{-4}$	.44
at	300°F	148.9°C	1.53×10^{-4}	$.96 \times 10^{-6}$	.43

Roelands temperature viscosity slope index

S = .55 re atmospheric pressure.

Elastohydrodynamic film thickness and traction.

Data taken at 15 lbf load (150 kpsi peak Hertzian pressure)

1 1/4 inch diameter steel ball loaded against a sapphire anvil.

Sliding speed	13.7 ips	27.4 ips
h_c (μ-inch)	2	3
h_m (μ-inch)	1	2
TC	.069	.061

Polyalkyl Aromatic plus additive.

Source NASA Lewis Research Center, Cleveland, Ohio.

Data supplied with the sample

Kinematic viscosity	at 100°F	37.6 cs
	at 210°F	6.1 cs

Data measured (40)

	100°F	210°F	300°F
	37.8°C	98.9°C	148.9°C
Viscosity cp (p = atm)	32.2	5.0	2.1
α_{OT} psi^{-1}	1.41×10^{-4}	1.39×10^{-4}	-
α^* psi^{-1}	1.17×10^{-4}	$.88 \times 10^{-4}$	-

Elastohydrodynamic film thickness and traction

Data taken at 15 lbf load (150 kpsi peak Hertzian pressure)

1 1/4 inch diameter steel ball loaded against a sapphire anvil.

Sliding speed	13.7 ips	27.4 ips	54.8 ips
h_c(μ-inch)	3	4	8
h_m(μ-inch)	2	2	4
TC	.055	.048	.042

Synthetic Paraffinic Hydrocarbon (XRM 109 F4)

Source NASA Lewis Research Center, Cleveland, Ohio.

Data measured

	100°F	210°F	300°F
	37.8°C	98.9°C	148.9°C
Viscosity cp	376	31.6	10.2
α_{OT} psi^{-1}	1.52×10^{-4}	1.37×10^{-4}	1.11×10^{-4}
α^* psi^{-1}	1.37×10^{-4}	1.04×10^{-4}	$.89 \times 10^{-4}$
Z	.44	.46	.47

Synthetic Paraffinic Hydrocarbon plus Antiwear Additive (XRM 177 F-4)

Source NASA Lewis Research Center, Cleveland, Ohio

Data measured

	100°F 378°C	210°F 98.9°C	300°F 148.9°C
Viscosity cp	37.6	31.6	10.2
α_{OT} psi^{-1}	1.52×10^{-4}	1.37×10^{-4}	1.11×10^{-4}
α^*	1.35×10^{-4}	1.07×10^{-4}	$.86 \times 10^{-4}$
Z	.44	.46	.46

Fluid XRM 177 F4 is of the same composition as the previous investigated fluid D (40). The base fluid is however not from the same lot.

Elastohydrodynamic film thickness and traction for fluid D. Data taken at 15 lbf load (150 kpsi peak Hertzian pressure) 1 1/4 inch diameter steel ball loaded against a sapphire anvil

Sliding speed	13.7 ips	27.4 ips	54.8 ips
h_c(μ-inch)	15	23	30
h_m(μ-inch)	7	13	19
TC	.058	.045	.035

Paraffinic Base Oil R-620-12 plus 11.5% Polyalkylmethacrylate (MW = $2.\times10^6$).

Data supplied with the sample

Base oil R-620-12

Source: Sun Oil Company

Viscosity 33.33 cs at 100°F (37.8°C) 5.336cs at 210°F (98.9°C)

SUS/100 156.2 SUS/210 43.74

Viscosity index (ASTM D-2270)	102
Flash point	410°F
Fire point	470°F
Pour point	5°F
Refractive index	1.4754
Density gramm/cm^3	.8596
Molecular weight (MW)	401 *

Polyalkylmethacrylate PL 4523. (PAMA)

Source Rohm and Haas Company

The polymer was in solution with a paraffinic base oil, a 150 neutral carrier oil similar to the base oil R-620-12. Their chemical composition are alike. They differ only in their molecular weight. The solution contains 19% polymer. It has a kinematic viscosity of 773 cs re 210°F (98.9°C). The molecular weight is 4.51×10^6 as measured with a permeation chromatography method, GPCM. An estimated molecular weight of $2. \times 10^6$ is however found by extrapolating from viscosity and molecular weight data for lower MW polyalkylmethacrylates, MW = 1.28×10^6, $.828 \times 10^6$ and $.5 \times 10^6$. It is believed that the GPP technique is not suitable for materials with high molecular weights. The molecular weight of $2. \times 10^6$ determined with viscosity measurements are therefore adhered to. The amount polymer reported, 11.5% is the volume concentration in the final solution.

---

*Calculated from viscosity data using the method of A. E. Hirschler, J. Inst. Petroleum, 32, 133-61, 1946.

Data measured

	100°F	210°F	300°F
R-620-12	37.8°C	98.9°F	148.9°C
Viscosity (cp)	29.2	4.5	1.9
Density (gramm/cm^3)	.849	.809	.777

APPENDIX B

MANUFACTURER'S SPECIFICATION ON THE VELOCITY TRANSDUCER

LVSYN TRANSDUCERS

HEWLETT PACKARD

IM-LVSYN-4

This information is prepared for:

LVsyn Model No. [illegible]

Serial No. _____

Working range _____ inches

Maximum usable stroke _____ inches

Sensitivity 55.5 millivolts per inch/second of velocity

☒ Standard LVsyn see reverse side

☐ Non-Standard LVsyn see reverse side

CALIBRATION CURVE OF YOUR LVSYN

The Sanborn LVsyn transducer measures linear (straight-line) velocity. Each transducer consists of only two parts; a shielded cylindrical coil assembly, and a high coercive force permanent magnet. The relative motion of the magnet and the coil generates a voltage, whose magnitude is proportional to the linear velocity, and whose polarity indicates the direction of motion.

The LVsyn transducer features extremely rugged construction; there are no springs, levers, bearings, or other delicate mechanisms to get out of order. The LVsyn is recommended for use with Sanborn instruments to measure motion, or as a control element in a servo feedback loop. The LVsyn can measure displacement by using an integrating circuit, or acceleration by using a differentiating circuit.

The magnet of this Sanborn LVsyn is a precision element. To maintain the accuracy and reliability designed into this transducer, observe the following warnings:

1. Do not subject the magnet to high external magnetic fields, or bring the magnet into contact with any magnetic material, such as the shield on the coil.
2. Do not handle the magnet roughly or try to bend the magnet. Do not drop the magnet onto a hard surface. Non-breakable magnets are available as standard item; see table.
3. Each magnet and coil is a matched pair; keep each pair together.

SENSITIVITY Depends on model used; see table.

DIMENSIONS Depends on model used; see table.

OUTPUT May be wired for single-ended or push-pull operation, using the color coded leads as shown in the figure below. Parallel operation also possible at one-quarter the source impedance values given.

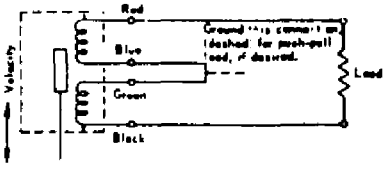

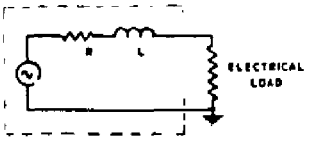

EQUIVALENT CIRCUIT An open-circuit voltage whose amplitude is proportional to the instantaneous velocity, and whose polarity indicates the direction of relative motion, in series with the LVsyn internal impedance as shown in the figure above. For values of internal impedance of each model see table on reverse side.

FREQUENCY RESPONSE Determined by the internal impedance of the LVsyn in conjunction with the electrical load applied.

EXCITATION None required; this is a voltage-generating transducer.

ACCELERATION Limited by maximum permissible stress in magnetic core.

MECHANICAL IMPEDANCE Practically a pure mass. See table.

STABILITY Calibration is reliable over life of unit, if magnet core is not subjected to strong external magnetic fields or otherwise mishandled.

ZERO DRIFT None; at zero relative velocity, the generated open-circuit output voltage is also zero.

OVERLOAD No damage if displacement limits are exceeded.

DISPLACEMENT LIMITS Nominal Working Range and Maximum Usable Stroke depend on the model LVsyn used. The table gives the values; the figure to the right defines the terms.

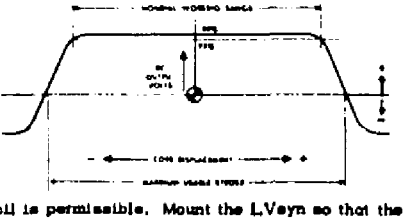

OTHER MEASUREMENTS Can measure displacement with a simple integrating circuit, or can measure acceleration with a simple differentiating circuit.

TEMPERATURE LIMITS -50°F to +200°F.

MAGNET DRIVE From either end, from non-magnetic rod or shaft.

MOUNTING Any position. Contact between the magnet and the inside of the coil is permissible. Mount the LVsyn so that the electrical centers ⊕ of the magnet and the coil coincide when the magnet is at the mid-point of its stroke (half-way between the most positive and the most negative excursions). This insures that the center of the range of displacements is at the center of the nominal working range. Find the point of coincidence by measuring the distance between the end of the coil and the end of the magnet, using the dimensions given in the chart. Do not confuse the two ends of the coil.

CALIBRATION CURVE The recording at the right is an actual record made with your transducer, with the magnet moving through the coil at a constant velocity. The central section of this recording corresponds to the LVsyn output curve above. Recalibration service is available at nominal charge.

STANDARD

MODEL NUMBER ("N" after model No. denotes non-breakable core)	NOMINAL OUTPUT SENSITIVITY millivolts MV/INCH/SEC (open circuit)	ELECTRICAL IMPEDANCE (coils connected in series) R ohms	L henrys	MAGNET CORE DISPLACEMENT inches Nominal Working Range	Maximum Usable Stroke	COIL AND HOUSING DIMENSIONS inches C_c	L_c	$(OD)_c$ +.000 −.005	$(ID)_c$	WT. grams W_c	MAGNET CORE DIMENSIONS inches L_m	$(OD)_m$ ±.002	T_h	WT. grams W_m
3LVA5	120	2,000	0.085	0.50	1.30	1.405	3.18	0.374	0.138	20	2.38	0.125	1-72NF	3.5
3LVA5-N	40	2,000	0.085	0.50	1.30	1.405	3.18	0.374	0.138	20	1.63	0.125	1-72NF	2.5
3LV1	90	2,500	0.085	1.0	1.90	1.937	4.22	0.374	0.138	25	3.00	0.125	1-72NF	4.5
3LV1-N	35	2,500	0.085	1.0	1.90	1.937	4.22	0.374	0.138	25	2.25	0.125	1-72NF	3.8
6LVA5	450	8,000	0.9	0.5	1.50	1.426	3.23	0.623	0.200	63	2.50	0.187	4-40NC	8.0
6LVA5-N	235	8,000	0.9	0.5	1.50	1.426	3.23	0.623	0.200	63	1.69	0.187	4-40NC	5.8
6LVA8	500	11,000	1.4	0.80	2.10	2.082	4.50	0.623	0.200	100	3.25	0.187	4-40NC	10
6LVA8-N	250	11,000	1.4	0.80	2.10	2.082	4.50	0.623	0.200	100	2.50	0.187	4-40NC	8.5
6LV1	500	13,000	1.6	1.0	2.3	2.312	5.00	0.623	0.200	110	3.50	0.187	4-40NC	11
6LV1-N	250	13,000	1.6	1.0	2.3	2.312	5.00	0.623	0.200	110	2.75	0.187	4-40NC	10
6LV2	500	19,000	2.4	2.0	3.4	3.312	7.00	0.623	0.200	150	4.50	0.187	4-40NC	15
6LV2-N	250	19,000	2.4	2.0	3.4	3.312	7.00	0.623	0.200	150	3.75	0.187	4-40NC	14
6LV3	500	25,000	3.2	3.0	4.2	4.312	9.00	0.623	0.200	200	5.25	0.187	4-40NC	17
6LV3-N	250	25,000	3.2	3.0	4.2	4.312	9.00	0.623	0.200	200	4.50	0.187	4-40NC	17
6LV4	500	32,000	4.0	4.0	5.5	5.437	11.25	0.623	0.200	240	6.75	0.187	4-40NC	22
6LV4-N	250	32,000	4.0	4.0	5.5	5.437	11.25	0.623	0.200	240	6.00	0.187	4-40NC	23
7LV3	650	18,000	2.8	3.0	4.6	4.687	9.75	0.748	0.312	270	5.75	0.250	4-40NC	34
7LV3-N	250	18,000	2.8	3.0	4.6	4.687	9.75	0.748	0.312	270	5.00	0.250	4-40NC	28
7LV4	650	21,000	3.4	4.0	5.5	5.437	11.25	0.748	0.312	300	6.75	0.250	4-40NC	40
7LV4-N	250	21,000	3.4	4.0	5.5	5.437	11.25	0.748	0.312	300	6.00	0.250	4-40NC	34
7LV6	350	11,500	1.9	6.0	8.0	7.687	15.75	0.748	0.312	420	9.25	0.250	4-40NC	54
7LV6-N	150	11,500	1.9	6.0	8.0	7.687	15.75	0.748	0.312	420	8.50	0.250	4-40NC	49
7LV9	350	17,000	2.8	9.0	11.0	11.187	22.75	0.748	0.312	610	11.75	0.250	4-40NC	69
7LV9-N	150	17,000	2.8	9.0	11.0	11.187	22.75	0.748	0.312	610	11.50	0.250	4-40NC	66

STANDARD

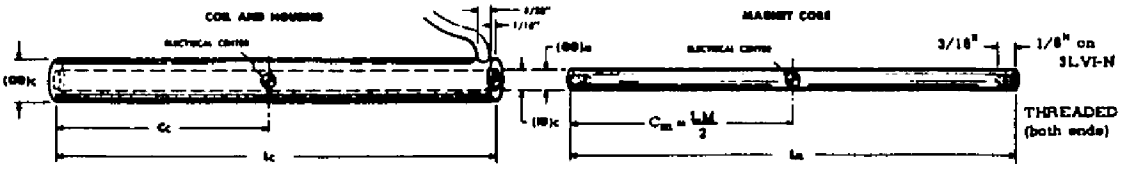

NON-STANDARD

Model No.	MAGNET CORE DISPLACEMENT inches Nominal Working Range	Maximum Usable Stroke	ELECTRICAL CHARACTERISTICS HIGH IMPEDANCE Nominal Output Sensitivity mv	Electrical Impedance coils connected in series R ohms	L henrys	MED-HI IMPEDANCE Nominal Output Sensitivity mv	Electrical Impedance coils connected in series R ohms	L henrys	MEDIUM IMPEDANCE Nominal Output Sensitivity mv	Electrical Impedance coils connected in series R ohms	L henrys	LOW IMPEDANCE Nominal Output Sensitivity mv	Electrical Impedance coils connected in series R ohms	L henrys
3LVA5	0.50	1.30	Same as standard											
3LV1	1.0	1.90	Same as Standard											
6LVA8	0.80	2.10	Same as Standard			200	1.15K	.27	140	870	0.11	45	90	0.011
6LV1	1.0	2.3	Same as Standard			200	2.6K	.3	140	990	0.12	45	100	0.013
6LV2	2.0	3.4	Same as Standard			200	3.5K	.45	140	1,500	0.18	45	150	0.019
6LV3	3.0	4.3	Same as Standard			200	4.7K	.6	140	1,900	0.25	45	200	0.025
6LV4	4.0	5.5	Same as Standard			200	6.0K	.75	140	2,500	0.31	45	250	0.032
7LV3	3.0	4.6	700	37,000	6.0	320	7.0K	1.1	210	2,000	0.46	69	290	0.047
7LV4	4.0	5.5	700	43,000	7.0	320	8.1K	1.3	210	3,300	0.53	69	340	0.055
7LV6	6.0	8.0	700	62,000	10	320	11.5K	1.8	210	4,700	0.76	69	480	0.078
7LV9	9.0	11.0	700	90,000	15	320	16.9K	2.75	210	6,900	1.10	70	700	0.12

R & L of each coil winding is ½ the value given in chart. Total impedance values given for series connection.
Voltage output given in open circuit ___ inch/sec. Dimensions are same as standard units.

NON-STANDARD

APPENDIX C

MEASURED RESULTS FOR THE INVESTIGATED LUBRICANTS

APPENDIX C

MEASURED RESULTS FOR THE INVESTIGATED LUBRICANTS

Table 14. Diester, 32°F

L/D = 1.35

P3	VISCP	TAUDYN	NSRATE	RE	LEOL
9956.	.2189+01	.5277+05	.2411+05	.8611-01	.4146-02
9950.	.2108+01	.5163+05	.2450+05	.9085-01	.4374-02
9948.	.2048+01	.5497+05	.2684+05	.1024+00	.4932-02
9945.	.1950+01	.1169+06	.5993+05	.2402+00	.1157-01
9946.	.1962+01	.1150+06	.5860+05	.2335+00	.1124-01
9944.	.1961+01	.1105+06	.5636+05	.2246+00	.1081-01
9941.	.1993+01	.1829+06	.9179+05	.3600+00	.1733-01
9937.	.1970+01	.1782+06	.9048+05	.3590+00	.1729-01
9933.	.2024+01	.1891+06	.9346+05	.3610+00	.1738-01
9935.	.1982+01	.2272+06	.1146+06	.4519+00	.2176-01
9933.	.2031+01	.2555+06	.1258+06	.4843+00	.2332-01
9929.	.1970+01	.2537+06	.1288+06	.5112+00	.2461-01
9930.	.2012+01	.2476+06	.1231+06	.4782+00	.2302-01
9926.	.1983+01	.3359+06	.1694+06	.6677+00	.3215-01
9929.	.1986+01	.3322+06	.1673+06	.6584+00	.3170-01
9926.	.1987+01	.3407+06	.1714+06	.6742+00	.3246-01
9928.	.1969+01	.3150+06	.1600+06	.6350+00	.3058-01
9925.	.1980+01	.3353+06	.1694+06	.6686+00	.3219-01
9924.	.1979+01	.4128+06	.2086+06	.8236+00	.3966-01
9923.	.1973+01	.4052+06	.2054+06	.8138+00	.3918-01
9924.	.1952+01	.4105+06	.2103+06	.8424+00	.4056-01
20066.	.5566+01	.1568+06	.2817+05	.3956-01	.1905-02
20055.	.5559+01	.1600+06	.2878+05	.4046-01	.1948-02
20050.	.5551+01	.1615+06	.2909+05	.4095-01	.1972-02
20048.	.5667+01	.1482+06	.2615+05	.3606-01	.1736-02
20062.	.5599+01	.3049+06	.5445+05	.7601-01	.3660-02
20050.	.5579+01	.3266+06	.5855+05	.8202-01	.3949-02
20047.	.5684+01	.3300+06	.5806+05	.7985-01	.3845-02
20042.	.5599+01	.5261+06	.9396+05	.1312+00	.6315-02
20039.	.5604+01	.4892+06	.8729+05	.1218+00	.5862-02
20035.	.5602+01	.5159+06	.9209+05	.1285+00	.6187-02
20031.	.5637+01	.7276+06	.1291+06	.1789+00	.8616-02
20027.	.5638+01	.6953+06	.1233+06	.1710+00	.8231-02
20022.	.5572+01	.7190+06	.1290+06	.1810+00	.8715-02
20059.	.5564+01	.9486+06	.1705+06	.2395+00	.1153-01
20054.	.5578+01	.9194+06	.1648+06	.2310+00	.1112-01
20054.	.5565+01	.9326+06	.1676+06	.2354+00	.1133-01
20048.	.5588+01	.9646+06	.1726+06	.2415+00	.1163-01
20046.	.5526+01	.1150+07	.2082+06	.2944+00	.1418-01
20042.	.5529+01	.1141+07	.2064+06	.2918+00	.1405-01
20041.	.5567+01	.1115+07	.2003+06	.2812+00	.1354-01
20039.	.5489+01	.1133+07	.2064+06	.2939+00	.1415-01

Table 14. Diester, 32°F (Continued)

L/D = 1.35

P3	VISCP	TAUDYN	NSRATE	RE	LEOL
29451.	.1447+02	.8463+06	.5847+05	.3158-01	.1520-02
29440.	.1434+02	.7376+06	.5142+05	.2802-01	.1349-02
29523.	.1437+02	.7905+06	.5500+05	.2991-01	.1440-02
29487.	.1457+02	.7962+06	.5465+05	.2932-01	.1411-02
29479.	.1429+02	.1232+07	.8620+05	.4715-01	.2270-02
29471.	.1419+02	.1234+07	.8692+05	.4786-01	.2304-02
29468.	.1441+02	.1279+07	.8877+05	.4817-01	.2319-02
29454.	.1395+02	.1698+07	.1218+06	.6824-01	.3286-02
29427.	.1445+02	.1736+07	.1202+06	.6499-01	.3129-02
29410.	.1419+02	.1772+07	.1249+06	.6883-01	.3314-02
29517.	.1438+02	.1828+07	.1271+06	.6908-01	.3326-02
29462.	.1409+02	.2394+07	.1699+06	.9426-01	.4539-02
29478.	.1389+02	.2296+07	.1652+06	.9295-01	.4475-02
29467.	.1385+02	.2285+07	.1650+06	.9309-01	.4482-02
29454.	.1406+02	.2708+07	.1926+06	.1071+00	.5155-02
29505.	.1400+02	.2799+07	.1999+06	.1116+00	.5373-02
29497.	.1431+02	.2800+07	.1956+06	.1068+00	.5144-02
29481.	.1384+02	.2850+07	.2059+06	.1162+00	.5597-02
29476.	.1404+02	.2774+07	.1976+06	.1100+00	.5295-02
29466.	.1291+02	.4893+07	.3790+06	.2295+00	.1105-01
29524.	.1328+02	.5015+07	.3776+06	.2222+00	.1070-01
29509.	.1362+02	.4637+07	.3405+06	.1955+00	.9411-02
29483.	.1407+02	.2138+05	.1520+04	.8444-03	.4066-04
29485.	.1293+02	.4682+07	.3620+06	.2187+00	.1053-01
29470.	.1339+02	.4372+07	.3265+06	.1905+00	.9174-02
29501.	.1222+02	.7572+07	.6195+06	.3962+00	.1908-01
29479.	.1251+02	.6703+07	.5358+06	.3348+00	.1612-01
29498.	.1357+02	.3942+07	.2906+06	.1674+00	.8061-02
29481.	.1294+02	.4978+07	.3846+06	.2323+00	.1118-01
29479.	.1275+02	.6624+07	.5196+06	.3186+00	.1534-01
29462.	.1228+02	.6176+07	.5029+06	.3200+00	.1541-01
29411.	.1232+02	.7040+07	.5713+06	.3623+00	.1744-01
29489.	.1248+02	.7271+07	.5824+06	.3646+00	.1755-01
29482.	.1190+02	.8715+07	.7325+06	.4813+00	.2317-01
30067.	.1440+02	.3525+06	.2448+05	.1329-01	.6400-03
30046.	.1438+02	.4024+06	.2798+05	.1520-01	.7321-03
30077.	.1435+02	.3799+06	.2648+05	.1443-01	.6947-03
30062.	.1427+02	.8830+06	.6189+05	.3390-01	.1632-02
30045.	.1426+02	.8237+06	.5778+05	.3168-01	.1525-02
30090.	.1441+02	.8649+06	.6003+05	.3257-01	.1568-02
30072.	.1416+02	.1313+07	.9274+05	.5118-01	.2464-02
30088.	.1424+02	.1253+07	.8798+05	.4827-01	.2324-02

Table 14. Diester, 32°F (Continued)

L/D = 1.35

30070.	.1420+02	.1341+07	.9442+05	.5198-01	.2503-02
30061.	.1397+02	.1775+07	.1270+06	.7103-01	.3420-02
30084.	.1436+02	.1834+07	.1277+06	.6950-01	.3346-02
30066.	.1399+02	.1830+07	.1309+06	.7314-01	.3521-02
30059.	.1395+02	.2361+07	.1692+06	.9482-01	.4565-02
30091.	.1401+02	.2349+07	.1676+06	.9350-01	.4502-02
30076.	.1385+02	.2413+07	.1742+06	.9829-01	.4733-02
30068.	.1391+02	.2839+07	.2041+06	.1147+00	.5522-02
30057.	.1370+02	.2888+07	.2107+06	.1202+00	.5787-02
30035.	.1380+02	.2805+07	.2032+06	.1151+00	.5542-02
30079.	.1377+02	.2919+07	.2119+06	.1203+00	.5790-02
39348.	.3372+02	.2047+07	.6070+05	.1407-01	.6775-03
39303.	.3414+02	.2092+07	.6127+05	.1403-01	.6754-03
39338.	.3344+02	.2978+07	.8907+05	.2082-01	.1003-02
39290.	.3340+02	.3113+07	.9319+05	.2181-01	.1050-02
39254.	.3203+02	.4035+07	.1260+06	.3074-01	.1480-02
39343.	.3275+02	.3978+07	.1215+06	.2899-01	.1396-02
39290.	.3138+02	.5410+07	.1724+06	.4293-01	.2067-02
39262.	.3145+02	.5260+07	.1672+06	.4157-01	.2001-02
39307.	.3080+02	.6290+07	.2042+06	.5181-01	.2495-02
39282.	.3051+02	.6305+07	.2067+06	.5294-01	.2549-02
39320.	.2481+02	.1305+08	.5261+06	.1658+00	.7981-02
39323.	.2700+02	.1162+08	.4301+06	.1245+00	.5994-02
40127.	.3402+02	.9003+06	.2646+05	.6079-02	.2927-03
40120.	.3532+02	.8768+06	.2482+05	.5494-02	.2645-03
40122.	.3444+02	.9552+06	.2774+05	.6296-02	.3031-03
40149.	.3510+02	.8075+06	.2301+05	.5125-02	.2467-03
40162.	.3392+02	.1967+07	.5800+05	.1337-01	.6435-03
40105.	.3329+02	.2042+07	.6132+05	.1440-01	.6932-03
40198.	.3405+02	.2094+07	.6149+05	.1411-01	.6796-03
40151.	.3332+02	.3019+07	.9060+05	.2125-01	.1023-02
40121.	.3286+02	.3052+07	.9287+05	.2209-01	.1063-02
40190.	.3348+02	.3010+07	.8990+05	.2099-01	.1010-02
40139.	.3235+02	.4188+07	.1295+06	.3128-01	.1506-02
40103.	.3194+02	.4225+07	.1323+06	.3237-01	.1558-02
40182.	.3248+02	.4187+07	.1289+06	.3101-01	.1493-02
40147.	.3146+02	.5416+07	.1722+06	.4278-01	.2060-02
40106.	.3139+02	.5383+07	.1715+06	.4271-01	.2056-02
40194.	.3188+02	.5481+07	.1719+06	.4216-01	.2030-02
40153.	.3151+02	.5450+07	.1730+06	.4291-01	.2066-02
40198.	.3075+02	.6394+07	.2080+06	.5286-01	.2545-02
40154.	.3062+02	.6401+07	.2090+06	.5335-01	.2569-02
40101.	.3066+02	.6458+07	.2106+06	.5368-01	.2585-02
40065.	.3067+02	.6333+07	.2065+06	.5264-01	.2534-02

Table 14. Diester, 32°F (Continued)

L/D = 14.9

P3	VISCP	TAUDYN	NSRATE	RE	LEOL
9860.	.1951+01	.9307+04	.4771+04	.9737-01	.4248-03
9852.	.1916+01	.9189+04	.4797+04	.9968-01	.4349-03
9848.	.1978+01	.1003+05	.5070+04	.1021+00	.4453-03
9849.	.1937+01	.1478+05	.7628+04	.1567+00	.6839-03
9843.	.1972+01	.1526+05	.7737+04	.1562+00	.6815-03
9873.	.1937+01	.1449+05	.7481+04	.1538+00	.6708-03
9867.	.1896+01	.1477+05	.7790+04	.1636+00	.7138-03
9866.	.1958+01	.1505+05	.7686+04	.1563+00	.6819-03
9862.	.1932+01	.2101+05	.1087+05	.2240+00	.9776-03
9861.	.1972+01	.2148+05	.1089+05	.2198+00	.9589-03
9866.	.1969+01	.2046+05	.1039+05	.2102+00	.9172-03
9874.	.1962+01	.2092+05	.1066+05	.2164+00	.9443-03
9872.	.1929+01	.2658+05	.1378+05	.2844+00	.1241-02
9868.	.1977+01	.2792+05	.1412+05	.2843+00	.1240-02
9865.	.1913+01	.2683+05	.1402+05	.2917+00	.1273-02
9861.	.1955+01	.2848+05	.1457+05	.2968+00	.1295-02
9866.	.1931+01	.8564+05	.4435+05	.9142+00	.3989-02
9866.	.1893+01	.6082+05	.3213+05	.6758+00	.2949-02
9865.	.1904+01	.8500+05	.4464+05	.9334+00	.4073-02
9883.	.2529+01	.1622+06	.6414+05	.1010+01	.4406-02
9888.	.2559+01	.1642+06	.6417+05	.9985+00	.4357-02
9893.	.2718+01	.1745+06	.6421+05	.9406+00	.4104-02
9897.	.1939+01	.2798+05	.1443+05	.2962+00	.1292-02
9896.	.1975+01	.2876+05	.1456+05	.2934+00	.1280-02
19891.	.5429+01	.2942+05	.5419+04	.3973-01	.1734-03
19874.	.5452+01	.2850+05	.5227+04	.3816-01	.1665-03
19865.	.5359+01	.2839+05	.5297+04	.3935-01	.1717-03
19859.	.5275+01	.2739+05	.5192+04	.3918-01	.1710-03
19853.	.5380+01	.4356+05	.8097+04	.5991-01	.2614-03
19889.	.5402+01	.4238+05	.7847+04	.5783-01	.2523-03
19887.	.5381+01	.4288+05	.7968+04	.5894-01	.2572-03
19882.	.5391+01	.4417+05	.8192+04	.6049-01	.2639-03
19876.	.5507+01	.6040+05	.1097+05	.7928-01	.3459-03
19870.	.5413+01	.5908+05	.1092+05	.8027-01	.3502-03
19865.	.5402+01	.6156+05	.1140+05	.8399-01	.3665-03
19878.	.5391+01	.5826+05	.1081+05	.7981-01	.3482-03
19871.	.5411+01	.5980+05	.1105+05	.8130-01	.3547-03
19866.	.5415+01	.7902+05	.1459+05	.1073+00	.4682-03
19864.	.5384+01	.8094+05	.1503+05	.1111+00	.4849-03
19894.	.5354+01	.7893+05	.1474+05	.1096+00	.4782-03
19892.	.5379+01	.7811+05	.1452+05	.1075+00	.4690-03
19893.	.5655+01	.2021+06	.3574+05	.2516+00	.1098-02

Table 14. Diester, 32°F (Continued)

L/D = 14.9

19890.	.5378+01	.1543+06	.2869+05	.2124+00	.9267-03
19891.	.5500+01	.8807+05	.1601+05	.1159+00	.5056-03
19889.	.5317+01	.1380+06	.2595+05	.1943+00	.8479-03
19884.	.5442+01	.1228+06	.2256+05	.1650+00	.7199-03
19885.	.5523+01	.1973+06	.3572+05	.2575+00	.1123-02
29896.	.1394+02	.2977+05	.2136+04	.6101-02	.2662-04
29881.	.1389+02	.2709+05	.1950+04	.5586-02	.2437-04
29879.	.1408+02	.3114+05	.2212+04	.6255-02	.2729-04
29875.	.1382+02	.3171+05	.2295+04	.6613-02	.2885-04
29868.	.1406+02	.6955+05	.4948+04	.1401-01	.6113-04
29857.	.1390+02	.7017+05	.5050+04	.1447-01	.6312-04
29843.	.1415+02	.7255+05	.5129+04	.1443-01	.6297-04
29856.	.1378+02	.1113+06	.8082+04	.2335-01	.1019-03
29855.	.1396+02	.1089+06	.7796+04	.2223-01	.9699-04
29853.	.1375+02	.1064+06	.7741+04	.2241-01	.9779-04
29873.	.1463+02	.1133+06	.7742+04	.2107-01	.9192-04
29869.	.1385+02	.1501+06	.1083+05	.3113-01	.1358-03
29864.	.1363+02	.1562+06	.1146+05	.3347-01	.1460-03
29864.	.1340+02	.1485+06	.1108+05	.3292-01	.1436-03
29865.	.1351+02	.1574+06	.1165+05	.3432-01	.1497-03
29865.	.1379+02	.7104+05	.5151+04	.1487-01	.6487-04
29855.	.1365+02	.6945+05	.5089+04	.1484-01	.6476-04
29861.	.1360+02	.2040+06	.1501+05	.4394-01	.1917-03
29858.	.1348+02	.1999+06	.1483+05	.4379-01	.1911-03
29856.	.1355+02	.2022+06	.1492+05	.4381-01	.1912-03
29854.	.1345+02	.6940+05	.5159+04	.1527-01	.6662-04
29853.	.1387+02	.1076+06	.7762+04	.2228-01	.9722-04
29856.	.1348+02	.1545+06	.1146+05	.3385-01	.1477-03
29851.	.1348+02	.2049+06	.1520+05	.4488-01	.1958-03
29874.	.1280+02	.4540+06	.3547+05	.1103+00	.4812-03
29874.	.1233+02	.5143+06	.4171+05	.1347+00	.5876-03
39807.	.3572+02	.7839+05	.2195+04	.2446-02	.1067-04
39800.	.3339+02	.7961+05	.2384+04	.2842-02	.1240-04
39814.	.3358+02	.8046+05	.2396+04	.2840-02	.1239-04
39809.	.3352+02	.7906+05	.2358+04	.2801-02	.1222-04
39819.	.3330+02	.7494+05	.2251+04	.2691-02	.1174-04

Table 14. Diester, 32°F (Continued)

L/D = 14.9

39820.	.3315+02	.7825+05	.2361+04	.2835-02	.1237-04
39817.	.3309+02	.1771+06	.5353+04	.6441-02	.2810-04
39807.	.3305+02	.1643+06	.4972+04	.5989-02	.2613-04
39798.	.3297+02	.1794+06	.5441+04	.6568-02	.2866-04
39796.	.3337+02	.1820+06	.5455+04	.6508-02	.2839-04
39790.	.3281+02	.2607+06	.7945+04	.9639-02	.4206-04
39788.	.3321+02	.2614+06	.7872+04	.9438-02	.4118-04
39822.	.3278+02	.2597+06	.7922+04	.9620-02	.4197-04
39820.	.3315+02	.2764+06	.8337+04	.1001-01	.4368-04
39813.	.3258+02	.3667+06	.1125+05	.1375-01	.5999-04
39816.	.3206+02	.3737+06	.1166+05	.1447-01	.6315-04
39817.	.3240+02	.3625+06	.1119+05	.1375-01	.5998-04
39823.	.3287+02	.3675+06	.1118+05	.1354-01	.5907-04
39820.	.3205+02	.4671+06	.1457+05	.1810-01	.7896-04
39815.	.3195+02	.4742+06	.1484+05	.1849-01	.8069-04
39812.	.3201+02	.4829+06	.1509+05	.1877-01	.8189-04
39811.	.3193+02	.4740+06	.1485+05	.1851-01	.8077-04

Table 14. Diester, 32°F (Continued)

L/D = 297

P3	VISCP	TAUDYN	NSRATE	RE	LEOL
4977.	.1092+01	.2526+04	.2313+04	.1393+00	.3050-04
4971.	.1084+01	.2620+04	.2417+04	.1466+00	.3212-04
4966.	.1078+01	.2600+04	.2411+04	.1470+00	.3220-04
4967.	.1080+01	.2567+04	.2377+04	.1447+00	.3169-04
4964.	.1092+01	.3970+04	.3636+04	.2190+00	.4795-04
4960.	.1101+01	.3991+04	.3624+04	.2163+00	.4738-04
4955.	.1082+01	.3920+04	.3622+04	.2201+00	.4819-04
4954.	.1101+01	.4063+04	.3690+04	.2203+00	.4825-04
4955.	.1090+01	.5449+04	.4999+04	.3015+00	.6604-04
4950.	.1089+01	.5593+04	.5137+04	.3101+00	.6792-04
4948.	.1090+01	.5538+04	.5079+04	.3062+00	.6706-04
4950.	.1079+01	.7672+04	.7113+04	.4336+00	.9495-04
4951.	.1076+01	.7565+04	.7029+04	.4294+00	.9403-04
4949.	.1078+01	.7760+04	.7201+04	.4393+00	.9621-04
9951.	.1923+01	.1960+04	.1019+04	.3485-01	.7631-05
9937.	.1926+01	.1977+04	.1027+04	.3504-01	.7673-05
9928.	.2019+01	.2016+04	.9983+03	.3250-01	.7118-05
9922.	.1994+01	.2178+04	.1093+04	.3603-01	.7891-05
9921.	.1944+01	.4796+04	.2467+04	.8340-01	.1827-04
9957.	.2007+01	.5137+04	.2559+04	.8382-01	.1836-04
9954.	.1994+01	.4997+04	.2505+04	.8258-01	.1809-04
9950.	.1961+01	.5026+04	.2563+04	.8592-01	.1882-04
9951.	.1940+01	.7163+04	.3692+04	.1251+00	.2740-04
9945.	.1939+01	.7314+04	.3771+04	.1278+00	.2800-04
9952.	.1944+01	.7149+04	.3677+04	.1243+00	.2723-04
9950.	.1963+01	.7506+04	.3824+04	.1281+00	.2805-04
9943.	.1955+01	.7379+04	.3774+04	.1269+00	.2779-04
9941.	.1945+01	.1049+05	.5394+04	.1823+00	.3993-04
9941.	.1938+01	.1025+05	.5291+04	.1795+00	.3932-04
9954.	.1924+01	.1008+05	.5235+04	.1788+00	.3917-04
9975.	.1947+01	.1019+05	.5232+04	.1766+00	.3869-04
9978.	.1954+01	.1040+05	.5326+04	.1792+00	.3925-04
9980.	.1937+01	.7294+04	.3766+04	.1278+00	.2799-04
9979.	.1931+01	.7534+04	.3902+04	.1329+00	.2910-04
9981.	.1934+01	.4576+04	.2366+04	.8044-01	.1762-04
20004.	.5512+01	.5568+04	.1010+04	.1205-01	.2639-05
19989.	.5586+01	.5866+04	.1050+04	.1236-01	.2707-05
19983.	.5568+01	.5858+04	.1052+04	.1242-01	.2721-05
19982.	.5406+01	.1425+05	.2636+04	.3205-01	.7020-05
19975.	.5409+01	.1447+05	.2675+04	.3251-01	.7121-05

Table 14. Diester, 32°F (Continued)

L/D = 297

19987.	.5469+01	.1329+05	.2431+04	.2922-01	.6399-05
19984.	.5263+01	.1302+05	.2474+04	.3090-01	.6766-05
19975.	.5525+01	.1313+05	.2375+04	.2826-01	.6190-05
19987.	.5443+01	.2137+05	.3926+04	.4741-01	.1038-04
19981.	.5477+01	.2109+05	.3851+04	.4622-01	.1012-04
19989.	.5588+01	.2125+05	.3803+04	.4474-01	.9799-05
19986.	.5535+01	.2162+05	.3907+04	.4641-01	.1016-04
19985.	.5521+01	.3014+05	.5459+04	.6500-01	.1423-04
19979.	.5478+01	.2893+05	.5281+04	.6337-01	.1388-04
19977.	.5533+01	.3066+05	.5541+04	.6584-01	.1442-04
19993.	.5389+01	.2841+05	.5272+04	.6432-01	.1409-04
19998.	.5391+01	.2880+05	.5341+04	.6513-01	.1426-04
19996.	.5469+01	.1421+05	.2598+04	.3123-01	.6839-05
19998.	.5457+01	.2075+05	.3802+04	.4579-01	.1003-04
19997.	.5446+01	.1398+05	.2567+04	.3099-01	.6786-05
19998.	.5354+01	.1368+05	.2554+04	.3137-01	.6869-05
19999.	.5384+01	.6103+04	.1133+04	.1384-01	.3031-05
19999.	.5315+01	.5779+04	.1087+04	.1345-01	.2945-05
29971.	.1370+02	.1449+05	.1058+04	.5077-02	.1112-05
29971.	.1410+02	.1525+05	.1081+04	.5040-02	.1104-05
29996.	.1415+02	.1511+05	.1068+04	.4961-02	.1087-05
29987.	.1365+02	.1503+05	.1101+04	.5300-02	.1161-05
29989.	.1335+02	.3276+05	.2454+04	.1209-01	.2647-05
29984.	.1365+02	.3354+05	.2458+04	.1184-01	.2593-05
29981.	.1386+02	.3412+05	.2462+04	.1168-01	.2558-05
29981.	.1386+02	.3565+05	.2572+04	.1220-01	.2671-05
29995.	.1435+02	.3532+05	.2461+04	.1127-01	.2468-05
29989.	.1429+02	.3701+05	.2590+04	.1192-01	.2610-05
29984.	.1462+02	.1627+05	.1113+04	.5005-02	.1096-05
29979.	.1358+02	.1494+05	.1100+04	.5325-02	.1166-05
29973.	.1052+02	.1376+02	.1308+01	.8171-05	.1789-08
29969.	.1418+02	.5418+05	.3822+04	.1772-01	.3882-05
29965.	.1430+02	.5461+05	.3818+04	.1755-01	.3844-05
29961.	.1421+02	.5377+05	.3784+04	.1751-01	.3834-05
39979.	.3187+02	.3570+05	.1120+04	.2310-02	.5060-06
39959.	.3345+02	.3678+05	.1100+04	.2162-02	.4734-06
40001.	.3398+02	.3415+05	.1005+04	.1944-02	.4258-06
39977.	.3515+02	.4082+05	.1161+04	.2171-02	.4755-06
39999.	.3381+02	.3781+05	.1118+04	.2175-02	.4763-06

Table 14. Diester, 32°F (Continued)

Averaged Data Points L/D = 297

P (psi)	V (cp)
.0	.57500+02
.49583+04	.10865+03
.99520+04	.19534+03
.19989+05	.54574+03
.29980+05	.13990+04
.39983+05	.33652+04

Table 15. Diester, 10°F

L/D = 1.35

P3	VISCP	TAUDYN	NSRATE	RE	LEOL
9978.	.4895+01	.1131+06	.2310+05	.3688-01	.1776-02
9963.	.4680+01	.1146+06	.2448+05	.4088-01	.1968-02
9977.	.4645+01	.1090+06	.2346+05	.3948-01	.1901-02
9967.	.4658+01	.2693+06	.5781+05	.9700-01	.4670-02
9963.	.4706+01	.2724+06	.5789+05	.9615-01	.4630-02
9959.	.4613+01	.2629+06	.5700+05	.9659-01	.4650-02
9955.	.4586+01	.2739+06	.5972+05	.1018+00	.4901-02
9971.	.4639+01	.2661+06	.5737+05	.9665-01	.4653-02
9968.	.4622+01	.2671+06	.5780+05	.9776-01	.4707-02
9973.	.4645+01	.2713+06	.5841+05	.9828-01	.4732-02
9971.	.4761+01	.2771+06	.5821+05	.9555-01	.4601-02
9966.	.4666+01	.2682+06	.5748+05	.9629-01	.4636-02
9970.	.4657+01	.4303+06	.9240+05	.1551+00	.7467-02
9966.	.4617+01	.4270+06	.9247+05	.1565+00	.7537-02
9968.	.4639+01	.4192+06	.9037+05	.1523+00	.7332-02
9968.	.4679+01	.4316+06	.9225+05	.1541+00	.7420-02
9965.	.4637+01	.4281+06	.9232+05	.1556+00	.7492-02
9964.	.4671+01	.4407+06	.9435+05	.1579+00	.7602-02
9965.	.4618+01	.5732+06	.1241+06	.2100+00	.1011-01
9967.	.4642+01	.5809+06	.1252+06	.2108+00	.1015-01
9971.	.4666+01	.5695+06	.1221+06	.2045+00	.9846-02
9972.	.4654+01	.7567+06	.1626+06	.2731+00	.1315-01
9966.	.4653+01	.7895+06	.1697+06	.2850+00	.1372-01
9969.	.4668+01	.5696+06	.1220+06	.2043+00	.9837-02
9975.	.4710+01	.7840+06	.1665+06	.2763+00	.1330-01
9967.	.4654+01	.7859+06	.1689+06	.2836+00	.1365-01
9972.	.4625+01	.9228+06	.1995+06	.3371+00	.1623-01
9972.	.4686+01	.9286+06	.1982+06	.3305+00	.1591-01
9976.	.4646+01	.9110+06	.1961+06	.3299+00	.1588-01
9981.	.4596+01	.9660+06	.2102+06	.3574+00	.1721-01
9979.	.4614+01	.9441+06	.2046+06	.3467+00	.1669-01
19688.	.1434+02	.4377+06	.3053+05	.1664-01	.8012-03
19688.	.1463+02	.3637+06	.2486+05	.1329-01	.6397-03
19688.	.1404+02	.3358+06	.2391+05	.1331-01	.6410-03
19689.	.1434+02	.7978+06	.5563+05	.3032-01	.1460-02
19689.	.1435+02	.7638+06	.5324+05	.2900-01	.1396-02
19685.	.1432+02	.8011+06	.5595+05	.3054-01	.1470-02
19682.	.1418+02	.1240+07	.8744+05	.4821-01	.2321-02
19684.	.1428+02	.1273+07	.8910+05	.4876-01	.2348-02
19682.	.1411+02	.1237+07	.8761+05	.4852-01	.2336-02
19684.	.1410+02	.1717+07	.1217+06	.6747-01	.3249-02

Table 15. Diester, 10°F (Continued)

L/D = 1.35

19682.	.1402+02	.1722+07	.1228+06	.6847-01	.3297-02
19682.	.1398+02	.1827+07	.1307+06	.7306-01	.3518-02
19681.	.1394+02	.2316+07	.1661+06	.9312-01	.4484-02
19679.	.1392+02	.2276+07	.1634+06	.9175-01	.4418-02
19685.	.1385+02	.2299+07	.1660+06	.9367-01	.4510-02
19690.	.1367+04	.6948+06	.5081+03	.2904-05	.1398-06
19675.	.1402+02	.1249+07	.8907+05	.4964-01	.2390-02
19676.	.1406+02	.1268+07	.9015+05	.5011-01	.2413-02
19676.	.1410+02	.1263+07	.8954+05	.4964-01	.2390-02
19675.	.1402+02	.1260+07	.8991+05	.5013-01	.2414-02
19671.	.1407+02	.1238+07	.8798+05	.4888-01	.2354-02
20047.	.1432+02	.3482+06	.2431+05	.1327-01	.6388-03
20034.	.1419+02	.3365+06	.2371+05	.1306-01	.6286-03
20031.	.1431+02	.3350+06	.2341+05	.1279-01	.6158-03
20032.	.1423+02	.8280+06	.5818+05	.3196-01	.1539-02
20025.	.1424+02	.8603+06	.6043+05	.3318-01	.1597-02
20045.	.1435+02	.8048+06	.5608+05	.3054-01	.1470-02
20039.	.1423+02	.1315+07	.9240+05	.5074-01	.2443-02
20036.	.1410+02	.1317+07	.9340+05	.5179-01	.2494-02
20035.	.1418+02	.1271+07	.8964+05	.4942-01	.2380-02
20030.	.1414+02	.1738+07	.1229+06	.6792-01	.3270-02
20027.	.1396+02	.1850+07	.1325+06	.7417-01	.3571-02
20028.	.1400+02	.1729+07	.1235+06	.6898-01	.3321-02
20029.	.1384+02	.2284+07	.1650+06	.9318-01	.4486-02
20025.	.1367+02	.2293+07	.1677+06	.9592-01	.4618-02
20047.	.1395+02	.2257+07	.1617+06	.9061-01	.4363-02
20045.	.1388+02	.2306+07	.1661+06	.9350-01	.4502-02
20037.	.1376+02	.2309+07	.1679+06	.9537-01	.4592-02
20032.	.1363+02	.2733+07	.2005+06	.1150+00	.5538-02
20038.	.1353+02	.2757+07	.2038+06	.1177+00	.5666-02
20038.	.1349+02	.2816+07	.2087+06	.1209+00	.5821-02
27664.	.3901+02	.2354+07	.6033+05	.1209-01	.5820-03
27898.	.3892+02	.2280+07	.5859+05	.1177-01	.5665-03
28130.	.3745+02	.3518+07	.9393+05	.1960-01	.9439-03
28163.	.3810+02	.3419+07	.8975+05	.1841-01	.8866-03
28250.	.3667+02	.4549+07	.1240+06	.2644-01	.1273-02
28373.	.3647+02	.4662+07	.1278+06	.2740-01	.1319-02
28339.	.3683+02	.4570+07	.1241+06	.2634-01	.1268-02
28345.	.3549+02	.5899+07	.1662+06	.3660-01	.1762-02
28412.	.3521+02	.5941+07	.1687+06	.3745-01	.1803-02
28459.	.3457+02	.6995+07	.2023+06	.4574-01	.2202-02
28457.	.3430+02	.7134+07	.2080+06	.4740-01	.2282-02

Table 15. Diester, 10°F (Continued)

L/D = 1.35

28442.	.2959+02	.1230+08	.4158+06	.1098+00	.5287-02
28422.	.2719+02	.1322+08	.4863+06	.1398+00	.6731-02
28863.	.2918+02	.1126+08	.3858+06	.1034+00	.4976-02
28850.	.2928+02	.1227+08	.4190+06	.1118+00	.5384-02
28892.	.3143+02	.1013+08	.3223+06	.8016-01	.3859-02
29008.	.2551+02	.1573+08	.6166+06	.1889+00	.9097-02
29028.	.2739+02	.1447+08	.5283+06	.1508+00	.7260-02
28989.	.2837+02	.1327+08	.4679+06	.1289+00	.6208-02
30119.	.3830+02	.9992+06	.2609+05	.5324-02	.2564-03
30109.	.3901+02	.9509+06	.2438+05	.4885-02	.2352-03
30089.	.4046+02	.1038+07	.2566+05	.4957-02	.2386-03
30076.	.3931+02	.9853+06	.2507+05	.4984-02	.2400-03
30119.	.4112+02	.9648+06	.2346+05	.4459-02	.2147-03
30122.	.3979+02	.9234+06	.2321+05	.4558-02	.2195-03
30113.	.3839+02	.2268+07	.5909+05	.1203-01	.5792-03
30121.	.3822+02	.2317+07	.6062+05	.1240-01	.5969-03
30113.	.3931+02	.2330+07	.5925+05	.1178-01	.5672-03
30113.	.3783+02	.3482+07	.9204+05	.1901-01	.9155-03
30124.	.3714+02	.3513+07	.9459+05	.1991-01	.9585-03
30119.	.3747+02	.3438+07	.9174+05	.1914-01	.9214-03
30105.	.3618+02	.4624+07	.1278+06	.2761-01	.1329-02
30115.	.3628+02	.4644+07	.1280+06	.2758-01	.1328-02
30100.	.3630+02	.4754+07	.1310+06	.2820-01	.1358-02
30109.	.3554+02	.5931+07	.1669+06	.3671-01	.1767-02
30093.	.3529+02	.5993+07	.1698+06	.3762-01	.1811-02
30114.	.3555+02	.6067+07	.1706+06	.3752-01	.1806-02
38771.	.9436+02	.5779+07	.6125+05	.5073-02	.2443-03
38761.	.9573+02	.5493+07	.5738+05	.4685-02	.2256-03
38726.	.9073+02	.8162+07	.8996+05	.7750-02	.3732-03
38713.	.9120+02	.8148+07	.8934+05	.7656-02	.3686-03
38764.	.9734+02	.5357+07	.5503+05	.4419-02	.2128-03
38739.	.9051+02	.8216+07	.9077+05	.7838-02	.3774-03
38769.	.9076+02	.8133+07	.8961+05	.7717-02	.3716-03
38739.	.8456+02	.1071+08	.1266+06	.1170-01	.5635-03
38717.	.8714+02	.1090+08	.1251+06	.1122-01	.5402-03
38678.	.7796+02	.1324+08	.1698+06	.1703-01	.8199-03
38590.	.7833+02	.1334+08	.1703+06	.1699-01	.8181-03
38551.	.7481+02	.1519+08	.2031+06	.2122-01	.1022-02
38610.	.7394+02	.1514+08	.2048+06	.2165-01	.1042-02
38573.	.6234+02	.2208+08	.3542+06	.4441-01	.2138-02
38695.	.4841+02	.2742+08	.5664+06	.9144-01	.4403-02
38680.	.6256+02	.2051+08	.3279+06	.4096-01	.1972-02

Table 15. Diester, 10°F (Continued)

L/D = 1.35

38706.	.5708+02	.2343+08	.4105+06	.5620-01	.2706-02
38711.	.5431+02	.2452+08	.4515+06	.6498-01	.3129-02
38687.	.4526+02	.2976+08	.6575+06	.1136+00	.5468-02
40116.	.9979+02	.2538+07	.2544+05	.1992-02	.9593-04
40114.	.1006+03	.2838+07	.2820+05	.2190-02	.1054-03
40118.	.9956+02	.2774+07	.2787+05	.2188-02	.1053-03
40126.	.9411+02	.5601+07	.5952+05	.4943-02	.2380-03
40148.	.9436+02	.5878+07	.6229+05	.5159-02	.2484-03
40108.	.9453+02	.5693+07	.6023+05	.4980-02	.2398-03
40111.	.8645+02	.8264+07	.9559+05	.8643-02	.4161-03
40114.	.8860+02	.8414+07	.9496+05	.8378-02	.4034-03
40116.	.8848+02	.8244+07	.9317+05	.8230-02	.3963-03
40081.	.8553+02	.9297+07	.1087+06	.9933-02	.4782-03
40114.	.8762+02	.9543+07	.1089+06	.9716-02	.4678-03
40077.	.8391+02	.1030+08	.1227+06	.1143-01	.5505-03
40128.	.8372+02	.1062+08	.1269+06	.1185-01	.5703-03
40099.	.8441+02	.1049+08	.1243+06	.1151-01	.5543-03
40063.	.8416+02	.1038+08	.1234+06	.1146-01	.5518-03

Table 15. Diester, 10°F (Continued)

L/D = 14.9

P3	VISCP	TAUDYN	NSRATE	RE	LEOL
39737.	.9575+02	.1808+06	.1888+04	.7851-03	.3426-05
39766.	.9943+02	.2229+06	.2242+04	.8977-03	.3917-05
39737.	.9545+02	.1926+06	.2018+04	.8417-03	.3673-05
39771.	.9387+02	.4856+06	.5173+04	.2194-02	.9572-05
39774.	.9506+02	.4932+06	.5188+04	.2173-02	.9480-05
39752.	.9560+02	.4852+06	.5075+04	.2113-02	.9221-05
39761.	.9186+02	.7346+06	.7997+04	.3466-02	.1512-04
39756.	.9223+02	.7340+05	.7959+04	.3435-02	.1499-04
39764.	.9169+02	.7251+06	.7909+04	.3434-02	.1498-04
39749.	.8750+02	.9438+06	.1079+05	.4907-02	.2141-04
39737.	.8716+02	.9726+06	.1116+05	.5097-02	.2224-04
39724.	.8957+02	.9172+06	.1024+05	.4552-02	.1986-04
29640.	.3808+02	.8771+05	.2303+04	.2408-02	.1051-04
29629.	.3812+02	.8807+05	.2311+04	.2413-02	.1053-04
29631.	.3784+02	.1947+06	.5146+04	.5413-02	.2362-04
29632.	.3720+02	.2045+06	.5497+04	.5882-02	.2566-04
29632.	.3698+02	.2979+06	.8055+04	.8672-02	.3784-04
29634.	.3693+02	.3024+06	.8188+04	.8826-02	.3851-04
29631.	.3636+02	.3994+06	.1098+05	.1203-01	.5247-04
29629.	.3626+02	.4111+06	.1134+05	.1245-01	.5432-04
29629.	.3568+02	.5238+06	.1468+05	.1638-01	.7147-04
29628.	.3571+02	.5230+06	.1465+05	.1633-01	.7125-04

Table 16. Dimethyl Siloxane DC - 200 - 50

100°F, L/D = 297

DC200-20CS,CAP4,100F,3-23-71

P3	VISCP	NSRATE	KEC	DELTAP	TAUDYN	REYN
5432.	.7502+00	.2398+05	.8678-01	.3065+03	.1799+05	.2661+01
5355.	.7395+00	.1628+05	.4003-01	.2052+03	.1204+05	.1833+01
5355.	.6985+00	.1748+05	.4614-01	.2080+03	.1221+05	.2084+01
5355.	.7046+00	.1945+05	.5709-01	.2335+03	.1370+05	.2298+01
5355.	.7301+00	.2781+05	.1168+00	.3460+03	.2031+05	.3172+01
5355.	.7415+00	.2382+05	.8563-01	.3009+03	.1766+05	.2674+01
5355.	.6832+00	.2270+05	.7777-01	.2642+03	.1551+05	.2766+01
11186.	.1272+01	.9391+04	.1331-01	.2034+03	.1194+05	.6149+00
11147.	.1144+01	.1199+05	.2170-01	.2336+03	.1371+05	.8728+00
11186.	.1236+01	.1658+05	.4152-01	.3493+03	.2050+05	.1117+01
11186.	.1211+01	.1449+05	.3168-01	.2990+03	.1755+05	.9957+00
11225.	.1208+01	.4636+05	.3244+00	.9543+03	.5601+05	.3194+01
11225.	.1252+01	.5275+05	.4200+00	.1125+04	.6606+05	.3507+01
11186.	.1386+01	.5874+05	.5209+00	.1387+04	.8140+05	.3530+01
11186.	.1196+01	.6374+05	.6133+00	.1299+04	.7622+05	.4438+01
11225.	.1128+01	.6494+05	.6366+00	.1248+04	.7324+05	.4794+01
19907.	.2573+01	.6591+04	.6558-02	.2889+03	.1696+05	.2133+00
19758.	.2526+01	.6314+04	.6017-02	.2717+03	.1595+05	.2081+00
20056.	.2542+01	.6787+04	.6954-02	.2939+03	.1725+05	.2223+00
19758.	.2442+01	.1247+05	.2347-01	.5187+03	.3045+05	.4252+00
19907.	.2517+01	.1578+05	.3761-01	.6769+03	.3973+05	.5222+00
19907.	.2669+01	.1179+05	.2097-01	.5359+03	.3146+05	.3677+00
19907.	.2576+01	.1300+05	.2549-01	.5704+03	.3348+05	.4200+00
19758.	.2336+01	.2370+05	.8482-01	.9433+03	.5537+05	.8450+00
19907.	.2421+01	.2814+05	.1195+00	.1161+04	.6813+05	.9678+00
19907.	.2448+01	.2053+05	.6365-01	.8566+03	.5028+05	.6983+00
29445.	.5311+01	.3630+04	.1989-02	.3285+03	.1928+05	.5692-01
29445.	.5338+01	.4183+04	.2641-02	.3804+03	.2233+05	.6525-01
29445.	.5200+01	.5130+04	.3972-02	.4545+03	.2668+05	.8213-01
29445.	.5207+01	.6850+04	.7084-02	.6077+03	.3567+05	.1095+00
29445.	.5371+01	.8397+04	.1064-01	.7684+03	.4510+05	.1302+00
29445.	.5245+01	.8460+04	.1080-01	.7561+03	.4438+05	.1343+00
38386.	.9816+01	.3177+04	.1523-02	.5312+03	.3118+05	.2695-01
38386.	.9931+01	.4045+04	.2469-02	.6844+03	.4017+05	.3391-01
38386.	.9723+01	.3847+04	.2234-02	.6374+03	.3741+05	.3295-01

Table 16. Dimethyl Siloxane DC - 200 - 50 (Continued)

100°F, L/D = 297

38386.	.9495+01	.3788+04	.2166-02	.6128+03	.3597+05	.3322-01
38386.	.9933+01	.4045+04	.2469-02	.6845+03	.4018+05	.3390-01
47775.	.1947+02	.2036+04	.6258-03	.6754+03	.3964+05	.8708-02
47775.	.2044+02	.1464+04	.3236-03	.5100+03	.2993+05	.5963-02
47626.	.2087+02	.1778+04	.4772-03	.6321+03	.3710+05	.7095-02
47626.	.1933+02	.1815+04	.4974-03	.5979+03	.3509+05	.7818-02
47626.	.1990+02	.1309+04	.2588-03	.4440+03	.2606+05	.5478-02
58803.	.4856+02	.6695+03	.6767-04	.5540+03	.3252+05	.1148-02
58803.	.4915+02	.5245+03	.4152-04	.4392+03	.2578+05	.8884-03
58654.	.4812+02	.5803+03	.5083-04	.4757+03	.2792+05	.1004-02
58803.	.4913+02	.6323+03	.6036-04	.5293+03	.3107+05	.1072-02
68936.	.1202+03	.2172+03	.7123-05	.4450+03	.2612+05	.1504-03
69234.	.1237+03	.2541+03	.9748-05	.5354+03	.3143+05	.1711-03
69234.	.1218+03	.2499+03	.9430-05	.5186+03	.3044+05	.1709-03
69085.	.1203+03	.2457+03	.9116-05	.5038+03	.2957+05	.1700-03
69085.	.1220+03	.1492+03	.3362-05	.3102+03	.1821+05	.1018-03
79070.	.3333+03	.6772+02	.6923-06	.3846+03	.2257+05	.1692-04
78921.	.4360+03	.6982+02	.7357-06	.5186+03	.3044+05	.1333-04
78921.	.4494+03	.5376+02	.4362-06	.4116+03	.2416+05	.9960-05

Table 16. Dimethyl Siloxane DC - 200 - 50 (Continued)

210°F, L/D = 297

DC200-20Cs,210F,CAP4,3 24-71

P3	VISCP	NSRATE	KEC	DELTAP	TAUDYN	REYN
5398.	.3346+00	.2399+05	.8409-01	.1368+03	.8027+04	.5778+01
5398.	.3152+00	.3952+05	.2282+00	.2122+03	.1246+05	.1010+02
5359.	.3271+00	.3003+05	.1317+00	.1673+03	.9822+04	.7398+01
5359.	.3269+00	.4409+05	.2840+00	.2456+03	.1441+05	.1087+02
5320.	.3368+00	.4330+05	.2739+00	.2485+03	.1458+05	.1036+02
11464.	.5769+00	.1549+05	.3506-01	.1523+03	.8938+04	.2164+01
11542.	.5615+00	.1539+05	.3461-01	.1473+03	.8643+04	.2209+01
11542.	.5561+00	.2185+05	.6973-01	.2070+03	.1215+05	.3166+01
11503.	.5375+00	.1880+05	.5164-01	.1722+03	.1011+05	.2819+01
11464.	.5401+00	.2685+05	.1053+00	.2471+03	.1450+05	.4006+01
19460.	.9025+00	.1493+05	.3256-01	.2296+03	.1347+05	.1333+01
19460.	.8864+00	.1847+05	.4981-01	.2789+03	.1637+05	.1679+01
19311.	.8800+00	.1267+05	.2345-01	.1900+03	.1115+05	.1160+01
19162.	.9639+00	.1834+05	.4911-01	.3011+03	.1767+05	.1533+01
19162.	.9428+00	.9528+04	.1396-01	.1530+03	.8982+04	.8143+00
49414.	.4624+01	.2076+04	.6293-03	.1635+03	.9597+04	.3617-01
49414.	.4248+01	.2358+04	.8124-03	.1707+03	.1002+05	.4473-01
49414.	.4669+01	.2209+04	.7131-03	.1758+03	.1032+05	.3813-01
49861.	.4876+01	.1904+04	.5298-03	.1582+03	.9285+04	.3147-01
49861.	.4645+01	.2187+04	.6988-03	.1731+03	.1016+05	.3794-01
49861.	.4388+01	.1957+04	.5592-03	.1463+03	.8585+04	.3593-01
66850.	.1150+02	.9423+03	.1297-03	.1846+03	.1084+05	.6602-02
66850.	.1132+02	.1547+04	.3498-03	.2084+03	.1752+05	.1101-01
66850.	.1117+02	.1555+04	.3531-03	.2960+03	.1737+05	.1121-01
66850.	.1079+02	.2068+04	.6248-03	.3803+03	.2232+05	.1544-01
66850.	.1126+02	.1235+04	.2298-03	.2370+03	.1391+05	.8834-02
66850.	.1140+02	.1845+04	.4972-03	.3583+03	.2103+05	.1304-01
79815.	.2239+02	.6943+03	.7043-04	.2649+03	.1555+05	.2499-02
79815.	.2121+02	.6051+03	.5348-04	.2187+03	.1284+05	.2298-02
79815.	.2043+02	.7538+03	.8302-04	.2623+03	.1540+05	.2974-02
79666.	.2124+02	.6646+03	.6452-04	.2405+03	.1412+05	.2521-02
79666.	.2245+02	.1017+04	.1510-03	.3988+03	.2282+05	.3650-02
79666.	.2037+02	.1106+04	.1787-03	.3938+03	.2253+05	.4375-02
79666.	.2151+02	.9671+03	.1366-03	.3545+03	.2081+05	.3622-02

Table 16. Dimethyl Siloxane DC - 200 - 50 (Continued)

300°F, L/D = 297

DC200-20Cs,300F,CAP4,3 25-71

P3	VISCP	NSRATE	KEC	DELTAP	TAUDYN	REYN
5350.	.2037+00	.3417+05	.1649+00	.1186+03	.6960+04	.1307+02
5350.	.2061+00	.4905+05	.3397+00	.1722+03	.1011+05	.1854+02
5350.	.1828+00	.7156+05	.7232+00	.2228+03	.1308+05	.3050+02
5350.	.1953+00	.7880+05	.8768+00	.2622+03	.1539+05	.3143+02
5389.	.1909+00	.6674+05	.6290+00	.2171+03	.1274+05	.2723+02
5389.	.1990+00	.5575+05	.4389+00	.1891+03	.1110+05	.2182+02
12194.	.3684+00	.2573+05	.9349-01	.1615+03	.9480+04	.5440+01
12234.	.3196+00	.3152+05	.1403+00	.1716+03	.1007+05	.7683+01
12194.	.3541+00	.4684+05	.3098+00	.2826+03	.1658+05	.1030+02
12194.	.3347+00	.4825+05	.3287+00	.2751+03	.1615+05	.1123+02
12194.	.3465+00	.4362+05	.2687+00	.2575+03	.1511+05	.9807+01
20354.	.5771+00	.2310+05	.7537-01	.2271+03	.1333+05	.3118+01
20354.	.5443+00	.3033+05	.1299+00	.2813+03	.1651+05	.4341+01
20354.	.6250+00	.1760+05	.4375-01	.1874+03	.1100+05	.2194+01
20354.	.5403+00	.1289+05	.2345-01	.1186+03	.6963+04	.1858+01
20354.	.5536+00	.1650+05	.3845-01	.1557+03	.9136+04	.2322+01
20354.	.5360+00	.1434+05	.2904-01	.1310+03	.7686+04	.2084+01
50159.	.2252+01	.4893+04	.3381-02	.1877+03	.1102+05	.1693+00
50159.	.2338+01	.6377+04	.5742-02	.2540+03	.1491+05	.2124+00
50308.	.2275+01	.5998+04	.5080-02	.2324+03	.1364+05	.2054+00
50308.	.2314+01	.6503+04	.5972-02	.2564+03	.1505+05	.2189+00
50308.	.2329+01	.5714+04	.4610-02	.2267+03	.1331+05	.1911+00
68638.	.4903+01	.3177+04	.1425-02	.2653+03	.1557+05	.5047-01
68638.	.4656+01	.4301+04	.2612-02	.3412+03	.2003+05	.7196-01
68638.	.4480+01	.2644+04	.9871-03	.2018+03	.1184+05	.4597-01
68638.	.4710+01	.4222+04	.2517-02	.3388+03	.1989+05	.6983-01
68638.	.4602+01	.3887+04	.2133-02	.3048+03	.1789+05	.6579-01
81603.	.7166+01	.1860+04	.4884-03	.2270+03	.1333+05	.2022-01
81603.	.7038+01	.2500+04	.8823-03	.2997+03	.1759+05	.2766-01
81603.	.7067+01	.2507+04	.8875-03	.3019+03	.1772+05	.2763-01
81603.	.6519+01	.3343+04	.1578-02	.3713+03	.2179+05	.3094-01
81603.	.7176+01	.3690+04	.1923-02	.4511+03	.2648+05	.4005-01

Table 16. Dimethyl Siloxane DC - 200 - 50 (Continued)

L/D = 297 Averaged Data Points

DC200-20CS,CAP4,100F,3-23-71

P (PSI)	V (CP)
.00000	.39100+02
.53657+04	.72110+02
.11194+05	.12259+03
.19878+05	.25050+03
.29445+05	.52787+03
.38386+05	.97799+03
.47685+05	.20003+04
.58765+05	.48742+04
.69115+05	.12161+05
.78921+05	.44270+05

ALPHA STAR= .96336-04
ALPHA OT= .13550-03

DC200-20CS,210F,CAP4,3 24-71

P (PSI)	V (CP)
.00000	.15200+02
.53667+04	.32812+02
.11503+05	.55443+02
.19311+05	.91511+02
.49638+05	.45749+03
.66850+05	.11242+04
.79730+05	.21371+04

ALPHA STAR= .95620-04
ALPHA OT= .20481-03

DC200-20CS,300F,CAP4,3 25-71

P (PSI)	V (CP)
.00000	.84600+01
.53631+04	.19630+02
.12202+05	.34464+02
.20354+05	.56270+02
.50249+05	.23016+03
.68638+05	.46701+03
.81603+05	.69932+03

ALPHA STAR= .95546-04
ALPHA OT= .24187-03

Table 17. Dimethyl Siloxane DC - 200 - 50, 75°F

L/D = 1.35

P3	VISCP	TAUDYN	NSRATE	RE	LEOL
30156.	.8818+01	.1228+06	.1393+05	.1234-01	.5943-03
30146.	.8567+01	.1258+06	.1468+05	.1340-01	.6451-03
30140.	.9039+01	.1243+06	.1375+05	.1189-01	.5726-03
30146.	.8813+01	.4416+06	.5011+05	.4444-01	.2140-02
30141.	.8915+01	.4359+06	.4890+05	.4287-01	.2064-02
30138.	.8989+01	.4326+06	.4813+05	.4185-01	.2015-02
30135.	.9075+01	.4609+06	.5078+05	.4374-01	.2106-02
30150.	.8741+01	.7268+06	.8316+05	.7436-01	.3580-02
30154.	.8739+01	.7046+06	.8063+05	.7212-01	.3473-02
30154.	.8750+01	.7328+06	.8376+05	.7482-01	.3602-02
30152.	.8718+01	.7426+06	.8518+05	.7637-01	.3677-02
30150.	.8751+01	.1057+07	.1208+06	.1079+00	.5193-02
30148.	.8701+01	.1052+07	.1210+06	.1087+00	.5231-02
30146.	.8722+01	.1047+07	.1201+06	.1076+00	.5182-02
30142.	.8755+01	.1059+07	.1209+06	.1080+00	.5198-02
30152.	.8609+01	.1416+07	.1645+06	.1494+00	.7191-02
30150.	.8615+01	.1343+07	.1559+06	.1414+00	.6810-02
30148.	.8725+01	.1391+07	.1595+06	.1428+00	.6878-02
30146.	.8694+01	.1332+07	.1532+06	.1377+00	.6630-02
30141.	.8593+01	.1644+07	.1913+06	.1740+00	.8380-02
30135.	.8643+01	.1715+07	.1984+06	.1795+00	.8641-02
30132.	.8635+01	.1696+07	.1964+06	.1778+00	.8560-02
30149.	.8443+01	.3253+07	.3852+06	.3567+00	.1717-01
30150.	.8036+01	.4809+07	.5985+06	.5821+00	.2803-01
30142.	.8254+01	.3946+07	.4781+06	.4527+00	.2180-01
30145.	.8482+01	.2906+07	.3426+06	.3157+00	.1520-01
30143.	.8436+01	.1868+07	.2214+06	.2052+00	.9878-02
30143.	.8235+01	.3791+07	.4604+06	.4370+00	.2104-01
30141.	.8113+01	.4850+07	.5978+06	.5760+00	.2773-01
30136.	.8055+01	.4721+07	.5861+06	.5687+00	.2738-01
30133.	.7796+01	.7644+07	.9805+06	.9830+00	.4733-01
30137.	.7645+01	.1071+08	.1401+07	.1433+01	.6899-01
30135.	.7985+01	.7846+07	.9826+06	.9619+00	.4631-01
30145.	.7768+01	.1033+08	.1330+07	.1339+01	.6445-01
30159.	.7894+01	.8907+07	.1128+07	.1117+01	.5380-01
29627.	.8359+01	.5120+07	.6125+06	.5727+00	.2757-01
29623.	.7494+01	.8468+07	.1130+07	.1178+01	.5674-01
29603.	.6738+01	.1694+08	.2515+07	.2917+01	.1405+00
29593.	.6799+01	.1539+08	.2264+07	.2602+01	.1253+00
29593.	.8373+01	.1302+08	.1555+07	.1452+01	.6990-01
29611.	.6482+01	.2057+08	.3174+07	.3828+01	.1843+00
29630.	.6777+01	.1712+08	.2526+07	.2913+01	.1403+00
29581.	.7205+01	.1291+08	.1792+07	.1944+01	.9358-01

Table 17. Dimethyl Siloxane DC - 200 - 50, 75°F (Continued)

L/D = 1.35

P3	VISCP	TAUDYN	NSRATE	RE	LEOL
40036.	.1967+02	.5770+07	.2933+06	.1166+00	.5612-02
40026.	.1870+02	.8492+07	.4542+06	.1899+00	.9144-02
40009.	.1649+02	.1932+08	.1172+07	.5554+00	.2674-01
39998.	.1696+02	.1636+08	.9644+06	.4444+00	.2140-01
39994.	.1854+02	.6642+07	.3581+06	.1510+00	.7268-02
39982.	.1565+02	.2585+08	.1652+07	.8248+00	.3971-01
40007.	.1552+02	.2860+08	.1843+07	.9280+00	.4468-01
40045.	.1553+02	.2705+08	.1742+07	.8768+00	.4222-01
40034.	.1915+02	.4603+07	.2403+06	.9807-01	.4722-02
40045.	.1937+02	.4608+07	.2379+06	.9599-01	.4622-02
40066.	.1515+02	.3174+08	.2094+07	.1080+01	.5200-01
40086.	.1911+02	.8878+07	.4647+06	.1901+00	.9152-02
40082.	.2041+02	.5136+07	.2517+06	.9640-01	.4641-02
40079.	.1790+02	.1377+08	.7693+06	.3360+00	.1618-01
40075.	.1686+02	.1981+08	.1175+07	.5445+00	.2622-01
40063.	.1738+02	.1430+08	.8224+06	.3698+00	.1780-01
40075.	.1497+02	.3262+08	.2179+07	.1137+01	.5476-01
40074.	.1462+02	.3541+08	.2422+07	.1295+01	.6233-01
40071.	.1392+02	.3814+08	.2739+07	.1538+01	.7403-01
40090.	.1418+02	.3806+08	.2684+07	.1480+01	.7125-01
40096.	.1696+02	.1435+08	.8456+06	.3896+00	.1876-01
40085.	.1967+02	.4550+07	.2313+06	.9192-01	.4426-02
40078.	.1533+02	.2215+08	.1445+07	.7369+00	.3548-01
40076.	.1404+02	.3335+08	.2376+07	.1323+01	.6372-01
40065.	.1347+02	.3965+08	.2944+07	.1708+01	.8226-01
40071.	.1876+02	.3855+07	.2055+06	.8561-01	.4122-02
40063.	.1412+02	.3843+08	.2722+07	.1507+01	.7257-01
40065.	.1425+02	.3578+08	.2510+07	.1377+01	.6628-01
40080.	.1596+02	.1978+08	.1240+07	.6072+00	.2923-01
40100.	.1648+02	.1413+08	.8573+06	.4065+00	.1957-01
40204.	.2201+02	.3555+06	.1615+05	.5734-02	.2761-03
40199.	.1886+02	.3189+06	.1691+05	.7005-02	.3373-03
40196.	.2152+02	.3707+06	.1723+05	.6260-02	.3014-03
40189.	.2134+02	.2785+06	.1305+05	.4782-02	.2302-03
40187.	.2153+02	.3128+06	.1453+05	.5275-02	.2540-03
40185.	.1961+02	.2687+06	.1370+05	.5459-02	.2628-03
40179.	.2015+02	.2613+06	.1297+05	.5030-02	.2422-03
40170.	.2020+02	.1074+07	.5317+05	.2057-01	.9904-03
40179.	.2042+02	.1082+07	.5300+05	.2029-01	.9769-03
40174.	.2055+02	.1044+07	.5081+05	.1932-01	.9303-03
40172.	.2035+02	.9734+06	.4783+05	.1837-01	.8847-03

Table 17. Dimethyl Siloxane DC - 200 - 50, 75°F (Continued)

L/D = 1.35

40171.	.2064+02	.1054+07	.5109+05	.1935-01	.9315-03
40165.	.2024+02	.1751+07	.8652+05	.3342-01	.1609-02
40166.	.2025+02	.1691+07	.8352+05	.3223-01	.1552-02
40164.	.2006+02	.1683+07	.8391+05	.3270-01	.1575-02
40161.	.2019+02	.1739+07	.8611+05	.3333-01	.1605-02
40158.	.1992+02	.2422+07	.1216+06	.4770-01	.2297-02
40157.	.2006+02	.2401+07	.1197+06	.4665-01	.2246-02
40155.	.2005+02	.2448+07	.1221+06	.4758-01	.2291-02
40151.	.1981+02	.3163+07	.1597+06	.6303-01	.3035-02
40151.	.1990+02	.3209+07	.1613+06	.6335-01	.3050-02
40144.	.1986+02	.3297+07	.1660+06	.6530-01	.3144-02
40147.	.1973+02	.3800+07	.1926+06	.7629-01	.3673-02
40144.	.1974+02	.3917+07	.1984+06	.7855-01	.3782-02
40141.	.1968+02	.4054+07	.2060+06	.8178-01	.3938-02
40171.	.1909+02	.8669+07	.4541+06	.1860+00	.8953-02
40174.	.1859+02	.1111+08	.5974+06	.2511+00	.1209-01
40175.	.1849+02	.1065+08	.5759+06	.2435+00	.1172-01
40166.	.1850+02	.5946+07	.3214+06	.1358+00	.6537-02
40169.	.1898+02	.4012+07	.2114+06	.8708-01	.4193-02
40174.	.1818+02	.1134+08	.6240+06	.2682+00	.1291-01
40176.	.1792+02	.1232+08	.6875+06	.2999+00	.1444-01
49606.	.5123+02	.1107+07	.2162+05	.3298-02	.1588-03
49601.	.5046+02	.1014+07	.2010+05	.3114-02	.1499-03
49593.	.5219+02	.1023+07	.1961+05	.2937-02	.1414-03
49584.	.4913+02	.2635+07	.5363+05	.8532-02	.4108-03
49583.	.4902+02	.2470+07	.5039+05	.8036-02	.3869-03
49573.	.4932+02	.2622+07	.5316+05	.8425-02	.4057-03
49573.	.4954+02	.2518+07	.5083+05	.8020-02	.3862-03
49593.	.4902+02	.4236+07	.8643+05	.1378-01	.6636-03
49596.	.4876+02	.4147+07	.8505+05	.1363-01	.6564-03
49592.	.4876+02	.4178+07	.8569+05	.1374-01	.6613-03
49593.	.4886+02	.4097+07	.8385+05	.1341-01	.6458-03
49585.	.4786+02	.5798+07	.1211+06	.1978-01	.9525-03
49582.	.4783+02	.5818+07	.1216+06	.1987-01	.9569-03
49583.	.4789+02	.5782+07	.1207+06	.1971-01	.9490-03
49584.	.4714+02	.7642+07	.1621+06	.2688-01	.1294-02
49582.	.4760+02	.7587+07	.1594+06	.2617-01	.1260-02
49586.	.4768+02	.7604+07	.1595+06	.2615-01	.1259-02
49584.	.4657+02	.9300+07	.1997+06	.3352-01	.1614-02
49584.	.4709+02	.9056+07	.1923+06	.3193-01	.1537-02
49583.	.4716+02	.9155+07	.1941+06	.3217-01	.1549-02
49587.	.4686+02	.9059+07	.1933+06	.3225-01	.1553-02

Table 17. Dimethyl Siloxane DC - 200 - 50, 75°F (Continued)

L/D = 14.9

P3	VISCP	TAUDYN	NSRATE	RE	LEOL
30065.	.8872+01	.3851+05	.4340+04	.1948-01	.8498-04
30065.	.8796+01	.3989+05	.4535+04	.2052-01	.8955-04
30064.	.8599+01	.6583+05	.7655+04	.3544-01	.1546-03
30064.	.8650+01	.6253+05	.7229+04	.3327-01	.1452-03
30060.	.8541+01	.8711+05	.1020+05	.4753-01	.2074-03
30059.	.8427+01	.8715+05	.1034+05	.4886-01	.2132-03
30060.	.8499+01	.1184+06	.1393+05	.6525-01	.2847-03
30060.	.8470+01	.1138+06	.1343+05	.6313-01	.2754-03
30059.	.8425+01	.1446+06	.1716+05	.8108-01	.3538-03
30056.	.8452+01	.1440+06	.1703+05	.8022-01	.3500-03
40048.	.2091+02	.3290+05	.1573+04	.2995-02	.1307-04
40048.	.1990+02	.3534+05	.1776+04	.3552-02	.1550-04
40044.	.2030+02	.3407+05	.1678+04	.3291-02	.1436-04
40039.	.2015+02	.9124+05	.4528+04	.8946-02	.3903-04
40040.	.2014+02	.9594+05	.4763+04	.9414-02	.4108-04
40039.	.2037+02	.9043+05	.4440+04	.8680-02	.3787-04
40036.	.1977+02	.1486+06	.7516+04	.1513-01	.6604-04
40036.	.1977+02	.1462+06	.7394+04	.1489-01	.6497-04
40031.	.1940+02	.2000+06	.1031+05	.2115-01	.9227-04
40025.	.1915+02	.2109+06	.1101+05	.2290-01	.9990-04
40021.	.1914+02	.2761+06	.1442+05	.2999-01	.1309-03
40017.	.1911+02	.2781+06	.1455+05	.3032-01	.1323-03
40015.	.1902+02	.2606+06	.1370+05	.2869-01	.1252-03
40016.	.1897+02	.3274+06	.1726+05	.3622-01	.1581-03
40015.	.1908+02	.3281+06	.1720+05	.3590-01	.1566-03
40013.	.1888+02	.3312+06	.1754+05	.3700-01	.1614-03
49527.	.5039+02	.7593+05	.1507+04	.1191-02	.5195-05
49526.	.5175+02	.8622+05	.1666+04	.1282-02	.5592-05
49527.	.4896+02	.2325+06	.4749+04	.3862-02	.1685-04
49520.	.4835+02	.2392+06	.4947+04	.4073-02	.1777-04
49517.	.4734+02	.3627+06	.7660+04	.6441-02	.2810-04
49514.	.4767+02	.3642+06	.7640+04	.6380-02	.2784-04
49512.	.4769+02	.3536+06	.7415+04	.6190-02	.2701-04
49508.	.4626+02	.4880+06	.1055+05	.9080-02	.3962-04
49508.	.4673+02	.4830+06	.1034+05	.8805-02	.3842-04
49506.	.4498+02	.6392+06	.1421+05	.1258-01	.5488-04
49504.	.4512+02	.6527+06	.1447+05	.1277-01	.5570-04
49501.	.4484+02	.6434+06	.1435+05	.1274-01	.5557-04
49498.	.4445+02	.7775+06	.1749+05	.1567-01	.6836-04
49498.	.4387+02	.7857+06	.1791+05	.1625-01	.7090-04

Table 17. Dimethyl Siloxane DC - 200 - 50, 75°F (Continued)

L/D = 14.9

P3	VISCP	TAUDYN	NSRATE	RE	LEOL
50032.	.4525+02	.8755+06	.1935+05	.1702-01	.7427-04
50034.	.3971+02	.1258+07	.3168+05	.3177-01	.1386-03
50047.	.3894+02	.1486+07	.3816+05	.3901-01	.1702-03
50038.	.3775+02	.1739+07	.4606+05	.4858-01	.2120-03
50046.	.3618+02	.2077+07	.5740+05	.6316-01	.2756-03
50034.	.2731+02	.3264+07	.1195+06	.1742+00	.7602-03
50050.	.3335+02	.2517+07	.7549+05	.9012-01	.3932-03
50067.	.3370+02	.2283+07	.6775+05	.8003-01	.3492-03
50057.	.3576+02	.2011+07	.5626+05	.6263-01	.2733-03
50056.	.3123+02	.2552+07	.8174+05	.1042+00	.4547-03
50039.	.2269+02	.4055+07	.1787+06	.3136+00	.1368-02
50050.	.2332+02	.3959+07	.1697+06	.2897+00	.1264-02
50053.	.2494+02	.3736+07	.1498+06	.2391+00	.1043-02
50096.	.3720+02	.1720+07	.4625+05	.4949-01	.2159-03
39813.	.1757+02	.8484+06	.4829+05	.1094+00	.4775-03
39811.	.1499+02	.1565+07	.1044+06	.2773+00	.1210-02
39793.	.1292+02	.2387+07	.1847+06	.5692+00	.2484-02
39741.	.1067+02	.3257+07	.3052+06	.1139+01	.4969-02
39723.	.1206+02	.2739+07	.2271+06	.7497+00	.3271-02
39821.	.1067+02	.3357+07	.3148+06	.1175+01	.5126-02
39832.	.1548+02	.1315+07	.8495+05	.2184+00	.9530-03
39823.	.1286+02	.2397+07	.1863+06	.5767+00	.2516-02
39812.	.1085+02	.3553+07	.3275+06	.1202+01	.5243-02
39812.	.1131+02	.2970+07	.2625+06	.9236+00	.4030-02
29711.	.7324+01	.8135+06	.1111+06	.6038+00	.2634-02
29702.	.6330+01	.1595+07	.2519+06	.1584+01	.6912-02
29689.	.6184+01	.1739+07	.2812+06	.1810+01	.7899-02
29700.	.6734+01	.1261+07	.1873+06	.1107+01	.4830-02
29708.	.6577+01	.1541+07	.2344+06	.1418+01	.6189-02
29704.	.6483+01	.1576+07	.2431+06	.1493+01	.6513-02
29720.	.6871+01	.1285+07	.1870+06	.1083+01	.4727-02

Table 18 Dimethyl Siloxane DC - 200 - 50, 75°F, L/D = 1.35

(Measurements with partially blocked capillary)

P3	VISCP	TAUDYN	NSRATE	RE	LEOL
39473.	.1785+02	.8965+07	.5024+06	.2200+00	.1059-01
39485.	.1777+02	.9753+07	.5489+06	.2415+00	.1163-01
39488.	.1862+02	.5796+07	.3112+06	.1306+00	.6288-02
39484.	.1661+02	.1467+08	.8833+06	.4156+00	.2001-01
39481.	.1595+02	.1843+08	.1155+07	.5662+00	.2726-01
39472.	.1646+02	.1455+08	.8838+06	.4196+00	.2020-01
39476.	.1550+02	.2016+08	.1301+07	.6560+00	.3159-01
39485.	.1650+02	.1481+08	.8978+06	.4253+00	.2048-01
39477.	.1581+02	.1806+08	.1142+07	.5648+00	.2719-01
39466.	.2477+02	.3099+08	.1251+07	.3947+00	.1901-01
39457.	.3907+02	.4376+07	.1120+06	.2241-01	.1079-02
39472.	.2121+02	.3549+08	.1674+07	.6169+00	.2970-01
39480.	.2127+02	.4052+08	.1905+07	.7000+00	.3370-01
39470.	.2341+02	.4037+08	.1725+07	.5759+00	.2773-01
39425.	.2666+02	.2401+08	.9006+06	.2640+00	.1271-01
39436.	.2390+02	.3331+08	.1394+07	.4559+00	.2195-01
39438.	.2905+02	.1991+08	.6855+06	.1845+00	.8881-02
39420.	.2466+02	.3479+08	.1411+07	.4472+00	.2153-01
39419.	.2244+02	.4428+08	.1973+07	.6872+00	.3309-01
39401.	.2647+02	.4389+08	.1658+07	.4895+00	.2357-01
39414.	.3238+02	.4382+08	.1353+07	.3266+00	.1572-01
49394.	.9065+02	.1073+08	.1184+06	.1021-01	.4914-03
49390.	.9028+02	.1924+08	.2131+06	.1845-01	.8883-03
49386.	.9155+02	.2124+08	.2320+06	.1981-01	.9539-03
49380.	.1036+03	.1184+08	.1143+06	.8625-02	.4153-03
49324.	.9433+02	.3148+08	.3337+06	.2766-01	.1332-02
49315.	.8085+02	.3803+08	.4704+06	.4547-01	.2190-02
49303.	.6748+02	.4458+08	.6607+06	.7653-01	.3685-02
49320.	.7678+02	.3812+08	.4964+06	.5053-01	.2433-02
49552.	.9830+02	.2322+08	.2362+06	.1878-01	.9044-03
49550.	.9795+02	.1871+08	.1910+06	.1524-01	.7340-03
49597.	.7886+02	.3926+08	.4979+06	.4935-01	.2376-02

Table 19. Dimethyl Siloxane DC - 200 - 50, 32°F,

L/D = 1.35

P3	VISCP	TAUDYN	NSRATE	RE	LEOL
4950.	.1710+01	.1302+06	.7616+05	.3482+00	.1676-01
4944.	.1721+01	.1336+06	.7763+05	.3525+00	.1697-01
4943.	.1727+01	.1325+06	.7672+05	.3473+00	.1672-01
4942.	.1702+01	.1810+06	.1063+06	.4882+00	.2351-01
4941.	.1707+01	.1835+06	.1075+06	.4923+00	.2371-01
4939.	.1727+01	.1924+06	.1114+06	.5042+00	.2428-01
4938.	.1686+01	.2396+06	.1421+06	.6586+00	.3171-01
4938.	.1726+01	.2505+06	.1451+06	.6572+00	.3164-01
4938.	.1690+01	.2342+06	.1386+06	.6408+00	.3085-01
4940.	.1537+01	.1019+07	.6628+06	.3370+01	.1623+00
4941.	.1387+01	.1973+07	.1423+07	.8019+01	.3861+00
4938.	.1393+01	.2175+07	.1561+07	.8759+01	.4217+00
4942.	.1493+01	.1344+07	.9002+06	.4712+01	.2269+00
4943.	.1518+01	.1094+07	.7208+06	.3712+01	.1787+00
4946.	.1350+01	.2618+07	.1938+07	.1122+02	.5402+00
4952.	.1396+01	.2913+07	.2087+07	.1169+02	.5626+00
4960.	.1328+01	.2890+07	.2177+07	.1282+02	.6171+00
4945.	.1394+01	.2013+07	.1444+07	.8092+01	.3896+00
4946.	.1323+01	.2994+07	.2263+07	.1337+02	.6438+00
4949.	.1342+01	.2975+07	.2216+07	.1290+02	.6213+00
9913.	.3234+01	.2333+06	.7214+05	.1743+00	.8395-02
9918.	.3025+01	.2424+06	.8015+05	.2071+00	.9972-02
9916.	.2997+01	.2533+06	.8451+05	.2204+00	.1061-01
9916.	.2990+01	.2436+06	.8147+05	.2130+00	.1025-01
9913.	.2997+01	.3488+06	.1164+06	.3035+00	.1461-01
9913.	.3063+01	.3558+06	.1162+06	.2964+00	.1427-01
9914.	.3049+01	.3387+06	.1111+06	.2848+00	.1371-01
9906.	.3040+01	.2419+06	.7959+05	.2047+00	.9854-02
9906.	.3025+01	.2560+06	.8461+05	.2186+00	.1053-01
9899.	.3050+01	.4634+06	.1519+06	.3893+00	.1875-01
9899.	.3046+01	.4713+06	.1547+06	.3971+00	.1912-01
9907.	.2988+01	.4599+06	.1539+06	.4026+00	.1939-01
9909.	.2989+01	.4623+06	.1547+06	.4046+00	.1948-01
9914.	.2775+01	.1152+07	.4150+06	.1169+01	.5628-01
9911.	.2719+01	.1882+07	.6923+06	.1990+01	.9581-01
9909.	.2529+01	.3159+07	.1249+07	.3860+01	.1859+00
9926.	.2410+01	.3834+07	.1591+07	.5162+01	.2485+00
9929.	.2582+01	.1731+07	.6704+06	.2030+01	.9774-01
9932.	.2594+01	.1827+07	.7044+06	.2122+01	.1022+00
9935.	.2220+01	.5778+07	.2603+07	.9168+01	.4414+00

Table 19. Dimethyl Siloxane DC - 200 - 50, 32°F,

L/D = 1.35 (Continued)

9947.	.2191+01	.6987+07	.3189+07	.1137+02	.5477+00
9921.	.2422+01	.4035+07	.1666+07	.5374+01	.2588+00
9920.	.2149+01	.5641+07	.2625+07	.9544+01	.4595+00
9920.	.2198+01	.6391+07	.2907+07	.1033+02	.4976+00
19865.	.7884+01	.6369+06	.8079+05	.8009-01	.3856-02
19867.	.7906+01	.6619+06	.8373+05	.8278-01	.3986-02
19866.	.7932+01	.6723+06	.8476+05	.8353-01	.4022-02
19859.	.8032+01	.8946+06	.1114+06	.1084+00	.5219-02
19861.	.7890+01	.9687+06	.1228+06	.1216+00	.5856-02
19855.	.7915+01	.8915+06	.1126+06	.1112+00	.5355-02
19852.	.7829+01	.1221+07	.1560+06	.1558+00	.7500-02
19846.	.7902+01	.1206+07	.1526+06	.1509+00	.7268-02
19847.	.7839+01	.1186+07	.1512+06	.1508+00	.7260-02
19858.	.7849+01	.1507+07	.1920+06	.1912+00	.9208-02
19856.	.7834+01	.1513+07	.1931+06	.1927+00	.9277-02
19852.	.7831+01	.1436+07	.1834+06	.1831+00	.8814-02
19859.	.7144+01	.3502+07	.4902+06	.5363+00	.2582-01
19854.	.7106+01	.4974+07	.6999+06	.7699+00	.3707-01
19857.	.7469+01	.2439+07	.3265+06	.3417+00	.1645-01
19848.	.7553+01	.2708+07	.3585+06	.3710+00	.1786-01
19857.	.6934+01	.5499+07	.7931+06	.8940+00	.4304-01
19850.	.6576+01	.8288+07	.1260+07	.1498+01	.7213-01
19844.	.6484+01	.1066+08	.1644+07	.1981+01	.9540-01
19847.	.6590+01	.9982+07	.1515+07	.1796+01	.8649-01
19854.	.7092+01	.5763+07	.8126+06	.8956+00	.4312-01
29936.	.2316+02	.1074+07	.4638+05	.1565-01	.7535-03
29937.	.2264+02	.3694+06	.1631+05	.5631-02	.2711-03
29939.	.2255+02	.2904+06	.1288+05	.4463-02	.2149-03
29941.	.2277+02	.3458+06	.1519+05	.5214-02	.2510-03
29922.	.2169+02	.3405+06	.1570+05	.5658-02	.2724-03
29925.	.2218+02	.1112+07	.5015+05	.1768-01	.8510-03
29926.	.2185+02	.1110+07	.5081+05	.1817-01	.8750-03
29919.	.2177+02	.1765+07	.8107+05	.2911-01	.1401-02
29919.	.2168+02	.1781+07	.8214+05	.2961-01	.1426-02
29911.	.2153+02	.2513+07	.1167+06	.4239-01	.2041-02
29912.	.2178+02	.1777+07	.8159+05	.2928-01	.1410-02
29927.	.2133+02	.2547+07	.1194+06	.4376-01	.2107-02
29928.	.2132+02	.2479+07	.1162+06	.4261-01	.2052-02
29921.	.2125+02	.3338+07	.1571+06	.5780-01	.2783-02
29919.	.2119+02	.3335+07	.1574+06	.5806-01	.2795-02
29918.	.2148+02	.3383+07	.1575+06	.5731-01	.2759-02

Table 19. Dimethyl Siloxane DC - 200 - 50, 32°F,

L/D = 1.35 (Continued)

29913.	.2141+02	.3256+07	.1521+06	.5552-01	.2673-02
29909.	.2143+02	.3912+07	.1825+06	.6658-01	.3206-02
29911.	.2123+02	.3956+07	.1863+06	.6859-01	.3303-02
29909.	.2153+02	.3961+07	.1840+06	.6679-01	.3216-02
29920.	.1865+02	.9168+07	.4917+06	.2061+00	.9923-02
29917.	.1918+02	.1089+08	.5676+06	.2313+00	.1114-01
29916.	.2077+02	.4671+07	.2249+06	.8465-01	.4076-02
29909.	.1914+02	.1140+08	.5955+06	.2431+00	.1171-01
29901.	.1904+02	.1216+08	.6387+06	.2622+00	.1263-01
29931.	.1861+02	.1121+08	.6026+06	.2531+00	.1219-01
29928.	.1818+02	.1190+08	.6544+06	.2813+00	.1355-01
29930.	.2008+02	.8065+07	.4016+06	.1563+00	.7526-02
29929.	.2030+02	.6849+07	.3375+06	.1300+00	.6257-02
29936.	.1860+02	.1087+08	.5844+06	.2456+00	.1182-01
39884.	.6646+02	.1062+07	.1598+05	.1879-02	.9048-04
39875.	.6800+02	.1105+07	.1625+05	.1868-02	.8994-04
39882.	.6576+02	.1127+07	.1713+05	.2037-02	.9805-04
39873.	.6575+02	.1095+07	.1665+05	.1979-02	.9529-04
39886.	.6664+02	.8763+06	.1315+05	.1542-02	.7426-04
39878.	.7012+02	.8270+06	.1179+05	.1315-02	.6329-04
39917.	.8257+02	.4224+07	.5116+05	.4843-02	.2332-03
39908.	.1586+03	.6025+07	.3799+05	.1872-02	.9013-04
39893.	.8526+02	.4061+07	.4763+05	.4366-02	.2102-03
39882.	.8432+02	.4124+07	.4891+05	.4534-02	.2183-03
39875.	.6900+02	.3258+07	.4721+05	.5348-02	.2575-03

Table 20. Dimethyl Siloxane DC - 200 - 50,

32°F, L/D = 1.35

P3	VISCP	TAUDYN	NSRATE	RE	LEOL
30238.	.2370+02	.3474+06	.1466+05	.4834-02	.2328-03
30241.	.2356+02	.3270+06	.1388+05	.4607-02	.2218-03
30236.	.2331+02	.3320+06	.1425+05	.4778-02	.2300-03
30227.	.2199+02	.1079+07	.4904+05	.1743-01	.8391-03
30226.	.2214+02	.1095+07	.4947+05	.1747-01	.8411-03
30222.	.2184+02	.1063+07	.4866+05	.1741-01	.8384-03
30220.	.2213+02	.1015+07	.4584+05	.1619-01	.7795-03
30220.	.2220+02	.1113+07	.5016+05	.1766-01	.8504-03
30220.	.2198+02	.1096+07	.4989+05	.1774-01	.8542-03
30245.	.2212+02	.1851+07	.8369+05	.2957-01	.1424-02
30245.	.2194+02	.1753+07	.7991+05	.2847-01	.1371-02
30234.	.2192+02	.1764+07	.8049+05	.2871-01	.1382-02
30235.	.2187+02	.1725+07	.7888+05	.2819-01	.1357-02
30232.	.2163+02	.2599+07	.1201+06	.4341-01	.2090-02
30229.	.2161+02	.2561+07	.1185+06	.4288-01	.2064-02
30228.	.2172+02	.2583+07	.1189+06	.4278-01	.2060-02
30227.	.2161+02	.2514+07	.1163+06	.4207-01	.2025-02
30225.	.2145+02	.3399+07	.1585+06	.5774-01	.2780-02
30221.	.2130+02	.3398+07	.1595+06	.5855-01	.2819-02
30219.	.2154+02	.3466+07	.1609+06	.5836-01	.2810-02
30218.	.2164+02	.3335+07	.1541+06	.5567-01	.2680-02
30216.	.2114+02	.4182+07	.1978+06	.7315-01	.3522-02
30210.	.2117+02	.4132+07	.1952+06	.7207-01	.3470-02
30205.	.2129+02	.4153+07	.1951+06	.7161-01	.3448-02
30202.	.2116+02	.4112+07	.1943+06	.7174-01	.3454-02
40345.	.6676+02	.9600+06	.1438+05	.1684-02	.8107-04
40340.	.7295+02	.9899+06	.1357+05	.1454-02	.6999-04
40333.	.7185+02	.1130+07	.1572+05	.1711-02	.8236-04
40327.	.6788+02	.3477+07	.5122+05	.5898-02	.2840-03
40324.	.7075+02	.3565+07	.5038+05	.5566-02	.2680-03
40323.	.6968+02	.3677+07	.5278+05	.5920-02	.2851-03
40325.	.7701+02	.3769+07	.4895+05	.4968-02	.2392-03
40325.	.7920+02	.3907+07	.4932+05	.4868-02	.2344-03
40326.	.8050+02	.3863+07	.4799+05	.4660-02	.2244-03
40318.	.8053+02	.6674+07	.8288+05	.8045-02	.3873-03
40321.	.8442+02	.6755+07	.8002+05	.7408-02	.3567-03
40310.	.8910+02	.7463+07	.8376+05	.7347-02	.3538-03
40310.	.9279+02	.7811+07	.8419+05	.7092-02	.3414-03
40311.	.9487+02	.8248+07	.8694+05	.7164-02	.3449-03
40300.	.1024+03	.1195+08	.1167+06	.8914-02	.4292-03
40296.	.1058+03	.1274+08	.1205+06	.8903-02	.4287-03
40292.	.1108+03	.1333+08	.1202+06	.8481-02	.4084-03
40276.	.1259+03	.1445+08	.1148+06	.7124-02	.3430-03
40258.	.1286+03	.1494+08	.1162+06	.7064-02	.3401-03
40321.	.1161+03	.1292+08	.1113+06	.7492-02	.3607-03

Table 21. Dimethyl Siloxane DC - 200 - 50, 100°F

L/D = 1.35

P3	VISCP	TAUDYN	NSRATE	RE	LEOL
30139.	.5977+01	.3008+06	.5033+05	.6582-01	.3169-02
30134.	.5914+01	.2959+06	.5004+05	.6614-01	.3184-02
30127.	.6057+01	.3047+06	.5030+05	.6491-01	.3125-02
30126.	.5913+01	.4782+06	.8087+05	.1069+00	.5147-02
30146.	.5961+01	.4524+06	.7589+05	.9950-01	.4791-02
30141.	.5883+01	.4547+06	.7728+05	.1027+00	.4944-02
30137.	.5899+01	.6821+06	.1156+06	.1532+00	.7376-02
30135.	.5934+01	.7053+06	.1189+06	.1565+00	.7537-02
30134.	.5891+01	.7277+06	.1235+06	.1639+00	.7891-02
30127.	.5835+01	.9406+06	.1612+06	.2160+00	.1040-01
30153.	.5897+01	.9204+06	.1561+06	.2068+00	.9959-02
30153.	.5874+01	.9370+06	.1595+06	.2123+00	.1022-01
40171.	.1254+02	.6364+06	.5077+05	.3166-01	.1524-02
40168.	.1241+02	.6212+06	.5006+05	.3153-01	.1518-02
40161.	.1273+02	.6469+06	.5084+05	.3122-01	.1503-02
40158.	.1233+02	.1030+07	.8353+05	.5295-01	.2550-02
40153.	.1264+02	.1061+07	.8390+05	.5187-01	.2497-02
40144.	.1250+02	.1060+07	.8485+05	.5307-01	.2555-02
40135.	.1231+02	.1493+07	.1212+06	.7695-01	.3705-02
40134.	.1216+02	.1459+07	.1200+06	.7716-01	.3715-02
40130.	.1230+02	.1435+07	.1167+06	.7418-01	.3572-02
40155.	.1212+02	.1941+07	.1601+06	.1032+00	.4971-02
40155.	.1208+02	.1938+07	.1604+06	.1038+00	.4998-02
40151.	.1198+02	.1966+07	.1641+06	.1071+00	.5156-02
49617.	.2806+02	.5059+06	.1803+05	.5023-02	.2419-03
49615.	.2731+02	.5516+06	.2020+05	.5779-02	.2783-03
49613.	.2767+02	.4953+06	.1790+05	.5059-02	.2436-03
49607.	.2680+02	.1410+07	.5259+05	.1534-01	.7384-03
49607.	.2705+02	.1390+07	.5138+05	.1485-01	.7148-03
49603.	.2699+02	.1320+07	.4889+05	.1416-01	.6817-03
49602.	.2643+02	.2267+07	.8578+05	.2537-01	.1221-02
49600.	.2629+02	.2285+07	.8691+05	.2584-01	.1244-02
49595.	.2607+02	.2166+07	.8311+05	.2492-01	.1200-02
49595.	.2600+02	.3107+07	.1195+06	.3593-01	.1730-02
49596.	.2546+02	.3030+07	.1190+06	.3654-01	.1759-02
49600.	.2563+02	.3158+07	.1232+06	.3759-01	.1810-02

Table 21. Dimethyl Siloxane DC - 200 - 50, 100°F (Continued)

L/D = 297

P3	VISCP	TAUDYN	NSRATE	RE	LEOL
30040.	.6563+01	.5790+04	.8822+03	.8837-02	.1935-05
30039.	.6890+01	.5217+04	.7572+03	.7224-02	.1582-05
30035.	.6562+01	.4904+04	.7474+03	.7488-02	.1640-05
30047.	.6546+01	.1463+05	.2236+04	.2245-01	.4917-05
30042.	.6484+01	.1433+05	.2210+04	.2241-01	.4908-05
30040.	.6505+01	.1393+05	.2141+04	.2164-01	.4739-05
30037.	.6491+01	.2171+05	.3344+04	.3387-01	.7418-05
30039.	.6465+01	.2189+05	.3386+04	.3443-01	.7540-05
30028.	.6450+01	.2290+05	.3550+04	.3618-01	.7923-05
30030.	.6479+01	.3064+05	.4728+04	.4798-01	.1051-04
30062.	.6487+01	.3255+05	.5018+04	.5086-01	.1114-04
30057.	.6431+01	.3345+05	.5201+04	.5317-01	.1164-04
40098.	.1376+02	.1051+05	.7642+03	.3653-02	.7999-06
40092.	.1264+02	.1071+05	.8470+03	.4405-02	.9646-06
40087.	.1355+02	.1135+05	.8379+03	.4066-02	.8905-06
40077.	.1313+02	.2733+05	.2081+04	.1041-01	.2281-05
40077.	.1302+02	.2728+05	.2096+04	.1058-01	.2318-05
40073.	.1326+02	.2869+05	.2164+04	.1073-01	.2350-05
40069.	.1302+02	.6439+05	.4945+04	.2497-01	.5468-05
40083.	.1332+02	.4681+05	.3514+04	.1734-01	.3797-05
40077.	.1340+02	.4581+05	.3418+04	.1676-01	.3671-05
40072.	.1332+02	.4561+05	.3423+04	.1689-01	.3699-05
49576.	.2933+02	.1874+05	.6390+03	.1432-02	.3137-06
49579.	.3155+02	.2059+05	.6525+03	.1360-02	.2978-06
49578.	.2755+02	.2009+05	.7292+03	.1740-02	.3811-06
49573.	.2894+02	.3835+05	.1325+04	.3011-02	.6595-06
49570.	.2907+02	.3697+05	.1272+04	.2877-02	.6300-06
49569.	.2999+02	.3868+05	.1290+04	.2827-02	.6191-06
49566.	.3002+02	.3771+05	.1256+04	.2750-02	.6023-06
49568.	.2912+02	.4200+05	.1442+04	.3256-02	.7131-06
49571.	.2893+02	.5954+05	.2058+04	.4677-02	.1024-05
49566.	.2885+02	.5872+05	.2035+04	.4638-02	.1016-05
49569.	.2912+02	.5393+05	.1852+04	.4181-02	.9157-06
49573.	.2874+02	.5279+05	.1837+04	.4202-02	.9203-06
49574.	.2868+02	.5091+05	.1775+04	.4069-02	.8910-06
49574.	.2898+02	.5137+05	.1773+04	.4023-02	.8809-06

Table 22. Polyalkyl Aromatic + Additive, 10°F

L/D = 1.35

P3	VTSCP	TAUDYN	PSRATE	RF	LEOL
9919.	.2001+02	.9042+07	.3476+06	.1044+00	.5029-02
9935.	.2102+02	.1407+08	.6692+06	.2488+00	.1198-01
9922.	.2896+02	.7755+07	.2678+06	.7225-01	.3479-02
9927.	.1731+02	.1816+08	.1049+07	.4737+00	.2281-01
9927.	.1582+02	.2050+08	.1296+07	.6401+00	.3082-01
9934.	.1479+02	.2158+08	.1459+07	.7708+00	.3711-01
9904.	.2442+02	.1208+08	.4948+06	.1584+00	.7626-02
9897.	.1267+02	.2496+08	.1969+07	.1215+01	.5846-01
9895.	.1010+02	.2872+08	.2844+07	.2201+01	.1060+00
9885.	.9047+01	.2992+08	.3307+07	.2858+01	.1376+00
9885.	.1065+02	.2781+08	.2611+07	.1916+01	.9224-01
9886.	.1053+02	.2082+08	.1250+07	.5954+00	.2867-01
9905.	.1657+02	.1751+08	.2430+06	.3970+00	.1911-01
9869.	.8885+01	.3032+08	.3413+07	.3002+01	.1445+00
9956.	.3644+02	.7046+06	.1934+05	.4148-02	.1997-03
9946.	.3688+02	.7297+06	.1979+05	.4194-02	.2019-03
9944.	.3659+02	.7360+06	.2011+05	.4297-02	.2069-03
10007.	.3307+02	.1843+07	.5573+05	.1317-01	.6341-03
9936.	.3349+02	.1896+07	.5661+05	.1321-01	.6362-03
9938.	.3208+02	.1923+07	.5993+05	.1460-01	.7030-03
9939.	.3229+02	.2903+07	.8989+05	.2176-01	.1048-02
9939.	.3232+02	.2824+07	.8738+05	.2113-01	.1017-02
9939.	.3311+02	.2924+07	.8829+05	.2084-01	.1003-02
9975.	.3241+02	.4005+07	.1236+06	.2980-01	.1435-02
9970.	.3189+02	.3982+07	.1248+06	.3060-01	.1473-02
9979.	.3169+02	.4002+07	.1263+06	.3114-01	.1499-02
9974.	.3065+02	.5106+07	.1666+06	.4247-01	.2045-02
9968.	.3053+02	.5013+07	.1642+06	.4204-01	.2024-02
9975.	.3019+02	.5080+07	.1683+06	.4356-01	.2097-02
9974.	.2555+02	.8532+07	.3339+06	.1022+00	.4918-02
997_.	.2313+02	.1099+08	.4753+06	.1606+00	.7735-02
9974.	.2539+02	.9691+07	.3817+06	.1175+00	.5656-02
9959.	.2467+02	.1050+08	.4255+06	.1348+00	.6492-02
9917.	.2953+02	.5268+07	.1784+06	.4722-01	.2273-02
9922.	.2916+02	.5517+07	.1892+06	.5071-01	.2442-02
9921.	.3215+02	.4034+07	.1255+06	.3050-01	.1468-02
9924.	.2478+02	.9822+07	.3963+06	.1250+00	.6018-02
9928.	.2606+02	.8212+07	.3152+06	.9454-01	.4552-02
9912.	.2323+02	.1275+08	.5491+06	.1848+00	.8896-02
19839.	.1345+03	.3418+07	.2541+05	.1476-02	.7107-04
19816.	.1416+03	.3450+07	.2436+05	.1344-02	.6473-04

Table 22. Polyalkyl Aromatic + Additive, 10°F (Continued)

L/D = 1.35

19804.	.1411+03	.3474+07	.2462+05	.1364-02	.6569-04
19852.	.1217+03	.7233+07	.5944+05	.3818-02	.1838-03
19832.	.1245+03	.7253+07	.5824+05	.3656-02	.1760-03
19826.	.1242+03	.7291+07	.5872+05	.3696-02	.1780-03
19806.	.1131+03	.1022+06	.9035+05	.6244-02	.3006-03
19802.	.1118+03	.1021+06	.9125+05	.6377-02	.3070-03
19816.	.1115+03	.1030+06	.9238+05	.6474-02	.3117-03
19992.	.1411+03	.8055+07	.5708+05	.3162-02	.1522-03
19979.	.1601+03	.6313+07	.3943+05	.1925-02	.9269-04
19956.	.1249+03	.9489+07	.7595+05	.4752-02	.2288-03
19957.	.5473+02	.2859+06	.5224+06	.7461-01	.3592-02
19934.	.3464+02	.1860+06	.2197+06	.2029-01	.9770-03
19942.	.4317+02	.3486+06	.9079+06	.1463+00	.7043-02
19984.	.3691+02	.2072+06	.2384+06	.2144-01	.1032-02
19992.	.3628+02	.3943+06	.1087+07	.2342+00	.1128-01
19965.	.9582+02	.1764+06	.1841+06	.1501-01	.7228-03
19996.	.3299+02	.4216+06	.1278+07	.3028+00	.1458-01
19972.	.9004+02	.1820+06	.2021+06	.1754-01	.8446-03
30026.	.4821+03	.1141+06	.2366+05	.3836-03	.1847-04
30002.	.4689+03	.1178+06	.2512+05	.4187-03	.2016-04
29994.	.4907+03	.1203+06	.2453+05	.3907-03	.1881-04
29975.	.4012+03	.1717+06	.4278+05	.8334-03	.4013-04
30039.	.4241+03	.1776+06	.4188+05	.7719-03	.3716-04
30020.	.4181+03	.1755+06	.4198+05	.7847-03	.3778-04
30009.	.3586+03	.2118+06	.5906+05	.1287-02	.6198-04
30000.	.3724+03	.2130+06	.5720+05	.1200-02	.5780-04
29983.	.3617+03	.2117+06	.5852+05	.1264-02	.6088-04
29971.	.2977+03	.2662+06	.9011+05	.2366-02	.1139-03
29960.	.2907+03	.2694+06	.9268+05	.2492-02	.1200-03
30079.	.3078+03	.2636+06	.8570+05	.2176-02	.1048-03
30090.	.2579+03	.3084+06	.1196+06	.3624-02	.1745-03
30065.	.2535+03	.3168+06	.1251+06	.3860-02	.1858-03
30060.	.2561+03	.3146+06	.1229+06	.3750-02	.1806-03
30066.	.2221+03	.3535+06	.1592+06	.5602-02	.2697-03
30052.	.2190+03	.3562+06	.1622+06	.5775-02	.2781-03
30041.	.2171+03	.3533+06	.1627+06	.5858-02	.2820-03
30039.	.2208+03	.3541+06	.1604+06	.5677-02	.2733-03
30030.	.2207+03	.3622+06	.1641+06	.5811-02	.2798-03

Table 22. Polyalkyl Aromatic + Additive, 10°F (Continued)

L/D = 14.9

P3	VISCP	TAUDYN	NSRATE	RF	LEOL
9906.	.3505+02	.7063+05	.2015+04	.2288-02	.9985-05
9906.	.3566+02	.6655+05	.1866+04	.2083-02	.9091-05
9914.	.3488+02	.6735+05	.1931+04	.2203-02	.9614-05
9902.	.3322+02	.1617+06	.4867+04	.5833-02	.2545-04
9900.	.3446+02	.1638+06	.4751+04	.5488-02	.2395-04
9895.	.3383+02	.1561+06	.4614+04	.5429-02	.2369-04
9913.	.3312+02	.2559+06	.7726+04	.9288-02	.4053-04
9912.	.3330+02	.2607+06	.7828+04	.9357-02	.4083-04
9906.	.3305+02	.2559+06	.7743+04	.9328-02	.4070-04
9901.	.3255+02	.3592+06	.1103+05	.1350-01	.5889-04
9897.	.3255+02	.3551+06	.1091+05	.1334-01	.5821-04
9911.	.3336+02	.3504+06	.1050+05	.1253-01	.5468-04
9905.	.3334+02	.3618+06	.1085+05	.1296-01	.5653-04
9902.	.3335+02	.3582+06	.1074+05	.1282-01	.5594-04
9916.	.3173+02	.4782+06	.1507+05	.1891-01	.8253-04
9912.	.3185+02	.4732+06	.1486+05	.1857-01	.8104-04
9910.	.3251+02	.4870+06	.1498+05	.1835-01	.8005-04
9907.	.3278+02	.4784+06	.1459+05	.1772-01	.7733-04
9902.	.3258+02	.4732+06	.1452+05	.1775-01	.7743-04
9900.	.3251+02	.4792+06	.1474+05	.1805-01	.7878-04
9896.	.3242+02	.4747+06	.1464+05	.1797-01	.7843-04
9895.	.3186+02	.5651+06	.1774+05	.2216-01	.9670-04
9886.	.3197+02	.5706+06	.1785+05	.2222-01	.9696-04
9885.	.3190+02	.5697+06	.1786+05	.2229-01	.9725-04
9874.	.2614+02	.9596+06	.3410+05	.4824-01	.2105-03
9896.	.2889+02	.8683+06	.3006+05	.4142-01	.1807-03
9885.	.2785+02	.9476+06	.3402+05	.4863-01	.2122-03
9885.	.2993+02	.6150+06	.2055+05	.2733-01	.1193-03
9876.	.2866+02	.9776+06	.3409+05	.4732-01	.2064-03
9872.	.3163+02	.7105+06	.2246+05	.2827-01	.1233-03
9869.	.2959+02	.7516+06	.2540+05	.3417-01	.1491-03
9686.	.3222+02	.3332+06	.1034+05	.1278-01	.5577-04
9665.	.3201+02	.3433+06	.1072+05	.1334-01	.5819-04
9710.	.3187+02	.3343+06	.1049+05	.1310-01	.5716-04
9707.	.3042+02	.4532+06	.1490+05	.1950-01	.8508-04
9706.	.3095+02	.4517+06	.1460+05	.1877-01	.8192-04
9720.	.3000+02	.5398+06	.1799+05	.2388-01	.1042-03
9707.	.3026+02	.5393+06	.1782+05	.2345-01	.1023-03
9745.	.2750+02	.9877+06	.3592+05	.5199-01	.2268-03
9766.	.2126+02	.1782+07	.8381+05	.1569+00	.6846-03
9771.	.1149+02	.2284+07	.1988+06	.6887+00	.3005-02
9774.	.1759+02	.2150+07	.1222+06	.2765+00	.1206-02

Table 22. Polyalkyl Aromatic + Additive, 10°F (Continued)

L/D = 14.9

9766.	.2426+02	.1443+07	.5948+05	.9761-01	.4259-03
9765.	.2367+02	.1267+07	.5352+05	.9002-01	.3928-03
9764.	.2571+02	.1041+07	.4049+05	.6270-01	.2736-03
9742.	.2436+02	.1253+07	.5142+05	.8402-01	.3666-03
9730.	.1502+02	.2573+07	.1713+06	.4539+00	.1980-02
9712.	.1577+02	.2868+07	.1819+06	.4594+00	.2004-02
9744.	.9672+01	.3012+07	.3115+06	.1282+01	.5594-02
9759.	.9505+01	.3074+07	.3234+06	.1355+01	.5911-02
19802.	.1327+03	.1217+07	.9168+04	.2750-02	.1200-04
19790.	.7426+02	.2445+07	.3292+05	.1765-01	.7699-04
19770.	.1105+03	.1410+07	.1275+05	.4594-02	.2004-04
19754.	.1039+03	.1569+07	.1511+05	.5790-02	.2526-04
19750.	.3480+02	.3963+07	.1139+06	.1303+00	.5684-03
19744.	.4865+02	.3481+07	.7159+05	.5861-01	.2557-03
19745.	.4863+02	.3480+07	.7156+05	.5858-01	.2556-03
19746.	.1631+03	.1021+07	.6262+04	.1529-02	.6671-05
19711.	.1323+03	.8127+06	.6145+04	.1850-02	.8070-05
19714.	.1102+03	.7127+06	.6467+04	.2336-02	.1019-04
19702.	.1045+03	.1355+07	.1297+05	.4941-02	.2156-04
19702.	.4112+02	.3682+07	.9441+05	.9141-01	.3988-03
19690.	.1298+03	.1153+07	.8879+04	.2723-02	.1188-04
19655.	.3695+02	.3998+07	.1082+06	.1166+00	.5087-03
19625.	.4145+02	.3792+07	.9150+05	.9789-01	.3835-03
19660.	.4984+02	.3527+07	.7076+05	.5651-01	.2466-03
19885.	.1508+03	.2912+06	.2098+04	.6014-03	.2624-05
19869.	.1406+03	.3005+06	.2134+04	.6034-03	.2633-05
19879.	.1390+03	.3242+06	.2332+04	.6680-03	.2915-05
19870.	.1320+03	.6439+06	.4877+04	.1471-02	.6416-05
19860.	.1296+03	.6610+06	.5091+04	.1561-02	.6810-05
19850.	.1316+03	.6492+06	.4934+04	.1493-02	.6514-05
19880.	.1317+03	.6891+06	.5231+04	.1581-02	.6898-05
19900.	.1221+03	.9770+06	.8002+04	.2609-02	.1138-04
19917.	.1247+03	.9577+06	.7680+04	.2452-02	.1070-04
19904.	.1246+03	.9992+06	.8021+04	.2563-02	.1118-04
29930.	.5150+03	.1094+07	.2123+04	.1641-03	.7161-06
29895.	.5340+03	.7606+06	.1424+04	.1062-03	.4633-06
29856.	.5690+03	.6052+06	.1064+04	.7442-04	.3247-06
29821.	.5907+03	.6663+06	.1128+04	.7602-04	.3317-06
29195.	.3709+03	.2816+07	.7591+04	.8147-03	.3555-05
29202.	.3746+03	.2970+07	.7925+04	.8416-03	.3672-05
29187.	.3952+03	.3116+07	.7884+04	.7941-03	.3465-05
29174.	.3992+03	.3170+07	.7941+04	.7919-03	.3455-05
29175.	.4063+03	.3088+07	.7601+04	.7448-03	.3250-05

Table 22. Polyalkyl Aromatic + Additive, 10°F (Continued)

L/D = 14.9

29164.	.3422+03	.3777+07	.1104+05	.1284-02	.5603-05
29167.	.3372+03	.3799+07	.1127+05	.1330-02	.5803-05
29139.	.3502+03	.3798+07	.1085+05	.1233-02	.5380-05
29142.	.3471+03	.3703+07	.1067+05	.1224-02	.5340-05
29129.	.3406+03	.3774+07	.1108+05	.1295-02	.5652-05
29795.	.7246+03	.9490+06	.1310+04	.7195-04	.3139-06
29747.	.6323+03	.5027+06	.6040+03	.2889-04	.1261-06
29670.	.6774+03	.7410+06	.1094+04	.6429-04	.2805-06
29649.	.4549+03	.8423+06	.1853+04	.1621-03	.7075-06
29735.	.4083+03	.2180+07	.5339+04	.5205-03	.2271-05
29707.	.3245+03	.3435+07	.1058+05	.1298-02	.5665-05
29700.	.7282+03	.3311+07	.4546+04	.2485-03	.1084-05
29710.	.3269+03	.2398+07	.7337+04	.8936-03	.3899-05
29721.	.5845+03	.1842+07	.3151+04	.2146-03	.9364-06
29700.	.7310+03	.1559+07	.2130+04	.1159-03	.5058-06
29681.	.3103+03	.3858+07	.1243+05	.1595-02	.6959-05
29660.	.3661+03	.3191+07	.8715+04	.9477-03	.4135-05
29649.	.4124+03	.2015+07	.4886+04	.4716-03	.2058-05
29550.	.4827+03	.9218+06	.1910+04	.1575-03	.6872-06
29540.	.4970+03	.1071+07	.2154+04	.1725-03	.7529-06
29517.	.4776+03	.1001+07	.2095+04	.1746-03	.7619-06
29502.	.4133+03	.2014+07	.4874+04	.4694-03	.2048-05
29480.	.4234+03	.2048+07	.4837+04	.4547-03	.1984-05
29462.	.4457+03	.2214+07	.4967+04	.4436-03	.1936-05
29439.	.3746+03	.2834+07	.7565+04	.8041-03	.3508-05
29441.	.3655+03	.2946+07	.8060+04	.8780-03	.3831-05
29432.	.3848+03	.3039+07	.7897+04	.8170-03	.3565-05
29402.	.3806+03	.3006+07	.7897+04	.8261-03	.3604-05
29460.	.3263+03	.3491+07	.1070+05	.1305-02	.5696-05
29370.	.3207+03	.3452+07	.1047+05	.1265-02	.5518-05
29395.	.3331+03	.3531+07	.1060+05	.1267-02	.5528-05
29390.	.2843+03	.4047+07	.1424+05	.1994-02	.8696-05
29402.	.2764+03	.3822+07	.1383+05	.1991-02	.8688-05
29411.	.2760+03	.3942+07	.1425+05	.2051-02	.8949-05
39390.	.1257+04	.2626+07	.2089+04	.6619-04	.2888-06
39310.	.1570+04	.3519+07	.2242+04	.5686-04	.2481-06
39321.	.1752+04	.3750+07	.2140+04	.4864-04	.2122-06
39310.	.1703+04	.3763+07	.2098+04	.4658-04	.2032-06
39232.	.1903+04	.3700+07	.1944+04	.4067-04	.1775-06
39191.	.1955+04	.3363+07	.1720+04	.3501-04	.1528-06
39409.	.1864+04	.3385+07	.1817+04	.3881-04	.1693-06
39280.	.1791+04	.3431+07	.1916+04	.4258-04	.1858-06

Table 22. Polyalkyl Aromatic + Additive, 10°F (Continued)

L/D = 14.9

39586.	.1733+04	.1365+07	.7875+03	.1809-04	.7492-07
39724.	.1975+04	.8403+06	.4252+03	.8565-05	.3737-07
39760.	.2289+04	.1706+07	.7714+03	.1341-04	.5853-07
39759.	.1866+04	.2868+07	.1537+04	.3278-04	.1430-06
39746.	.1656+04	.3057+07	.1846+04	.4436-04	.1936-06
39754.	.1471+04	.3640+07	.2475+04	.6697-04	.2922-06
39750.	.1808+04	.3711+07	.2053+04	.4521-04	.1973-06
39736.	.2074+04	.1044+07	.5033+03	.9663-05	.4216-07

Table 23. XRM 109 F4, Synthetic Paraffinic Oil,

Plot, L/D = 297

XRM 109 F4 100 F

P3	VISCP	NSR TE	KEC	DELTAP	TAUDYN	REYN
4752.	.7909+01	.3476+04	.1440-02	.4733+03	.2749+05	.2889-01
4751.	.8049+01	.3204+04	.1223-02	.4440+03	.2579+05	.2617-01
4756.	.8152+01	.3298+04	.1297-02	.4630+03	.2689+05	.2660-01
9781.	.1531+02	.2109+04	.5302-03	.5561+03	.3230+05	.9055-02
9760.	.1525+02	.2144+04	.5479-03	.5630+03	.3270+05	.9243-02
9777.	.1524+02	.2012+04	.4824-03	.5278+03	.3066+05	.8681-02
19796.	.4304+02	.2035+04	.4937-03	.1508+04	.8760+05	.3108-02
19798.	.4309+02	.2064+04	.5079-03	.1531+04	.8894+05	.3150-02
19767.	.4345+02	.2039+04	.4954-03	.1525+04	.8859+05	.3085-02
29882.	.1257+03	.6880+03	.5641-04	.1489+04	.8647+05	.3598-03
29862.	.1210+03	.7381+03	.6493-04	.1538+04	.8933+05	.4009-03
29873.	.1382+03	.6371+03	.4838-04	.1516+04	.8802+05	.3032-03
39874.	.3007+03	.5175+03	.3191-04	.2679+04	.1556+06	.1131-03
39874.	.3007+03	.5244+03	.3278-04	.2715+04	.1577+06	.1147-03
39862.	.3143+03	.5343+03	.3403-04	.2892+04	.1680+06	.1117-03

Averaged Data Points

XR 109 F4 100 F

P (PSI)	V (CP)
.00000	.37600+03
.47530+04	.80367+03
.97724+04	.15267+04
.19794+05	.43194+04
.29879+05	.12829+05
.39870+05	.30525+05

Table 23. XRM 109 F4, Synthetic Paraffinic Oil,

Plot, L/D = 297 (Continued)

XRM 109 F4 210 F

P3	VISCP	NSRATE	KEC	DELTAP	TAUDYN	REYN
4946.	.6273+00	.4707+04	.2641-02	.5084+02	.2953+04	.4933+00
4947.	.6290+00	.4755+04	.2695-02	.5150+02	.2991+04	.4970+00
4946.	.6305+00	.4876+04	.2833-02	.5293+02	.3074+04	.5084+00
9988.	.9991+00	.4640+04	.2566-02	.7981+02	.4635+04	.3053+00
9982.	.1005+01	.4664+04	.2592-02	.8067+02	.4685+04	.3052+00
9997.	.1014+01	.4842+04	.2795-02	.8454+02	.4910+04	.3140+00
9992.	.1001+01	.4677+04	.2607-02	.8064+02	.4683+04	.3070+00
20027.	.2375+01	.3233+04	.1246-02	.1322+03	.7678+04	.8948-01
20022.	.2364+01	.3342+04	.1331-02	.1360+03	.7901+04	.9295-01
20020.	.2348+01	.3371+04	.1354-02	.1363+03	.7914+04	.9438-01
30168.	.4856+01	.2079+04	.5150-03	.1738+03	.1009+05	.2814-01
30184.	.4921+01	.2055+04	.5032-03	.1741+03	.1011+05	.2745-01
30180.	.4937+01	.2091+04	.5211-03	.1777+03	.1032+05	.2785-01
40250.	.9672+01	.1242+04	.1839-03	.2069+03	.1201+05	.8443-02
40245.	.1061+02	.1255+04	.1878-03	.2165+03	.1257+05	.8240-02
40242.	.9694+01	.1299+04	.2010-03	.2167+03	.1259+05	.8807-02
49609.	.1724+02	.1269+04	.1918-03	.3765+03	.2187+05	.4839-02
49609.	.1741+02	.1265+04	.1907-03	.3793+03	.2203+05	.4775-02
49605.	.1750+02	.1263+04	.1900-03	.3805+03	.2210+05	.4742-02
60467.	.3647+02	.3964+03	.1892-04	.2502+03	.1453+05	.7182-03
60487.	.3098+02	.4422+03	.2330-04	.2359+03	.1370+05	.9384-03
60523.	.2887+02	.5104+03	.3105-04	.2537+03	.1474+05	.1162-02
60480.	.2889+02	.5060+03	.3052-04	.2517+03	.1462+05	.1151-02

Averaged Data Points

XRM 109 F4 210 F

P (PSI)	V (CP)
.00000	.31600+02
.49462+04	.62895+02
.99898+04	.10047+03
.20023+05	.23623+03
.30184+05	.49047+03
.40246+05	.97936+03
.49608+05	.17384+04
.60497+05	.29581+04

Table 23. XRM 109 F4, Synthetic Paraffinic Oil,

Plot, L/D = 297 (Continued)

XRM 109 F4 300 F

P3	VISCP	NSRATE	KEC	DELTAP	TAUDYN	REYN
5[illegible]31.	.1933+0[illegible]	.6488+04	.5018-02	.2159+02	.1254+04	.2207+01
5[illegible]30.	.1942+0[illegible]	.6222+04	.4614-02	.2080+02	.1208+04	.2107+01
5[illegible]33.	.1961+0[illegible]	.6314+04	.4751-02	.2067+02	.1200+04	.2183+01
10073.	.2836+0[illegible]	.6305+04	.4738-02	.3079+02	.1788+04	.1461+01
~~10063.~~	~~.2836+00~~	~~.6325+04~~	~~.4766-02~~	~~.3089+02~~	~~.1794+04~~	~~.1466+01~~
10063.	.2828+00	.6307+04	.4742-02	.3071+02	.1783+04	.1467+01
10061.	.2800+0[illegible]	.6261+04	.4672-02	.3018+02	.1753+04	.1470+01
20122.	.5848+0[illegible]	.4691+04	.2623-02	.4723+02	.2743+04	.5274+00
20113.	.5867+00	.4501+04	.2415-02	.4547+02	.2641+04	.5043+00
20110.	.5842+0[illegible]	.4543+04	.2459-02	.4569+02	.2654+04	.5112+00
~~20105.~~	~~.5859+00~~	~~.4765+04~~	~~.2706-02~~	~~.4807+02~~	~~.2792+04~~	~~.5346+00~~
30260.	.1078+01	.4518+04	.2433-02	.8383+02	.4869+04	.2756+00
30258.	.1081+01	.4694+04	.2626-02	.8737+02	.5074+04	.2854+00
30253.	.1100+01	.4685+04	.2616-02	.8871+02	.5152+04	.2801+00
40369.	.1871+01	.3195+04	.1216-02	.1029+03	.5978+04	.1122+00
40362.	.1678+01	.3256+04	.1264-02	.1053+03	.6116+04	.1140+00
~~40359.~~	~~.1697+01~~	~~.3254+04~~	~~.1262-02~~	~~.1063+03~~	~~.6174+04~~	~~.1127+00~~
49698.	.3034+01	.2044+04	.4982-03	.1068+03	.6202+04	.4431-01
49676.	.3229+01	.2033+04	.4927-03	.1130+03	.6565+04	.4139-01

Averaged Data Points

XRM 109 F4 300

P (PSI)	V (CP)
.00000	.16220+02
~~.50313+04~~	~~.19251+02~~
.10065+05	.28248+02
.20112+05	.58539+02
.30257+05	.10861+03
~~.40363+05~~	~~.10823+03~~
.49687+05	.31313+03

Table 24. XRM 177 F4, Synthetic Paraffinic Oil,

Plot, L/D = 297

FLUID XRM 177F4 100°F

P3	VISCP	NSRATE	KEC	DELTAP	TAUDYN	REYN
4699.	.7711+01	.3662+04	.1598-02	.4862+03	.2824+05	.3122-01
4700.	.7682+01	.3718+04	.1647-02	.4917+03	.2856+05	.3182-01
4709.	.7591+01	.3751+04	.1677-02	.4903+03	.2847+05	.3248-01
9668.	.1472+02	.2273+04	.6155-03	.5761+03	.3346+05	.1015-01
9641.	.1445+02	.2352+04	.6594-03	.5851+03	.3398+05	.1070-01
9631.	.1492+02	.2213+04	.5836-03	.5686+03	.3302+05	.9747-02
19618.	.3934+02	.2157+04	.5546-03	.1461+04	.8487+05	.3605-02
19675.	.4105+02	.2148+04	.5498-03	.1518+04	.8818+05	.3439-02
19657.	.4216+02	.2222+04	.5885-03	.1613+04	.9369+05	.3465-02
19654.	.4256+02	.2236+04	.5957-03	.1638+04	.9516+05	.3453-02
29609.	.1113+03	.8812+03	.9254-04	.1689+04	.9811+05	.5203-03
29575.	.1106+03	.9230+03	.1015-03	.1757+04	.1020+06	.5489-03
29549.	.1089+03	.9559+03	.1089-03	.1793+04	.1041+06	.5770-03
39515.	.3125+03	.4825+03	.2775-04	.2596+04	.1508+06	.1015-03
39486.	.3097+03	.5060+03	.3052-04	.2698+04	.1567+06	.1074-03
39462.	.2707+03	.6092+03	.4423-04	.2840+04	.1649+06	.1479-03

Averaged Data Points

FLUID XRM 177F4 100°F

P (PSI)	V (CP)
.00000	.37600+03
.47029+04	.76613+03
.96466+04	.14697+04
.19651+05	.41280+04
.29578+05	.11027+05

Table 24. XRM 177 F4, Synthetic Paraffinic Oil, Plot, L/D = 297 (Continued)

FLUID XRM 177F4 210 F

P3	VISCP	NSRATE	KEC	DELTAP	TAUDYN	REYN
4945.	.6359+00	.4991+04	.2968-02	.5464+02	.3173+04	.5160+00
4941.	.6359+00	.5002+04	.2982-02	.5476+02	.3181+04	.5171+00
4949.	.6384+00	.5181+04	.3200-02	.5695+02	.3308+04	.5336+00
4956.	.6196+00	.5141+04	.3150-02	.5485+02	.3185+04	.5454+00
9923.	.9999+00	.5327+04	.3382-02	.9171+02	.5326+04	.3502+00
9931.	.9999+00	.5236+04	.3268-02	.9015+02	.5236+04	.3443+00
9921.	.1003+01	.5140+04	.3149-02	.8877+02	.5155+04	.3369+00
9933.	.9830+00	.5140+04	.3149-02	.8700+02	.5053+04	.3438+00
19985.	.2301+01	.3623+04	.1564-02	.1436+03	.8338+04	.1035+00
19996.	.2273+01	.3725+04	.1654-02	.1458+03	.8468+04	.1077+00
19993.	.2274+01	.3694+04	.1627-02	.1447+03	.8402+04	.1068+00
19990.	.2261+01	.3582+04	.1529-02	.1395+03	.8100+04	.1041+00
30008.	.4765+01	.2237+04	.5964-03	.1835+03	.1066+05	.3087-01
30036.	.4607+01	.2291+04	.6254-03	.1817+03	.1055+05	.3269-01
30023.	.4785+01	.2245+04	.6008-03	.1850+03	.1074+05	.3085-01
30010.	.4720+01	.2260+04	.6090-03	.1837+03	.1067+05	.3148-01
40017.	.9377+01	.1477+04	.2598-03	.2384+03	.1385+05	.1035-01
39996.	.9007+01	.1599+04	.3048-03	.2480+03	.1440+05	.1167-01
40026.	.9240+01	.1516+04	.2739-03	.2412+03	.1401+05	.1079-01
40009.	.9486+01	.1431+04	.2440-03	.2337+03	.1357+05	.9915-02
40271.	.9792+01	.1431+04	.2439-03	.2412+03	.1401+05	.9604-02
40293.	.1017+02	.1355+04	.2187-03	.2372+03	.1378+05	.8755-02
40288.	.9095+01	.1473+04	.2586-03	.2307+03	.1340+05	.1065-01
40299.	.9310+01	.1542+04	.2833-03	.2471+03	.1435+05	.1089-01
40285.	.9583+01	.1451+04	.2509-03	.2394+03	.1390+05	.9953-02
40302.	.9232+01	.1553+04	.2874-03	.2468+03	.1433+05	.1106-01
40289.	.9024+01	.1569+04	.2933-03	.2437+03	.1416+05	.1143-01
40302.	.9186+01	.1577+04	.2963-03	.2494+03	.1448+05	.1128-01
40296.	.9359+01	.1577+04	.2963-03	.2541+03	.1476+05	.1107-01
49718.	.1749+02	.7241+03	.6250-04	.2181+03	.1266+05	.2722-02
49690.	.1738+02	.1439+04	.2468-03	.4306+03	.2501+05	.5444-02
49705.	.1684+02	.1587+04	.3001-03	.4601+03	.2672+05	.6194-02
49692.	.1734+02	.1624+04	.3142-03	.4848+03	.2816+05	.6155-02

Averaged Data Points

FLUID XRM 177F4 210 F

P (PSI)	V (CP)
.00000	.31600+02
.49475+04	.63243+02
.99268+04	.99644+02
.19991+05	.22776+03
.30020+05	.47191+03
.40206+05	.93740+03
.49704+05	.17434+04

Table 24. XRM 177 F4, Synthetic Paraffinic Oil,

Plot, L/D = 297 (Continued)

FLUID XRM 177F4 300 F

P3	VISCP	NSRATE	KEC	DELTAP	TAUDYN	REYN
4900.	.1853+00	.6977+04	.5802-02	.2226+02	.1293+04	.2476+01
4899.	.1796+00	.7050+04	.5924-02	.2181+02	.1266+04	.2580+01
4898.	.1825+00	.7189+04	.6159-02	.2259+02	.1312+04	.2589+01
9895.	.2885+00	.5440+04	.3527-02	.2703+02	.1570+04	.1239+01
9888.	.2846+00	.7436+04	.6590-02	.3644+02	.2117+04	.1718+01
9892.	.2861+00	.7147+04	.6088-02	.3521+02	.2045+04	.1642+01
9884.	.2845+00	.7519+04	.6738-02	.3683+02	.2139+04	.1737+01
19924.	.5603+00	.5600+04	.3738-02	.5403+02	.3138+04	.6570+00
19905.	.5612+00	.5432+04	.3517-02	.5249+02	.3048+04	.6363+00
19885.	.5497+00	.5396+04	.3471-02	.5108+02	.2966+04	.6454+00
29554.	.9974+00	.5453+04	.3544-02	.9365+02	.5439+04	.3594+00
29547.	.9949+00	.5342+04	.3401-02	.9150+02	.5314+04	.3530+00
29542.	.9935+00	.5331+04	.3387-02	.9118+02	.5296+04	.3527+00
29540.	.9859+00	.5465+04	.3560-02	.9278+02	.5388+04	.3640+00
40139.	.1749+01	.3850+04	.1767-02	.1160+03	.6735+04	.1447+00
40125.	.1739+01	.3871+04	.1786-02	.1159+03	.6732+04	.1463+00
40123.	.1745+01	.3911+04	.1823-02	.1175+03	.6823+04	.1474+00
40117.	.1755+01	.3632+04	.1572-02	.1097+03	.6374+04	.1361+00
51390.	.3000+01	.2397+04	.6850-03	.1238+03	.7192+04	.5254-01
51377.	.3097+01	.2436+04	.7075-03	.1299+03	.7546+04	.5172-01
51364.	.3095+01	.2408+04	.6911-03	.1283+03	.7453+04	.5115-01
51357.	.3129+01	.2293+04	.6264-03	.1235+03	.7173+04	.4817-01

Averaged Data Points

XRM 177 F4 300 F

P (PSI)	V (CP)
.00000	.1[illegible]220+02
.48992+04	.1[illegible]247+02
.98698+04	.2[illegible]595+02
.19905+05	.5[illegible]5708+02
.29546+05	.9[illegible]9291+02
.40126+05	.1747[illegible]+03
.51372+05	.3[illegible]802+03

Table 25. XRM 177 F4, Synthetic Paraffinic Oil,

100°F, L/D = 1.35

P3	VISCP	TAUDYN	NSRATE	RE	LEOL
4833.	.7893+01	.9355+06	.1185+06	.1174+00	.5652-02
4828.	.7809+01	.9454+06	.1211+06	.1212+00	.5835-02
4833.	.8037+01	.1246+07	.1550+06	.1508+00	.7260-02
4831.	.7976+01	.9648+06	.1210+06	.1185+00	.5707-02
4812.	.8000+01	.1261+07	.1576+06	.1540+00	.7412-02
4828.	.7835+01	.1511+07	.1929+06	.1925+00	.9267-02
4821.	.7863+01	.1526+07	.1941+06	.1930+00	.9291-02
4826.	.6480+01	.7553+07	.1166+07	.1406+01	.6769-01
4840.	.5187+01	.1191+08	.2296+07	.3460+01	.1666+00
4852.	.7684+01	.2611+07	.3397+06	.3456+00	.1664-01
4849.	.7314+01	.4083+07	.5583+06	.5966+00	.2873-01
4857.	.7154+01	.5389+07	.7533+06	.8230+00	.3962-01
4850.	.8560+01	.2433+07	.2842+06	.2595+00	.1250-01
4865.	.4695+01	.1364+08	.2905+07	.4837+01	.2329+00
4872.	.6060+01	.9099+07	.1501+07	.1936+01	.9323-01
4838.	.6940+01	.7620+07	.1098+07	.1237+01	.5955-01
4835.	.6407+01	.7412+07	.1157+07	.1411+01	.6794-01
4859.	.5731+01	.9723+07	.1697+07	.2314+01	.1114+00
4861.	.4728+01	.1319+08	.2790+07	.4612+01	.2220+00
4851.	.4458+01	.1415+08	.3173+07	.5563+01	.2678+00
5008.	.7877+01	.1016+06	.1290+05	.1280-01	.6162-03
5007.	.8094+01	.9205+05	.1137+05	.1098-01	.5287-03
5002.	.8360+01	.1017+06	.1217+05	.1138-01	.5478-03
5006.	.8479+01	.3808+06	.4492+05	.4140-01	.1994-02
5010.	.8049+01	.3790+06	.4708+05	.4572-01	.2201-02
5011.	.8013+01	.3875+06	.4836+05	.4718-01	.2271-02
5011.	.8086+01	.6396+06	.7910+05	.7645-01	.3681-02
5012.	.8128+01	.6468+06	.7957+05	.7652-01	.3684-02
5013.	.7980+01	.6270+06	.7856+05	.7695-01	.3705-02
5013.	.7900+01	.8842+06	.1119+06	.1107+00	.5332-02
5015.	.8071+01	.9024+06	.1118+06	.1083+00	.5213-02
5012.	.7924+01	.9318+06	.1176+06	.1160+00	.5585-02
5013.	.8180+01	.9087+06	.1111+06	.1061+00	.5111-02
5015.	.7926+01	.1215+07	.1533+06	.1511+00	.7277-02
5015.	.7825+01	.1247+07	.1594+06	.1592+00	.7667-02
5013.	.7926+01	.1282+07	.1617+06	.1595+00	.7678-02
5015.	.7816+01	.1538+07	.1968+06	.1968+00	.9476-02
5015.	.7806+01	.1566+07	.2006+06	.2009+00	.9673-02
5015.	.8111+01	.1563+07	.1927+06	.1857+00	.8941-02

Table 25. XRM 177 F4, Synthetic Paraffinic Oil,

100°F, L/D = 1.35 (Continued)

9894.	.1584+02	.1279+07	.8071+05	.3982-01	.1917-02
9902.	.1509+02	.1284+07	.8505+05	.4404-01	.2120-02
9903.	.1541+02	.1234+07	.8012+05	.4064-01	.1957-02
9904.	.1588+02	.1792+07	.1128+06	.5553-01	.2674-02
9903.	.1537+02	.1808+07	.1176+06	.5982-01	.2880-02
9899.	.1555+02	.1783+07	.1146+06	.5761-01	.2774-02
9892.	.1506+02	.2402+07	.1595+06	.8280-01	.3986-02
9896.	.1515+02	.2383+07	.1573+06	.8114-01	.3907-02
9896.	.1508+02	.2439+07	.1617+06	.8379-01	.4035-02
9885.	.1481+02	.2899+07	.1958+06	.1034+00	.4978-02
9900.	.1478+02	.2923+07	.1978+06	.1046+00	.5035-02
9908.	.1499+02	.2898+07	.1934+06	.1008+00	.4856-02
9904.	.1303+02	.7111+07	.5458+06	.3274+00	.1577-01
9918.	.1438+02	.4295+07	.2987+06	.1624+00	.7820-02
9902.	.1090+02	.1306+08	.1199+07	.8598+00	.4140-01
9909.	.1238+02	.8198+07	.6622+06	.4181+00	.2013-01
9909.	.1255+02	.9533+07	.7597+06	.4732+00	.2278-01
9904.	.1177+02	.1050+08	.8920+06	.5924+00	.2853-01
9911.	.1348+02	.6166+07	.4575+06	.2653+00	.1277-01
9906.	.8720+01	.1907+08	.2187+07	.1960+01	.9437-01
9919.	.1132+02	.1213+08	.1072+07	.7398+00	.3562-01
9931.	.8980+01	.1656+08	.1844+07	.1605+01	.7727-01
9897.	.9212+01	.1702+08	.1848+07	.1568+01	.7549-01
9892.	.1117+02	.1216+08	.1089+07	.7618+00	.3668-01
9897.	.7989+01	.2069+08	.2590+07	.2534+01	.1220+00
9884.	.7148+01	.2343+08	.3278+07	.3584+01	.1726+00
9890.	.6955+01	.2431+08	.3495+07	.3927+01	.1891+00
9901.	.7071+01	.2387+08	.3376+07	.3731+01	.1797+00
9918.	.7043+01	.2438+08	.3462+07	.3841+01	.1850+00
10084.	.1513+02	.2212+06	.1462+05	.7557-02	.3639-03
10082.	.1558+02	.2304+06	.1479+05	.7423-02	.3574-03
10078.	.1571+02	.2344+06	.1492+05	.7421-02	.3573-03
10075.	.1523+02	.2280+06	.1497+05	.7679-02	.3697-03
10074.	.1542+02	.7295+06	.4731+05	.2398-01	.1155-02
10073.	.1515+02	.7323+06	.4835+05	.2495-01	.1201-02
10071.	.1493+02	.7779+06	.5211+05	.2729-01	.1314-02
10070.	.1510+02	.7546+06	.4996+05	.2586-01	.1245-02
10077.	.1506+02	.1215+07	.8066+05	.4185-01	.2015-02
10077.	.1515+02	.1225+07	.8087+05	.4173-01	.2009-02
10075.	.1520+02	.1215+07	.7994+05	.4112-01	.1980-02
10075.	.1473+02	.1748+07	.1187+06	.6296-01	.3031-02
10074.	.1493+02	.1728+07	.1157+06	.6057-01	.2916-02
10076.	.1499+02	.1689+07	.1127+06	.5874-01	.2828-02

Table 25. XRM 177 F4, Synthetic Paraffinic Oil,

100°F, L/D = 1.35 (Continued)

10075.	.1472+02	.2346+07	.1593+06	.8460-01	.4074-02
10077.	.1459+02	.2297+07	.1574+06	.8432-01	.4060-02
10079.	.1465+02	.2343+07	.1599+06	.8532-01	.4108-02
10077.	.1445+02	.2859+07	.1978+06	.1070+00	.5152-02
10077.	.1443+02	.2798+07	.1939+06	.1050+00	.5055-02
10077.	.1442+02	.2770+07	.1920+06	.1041+00	.5011-02
20214.	.4845+02	.7170+06	.1480+05	.2387-02	.1150-03
20210.	.4782+02	.6884+06	.1440+05	.2353-02	.1133-03
20208.	.4795+02	.7914+06	.1651+05	.2691-02	.1296-03
20206.	.4492+02	.2286+07	.5089+05	.8854-02	.4263-03
20208.	.4513+02	.2218+07	.4914+05	.8511-02	.4098-03
20202.	.4557+02	.2179+07	.4782+05	.8201-02	.3949-03
20207.	.4427+02	.3630+07	.8200+05	.1448-01	.6971-03
20206.	.4391+02	.3597+07	.8192+05	.1458-01	.7021-03
20207.	.4375+02	.3457+07	.7901+05	.1412-01	.6797-03
20211.	.4273+02	.4924+07	.1152+06	.2108-01	.1015-02
20209.	.4292+02	.4987+07	.1162+06	.2116-01	.1019-02
20212.	.4265+02	.4949+07	.1160+06	.2126-01	.1024-02
20219.	.4321+02	.4945+07	.1144+06	.2070-01	.9968-03
20204.	.4126+02	.6447+07	.1563+06	.2960-01	.1425-02
20216.	.4138+02	.6495+07	.1570+06	.2965-01	.1428-02
20217.	.4109+02	.6634+07	.1615+06	.3072-01	.1479-02
19952.	.4594+02	.2281+07	.4965+05	.8446-02	.4067-03
19963.	.4503+02	.2289+07	.5082+05	.8821-02	.4247-03
19975.	.4490+02	.2287+07	.5093+05	.8866-02	.4269-03
19954.	.4244+02	.3498+07	.8242+05	.1518-01	.7309-03
19963.	.4248+02	.3672+07	.8646+05	.1591-01	.7661-03
19959.	.4371+02	.3505+07	.8019+05	.1434-01	.6904-03
19948.	.4266+02	.4855+07	.1138+06	.2085-01	.1004-02
19955.	.4227+02	.4766+07	.1128+06	.2085-01	.1004-02
19950.	.4165+02	.4775+07	.1147+06	.2152-01	.1036-02
19946.	.4045+02	.6429+07	.1590+06	.3072-01	.1479-02
19941.	.4042+02	.6359+07	.1573+06	.3042-01	.1465-02
19936.	.4047+02	.6481+07	.1601+06	.3093-01	.1489-02
19935.	.4041+02	.6683+07	.1654+06	.3199-01	.1540-02
19926.	.3961+02	.7807+07	.1971+06	.3889-01	.1873-02
19971.	.3933+02	.7974+07	.2027+06	.4028-01	.1940-02
19956.	.3932+02	.7937+07	.2018+06	.4012-01	.1932-02
19969.	.3328+02	.1324+08	.3979+06	.9345-01	.4499-02
19968.	.2948+02	.1845+08	.6258+06	.1659+00	.7988-02
19969.	.3453+02	.1386+08	.4014+06	.9085-01	.4374-02
19952.	.2365+02	.2411+08	.1020+07	.3371+00	.1623-01
19950.	.2047+02	.3127+08	.1528+07	.5834+00	.2809-01

Table 25. XRM 177 F4, Synthetic Paraffinic Oil,

100°F, L/D = 1.35 (Continued)

19943.	.3120+02	.1646+08	.5274+06	.1321+00	.6362-02
19959.	.1606+02	.3954+08	.2461+07	.1198+01	.5766-01
19958.	.2639+02	.2183+08	.8270+06	.2449+00	.1179-01
19936.	.2118+02	.2926+08	.1382+07	.5098+00	.2455-01
19923.	.1788+02	.3519+08	.1968+07	.8606+00	.4144-01
19941.	.2495+02	.2253+08	.9031+06	.2829+00	.1362-01
19942.	.2908+02	.1831+08	.6296+06	.1692+00	.8148-02
19938.	.1592+02	.3846+08	.2416+07	.1186+01	.5712-01
19955.	.1732+02	.3511+08	.2028+07	.9152+00	.4406-01
19943.	.1581+02	.3795+08	.2400+07	.1187+01	.5713-01
20224.	.4102+02	.6681+07	.1629+06	.3104-01	.1494-02
20217.	.4038+02	.7580+07	.1877+06	.3633-01	.1749-02
20208.	.3991+02	.7642+07	.1915+06	.3750-01	.1805-02
20212.	.4009+02	.7720+07	.1926+06	.3754-01	.1808-02
20210.	.4009+02	.7668+07	.1913+06	.3730-01	.1796-02
30411.	.1305+03	.1799+07	.1379+05	.8258-03	.3976-04
30405.	.1302+03	.1775+07	.1363+05	.8181-03	.3939-04
30401.	.1228+03	.2171+07	.1767+05	.1124-02	.5414-04
30405.	.1173+03	.5609+07	.4780+05	.3184-02	.1533-03
30402.	.1157+03	.5493+07	.4746+05	.3205-02	.1543-03
30406.	.1186+03	.5898+07	.4973+05	.3278-02	.1578-03
30409.	.1076+03	.9368+07	.8710+05	.6329-02	.3047-03
30406.	.1106+03	.8734+07	.7897+05	.5581-02	.2687-03
30411.	.1082+03	.9186+07	.8488+05	.6130-02	.2951-03
30410.	.1082+03	.9103+07	.8412+05	.6077-02	.2926-03
30111.	.1238+03	.2007+07	.1621+05	.1023-02	.4926-04
30107.	.1235+03	.1926+07	.1559+05	.9865-03	.4750-04
30102.	.1249+03	.2002+07	.1602+05	.1003-02	.4828-04
30103.	.1172+03	.5843+07	.4987+05	.3327-02	.1602-03
30099.	.1145+03	.5775+07	.5046+05	.3445-02	.1659-03
30102.	.1172+03	.5575+07	.4757+05	.3172-02	.1527-03
30096.	.1079+03	.8971+07	.8312+05	.6020-02	.2898-03
30096.	.1068+03	.9108+07	.8532+05	.6247-02	.3008-03
30088.	.1069+03	.8722+07	.8160+05	.5967-02	.2873-03
30092.	.9921+02	.1189+08	.1199+06	.9444-02	.4547-03
30096.	.1000+03	.1192+08	.1192+06	.9320-02	.4487-03
30096.	.9908+02	.1173+08	.1184+06	.9337-02	.4495-03
30091.	.9370+02	.1491+08	.1591+06	.1327-01	.6391-03
30086.	.9151+02	.1490+08	.1628+06	.1390-01	.6695-03
30078.	.9152+02	.1487+08	.1625+06	.1388-01	.6681-03
30075.	.9415+02	.1454+08	.1545+06	.1282-01	.6174-03
30095.	.8901+02	.1701+08	.1911+06	.1678-01	.8081-03
30084.	.8903+02	.1672+08	.1878+06	.1649-01	.7940-03

Table 25. XRM 177 F4, Synthetic Paraffinic Oil, 100°F, L/D = 1.35 (Continued)

30124.	.8943+02	.1895+08	.2119+06	.1852-01	.8918-03
30111.	.8443+02	.1969+08	.2333+06	.2159-01	.1040-02
30098.	.7922+02	.1972+08	.2489+06	.2455-01	.1182-02
30093.	.5940+02	.3376+08	.5683+06	.7477-01	.3600-02
30090.	.5510+02	.4138+08	.7511+06	.1066+00	.5130-02
30109.	.4528+02	.4422+08	.9766+06	.1686+00	.8118-02
30109.	.5982+02	.3351+08	.5602+06	.7319-01	.3524-02
30084.	.7030+02	.2814+08	.4004+06	.4452-01	.2143-02
30088.	.6525+02	.2888+08	.4426+06	.5303-01	.2553-02
30090.	.7541+02	.2210+08	.2931+06	.3038-01	.1463-02
30081.	.6225+02	.3288+08	.5281+06	.6631-01	.3193-02
30083.	.4487+02	.4458+08	.9934+06	.1730+00	.8331-02
30084.	.4712+02	.4122+08	.8748+06	.1451+00	.6986-02
40186.	.3048+03	.4082+07	.1339+05	.3434-03	.1653-04
40186.	.3096+03	.4373+07	.1412+05	.3565-03	.1717-04
40183.	.2907+03	.4301+07	.1479+05	.3977-03	.1915-04
40178.	.2518+03	.1230+08	.4885+05	.1516-02	.7301-04
40181.	.2556+03	.1162+08	.4548+05	.1391-02	.6697-04
40176.	.2534+03	.1229+08	.4850+05	.1496-02	.7204-04
40189.	.2478+03	.1233+08	.4978+05	.1570-02	.7561-04
40166.	.2269+03	.1826+08	.8048+05	.2773-02	.1335-03
40168.	.2268+03	.1808+08	.7971+05	.2747-02	.1322-03
40168.	.2276+03	.1805+08	.7929+05	.2723-02	.1311-03
40164.	.2050+03	.2288+08	.1116+06	.4257-02	.2050-03
40162.	.2056+03	.2311+08	.1124+06	.4271-02	.2056-03
40157.	.2037+03	.2310+08	.1134+06	.4351-02	.2095-03
40162.	.1817+03	.2780+08	.1530+06	.6583-02	.3169-03
40169.	.1815+03	.2815+08	.1551+06	.6678-02	.3215-03
40168.	.1828+03	.2815+08	.1540+06	.6584-02	.3170-03
40168.	.1824+03	.2857+08	.1567+06	.6715-02	.3233-03
40164.	.1477+03	.4140+08	.2803+06	.1483-01	.7143-03
40199.	.1192+03	.4780+08	.4010+06	.2630-01	.1266-02

Table 25. XRM 177 F4, Synthetic Paraffinic Oil, 100°F, L/D = 14.9 (Continued)

P_3	VISCP	TAUDYN	NSRATE	RE	LEOL
4958.	.7912+01	.3552+05	.4489+04	.2259-01	.9856-04
4957.	.7901+01	.3883+05	.4915+04	.2477-01	.1081-03
4956.	.8108+01	.3683+05	.4542+04	.2230-01	.9729-04
4955.	.7928+01	.3702+05	.4670+04	.2345-01	.1023-03
4962.	.7946+01	.6080+05	.7651+04	.3833-01	.1672-03
4960.	.7851+01	.6283+05	.8003+04	.4058-01	.1770-03
4963.	.8002+01	.6089+05	.7610+04	.3786-01	.1652-03
4960.	.7919+01	.6323+05	.7984+04	.4014-01	.1751-03
4960.	.7964+01	.8494+05	.1067+05	.5332-01	.2326-03
4961.	.7799+01	.8483+05	.1088+05	.5552-01	.2422-03
4960.	.7819+01	.8820+05	.1128+05	.5742-01	.2506-03
4956.	.7880+01	.8761+05	.1112+05	.5617-01	.2451-03
4958.	.7909+01	.1148+06	.1451+05	.7304-01	.3187-03
4959.	.7811+01	.1164+06	.1490+05	.7595-01	.3314-03
4958.	.7882+01	.1211+06	.1536+05	.7759-01	.3385-03
4958.	.7786+01	.1205+06	.1548+05	.7915-01	.3453-03
4964.	.7864+01	.1443+06	.1836+05	.9293-01	.4055-03
4964.	.7896+01	.1419+06	.1797+05	.9060-01	.3953-03
4963.	.7862+01	.1423+06	.1810+05	.9163-01	.3998-03
4963.	.7743+01	.1457+06	.1881+05	.9673-01	.4221-03
4967.	.7875+01	.1455+06	.1848+05	.9342-01	.4076-03
4960.	.7603+01	.3124+06	.4109+05	.2152+00	.9388-03
4960.	.7751+01	.2379+06	.3070+05	.1576+00	.6878-03
4961.	.7244+01	.5181+06	.7151+05	.3930+00	.1715-02
4968.	.7497+01	.4886+06	.6517+05	.3461+00	.1510-02
4963.	.7499+01	.4028+06	.5372+05	.2852+00	.1244-02
4963.	.7663+01	.3526+06	.4601+05	.2390+00	.1043-02
4967.	.7256+01	.4677+06	.6445+05	.3536+00	.1543-02
4966.	.6668+01	.8287+06	.1243+06	.7420+00	.3237-02
4968.	.6902+01	.8436+06	.1222+06	.7049+00	.3076-02
4976.	.6566+01	.9800+06	.1493+06	.9050+00	.3949-02
4964.	.6586+01	.9260+06	.1406+06	.8499+00	.3708-02
4972.	.6739+01	.8859+06	.1315+06	.7767+00	.3389-02
4982.	.7293+01	.6142+06	.8423+05	.4598+00	.2006-02
4742.	.7559+01	.3271+06	.4327+05	.2279+00	.9944-03
4736.	.6412+01	.9775+06	.1524+06	.9465+00	.4130-02
4728.	.5463+01	.1539+07	.2817+06	.2053+01	.8957-02
4749.	.6244+01	.1111+07	.1780+06	.1135+01	.4951-02
4748.	.6753+01	.8133+06	.1204+06	.7101+00	.3098-02
4771.	.7164+01	.5321+06	.7428+05	.4128+00	.1801-02
9721.	.1188+02	.1392+07	.1172+06	.3927+00	.1713-02
9735.	.1099+02	.1754+07	.1596+06	.5784+00	.2524-02
9754.	.1393+02	.8094+06	.5811+05	.1661+00	.7246-03

Table 25. XRM 177 F4, Synthetic Paraffinic Oil,

100°F, L/D = 14.9 (Continued)

9723.	.1352+02	.7986+06	.5908+05	.1740+00	.7592-03
9717.	.1289+02	.9401+06	.7293+05	.2252+00	.9828-03
9702.	.1417+02	.5989+06	.4225+05	.1187+00	.5178-03
9694.	.1040+02	.1778+07	.1709+06	.6539+00	.2853-02
9698.	.9519+01	.2131+07	.2239+06	.9364+00	.4086-02
9737.	.9648+01	.2099+07	.2176+06	.8978+00	.3917-02
9745.	.8462+01	.2563+07	.3029+06	.1425+01	.6217-02
9744.	.1007+02	.1969+07	.1955+06	.7726+00	.3371-02
9928.	.1420+02	.2959+06	.2083+05	.5840-01	.2548-03
9927.	.1415+02	.4449+06	.3145+05	.8850-01	.3861-03
9914.	.1364+02	.6255+06	.4587+05	.1339+00	.5844-03
9918.	.1346+02	.9276+06	.6892+05	.2039+00	.8895-03
9914.	.1405+02	.6774+06	.4823+05	.1367+00	.5963-03
9915.	.1493+02	.4099+06	.2746+05	.7324-01	.3196-03
9911.	.1281+02	.9842+06	.7680+05	.2386+00	.1041-02
9982.	.1571+02	.2949+05	.1877+04	.4755-02	.2075-04
9982.	.1478+02	.2852+05	.1930+04	.5199-02	.2268-04
9979.	.1509+02	.2891+05	.1915+04	.5051-02	.2204-04
9978.	.1489+02	.7439+05	.4997+04	.1336-01	.5831-04
9978.	.1489+02	.7331+05	.4922+04	.1316-01	.5741-04
9974.	.1477+02	.7505+05	.5081+04	.1369-01	.5974-04
9973.	.1487+02	.7349+05	.4942+04	.1323-01	.5772-04
9973.	.1455+02	.1162+06	.7990+04	.2186-01	.9540-04
9972.	.1471+02	.1165+06	.7919+04	.2142-01	.9347-04
9972.	.1459+02	.1174+06	.8050+04	.2197-01	.9586-04
9970.	.1451+02	.1630+06	.1123+05	.3083-01	.1345-03
9970.	.1452+02	.1661+06	.1144+05	.3137-01	.1369-03
9971.	.1455+02	.1631+06	.1121+05	.3068-01	.1339-03
9971.	.1452+02	.1654+06	.1139+05	.3125-01	.1363-03
9973.	.1440+02	.2172+06	.1508+05	.4168-01	.1818-03
9972.	.1435+02	.2181+06	.1519+05	.4214-01	.1839-03
9972.	.1437+02	.2177+06	.1515+05	.4195-01	.1830-03
9972.	.1441+02	.2275+06	.1578+05	.4360-01	.1902-03
9970.	.1429+02	.2677+06	.1873+05	.5218-01	.2277-03
9970.	.1428+02	.2595+06	.1817+05	.5065-01	.2210-03
9976.	.1427+02	.2647+06	.1855+05	.5173-01	.2257-03
9922.	.1339+02	.6686+06	.4993+05	.1485+00	.6478-03
9925.	.1351+02	.7046+06	.5214+05	.1536+00	.6702-03
20016.	.4449+02	.7890+05	.1773+04	.1587-02	.6923-05
20014.	.4592+02	.8058+05	.1755+04	.1521-02	.6637-05
20013.	.4667+02	.7449+05	.1596+04	.1361-02	.5940-05
20008.	.4463+02	.2205+06	.4941+04	.4408-02	.1923-04
20008.	.4418+02	.2206+06	.4993+04	.4499-02	.1963-04

Table 25. XRM 177 F4, Synthetic Paraffinic Oil, 100°F, L/D = 14.9 (Continued)

20011.	.4461+02	.2327+06	.5216+04	.4655-02	.2031-04
20005.	.4433+02	.3575+06	.8064+04	.7241-02	.3160-04
20003.	.4368+02	.3597+06	.8235+04	.7505-02	.3275-04
20001.	.4404+02	.3624+06	.8228+04	.7437-02	.3245-04
20001.	.4358+02	.5066+06	.1163+05	.1062-01	.4634-04
19998.	.4281+02	.4968+06	.1161+05	.1079-01	.4709-04
19999.	.4350+02	.5009+06	.1151+05	.1054-01	.4597-04
20003.	.4267+02	.6588+06	.1544+05	.1441-01	.6285-04
20003.	.4229+02	.6491+06	.1535+05	.1445-01	.6303-04
20004.	.4190+02	.7796+06	.1861+05	.1768-01	.7713-04
20004.	.4198+02	.7827+06	.1865+05	.1768-01	.7715-04
20001.	.4143+02	.7791+06	.1881+05	.1807-01	.7885-04
19646.	.4051+02	.9843+06	.2430+05	.2387-01	.1042-03
19628.	.4123+02	.7236+06	.1755+05	.1695-01	.7394-04
19625.	.3885+02	.1215+07	.3128+05	.3206-01	.1399-03
19619.	.3648+02	.1409+07	.3861+05	.4214-01	.1839-03
19614.	.2003+02	.3567+07	.1780+06	.3538+00	.1544-02
19608.	.3168+02	.2161+07	.6821+05	.8570-01	.3739-03
19619.	.3888+02	.1119+07	.2878+05	.2946-01	.1285-03
19617.	.1714+02	.3863+07	.2253+06	.5232+00	.2283-02
19612.	.3364+02	.1776+07	.5281+05	.6250-01	.2727-03
19619.	.2632+02	.2821+07	.1072+06	.1621+00	.7072-03
19633.	.3044+02	.2295+07	.7538+05	.9857-01	.4301-03
19641.	.2597+02	.2867+07	.1104+06	.1692+00	.7385-03
19639.	.1766+02	.3806+07	.2155+06	.4857+00	.2119-02
19639.	.1620+02	.4124+07	.2546+06	.6257+00	.2730-02
19642.	.3038+02	.2222+07	.7314+05	.9584-01	.4182-03
19654.	.2536+02	.2915+07	.1150+06	.1804+00	.7873-03
19675.	.3827+02	.9232+06	.2412+05	.2509-01	.1095-03
29859.	.1155+03	.1575+06	.1363+04	.4697-03	.2050-05
29868.	.1208+03	.1631+06	.1350+04	.4450-03	.1942-05
29870.	.1203+03	.1921+06	.1597+04	.5287-03	.2307-05
29862.	.1169+03	.5162+06	.4414+04	.1503-02	.6557-05
29848.	.1145+03	.4951+06	.4323+04	.1502-02	.6556-05
29844.	.1190+03	.5115+06	.4297+04	.1437-02	.6270-05
29850.	.1142+03	.7965+06	.6977+04	.2433-02	.1062-04
29854.	.1139+03	.8098+06	.7109+04	.2485-02	.1084-04
29857.	.1134+03	.8128+06	.7170+04	.2518-02	.1099-04
29850.	.1109+03	.1135+07	.1023+05	.3673-02	.1603-04
29857.	.1120+03	.1119+07	.9987+04	.3548-02	.1548-04
29872.	.1114+03	.1129+07	.1013+05	.3619-02	.1579-04
29870.	.1065+03	.1431+07	.1344+05	.5022-02	.2191-04
29874.	.1074+03	.1441+07	.1342+05	.4974-02	.2170-04

Table 25. XRM 177 F4, Synthetic Paraffinic Oil,

100°F, L/D = 14.9 (Continued)

29881.	.1066+03	.1436+07	.1347+05	.5027-02	.2193-04
29877.	.1070+03	.1427+07	.1334+05	.4967-02	.2167-04
29886.	.1048+03	.1694+07	.1617+05	.6142-02	.2680-04
29877.	.1033+03	.1688+07	.1634+05	.6300-02	.2749-04
29891.	.1038+03	.1711+07	.1648+05	.6320-02	.2758-04
29909.	.1051+03	.1707+07	.1624+05	.6148-02	.2683-04
29869.	.1026+03	.1665+07	.1622+05	.6290-02	.2744-04
29853.	.1023+03	.1719+07	.1680+05	.6540-02	.2854-04
29851.	.1063+03	.1452+07	.1367+05	.5120-02	.2234-04
29839.	.1053+03	.1436+07	.1363+05	.5152-02	.2248-04
29838.	.1103+03	.1135+07	.1029+05	.3712-02	.1620-04
29839.	.1095+03	.1124+07	.1027+05	.3734-02	.1629-04
29850.	.1124+03	.8354+06	.7429+04	.2630-02	.1148-04
29835.	.1128+03	.8196+06	.7268+04	.2566-02	.1120-04
29838.	.1179+03	.5568+06	.4723+04	.1595-02	.6959-05
29844.	.1180+03	.5564+06	.4717+04	.1592-02	.6946-05
29844.	.8350+02	.2698+07	.3231+05	.1541-01	.6722-04
29848.	.6226+02	.3863+07	.6204+05	.3967-01	.1731-03
29864.	.6650+02	.3825+07	.5752+05	.3443-01	.1502-03
29863.	.8275+02	.3149+07	.3806+05	.1831-01	.7988-04
29881.	.9994+02	.1851+07	.1852+05	.7375-02	.3218-04
29898.	.8297+02	.3022+07	.3643+05	.1748-01	.7627-04
29891.	.6330+02	.3994+07	.6310+05	.3969-01	.1732-03
30165.	.1214+03	.2185+06	.1799+04	.5899-03	.2574-05
30166.	.1212+03	.2024+06	.1670+04	.5488-03	.2395-05
30164.	.1248+03	.1984+06	.1590+04	.5075-03	.2214-05
30162.	.1201+03	.5501+06	.4579+04	.1517-02	.6620-05
30159.	.1164+03	.5905+06	.5073+04	.1735-02	.7570-05
30156.	.1174+03	.6013+06	.5120+04	.1736-02	.7574-05
30155.	.1168+03	.5806+06	.4972+04	.1695-02	.7395-05
30150.	.1152+03	.9360+06	.8125+04	.2808-02	.1225-04
30177.	.1149+03	.9436+06	.8216+04	.2848-02	.1243-04
30173.	.1154+03	.9363+06	.8113+04	.2799-02	.1221-04
39589.	.2969+03	.4746+06	.1598+04	.2143-03	.9351-06
39595.	.2914+03	.4195+06	.1440+04	.1967-03	.8582-06
39605.	.3015+03	.4479+06	.1486+04	.1962-03	.8562-06
39611.	.2786+03	.1160+07	.4163+04	.5949-03	.2596-05
39600.	.2790+03	.1164+07	.4174+04	.5956-03	.2599-05
39607.	.2826+03	.1193+07	.4222+04	.5947-03	.2595-05
39604.	.2750+03	.1129+07	.4104+04	.5942-03	.2593-05
39615.	.2620+03	.1829+07	.6984+04	.1061-02	.4631-05
39608.	.2620+03	.1859+07	.7096+04	.1078-02	.4705-05
39615.	.2620+03	.1786+07	.6818+04	.1036-02	.4521-05

Table 25. XRM 177 F4, Synthetic Paraffinic Oil,

100°F, L/D = 14.9 (Continued)

39613.	.2449+03	.2573+07	.1051+05	.1708-02	.7453-05
39622.	.2490+03	.2445+07	.9818+04	.1570-02	.6849-05
39631.	.2466+03	.2523+07	.1023+05	.1652-02	.7207-05
39636.	.2489+03	.2500+07	.1004+05	.1606-02	.7007-05
39643.	.2326+03	.3107+07	.1336+05	.2287-02	.9980-05
39650.	.2334+03	.3075+07	.1317+05	.2247-02	.9802-05
39660.	.2323+03	.3061+07	.1318+05	.2259-02	.9856-05
39742.	.2303+03	.2891+07	.1256+05	.2171-02	.9472-05
39731.	.2247+03	.2973+07	.1323+05	.2343-02	.1022-04
39738.	.2315+03	.2942+07	.1271+05	.2184-02	.9531-05
39738.	.2291+03	.3059+07	.1335+05	.2320-02	.1012-04
39736.	.2262+03	.2985+07	.1320+05	.2323-02	.1013-04
39731.	.2440+03	.2431+07	.9963+04	.1626-02	.7093-05
39736.	.2472+03	.2491+07	.1008+05	.1623-02	.7081-05
39742.	.2424+03	.2463+07	.1016+05	.1669-02	.7281-05
39750.	.2003+03	.4088+07	.2041+05	.4055-02	.1769-04
39751.	.2128+03	.3866+07	.1817+05	.3398-02	.1483-04
39752.	.1974+03	.4294+07	.2176+05	.4389-02	.1915-04
39743.	.1953+03	.3921+07	.2008+05	.4094-02	.1786-04
39745.	.1799+03	.4591+07	.2551+05	.5646-02	.2463-04
39728.	.1518+03	.5233+07	.3446+05	.9035-02	.3942-04
39749.	.1389+03	.5506+07	.3965+05	.1137-01	.4959-04
40241.	.3070+03	.4055+06	.1321+04	.1713-03	.7473-06
40237.	.2868+03	.4417+06	.1540+04	.2138-03	.9328-06
40236.	.2897+03	.4366+06	.1507+04	.2071-03	.9036-06
40232.	.2889+03	.9091+06	.3146+04	.4335-03	.1892-05
40233.	.2896+03	.9405+06	.3247+04	.4463-03	.1947-05
40231.	.2815+03	.9586+06	.3405+04	.4815-03	.2101-05

Table 26. B3J: Paraffinic Mineral Oil R-620-12 + 11.5 per cent Polyalkylmethacrylate PL 4523 (MW = .2+07), 100°F

L/D = 14.9

T3	VISCP	TAUDYN	NSRATE	RE	LEOL
4777.	.1139+02	.2209+05	.1945+04	.6821-02	.2976-04
4748.	.1113+02	.5579+05	.5012+04	.1792-01	.7819-04
4739.	.1116+02	.5436+05	.4870+04	.1737-01	.7580-04
4751.	.1097+02	.5376+05	.4900+04	.1778-01	.7759-04
4742.	.1130+02	.6852+05	.7300+04	.2736-01	.1194-03
4737.	.1141+02	.9016+05	.7905+04	.2759-01	.1204-03
4730.	.1137+02	.8422+05	.7407+04	.2593-01	.1132-03
4667.	.1201+02	.1309+06	.1038+05	.3276-01	.1429-03
4721.	.1414+02	.1084+06	.7665+04	.2158-01	.9415-04
4726.	.1215+02	.1291+06	.1062+05	.3476-01	.1517-03
4711.	.1211+02	.1252+06	.1033+05	.3395-01	.1481-03
4714.	.1204+02	.1753+06	.1456+05	.4814-01	.2101-03
4713.	.1239+02	.1667+06	.1345+05	.4320-01	.1885-03
4717.	.1208+02	.1704+06	.1411+05	.4649-01	.2029-03
4724.	.1273+02	.8102+06	.6364+05	.1990+00	.8683-03
4730.	.1283+02	.8324+06	.6489+05	.2014+00	.8786-03
4734.	.1402+02	.8945+06	.6381+05	.1812+00	.7906-03
4962.	.1007+02	.7788+06	.7736+05	.3059+00	.1335-02
4751.	.9281+01	.1562+07	.1683+06	.7219+00	.3150-02
4761.	.1197+02	.1396+07	.1166+06	.3878+00	.1692-02
4741.	.1291+02	.9789+06	.7580+05	.2337+00	.1020-02
4745.	.1328+02	.1057+07	.7961+05	.2386+00	.1041-02
4723.	.1206+02	.2168+07	.1798+06	.5937+00	.2590-02
4730.	.1275+02	.2293+07	.1799+06	.5617+00	.2451-02
4726.	.1326+02	.1285+07	.9690+05	.2910+00	.1270-02
4728.	.1328+02	.1291+07	.9728+05	.2917+00	.1273-02
4710.	.1512+02	.5464+06	.3638+05	.9642-01	.4207-03
4734.	.1584+02	.4663+06	.2944+05	.7397-01	.3227-03
4720.	.1320+02	.2380+07	.1803+06	.5438+00	.2373-02
4726.	.1007+02	.1238+07	.1229+06	.4856+00	.2119-02
4735.	.6854+01	.2168+07	.3162+06	.1837+01	.8014-02
4713.	.1007+02	.1136+07	.1128+06	.4456+00	.1944-02
9734.	.2225+02	.4906+05	.2205+04	.3946-02	.1722-04
9714.	.2248+02	.5084+05	.2262+04	.4007-02	.1748-04
9716.	.2259+02	.1118+06	.4948+04	.8721-02	.3805-04
9716.	.2292+02	.1148+06	.5009+04	.8702-02	.3797-04
9708.	.2351+02	.1779+06	.7566+04	.1281-01	.5589-04
9688.	.2322+02	.1721+06	.7414+04	.1271-01	.5547-04
9674.	.2432+02	.2567+06	.1055+05	.1727-01	.7535-04
9682.	.2342+02	.1829+06	.7810+04	.1328-01	.5794-04
9688.	.2436+02	.2665+06	.1094+05	.1788-01	.7800-04
9688.	.2378+02	.2508+06	.1055+05	.1767-01	.7708-04

Table 26. B3J: Paraffinic Mineral Oil R-620-12 + 11.5 per cent Polyalkylmethacrylate PL 4523 (MW = .2 + 07), 100°F (Continued)

L/D = 14.9

9691.	.2464+02	.3618+06	.1456+05	.2334-01	.1018-03
9688.	.2491+02	.3682+06	.1476+05	.2362-01	.1031-03
9684.	.2463+02	.3636+06	.1473+05	.2375-01	.1036-03
9679.	.2575+02	.4530+06	.1758+05	.2717-01	.1186-03
9688.	.2572+02	.4430+06	.1722+05	.2666-01	.1163-03
9680.	.2561+02	.4413+06	.1723+05	.2679-01	.1169-03
9654.	.2554+02	.1054+07	.4476+05	.7574-01	.3305-03
9678.	.2564+02	.6879+06	.2683+05	.4165-01	.1817-03
9693.	.2575+02	.1000+07	.4211+05	.7058-01	.3080-03
9670.	.1906+02	.1533+07	.8042+05	.1679+00	.7328-03
9695.	.1837+02	.1769+07	.9527+05	.2086+00	.9101-03
9675.	.2624+02	.1240+07	.4726+05	.7168-01	.3128-03
9670.	.2079+02	.2230+07	.1073+06	.2054+00	.8962-03
9640.	.1545+02	.2725+07	.1763+06	.4542+00	.1982-02
9641.	.2697+02	.1088+07	.4034+05	.5955-01	.2598-03
9628.	.1563+02	.2758+07	.1764+06	.4493+00	.1961-02
9635.	.2753+02	.4919+06	.1787+05	.2584-01	.1127-03
9625.	.1651+02	.2913+07	.1765+06	.4255+00	.1857-02
19665.	.1733+02	.1814+06	.1047+05	.2406-01	.1050-03
19671.	.1705+02	.1868+06	.1095+05	.2557-01	.1116-03
19666.	.1904+02	.4942+06	.2595+05	.5426-01	.2368-03
19647.	.1705+02	.4293+06	.2518+05	.5877-01	.2564-03
19647.	.1660+02	.6725+06	.4052+05	.9718-01	.4240-03
19670.	.1621+02	.6566+06	.4052+05	.9953-01	.4343-03
19669.	.1817+02	.9043+06	.5593+05	.1377+00	.6009-03
19666.	.1625+02	.8659+06	.5324+05	.1303+00	.5687-03
19663.	.1614+02	.1142+07	.7073+05	.1744+00	.7612-03
19645.	.1630+02	.1157+07	.7099+05	.1734+00	.7566-03
19651.	.1686+02	.1222+07	.7242+05	.1708+00	.7454-03
19652.	.1524+02	.1294+07	.8471+05	.2207+00	.9631-03
19644.	.1550+02	.1379+07	.8896+05	.2285+00	.9969-03
19657.	.1261+02	.1619+07	.1284+06	.4053+00	.1768-02
19674.	.8191+01	.2682+07	.3274+06	.1591+01	.6942-02

Table 26. B3j: Paraffinic Mineral Oil R-620-12 + 11.5 per cent Polyalkylmethacrylate PL 4523 (MW = .2 + 07), 100°F (Continued)

L/D = 297

P3	VISCP	TAUDYN	NSR*TL	RF	FLOL
4980.	.1156+02	.1006+05	.8716+03	.8956-02	.1885-05
4984.	.1157+02	.9872+04	.8530+03	.8845-02	.1861-05
4985.	.1168+02	.1094+05	.9365+03	.9529-02	.1954-05
4970.	.1067+02	.2421+05	.2268+04	.1397-01	.3060-05
4975.	.1085+02	.2512+05	.2315+04	.1402-01	.3071-05
4973.	.1111+02	.2538+05	.2285+04	.1353-01	.2962-05
4979.	.1141+02	.2469+05	.2161+04	.1256-01	.2751-05
4972.	.1095+02	.4230+05	.3863+04	.2310-01	.5060-05
4967.	.1100+02	.4166+05	.3788+04	.2265-01	.4960-05
4967.	.1080+02	.4151+05	.3822+04	.2313-01	.5066-05
4966.	.1039+02	.5477+05	.5270+04	.3333-01	.7300-05
4967.	.1036+02	.5373+05	.5185+04	.3290-01	.7205-05
4965.	.1060+02	.5511+05	.5197+04	.3222-01	.7056-05
4965.	.1064+02	.5643+05	.5306+04	.3280-01	.7183-05
4965.	.1075+02	.5677+05	.5283+04	.3232-01	.7079-05
4984.	.1084+02	.5682+05	.5240+04	.3177-01	.6956-05
4980.	.1081+02	.5518+05	.5106+04	.3107-01	.6804-05
4985.	.1112+02	.5367+05	.4828+04	.2856-01	.6254-05
9861.	.2278+02	.2544+05	.1117+04	.3224-02	.7060-06
9871.	.2361+02	.2767+05	.1131+04	.3288-02	.7200-06
9865.	.2410+02	.2459+05	.1020+04	.2782-02	.6093-06
9866.	.2256+02	.5217+05	.2313+04	.6740-02	.1476-05
9865.	.2592+02	.5267+05	.2032+04	.6052-02	.1325-05
9850.	.2406+02	.5746+05	.2386+04	.6512-02	.1426-05
9850.	.2414+02	.5301+05	.2201+04	.5954-02	.1304-05
9511.	.2154+02	.2075+05	.9643+03	.2946-02	.6452-06
9517.	.2297+02	.2230+05	.9706+03	.2778-02	.6083-06
9520.	.2298+02	.5062+05	.2210+04	.6345-02	.1390-05
9492.	.2356+02	.5319+05	.2257+04	.6297-02	.1379-05
9571.	.2273+02	.7303+05	.3214+04	.9296-02	.2036-05
9557.	.2343+02	.8184+05	.3493+04	.9803-02	.2147-05
9560.	.2599+02	.9335+05	.3591+04	.9084-02	.1989-05
9550.	.2551+02	.9447+05	.3704+04	.9547-02	.2091-05
9552.	.2607+02	.9596+05	.4767+04	.1570-01	.3439-05
9542.	.2413+02	.1286+06	.5332+04	.1453-01	.3182-05
9549.	.2550+02	.1288+06	.5050+04	.1302-01	.2851-05
9546.	.2504+02	.1305+06	.5210+04	.1368-01	.2996-05
19532.	.9040+02	.8422+05	.9316+03	.6774-03	.1484-06
19507.	.1026+03	.1022+06	.9961+03	.6385-03	.1398-06
19469.	.1006+03	.1045+06	.1037+04	.6768-03	.1482-06
19479.	.7357+02	.1763+06	.2396+04	.2141-02	.4689-06
19190.	.5585+02	.1178+06	.2108+04	.2482-02	.5435-06
19455.	.6550+02	.1712+06	.2050+04	.1614-02	.3534-06
19490.	.6451+02	.1731+06	.2048+04	.1593-02	.3489-06
19449.	.6695+02	.1716+06	.1929+04	.1426-02	.3123-06

Table 27. B3J: Paraffinic Mineral Oil R-620-12 + 11.5 per cent Polyalkylmethacrylate PL 4523 (MW = .2 + 07), 100°F

L/D = 1.35

P3	VISCP	TAUDYN	NSRATE	RE	LEOL
4754.	.5130+02	.8410+07	.1639+06	.2498-01	.1203-02
4778.	.6256+02	.1284+08	.2052+06	.2563-01	.1234-02
4782.	.4629+02	.5956+07	.1287+06	.2173-01	.1046-02
4765.	.3877+02	.1543+08	.3981+06	.8024-01	.3864-02
4795.	.4900+02	.1178+08	.2404+06	.3835-01	.1846-02
4806.	.3690+02	.1911+08	.5178+06	.1097+00	.5281-02
4804.	.5290+02	.1391+08	.2630+06	.3886-01	.1871-02
4817.	.2708+02	.2306+08	.8515+06	.2458+00	.1183-01
4824.	.3497+02	.1831+08	.5236+06	.1170+00	.5634-02
4830.	.4751+02	.8502+07	.1789+06	.2943-01	.1417-02
4830.	.5971+02	.3102+08	.5196+06	.6802-01	.3275-02
4850.	.2973+02	.3105+08	.1044+07	.2745+00	.1322-01
4861.	.3586+02	.2620+08	.7305+06	.1592+00	.7666-02
4802.	.8074+02	.9507+07	.1177+06	.1140-01	.5488-03
4808.	.1021+03	.1359+08	.1331+06	.1019-01	.4904-03
4824.	.2792+02	.3275+08	.1173+07	.3284+00	.1581-01
4815.	.4778+02	.1838+08	.3848+06	.6295-01	.3031-02
4973.	.5141+02	.1186+07	.2307+05	.3508-02	.1689-03
4990.	.4956+02	.1162+07	.2344+05	.3697-02	.1780-03
4963.	.5191+02	.1115+07	.2148+05	.3234-02	.1557-03
4995.	.5059+02	.2684+07	.5315+05	.8226-02	.3961-03
4996.	.4849+02	.2808+07	.5791+05	.9335-02	.4494-03
4992.	.5284+02	.2993+07	.5475+05	.8099-02	.3899-03
4984.	.5101+02	.2871+07	.5629+05	.8626-02	.4153-03
4982.	.5107+02	.4485+07	.8783+05	.1344-01	.6472-03
4975.	.4785+02	.4299+07	.8986+05	.1468-01	.7068-03
4971.	.4812+02	.4486+07	.9324+05	.1515-01	.7292-03
4972.	.5701+02	.1333+07	.2339+05	.3207-02	.1544-03
4969.	.5239+02	.1366+07	.2608+05	.3891-02	.1873-03
4965.	.5190+02	.1313+07	.2529+05	.3808-02	.1834-03
4962.	.5570+02	.3147+07	.5649+05	.7927-02	.3817-03
4959.	.4991+02	.2934+07	.5879+05	.9207-02	.4433-03
4961.	.9531+04	.1712+07	.1796+03	.1473-06	.7092-08
4955.	.4758+02	.4364+07	.9170+05	.1506-01	.7252-03
4953.	.4796+02	.4476+07	.9332+05	.1521-01	.7323-03
4973.	.4955+02	.6039+07	.1219+06	.1922-01	.9255-03
4975.	.4627+02	.5836+07	.1261+06	.2131-01	.1026-02
4975.	.5355+02	.6768+07	.1264+06	.1945-01	.9382-03
4975.	.5131+02	.6214+07	.1211+06	.1844-01	.8881-03
4975.	.4279+02	.7178+07	.1681+06	.3077-01	.1482-02
4965.	.4409+02	.7472+07	.1695+06	.3004-01	.1447-02
4965.	.4801+02	.8075+07	.1682+06	.2738-01	.1318-02

Table 27. B3J: Paraffinic Mineral Oil R-620-12 + 11.5 per cent Polyalkylmethacrylate PL 4523 (MW = .2 + 07), 100°F (Continued)

L/D = 1.35

4989.	.3617+02	.9499+07	.1033+06	.2194-01	.1056-02
4985.	.3536+02	.1165+08	.1991+06	.2677-01	.1289-02
4992.	.3247+02	.1082+08	.2061+06	.3070-01	.1478-02
4974.	.3567+02	.1104+08	.2036+06	.2995-01	.1442-02
4975.	.7734+02	.8224+07	.1053+06	.1073-01	.5169-03
4980.	.3059+02	.9981+07	.1973+06	.3048-01	.1468-02
9969.	.1013+03	.2364+07	.3335+05	.1802-02	.8677-04
9945.	.9123+02	.2551+07	.3796+05	.2396-02	.1153-03
9945.	.9797+02	.2767+07	.3824+05	.2253-02	.1085-03
9924.	.3761+02	.5676+07	.5614+05	.3556-02	.2242-03
9885.	.9621+02	.5774+07	.6061+05	.4875-02	.2347-03
9935.	.9595+02	.5775+07	.6019+05	.4903-02	.2361-03
9947.	.1100+03	.6441+07	.6755+05	.4160-02	.2003-03
9925.	.9511+02	.8610+07	.9053+05	.7440-02	.3582-03
9939.	.9575+02	.8733+07	.9121+05	.7446-02	.3585-03
9931.	.9610+02	.8796+07	.9152+05	.7444-02	.3584-03
9925.	.3361+02	.9020+07	.9636+05	.8046-02	.3874-03
9737.	.1706+03	.9739+07	.5707+05	.2614-02	.1259-03
9746.	.5630+02	.2541+08	.4514+06	.6267-01	.3017-02
9746.	.1198+03	.1844+08	.1540+06	.1005-01	.4838-03
9735.	.1533+03	.1713+08	.1118+06	.5698-02	.2744-03
9741.	.1644+03	.1114+08	.6779+05	.3224-02	.1552-03
9757.	.3832+02	.3293+08	.8593+06	.1753+00	.8439-02
9753.	.2795+03	.6704+07	.2398+05	.6706-03	.3229-04
9743.	.4647+02	.2981+08	.6416+06	.1079+00	.5196-02
9744.	.5525+02	.3445+08	.6236+06	.8823-01	.4248-02
9740.	.3875+02	.3406+08	.8791+06	.1773+00	.8537-02
9758.	.7980+02	.2132+08	.2672+06	.2617-01	.1260-02
9752.	.1888+03	.1362+08	.7215+05	.2986-02	.1438-03
9746.	.1973+03	.1051+08	.5327+05	.2110-02	.1016-03
9773.	.2049+03	.1140+08	.5563+05	.2122-02	.1022-03
9780.	.2268+03	.6346+07	.2798+05	.9640-03	.4642-04
9766.	.2277+03	.6378+07	.2801+05	.9612-03	.4628-04
9771.	.1155+03	.1940+08	.1680+06	.1137-01	.5475-03
9736.	.1594+03	.1737+08	.1089+06	.5341-02	.2571-03
9798.	.1632+03	.1629+08	.9984+05	.4782-02	.2302-03
9822.	.2169+03	.1070+08	.4933+05	.1778-02	.8559-04
9814.	.5761+02	.2798+08	.4856+06	.6588-01	.3172-02
9838.	.7821+02	.2289+08	.2927+06	.2925-01	.1408-02
9849.	.7325+02	.2326+08	.3175+06	.3387-01	.1631-02
9839.	.1295+03	.1716+08	.1325+06	.7994-02	.3849-03
9857.	.4246+02	.3120+08	.7347+06	.1352+00	.6512-02
9844.	.4312+02	.3168+08	.7347+06	.1332+00	.6412-02

Table 27. B3J: Paraffinic Mineral Oil R-620-12 + 11.5 per cent Polyalkylmethacrylate PL 4523 (MW = .2 + 07), 100°F (Continued)

L/D = 1.35

19829.	.8291+03	.8858+07	.1068+05	.1007-03	.4850-05
19806.	.4309+03	.1430+08	.3318+05	.6020-03	.2898-04
19803.	.6172+03	.8807+07	.1427+05	.1807-03	.8699-05
19860.	.5017+03	.1167+08	.2327+05	.3624-03	.1745-04
19853.	.5501+03	.1096+08	.1992+05	.2831-03	.1363-04
19829.	.5629+03	.1080+08	.1919+05	.2665-03	.1283-04
19812.	.4932+03	.1120+08	.2270+05	.3598-03	.1732-04
19816.	.3293+03	.1775+08	.5392+05	.1280-02	.6163-04
19801.	.3306+03	.1756+08	.5313+05	.1256-02	.6049-04
19805.	.3223+03	.1738+08	.5393+05	.1308-02	.6297-04
19808.	.3296+03	.1771+08	.5374+05	.1274-02	.6136-04
19803.	.2573+03	.2232+08	.8675+05	.2636-02	.1269-03
19994.	.3749+03	.9685+07	.2583+05	.5386-03	.2593-04
19969.	.3877+03	.9712+07	.2505+05	.5049-03	.2431-04
19959.	.3631+03	.9136+07	.2516+05	.5416-03	.2608-04
19814.	.2572+03	.2203+08	.8564+05	.2603-02	.1253-03
19788.	.2634+03	.2197+08	.8340+05	.2475-02	.1192-03
19799.	.2544+03	.2203+08	.8660+05	.2661-02	.1281-03
19793.	.2144+03	.2544+08	.1187+06	.4327-02	.2083-03
19786.	.2113+03	.2517+08	.1191+06	.4406-02	.2121-03
19770.	.2116+03	.2501+08	.1182+06	.4367-02	.2103-03
19777.	.2124+03	.2505+08	.1179+06	.4340-02	.2090-03
19762.	.2083+03	.2463+08	.1183+06	.4440-02	.2138-03
19776.	.1762+03	.2771+08	.1573+06	.6978-02	.3360-03
19775.	.1705+03	.2783+08	.1632+06	.7479-02	.3601-03
19780.	.1701+03	.2789+08	.1639+06	.7533-02	.3627-03

Table 27. B3J: Paraffinic Mineral Oil R-620-12 + 11.5 per cent Polyalkylmethacrylate PL 4523 (MW = .2 + 07), 100°F (Continued)

L/D = 14.9

P3	VISCP	TAUDYN	NSRATE	RE	LEOL
4811.	.9113+01	.4776+06	.5241+05	.2290+00	.9990-03
4813.	.6402+01	.1214+07	.1445+06	.6849+00	.2988-02
4571.	.9964+01	.9100+06	.9133+05	.3649+00	.1592-02
4803.	.1064+02	.4908+06	.4613+05	.1726+00	.7531-03
4790.	.1032+02	.1888+07	.1829+06	.7055+00	.3078-02
4810.	.1102+02	.2018+07	.1831+06	.6617+00	.2887-02
4798.	.1053+02	.9843+06	.9352+05	.3537+00	.1543-02
4805.	.1079+02	.7867+06	.7289+05	.2688+00	.1173-02
4817.	.8733+01	.8584+06	.9830+05	.4481+00	.1955-02
4817.	.9027+01	.5879+06	.6513+05	.2872+00	.1253-02
4821.	.7676+01	.1216+07	.1584+06	.8216+00	.3585-02
4821.	.1122+02	.9532+06	.8496+05	.3015+00	.1315-02
4805.	.6762+01	.1672+07	.2472+06	.1455+01	.6349-02
4802.	.9149+01	.5385+06	.5887+05	.2561+00	.1118-02
4806.	.6323+01	.1937+07	.3063+06	.1928+01	.8413-02
4894.	.1462+02	.2340+06	.1601+05	.4361-01	.1905-03
4910.	.1290+02	.4164+06	.3228+05	.8962-01	.4347-03
4919.	.1486+02	.5167+06	.3572+05	.9830-01	.4289-03
4927.	.1474+02	.6352+06	.5668+05	.1531+00	.6681-03
4931.	.1609+02	.8456+06	.6685+05	.1033+00	.4508-03
4926.	.1453+02	.5549+06	.3818+05	.1046+00	.4563-03
4939.	.1504+02	.8241+06	.5478+05	.1449+00	.6324-03
4950.	.1262+02	.1258+07	.9965+05	.3143+00	.1371-02
4927.	.1603+02	.1257+07	.9726+05	.2996+00	.1307-02
4930.	.1509+02	.1138+07	.7541+05	.1990+00	.8682-03
4902.	.1246+02	.8612+06	.6909+05	.2207+00	.9626-03
4904.	.1243+02	.7938+06	.6384+05	.2044+00	.8917-03
4890.	.1192+02	.9370+06	.7859+05	.2624+00	.1145-02
4905.	.1110+02	.1133+07	.1015+06	.3621+00	.1580-02
4904.	.1120+02	.1209+07	.1079+06	.3836+00	.1674-02
4922.	.1121+02	.1101+07	.9816+05	.3485+00	.1521-02
4920.	.1140+02	.1069+07	.9301+05	.3222+00	.1406-02
4930.	.1187+02	.8677+06	.7316+05	.2452+00	.1070-02
4940.	.1202+02	.1335+07	.1298+06	.5022+00	.2191-02
4929.	.1194+02	.2170+05	.1803+04	.6643-02	.2898-04
4929.	.1155+02	.2197+05	.1902+04	.6552-02	.2859-04
4925.	.1194+02	.2186+05	.1824+04	.6059-02	.2644-04
4940.	.1169+02	.5520+05	.4722+04	.1608-01	.7018-04
4939.	.1160+02	.6050+05	.5171+04	.1765-01	.7702-04
4940.	.1181+02	.5947+05	.5034+04	.1696-01	.7401-04
4937.	.1215+02	.9232+05	.7580+04	.2477-01	.1081-03

Table 27. B3J: Paraffinic Mineral Oil R-620-12 + 11.5 per cent Polyalkylmethacrylate PL 4523 (MW = .2 + 07), 100°F (Continued)

L/D = 14.9

4934.	.1197+02	.9372+05	.7830+04	.2604-01	.1136-03
4933.	.1211+02	.9539+05	.7881+04	.2592-01	.1131-03
4932.	.1262+02	.1308+06	.1037+05	.3271-01	.1427-03
4930.	.1261+02	.1311+06	.1039+05	.3282-01	.1432-03
4926.	.1298+02	.1889+06	.1455+05	.4462-01	.1947-03
4925.	.1310+02	.1947+06	.1477+05	.4460-01	.1946-03
4924.	.1313+02	.1945+06	.1481+05	.4488-01	.1958-03
4924.	.1346+02	.2349+06	.1746+05	.5164-01	.2253-03
4923.	.1341+02	.2316+06	.1727+05	.5130-01	.2238-03
4924.	.1344+02	.2337+06	.1739+05	.5153-01	.2248-03
9890.	.2524+02	.4943+05	.1959+04	.3090-02	.1348-04
9891.	.2575+02	.5286+05	.2053+04	.3174-02	.1385-04
9882.	.2471+02	.5365+05	.2171+04	.3497-02	.1526-04
9876.	.2649+02	.1372+06	.4817+04	.6731-02	.2937-04
9871.	.2664+02	.1392+06	.4862+04	.6758-02	.2949-04
9866.	.2745+02	.1395+06	.5083+04	.7372-02	.3217-04
9895.	.3033+02	.2393+06	.7899+04	.1038-01	.4528-04
9892.	.3019+02	.2426+06	.8034+04	.1059-01	.4622-04
9887.	.3027+02	.2415+06	.7978+04	.1049-01	.4577-04
9886.	.3140+02	.3463+06	.1103+05	.1399-01	.6102-04
9885.	.3071+02	.3520+06	.1146+05	.1486-01	.6483-04
9881.	.3252+02	.3426+06	.1054+05	.1291-01	.5635-04
9877.	.3221+02	.4564+06	.1417+05	.1751-01	.7642-04
9879.	.3177+02	.4599+06	.1466+05	.1830-01	.8115-04
9879.	.3232+02	.4627+06	.1432+05	.1764-01	.7695-04
9881.	.3117+02	.4713+06	.1512+05	.1931-01	.8425-04
9877.	.3350+02	.5934+06	.1767+05	.2094-01	.9136-04
9881.	.3410+02	.5874+06	.1722+05	.2011-01	.8773-04
9876.	.3325+02	.5898+06	.1774+05	.2123-01	.9264-04
9773.	.2298+02	.6023+06	.2621+05	.4540-01	.1981-03
9749.	.2100+02	.1035+07	.4929+05	.9344-01	.4077-03
9753.	.2421+02	.4487+06	.1853+05	.3047-01	.1329-03
9733.	.2048+02	.1440+07	.7032+05	.1367+00	.5963-03
9721.	.2007+02	.1548+07	.7712+05	.1530+00	.6676-03
9714.	.1871+02	.2251+07	.1203+06	.2559+00	.1116-02
9704.	.2001+02	.1341+07	.6701+05	.1334+00	.5818-03
9703.	.2048+02	.1046+07	.5108+05	.9930-01	.4333-03
9696.	.1644+02	.2640+07	.1606+06	.3890+00	.1697-02
9741.	.1855+02	.3563+06	.1921+05	.4124-01	.1799-03
9731.	.1474+02	.1298+07	.8808+05	.2380+00	.1038-02
9727.	.1688+02	.1115+07	.6606+05	.1558+00	.6796-03
9711.	.1076+02	.2483+07	.2308+06	.8539+00	.3726-02
9715.	.1061+02	.2640+07	.2489+06	.9344+00	.4077-02

Table 27. B3J: Paraffinic Mineral Oil R-620-12 + 11.5 per cent Polyalkylmethacrylate PL 4523 (MW = .2 + 07), 100°F (Continued)

L/D = 14.9

[illegible]	[illegible]	.3633+06	[illegible]	.1702-01	.7425-04
[illegible]	[illegible]	.5271+06	[illegible]	[illegible]	[illegible]
[illegible]	[illegible]	.7490+06	[illegible]	.3383-01	.1476-03
[illegible]	[illegible]	.5058+06	[illegible]	[illegible]	[illegible]
[illegible]	[illegible]	.6770+06	[illegible]	.3760-01	.1640-03
[illegible]	[illegible]	.1005+07	[illegible]	.4380-01	.1911-03
[illegible]	[illegible]	.6859+06	[illegible]	.2990-01	.1317-03
19707.	.6597+02	.3443+06	.5219+04	.3149-02	.1374-04
19683.	.6571+02	.3466+06	.5439+04	.3399-02	.1483-04
19669.	.7716+02	.3723+06	.4825+04	.2489-02	.1086-04
19666.	.7739+02	.5894+06	.7617+04	.3918-02	.1710-04
19723.	.8494+02	.6639+06	.7816+04	.3663-02	.1598-04
19722.	.8386+02	.9214+06	.1099+05	.5216-02	.2276-04
19714.	.8682+02	.9085+06	.1046+05	.4798-02	.2094-04
19717.	.8432+02	.9263+06	.1099+05	.5186-02	.2263-04
19694.	.1190+03	.5153+06	.4332+04	.1450-02	.6325-05
19679.	.1064+03	.4979+06	.4679+04	.1751-02	.7638-05
19677.	.9480+02	.7228+06	.7624+04	.3202-02	.1397-04
19669.	.9295+02	.7278+06	.7830+04	.3354-02	.1463-04
19673.	.8597+02	.9432+06	.1097+05	.5081-02	.2217-04
19657.	.7860+02	.8224+06	.1046+05	.5299-02	.2312-04
19703.	.7705+02	.8536+06	.1108+05	.5724-02	.2497-04
19699.	.8201+02	.8687+06	.1059+05	.5142-02	.2244-04
19685.	.7736+02	.1110+07	.1435+05	.7384-02	.3222-04
19678.	.7723+02	.1127+07	.1459+05	.7519-02	.3281-04
19639.	.7947+02	.1138+07	.1432+05	.7175-02	.3130-04
19569.	.7755+02	.1379+07	.1778+05	.9127-02	.3982-04
19512.	.8244+02	.1389+07	.1685+05	.8135-02	.3549-04
19464.	.8400+02	.1410+07	.1679+05	.7956-02	.3471-04
19609.	.6798+02	.2285+07	.3361+05	.1968-01	.8588-04
19572.	.7699+02	.1983+07	.2575+05	.1332-01	.5810-04
19560.	.5230+02	.2763+07	.5284+05	.4022-01	.1755-03
[illegible]	[illegible]	.3235+06	[illegible]	.6503-03	.2837-05
19954.	.1236+03	.2305+06	.1864+04	.6002-03	.2619-05
19939.	.1357+03	.2761+06	.2035+04	.5969-03	.2604-05
19930.	.1372+03	.2584+06	.1884+04	.5467-03	.2385-05
19922.	.1445+03	.6843+06	.4735+04	.1304-02	.5690-05
19930.	.1417+03	.7153+06	.5047+04	.1418-02	.6187-05
19910.	.1430+03	.7170+06	.5013+04	.1394-02	.6040-05
19911.	.1374+03	.1086+07	.7900+04	.2289-02	.9965-05
19907.	.1340+03	.1059+07	.7866+04	.2327-02	.1015-04
19902.	.1349+03	.1074+07	.7965+04	.2351-02	.1026-04

Table 27. B3J: Paraffinic Mineral Oil R-620-12 + 11.5 per cent Polyalkylmethacrylate PL 4523 (MW = .2 + 07), 100°F (Continued)

L/D = 14.9

19640.	.4559+02	.2055+07	.4508+05	.3936-01	.1717-03
19635.	.5847+02	.1537+07	.2629+05	.1790-01	.7808-04
19643.	.3920+02	.2503+07	.6384+05	.6483-01	.2829-03
19682.	.3545+02	.2702+07	.7624+05	.8563-01	.3736-03
19690.	.3398+02	.2941+07	.8657+05	.1014+00	.4426-03
19729.	.3367+02	.2992+07	.8885+05	.1050+00	.4583-03
19727.	.3251+02	.3172+07	.9758+05	.1195+00	.5214-03
19742.	.2749+02	.3418+07	.1243+06	.1801+00	.7856-03

Table 27. B3J: Paraffinic Mineral Oil R-620-12 + 11.5 per cent Polyalkylmethacrylate PL 4523 (MW = .2 + 07), 100°F (Continued)

L/D = 297

P3	VISCP	TAUDYN	NSRATE	RE	LEOL
4785.	.1087+02	.1069+05	.9838+03	.5952-02	.1303-05
4780.	.1113+02	.1068+05	.9598+03	.5668-02	.1241-05
4787.	.1060+02	.1053+05	.9935+03	.6161-02	.1349-05
4786.	.1028+02	.2295+05	.2233+04	.1428-01	.3128-05
4788.	.9892+01	.2212+05	.2236+04	.1486-01	.3255-05
4798.	.9777+01	.2288+05	.2341+04	.1574-01	.3447-05
4797.	.9806+01	.3508+05	.3578+04	.2399-01	.5253-05
4790.	.9947+01	.3607+05	.3627+04	.2397-01	.5249-05
4783.	.9867+01	.3570+05	.3618+04	.2410-01	.5279-05
4796.	.9200+01	.4481+05	.4870+04	.3480-01	.7622-05
4801.	.9939+01	.4961+05	.4991+04	.3301-01	.7230-05
4797.	.9822+01	.4991+05	.5082+04	.3401-01	.7449-05
4785.	.9911+01	.6615+05	.6674+04	.4427-01	.9695-05
4778.	.9551+01	.6402+05	.6702+04	.4613-01	.1010-04
4801.	.9664+01	.6632+05	.6863+04	.4668-01	.1022-04
4810.	.9597+01	.7515+05	.7831+04	.5364-01	.1175-04
4798.	.9270+01	.7442+05	.8029+04	.5694-01	.1247-04
4810.	.9684+01	.7647+05	.7897+04	.5361-01	.1174-04
4801.	.7743+01	.1396+06	.1803+05	.1531+00	.3353-04
4817.	.7730+01	.1578+06	.2042+05	.1736+00	.3803-04
4812.	.6808+01	.1640+06	.2409+05	.2327+00	.5095-04
4808.	.8242+01	.1676+06	.2033+05	.1622+00	.3551-04
4771.	.9404+01	.1463+06	.1555+05	.1087+00	.2381-04
4749.	.1045+02	.1241+06	.1187+05	.7468-01	.1635-04
4723.	.1173+02	.1150+06	.9804+04	.5495-01	.1203-04
4745.	.9463+01	.1358+06	.1435+05	.9970-01	.2183-04
9759.	.2164+02	.2041+05	.9432+03	.2866-02	.6276-06
9728.	.2355+02	.2302+05	.9776+03	.2729-02	.5976-06
9712.	.2479+02	.2454+05	.9898+03	.2624-02	.5747-06
9689.	.2494+02	.5557+05	.2228+04	.5875-02	.1287-05
9734.	.2846+02	.6735+05	.2366+04	.5465-02	.1197-05
9728.	.2903+02	.6792+05	.2339+04	.5297-02	.1160-05
9733.	.2903+02	.6729+05	.2318+04	.5248-02	.1149-05
9704.	.2862+02	.1038+06	.3603+04	.8219-02	.1800-05
9696.	.2443+02	.9017+05	.3691+04	.9934-02	.2176-05
9701.	.2454+02	.8833+05	.3599+04	.9640-02	.2111-05
9712.	.2429+02	.1196+06	.4925+04	.1333-01	.2919-05
9687.	.2364+02	.1196+06	.5059+04	.1407-01	.3081-05
9689.	.2270+02	.1512+06	.6659+04	.1928-01	.4223-05
9689.	.2274+02	.1465+06	.6441+04	.1862-01	.4077-05
9691.	.2280+02	.1481+06	.6495+04	.1873-01	.4102-05

Table 27. B3J: Paraffinic Mineral Oil R-620-12 + 11.5 per cent Polyalkylmethacrylate PL 4523 (MW = .2 + 07), 100°F (Continued)

L/D = 297

19744.	.8536+02	.6904+05	.8087+03	.6228-03	.1364-06
19725.	.8592+02	.7542+05	.8778+03	.6716-03	.1471-06
19700.	.9075+02	.7843+05	.8642+03	.6261-03	.1371-06
19667.	.8859+02	.7438+05	.8396+03	.6231-03	.1365-06
19658.	.6857+02	.1478+06	.2155+04	.2066-02	.4525-06
19659.	.7478+02	.1589+06	.2125+04	.1868-02	.4091-06
19633.	.7405+02	.1656+06	.2239+04	.1987-02	.4352-06
19643.	.7561+02	.1656+06	.2190+04	.1904-02	.4171-06

Table 28. B3J: Paraffinic Mineral Oil R-620-12 + 11.5 per cent Polyalkylmethacrylate PL 4523 (MW = .2 + 07), Plot, L/D = 297

FL [illegible] F

P	VISCP	VSR TE	KEC	DELTAP	TAUDYN	REYN
4745.	.3920+02	.8361+03	.8332-04	.5652+03	.3282+05	.1400-02
4753.	.4117+02	.8979+03	.9610-04	.5866+03	.3697+05	.1434-02
4741.	.3809+02	.8963+03	.9575-04	.6002+03	.3486+05	.1515-02
4764.	.3954+02	.2120+04	.5354-03	.1443+04	.8381+05	.3524-02
4757.	.4177+02	.2171+04	.5618-03	.1561+04	.9068+05	.3417-02
4764.	.4150+02	.2238+04	.5970-03	.1561+04	.9064+05	.3633-02
9759.	.[illegible]+02	.9358+03	.1043-03	.1585+04	.9206+05	.6250-03
9739.	.11[illegible]+03	.7623+03	.6929-04	.1453+04	.8439+05	.4529-03
9646.	.1113+03	.7313+03	.6374-04	.1401+04	.8138+05	.4320-03
9540.	.1101+03	.7141+03	.6077-04	.1426+04	.8284+05	.4046-03
9751.	.1041+03	.6829+03	.7681-04	.1042+04	.8376+05	.5059-03
9833.	.1006+03	.6815+03	.7657-04	.1471+04	.8543+05	.4944-03

FL 83J 100 F

P	VISCP	VSR TE	KEC	DELTAP	TAUDYN	REYN
4788.	.9973+01	.2270+04	.6164-03	.3878+03	.2252+05	.1510-01
4781.	.1[illegible]+02	.2250+04	.6075-03	.3918+03	.2276+05	.1472-01
4767.	.1[illegible]+02	.2185+04	.5665-03	.3826+03	.2219+05	.1408-01
9726.	.2234+02	.2191+04	.5719-03	.8426+03	.4893+05	.6446-02
9712.	.[illegible]+02	.2[illegible]+04	.6280-03	.8642+03	.5019+05	.6902-02
9713.	.2290+02	.2202+04	.5777-03	.8609+03	.5052+05	.6307-02
19613.	.1[illegible]+03	.6[illegible]+03	.5527-04	.1176+04	.6829+05	.4465-03
19791.	.9530+02	.7200+03	.6193-04	.1154+04	.6874+05	.4970-03
19783.	.8644+02	.6486+03	.8577-04	.1263+04	.7333+05	.6452-03

Averaged Data Points

FL 83J 75 F

P (PSI)	V (CP)
.00000	.10000+04
.47541+04	.4[illegible]184+04
.96455+04	.1[illegible]954+05

FL 83J 100 F

P (PSI)	V (CP)
.00000	.42000+03
.47652+04	.1[illegible]953+04
.97187+04	.2[illegible]2384+04
.19797+05	.94024+04

Table 28. B3J: Paraffinic Mineral Oil R-620-12 + 11.5 per cent Polyalkylmethacrylate PL 4523 (MW = .2 + 07), Plot, L/D = 297 (Continued)

FL B3J 150 F

P3	VISCP	NSRATE	KEC	DELTAP	TAUDYN	REYN
4740.	.3019+01	.4890+04	.2850-02	.2542+03	.1476+05	.1065+00
4734.	.2875+01	.5151+04	.3162-02	.2550+03	.1481+05	.1178+00
9711.	.5111+01	.3557+04	.1508-02	.3130+03	.1818+05	.4575-01
9689.	.5152+01	.3561+04	.1511-02	.3159+03	.1835+05	.4544-01
9695.	.5124+01	.3575+04	.1524-02	.3154+03	.1832+05	.4587-01
19750.	.1324+02	.2209+04	.5815-03	.5034+03	.2924+05	.1097-01
19738.	.1313+02	.2280+04	.6194-03	.5154+03	.2993+05	.1142-01
19719.	.1283+02	.2234+04	.5948-03	.4936+03	.2867+05	.1144-01
29865.	.3377+02	.9420+03	.1056-03	.5478+03	.3182+05	.1834-02
29837.	.3593+02	.8493+03	.8597-04	.5254+03	.3051+05	.1554-02
29813.	.3645+02	.8483+03	.8577-04	.5325+03	.3093+05	.1530-02

FL B3J 190 F

P3	VISCP	NSRATE	KEC	DELTAP	TAUDYN	REYN
4776.	.1713+01	.6660+04	.5286-02	.1964+03	.1141+05	.2557+00
4779.	.1756+01	.6526+04	.5076-02	.1973+03	.1146+05	.2443+00
4779.	.1712+01	.6563+04	.5134-02	.1934+03	.1123+05	.2521+00
4779.	.1683+01	.6764+04	.5452-02	.1960+03	.1138+05	.2642+00
4788.	.1701+01	.6800+04	.5510-02	.1991+03	.1156+05	.2628+00
9761.	.2716+01	.5000+04	.2979-02	.2338+03	.1358+05	.1210+00
9748.	.2736+01	.5076+04	.3070-02	.2391+03	.1389+05	.1220+00
9749.	.2709+01	.5198+04	.3220-02	.2424+03	.1408+05	.1261+00
19779.	.5833+01	.3456+04	.1424-02	.3471+03	.2016+05	.3896-01
19775.	.5750+01	.3666+04	.1602-02	.3630+03	.2108+05	.4192-01
19763.	.5875+01	.3387+04	.1367-02	.3426+03	.1990+05	.3790-01
29789.	.1370+02	.1500+04	.2681-03	.3553+03	.2064+05	.7165-02
29778.	.1361+02	.1485+04	.2627-03	.3531+03	.2051+05	.7065-02
29767.	.1375+02	.1486+04	.2633-03	.3518+03	.2043+05	.7108-02
39695.	.2860+02	.8636+03	.8890-04	.4253+03	.2470+05	.1985-02
39641.	.3152+02	.7155+03	.6102-04	.3884+03	.2256+05	.1492-02
39597.	.2794+02	.8106+03	.7830-04	.3899+03	.2265+05	.1907-02
39566.	.2790+02	.8032+03	.7689-04	.3859+03	.2241+05	.1892-02

Averaged Data Points

FL B3J 150 F

P (PSI)	V (CP)
.00000	.15500+03
.47369+04	.29473+03
.96952+04	.51290+03
.19735+05	.13066+04
.29838+05	.35385+04

FL B3J 190 F

P (PSI)	V (CP)
.00000	.10000+03
.47804+04	.17128+03
.97525+04	.27204+03
.19772+05	.58191+03
.29778+05	.13774+04
.39625+05	.28990+04

APPENDIX D

CONVERSION FACTORS

Heat conductivity

1 Btu/h ft°F = .216 lbf/°F sec

1 lbf/°F sec = 4.62 Btu/h ft°F = .08 Watt/°C cm = 8.00 N/°C sec

1 Watt/°C cm = 57.79 Btu/h°F ft = 12.5 lbf/°F sec

Specific heat per unit mass

1 Btu/lbm°F = 1 cal/gramm °C = 9336 lbf in/lbm °F

Density

1 lbm/ft^3 = .5787 x 10^{-3} lbm/in^3 = .016018 gramm/cm^3

1 gramm/cm^3 = .3613 x 10^{-2} lbm/in^3 = 62.43 lbm/ft^3

Specific heat per unit volume

1 lbf/in^2°F = 2.964 x 10^{-3} cal/cm^3°C = 1.241 N/cm^2 °C

1 cal/cm^2°C = 3.374 x 10^2 lbf/in^2°F = 418.68 N/cm^2°C

Heat diffusivity

1 in^2/sec = 6.45 cm^2/sec

1 cm^2/sec = .155 in^2/sec

Force

1 kp = 2.2046 lbf = 980665 dyn = 1000 gramf $\tilde{=}$ 9.8 Newton

1 N = .22481 lbf = 10^5 dyn $\tilde{=}$ .102 kp

1 lbf = .4535924 kp = 4.44822 Newton = 444822 dyn

1 dyn = 1.0197 x 10^{-3} gramf = 2.2481 x 10^{-6} lbf

Mass

1 kgm = 2.20462 lbm

1 lbm = .4535924 kgm

Length

1 in = 2.54 cm = .833 ft = 25400 my (micron) = $2.54 \cdot 10^8$ Å

1 m = 39.3701 in = 10^6 my (micron) = 10^{10} Å

1 µin = 254 Å = .0254 my (micron)

1 my(micron) = 10000Å = 39.37 µinch

1 Å = 10^{-4} my(micron) = 3.937×10^{-3} µinch

Pressure (stress)

1 dyn/cm^2 = 1.4504×10^{-5} psi = 1.0197×10^{-3} gramm/cm^2

1 psi = 68948 dyn/cm^2

1 kp/cm^2 ≃ 14.22 psi

Temperature

-459.67 °F = 0°R (Rankine)

-273.15°C = 0°K (Kelvin)

Viscosity:

1 Poise(P) = 1 dyn sec/cm^2 = 100 cp = $.14504 \cdot 10^{-4}$ Reyn (psi x sec)

1 Reyn (lbf sec/in^2) = $6.8948 \cdot 10^6$ cp = $6.8948 \cdot 10^4$ P

1 µ Reyn ≃ 6.895 cp

1 kp sec/m^2 = 98.0665 P = 9806.65 cp ≃ $.1422 \times 10^{-2}$ Reyn

1 stoke(St) = 100 cs

APPENDIX E

PROGRAM TO CALCULATE ESTIMATED TEMPERATURES AND APPROXIMATED FLOW CURVES

```
CH. 13
      DIMENSION A(10,11),RH(10),IR(10),JC(10),X(10),PPV(11),PPPV(11),
     1 [illegible](10),[illegible](10),TRR(10),CER(10),IRDPH(11),AA(11),RR(11),
     2 [illegible](11),[illegible](11),PDV(11),PV(11),AV(11),PAV(11),SV(11),PSV(11)
      REAL R1,R2
      READ(5,500)R1,R2,8
      N=8
      DO 5 I=1,N
      RH(1)=.95
      RH(2)=.9
      RH(3)=.85
      RH(4)=.8
      RH(5)=.75
      RH(6)=.6
      RH(7)=.4
      RH(8)=.2
C     READ(5,500)RH(I)
C     WRITE(6,500)RH(I)
      NN=N+1
      DO 6 J=1,NN
      RH2=RH(I)**2.
      RH22=1-RH2
      A(I,J)=R1*RH22*(1-RH2**(J))+((J)*2.)**2.*(RH2)**((J)-1)
      IF((J).GT.N)A(I,J)=R2*RH2
    6 CONTINUE
    5 CONTINUE
  500 FORMAT()
      DO 17 I=1,N
C     PRINT 500,(A(I,J),J=1,NN)
   17 CONTINUE
      CALL ESTMED(A,10,IR,JC,N,1.0E-10,X,IERR1)
      IF(IERR1.EQ.-1)WRITE(6,501)
  501 FORMAT(1H ,'IERR1=-1')
      IF(IERR1.EQ.-1)GO TO 90
C     WRITE(6,500)(X(I),I=1,N)
      DO 19 I=1,N
      T(I)=X(1)*(1-(RH(I)**2.))+X(2)*(1-(RH(I)**4.))+
     1 X(3)*(1-(RH(I)**6.))+X(4)*(1-(RH(I)**8.))+
     2 X(5)*(1-(RH(I)**10.))+X(6)*(1-(RH(I)**12.))+
     3 X(7)*(1-(RH(I)**14.))+X(8)*(1-(RH(I)**16.))
      TR(I)=-(2.*X(1)*RH(I)+4.*X(2)*(RH(I)**3.)+
     1 6.*X(3)*(RH(I)**5.)+8.*X(4)*(RH(I)**7.)+
     2 10.*X(5)*(RH(I)**9.)+12.*X(6)*(RH(I)**11.)+
     3 14.*X(7)*(RH(I)**13.)+16.*X(8)*(RH(I)**15.))
```

```
      TRR(I)=-(2.*X(1)+12.*((2)*(RH(I)**2.)+
     1 30.*X(3)*(RH(I)**6.)+56.*X(4)*(RH(I)**8.)+
     2 90.*X(5)*(RH(I)**10.)+132.*X(6)*(RH(I)**12.)+
     3 182.*X(7)*(RH(I)**12.)+240.*X(8)*(RH(I)**14.))
      CER(I)=R1*(1-(RH(I)**2.))*T(I)-TRR(I)-TR(I)/RH(I)-
     1 R2*(RH(I)**2.)
      RH(0)=1.
      PV(0)=0.
      V(0)=0.
      PPV(0)=0.
      PV(0)=0.
      T(0)=0.
      SV(0)=0.
      PSV(0)=0.
      DV(I)=(RH(I-1)**2.-RH(I)**2.)/2.
      V(I)=DV(I)+V(I-1)
      WRITE(6,500)V(I)
      PPV(I)=EXP((3*T(I-1)))
      PPPV(I)=EXP((3*T(I)))
      DPV(I)=(PPV(I-1)*PPPV(I)+RH(I)*PPPV(I))*.5*(RH(I-1)-RH(I))
      PV(I)=PV(I-1)+DPV(I)
      WRITE(6,500)T(I-1),T(I),PV(I),PPV(I),PPPV(I)
      AV(I)=(V(I)*RH(I)+V(I-1)*RH(I-1))*(RH(I-1)-RH(I))*3.14
      APV(I)=(PV(I)*RH(I)+PV(I-1)*RH(I-1))*(RH(I-1)-RH(I))*3.14
      SV(I)=AV(I)+SV(I-1)
      PSV(I)=PAV(I)+PSV(I-1)
      RR(I)=R1*T(I)*(1-RH(I)**2.)
      TRDRH(I)=TR(I)/RH(I)
      RR(I)=R2*(RH(I)**2.)
      WRITE(6,500)T(I),CER(I),AA(I),TRR(I),TRDRH(I),RR(I)
      WRITE(6,500)V(I),PV(I),AV(I),PAV(I),SV(I),PSV(I)
   10 CONTINUE
      TV=V(N)+(RH(N)**2.)*.5
      PTV=PV(N)+(RH(N)**2.)*.5*(EXP(B*T(N)))
      TSV=SV(N)+(RH(N)**2.)*V(N)*3.14
      PTSV=PSV(N)+PV(N)*(RH(N)**2.)*3.14
      SX=X(1)+X(2)+X(3)+X(4)+X(5)+X(6)+X(7)+X(8)
      WRITE(6,500)SX,TV,PTV,TSV,PTSV
      STOP
      END
```

APPENDIX F

AUXILIARY DIAGRAMS FOR CHAPTER IV

Figures 46, 47, and 48 are prepared in order to facilitate the determination of π_3 and E. Figure 46 shows the slope parameter π_3 as function of η_{100} and η_{210}. Entrance to the figure is the two viscosities measured at constant pressure, at temperatures 100°F and 210°F, and applied in units of centipoise.

An ASTM chart may be used to determine these viscosities η_{100} and η_{210} if existing data are collected at other temperatures. This data should however have been collected at the same pressure. The characteristics of Figure 46 are calculated with

$$(\ln \eta_{100})/\ln \eta_{210}) = (559.67/669.67)^{-\pi_3} \qquad \text{(F-1)}$$

which gives straight lines in a log-log (or linear) representation for constant π_3. Intermediate values might easily be calculated from equation (F-1) for greater accuracy than obtainable from the graph of Figure 46. The expression (F-1) is derived from equation (22) Chapter IV. The numbers 559.67 and 669.67 are, in °Rankine, the standard temperatures 100°F and 210°F used often in viscometric measurement.

Figure 47 and 48 show the temperature E, in °Rankine, as function of η_{100} and π_3. Figure 47 gives relatively high resolution for lubricants with π_3 in the range 1 to 2, particularly siloxanes. Figure 48 gives relatively high resolution for lubricants with π_3 in the range

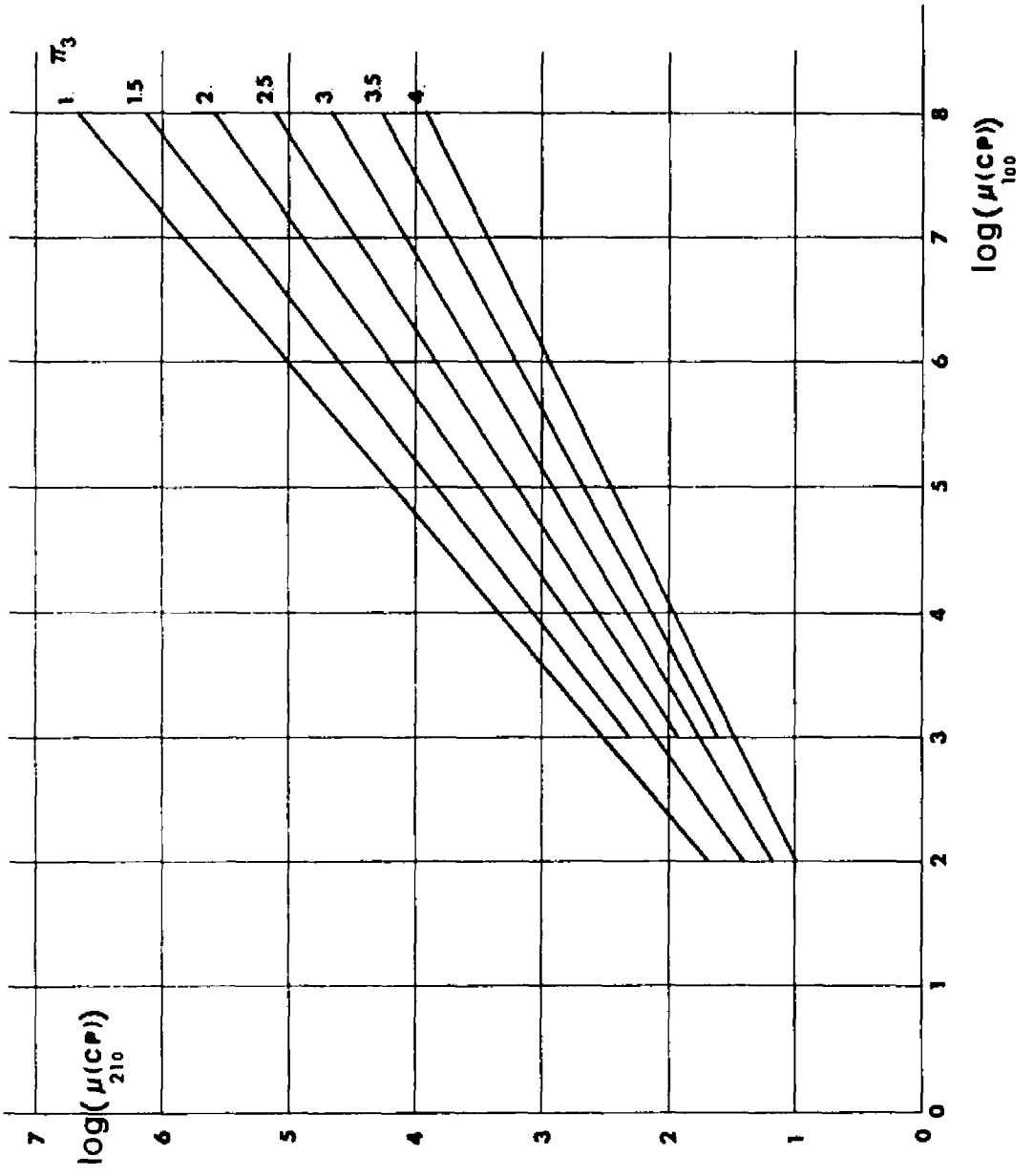

Figure 46. The Temperature Viscosity Coefficient π_3.

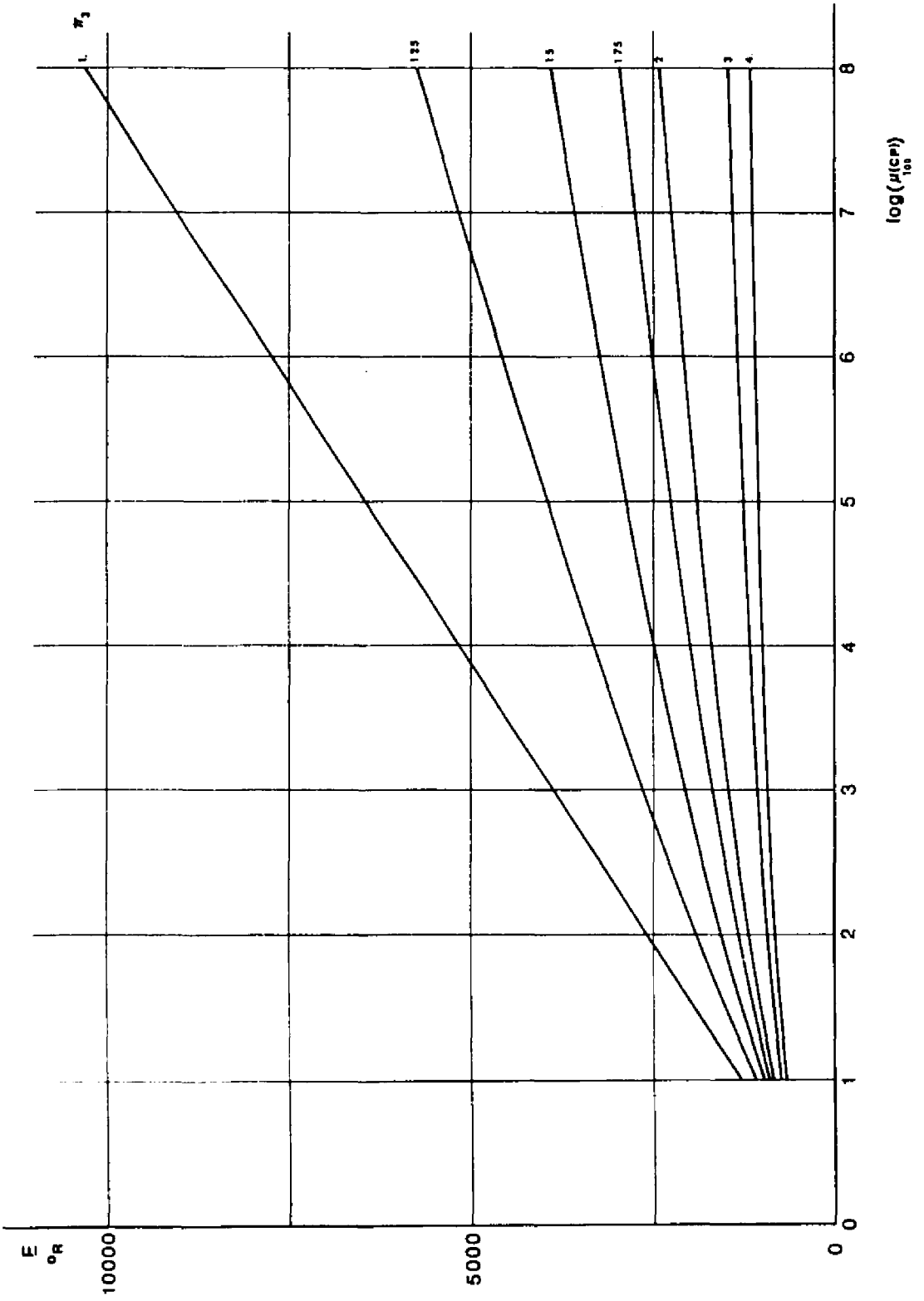

Figure 47. The Temperature E (°R).

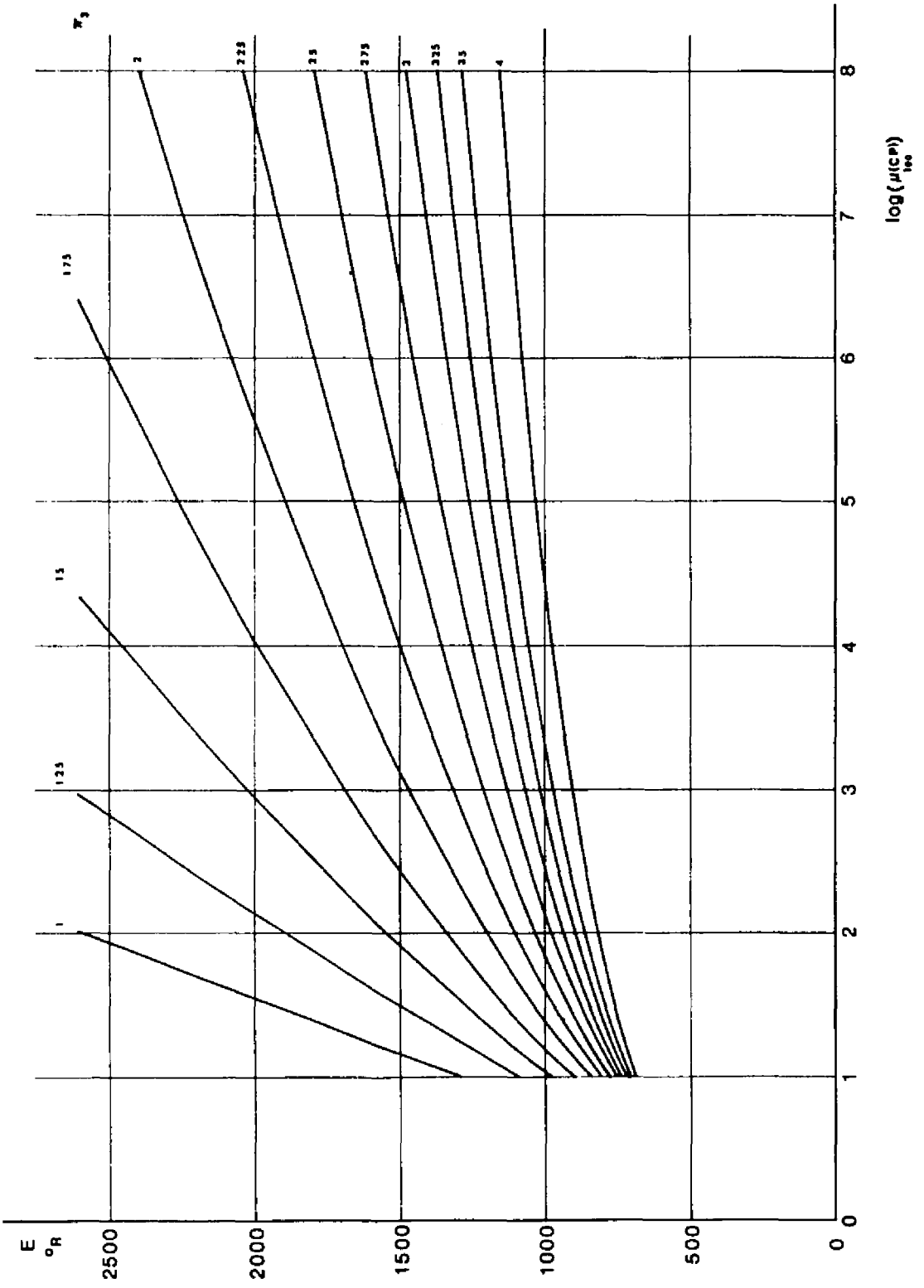

Figure 48. The Temperature E (^{o}R).

2 to 4, mineral oils and many synthetic lubricants.

The calculated values of E plotted in Figures 47 and 48 are found also in Table 29.

Table 29. The Temperature E as Function of the Viscosity at 100°F (cp) and π_3.

log η	8	7	6	5	4	3	2
π_3							
1.0	10310	9021	7732	6443	5155	3866	2577
1.125	7458	6624	5776	4911	4028	3119	2175
1.25	5757	5174	4573	3953	3306	2627	1899
1.5	3904	3571	3222	2854	2459	2030	1549
1.75	2958	2741	2509	2261	1999	1689	1340
2.0	2402	2247	2080	1899	1699	1471	1201
2.25	2043	1925	1798	1658	1501	1321	1103
2.5	1795	1702	1600	1487	1360	1213	1031
2.75	1615	1538	1454	1361	1255	1130	975
3.0	1478	1413	1343	1264	1173	1066	931
3.25	1372	1317	1256	1187	1108	1014	895
3.5	1287	1239	1185	1125	1056	972	866
4.0	1160	1121	1079	1031	975	907	820

APPENDIX G

EXAMPLE OF FILM CALCULATION OF AN ELASTOHYDRODYNAMIC POINT CONTACT IN PURE SLIDING

Estimate of the Temperature of the Moving Colder Surface

The surfaces are subject to the actual film shear stress in the contact area. The sliding generates a heating of the moving surface during the passage of the contact region. A part of the generated heat is transported out of the contact by convection due to the increased temperatures of the moving surface. The stationary surface will rapidly reach a relatively high temperature because of low ability to conduct heat away from the contact. The stationary surface operates therefore under conditions which are nearly adiabatic and the temperatures of the surface are near the maximum attainable film temperatures.

The shear stress increases from zero at the inlet to a maximum level and decreases then again to zero at the outlet. The quantities that characterizes the lubrication, maximum film temperature and shear stress, are not very sensitive to variations in the temperatures of the cold moving surface. Application of the average shear stress instead of the actual local shear stress can therefore be justified as a starting point for the film calculation.

The temperature distribution for a moving circular source seems not to have been treated in sufficient detail so far in the literature

but can be approximated with the solution for the square source with ℓ = a, a = radius of the contact area, along the centerline. The calculated values for the square source will expectedly be slightly higher than the actual temperatures along the centerline for a circular contact. The error introduced by assuming a square source instead of a circular source is expectedly not significant when the weak dependency of the shear stress and maximum temperature of the film is considered. A more detailed, and lengthy, analysis will advantageously take these effects into account achieving greater accuracy.

The literature shows several methods of solution of the temperature distribution of a moving plane rectangular heat source with constant heat flux per unit area, Blok 1937 (70), Jaeger 1942 (71) and Carslaw and Jaeger, 1962 (72). The temperature distribution for an infinitely wide band source is a particularly simplified situation of a rectangular heat source. A comparison, Jaeger 1942 (71), is made of the temperature distributions at the centerline of square sources with infinitely wide band sources. The comparison is carried out in terms of dimensionless temperatures ($\pi k_t (UN)\Delta T/2\kappa q_o$), lengths ($x_1/\ell$) and velocities ($V = (UN)\ell/4\kappa$), where (UN) is the moving velocity, ℓ is the half side length of the square or the half of the width of the band and κ is the thermal diffusivity of the moving surface. It is shown that the temperatures for the square source and for the band source are of equal magnitude when $V \geq 1$.

The insensitivity of the calculated surface temperature to the ratio length/width of the contact configuration implied by high values

of the speed parameter V shows that the temperature profile of the sliding area is determined primarily by heat conduction perpendicular to the surface when $V > 1$. Heat conduction in the two other main directions have then only a small influence on the temperature profile. The heating of the moving surface can therefore be approximated with a one directional constant heat flux perpendicular to the plane of the surface when $V > 1$. The temperature at a location can be determined by the expression

$$\Delta T = 2q_1 ((\kappa t_r)/\pi)^{1/2} \qquad (A\text{-}1)$$

Jakob (73) where $q_1 = \tau \times (UN)/k_{t_{ball}}$ and τ is the average shear stress. t_r is the time of exposure to the heat flux at the location under investigation. ΔT is the temperature increase over the temperature of the environment.

Film Calculation with Fluid D as Lubricant

Operating Parameters

Lubricant: Synthetic Paraffinic Oil, fluid D (40). This fluid is similar in composition to the investigated fluid XRM 177 F4, however, from another lot.

Stationary Bearing Surface: Sapphire, flat surface. Coefficient of heat conduction k_t: 3.14 lbf/°F sec.

Thermal diffusivity $123. \times 10^{-4}$ in^2/sec

Moving Bearing Surface: Steel 52100, radius .625 inch.

Coefficient of heat conduction k_t: 4.34 lbf/°F sec.

Thermal diffusivity : 149 x 10^{-4} in^2/sec

Sliding velocity (UN): 54.8 inch/sec

Load: W = 15 lbf Hertzian contact radius 6.98 x 10^{-3} inch and maximum Hertzian pressure of 148 kpsi. In the example these numbers are rounded to 7 x 10^{-3} in and 150 kpsi. Hertzian pressure distribution is assumed.

Film thickness h. Centerline film thickness: 30 μ inch. Minimum film thickness: 19 μ inch. Both quantities are measured (39).

Traction Coefficient TC: 3.5% A traction force of .525 lbf and an average shear stress of about 3400 psi. The traction coefficient is measured (39).

Calculation of the temperature of the moving surface

The temperatures for the moving surface with fluid D, synthetic paraffinic oil, as the lubricant, is calculated along the centerline for intervals of 10^{-3} inch. The calculations are performed with equation (A-1) and environment temperature assumed 90°F, ~32°C. A preliminary estimate of the shear stress in the film has shown that the average stress in the high pressure area of the contact was smaller than the measured average shear stress for the total contact. Preliminary estimated values were in the range 1800 - 2600 psi. A value of 2400 psi was selected for the calculation of the temperatures of the moving surface to demonstrate the further steps in the film calculation. Table 30 gives the calculated surface temperatures and also the Hertzian pressures for the intervals of 10^{-3} inch.

Table 30. Hertzian Pressures and Temperatures of the Moving Surface

Fluid D (UN) = 54.8 ips W = 15 lbf $\tau_{average}$ = 2400 psi $k_{t_{ball}}$ = 4.34 lbf/°R sec

Position	Hertzian Pressure kpsi	Temperature of Moving Surface °F	°C	
0	0	90	32	Inlet
1	75	108	42	
2	104	115	46	
3	122	121	49	
4	134	126	52	
5	142	130	54	
6	147	134	57	
7	150	137	58	Center
8	147	141	60	
9	142	144	62	
10	134	147	64	
11	122	150	66	
12	104	152	67	
13	75	155	68	
14	0	157	70	Outlet

The distance between each position is 10^{-3} in.

Determination of Maximum Temperature and Shear Stress Through Dimensionless Charts

The maximum pressure in the contact 150 kpsi, at r = 0, is selected to demonstrate the method. For the lubricant, fluid D, the viscosities are $\eta_{100} = 6.6 \times 10^7$ cp and η_{210} 1.6×10^5 cp. These values can be either measured directly or extrapolated from pressure viscosity diagrams.

The maximum temperature

1. η_{100} and η_{210} determine $\pi_3 = 2.26$ (Figure 49).
2. η_{100} and π_3 determine E = 2000°R (Figure 50).
3. π_2 is then (459.67 + 137)/2000 = .304 (Table 30).
4. Calculation of π_4 yields $\pi_4 = 6.4 \times 10^{-6}$ in that
   $c_1 = 1/6.895 \times 10^6$ Reyn $(\pi_4 = c_1(UN)^2/2k_tE)$.
5. $I_2 = 6.4 \times 10^{-9}$ (Figure 51).
6. $I_2 + \pi_4 \cong 6.4 \times 10^{-6}$.
7. A line parallel with the π_1 and π_2 axis intersects the curve $\pi_3 = 2.26$ at $\pi_1 = .4$. The maximum temperature at the adiabatic wall is thus .4 x E = 800°R or <u>340°F</u>.

The shear stress

1. Interpolation should be carried out between $\pi_3 = 2$ and $\pi_3 = 2.5$
2. When $\pi_3 = 2$ then E = 2370°R (Figure 50, $\eta = 6.6 \times 10^7$)
   $\pi_2 = 597/2370 = .252$ and
   $\pi_1 = 800/2370 = .338$

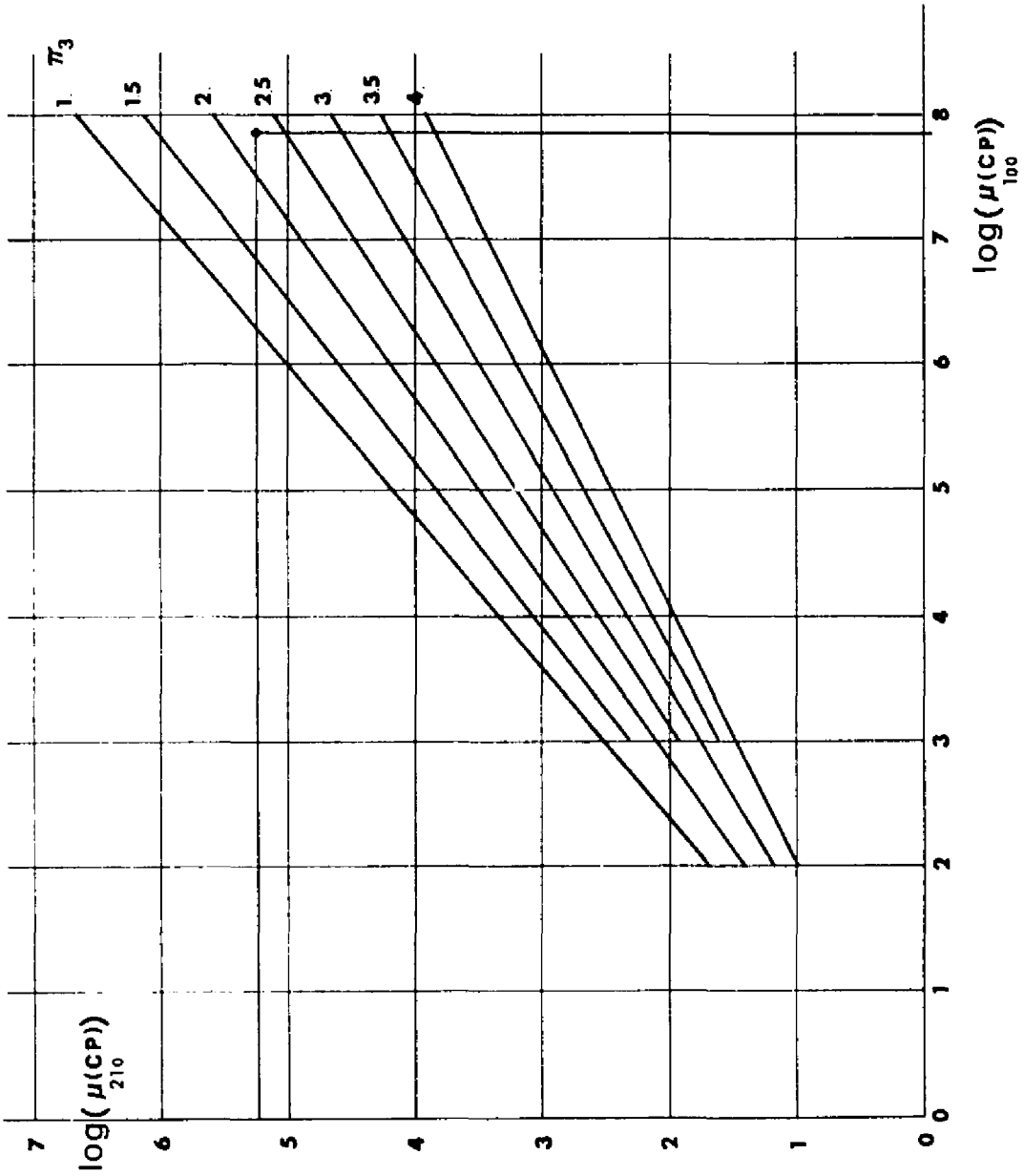

Figure 49. Determination of π_3.

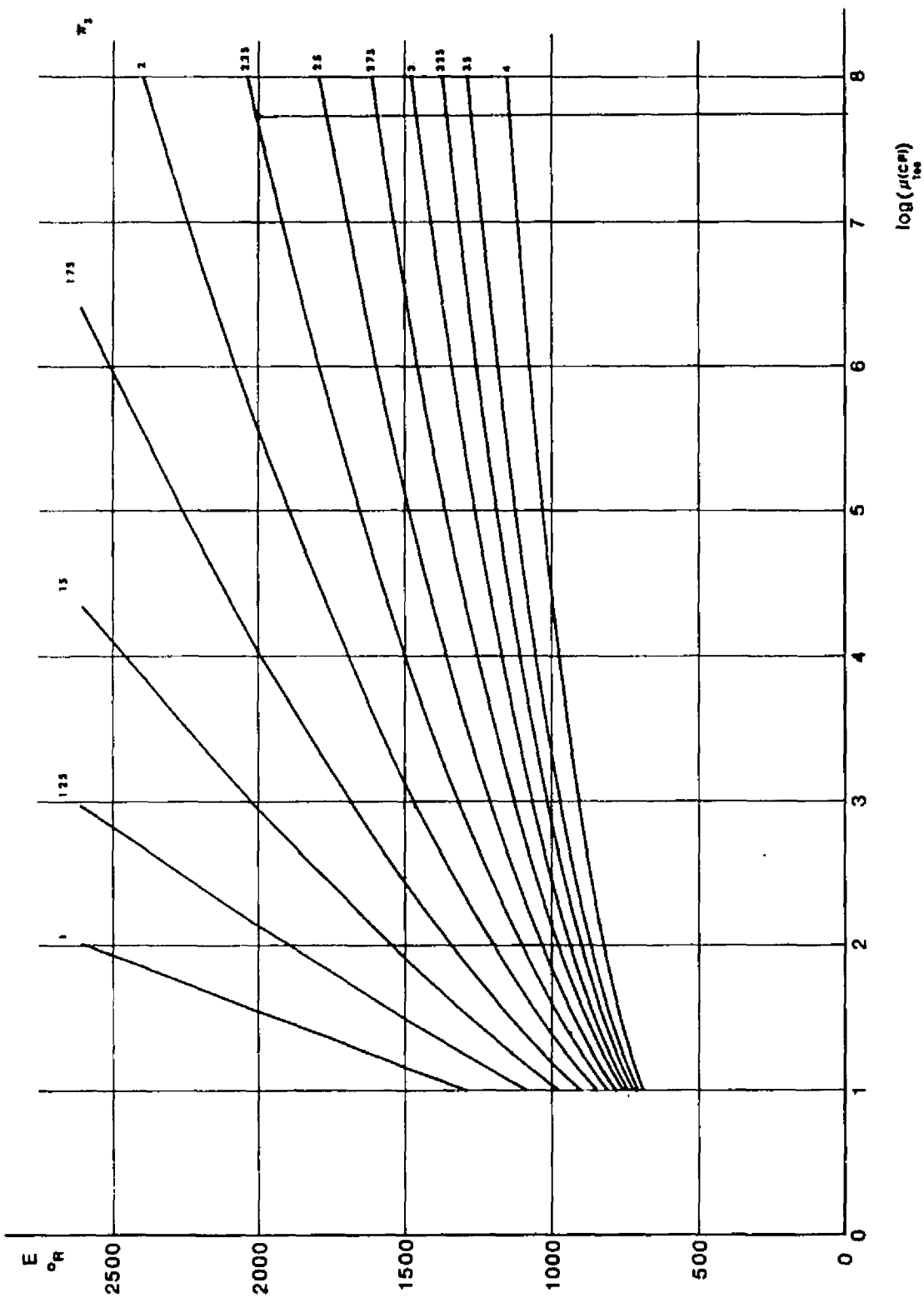

Figure 50. Determination of E (°R).

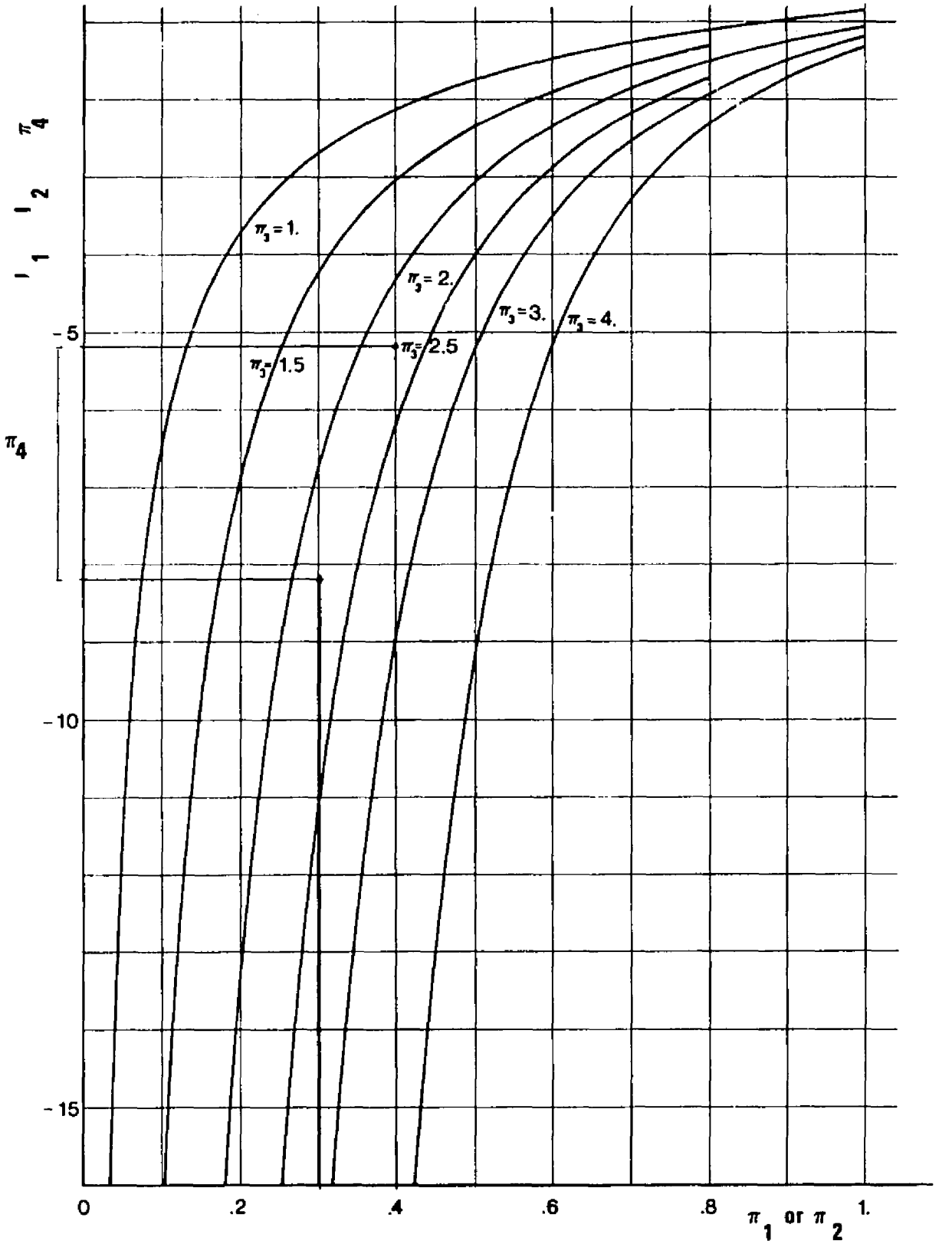

Figure 51. Determination of π_1.

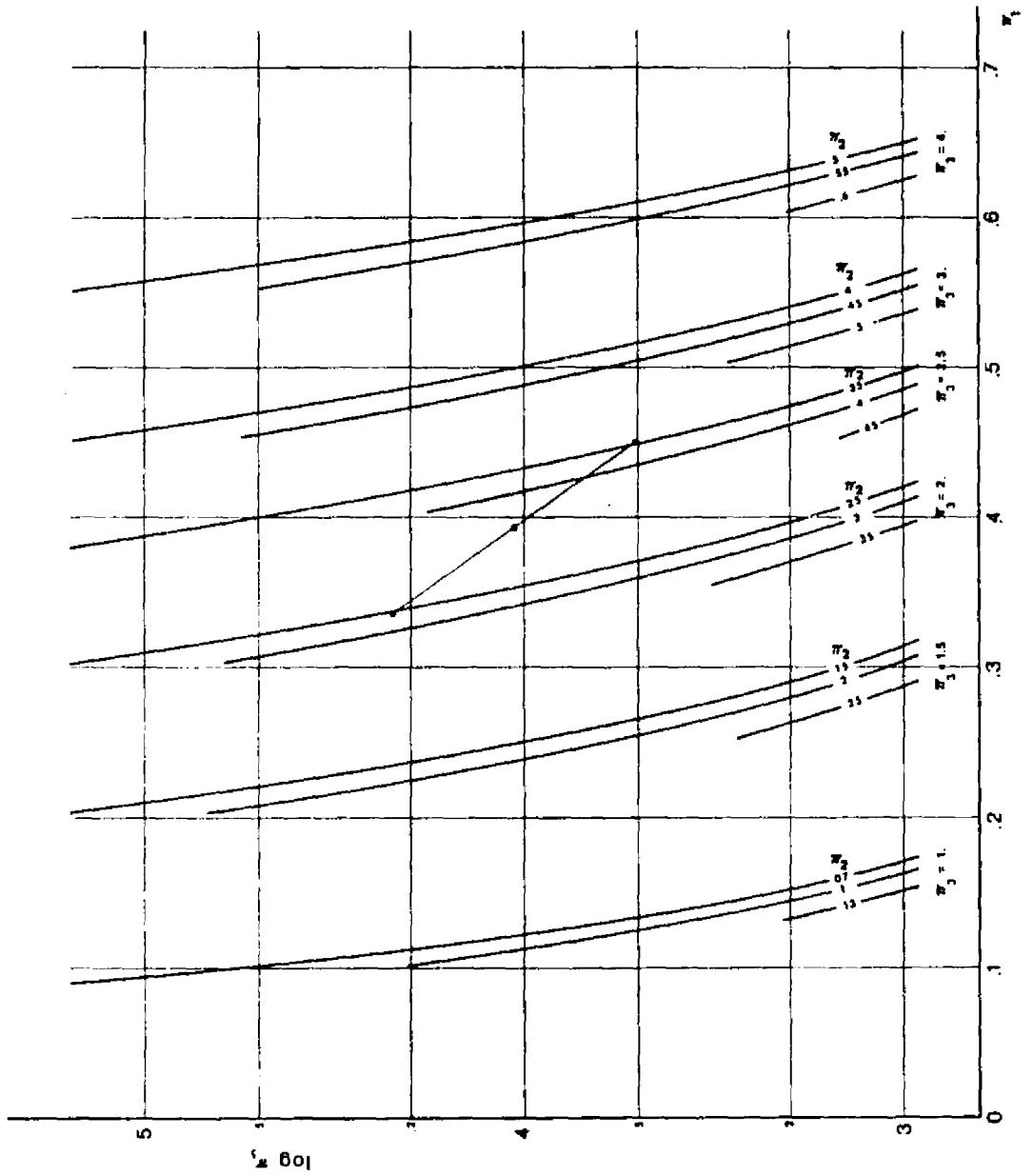

Figure 52. Determination of π_5.

3. When $\pi_3 = 2.5$ then E = 1778°R

   $\pi_2 = 597/1778 = .336$ and

   $\pi_1 = 800/1778 = .450$

4. Linear interpolation on Figure 52 yields direct

   $\pi_5 = 1.09 \times 10^4$. The shear stress is then

   2790 psi at the center of the contact.

Film Behavior in the Non-adiabatic Wall Case

The dimensionless charts give a direct access to estimates of the maximum film temperature and the shear stress in the case of adiabatic conditions at the stationary wall. The use of the charts can be extended to the non-adiabatic cases as discussed in Chapter IV by observing the symmetric film situation about the adiabatic plane, whether this is located inside or outside the actual film, see also Table 11 of Chapter IV.

In a different approach a program has been developed which will give direct detailed dimensional information about temperature and velocity profiles, shear stress and shear rates, temperature gradients and average radiation temperature of the film. The program is particularly applicable in non-adiabatic wall cases. It accepts as input

1.	Viscosity at T_H°F and p psi	$\eta_{T_H}\|_p$	cp
2.	The temperature T_H°F	669.67°R	*
3.	Viscosity at T_L°F and p psi	$\eta_{T_L}\|_p$	cp
4.	The temperature T_L°F	559.67°R	**
5.	The coefficient of heat conductivity of the lubricant	k_t	lbf/°R sec
6.	The velocity of the moving bearing surface	(UN)	in/sec
7.	The film thickness	h	in
8.	The temperature of the hot stationary wall	T_1	°R
9.	The temperature of the cold moving wall	T_2	°R

Output is yielded as

π_3		
E	Temperature	°R
$T,_3(0)$	Temperature gradient	°F/in
$T,_3(h)$	Temperature gradient	°F/in
τ	Shear stress	psi
T_1	Temperature	°R and °F
T_2	Temperature	°R and °F
$T_{\text{radiation Average}}$		°R and °F

---

*669.67°R = 210°F

**559.67°R = 100°F

Each run takes about 250 msec (JJA31). A version of the program (JJA21) gives extended print-out of intermediate results. It delivers also values inside the film of

x_3	Coordinate inch
$T(x_3)$	Temperature °F
$u(x_3)$	Velocity inch/sec
$T,_3$	Temperature gradient °F/inch
$u,_3$	Shear rate sec^{-1}
$\eta(x_3)$	Viscosity Reyn, lbf sec/in^2
$ER(x_3)$	

Where $ER(x_3)$ is the error or the deviation from zero when the calculated values are inserted in the dimensional counterpart to equation (26), Chapter IV. Sufficient information is available to plot desired profiles in the film. Each run takes about 3000 msec.

The limited print out program JJA31 has been used to map out the film behavior at different locations with Fluid D as lubricant. The temperature of the stationary wall T_1 is selected as independent variable. The position of the selected locations, (along the centerline) the Hertzian pressure and the estimated temperature of the cold wall is summarized in Table 31. Figure 53 shows the results of the calculations performed for one location. The maximum film temperature is found as $T,_3(0)$ is extrapolated to $T,_3(0) = 0$ and is about 342°F. This corresponds well with previous estimated maximum temperature of 340°F from the dimensionless charts.

The diagram, Figure 53, covers situations 1, 2 and 3 of Table

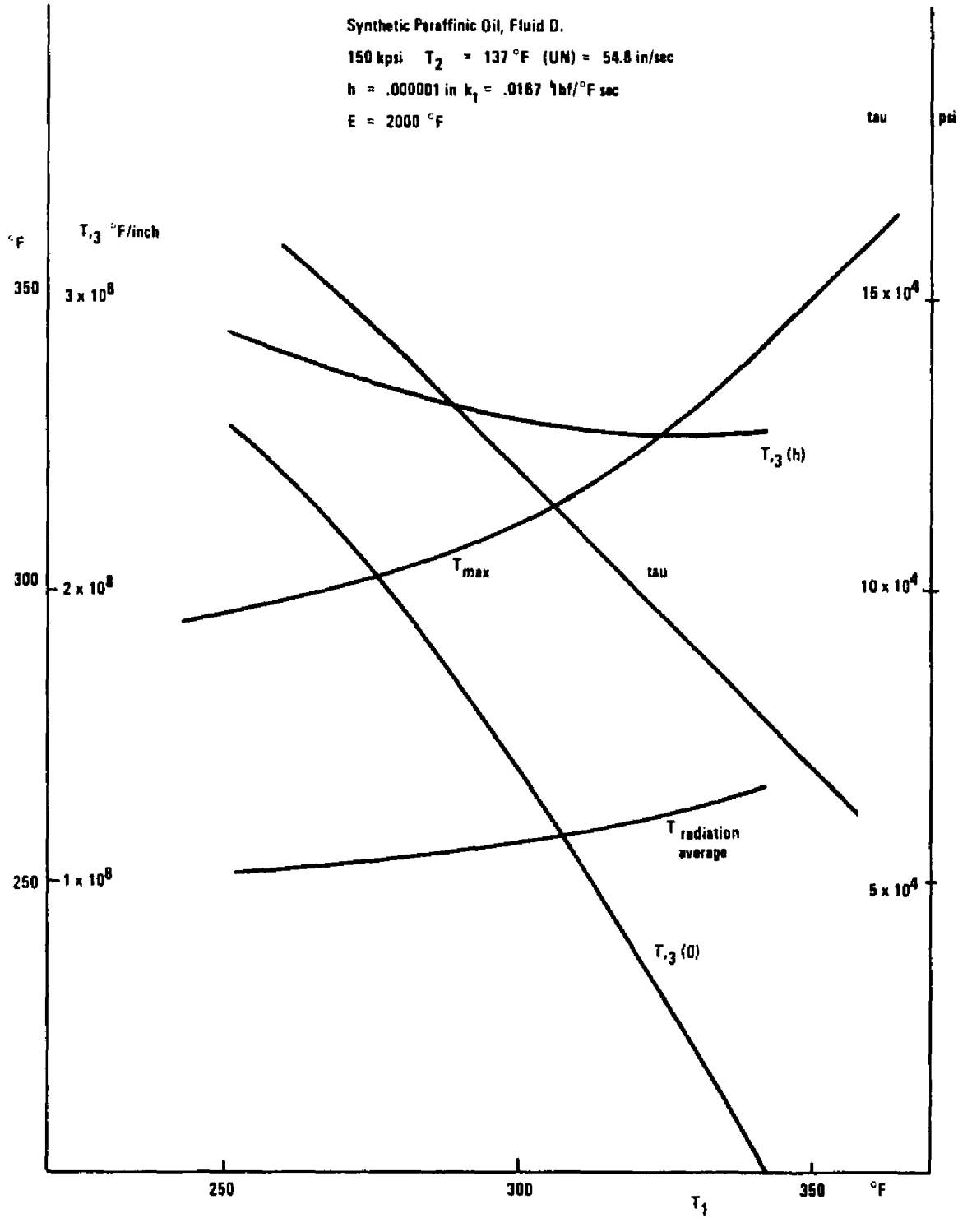

Figure 53. Extrapolation Procedure to Determine T_{max} and the Corresponding Shear Stress.

11, Chapter IV. Situation 1 is equal to the range $T_1 > 342°F$ in Figure 53, situation 2 corresponds to $T_1 = 342°F$ and situation 3 covers $137°F < T_1 < 342°F$. The temperature gradient $T,_3(0)$ and the shear stress are to a very good approximation linear functions in a wide temperature range of T_1 about $T_{1\ max}$. The temperature gradient $T,_3(h)$ is very nearly constant in the same wide temperature range of T_1 about $T_{1\ max}$. The increased heat dissipation, which will be generated when T_1 deviates to temperatures lower than $T_{1\ max}$ is therefore nearly totally conducted away through the stationary wall. The two curves $T,_3(0)$ and $T,_3(h)$ will have the same ordinate and tangent when $T_1 = 137°F$. (Situation 4, symmetry, of Table 11, Chapter IV). The curve for the maximum film temperature T_{max} shows the general behavior predicted by equations (48)(49) (50) and (51) Chapter IV. The curve for the average radiation temperature of the film is seen to have a comparatively weak dependency of the wall temperature T_1.

Extrapolation graphs similar to Figure 53 can be prepared for any location in the contact area. Table 31 shows data obtained from such interpolation graphs from locations on the centerline. Table 31 shows Hertzian pressures at each location, the viscosities η_{100} and η_{210}, the temperature E and the temperature viscosity coefficient π_3 at each pressure. The temperature T_2 of the moving surface is determined from equation (A1) assuming, in this case $\tau = 2000$ psi, $k_{t\ ball} = 4.34$ lbf/°F sec, $\kappa_{ball} = 14.9 \times 10^{-3}$ in^2/sec and (UN) = 54.8 inch/sec. Table 31 shows also the wall temperatures and shear stress (re h = .000001 inch) obtained by extrapolation.

Table 31. Temperature and Shear Stress Calculation at the Center of a Point Contact. W = 15 lbf. Sliding Velocity = 54.8 inch/sec. Lubricant: Fluid D.

	p kpsi 0	η_{100} cp	η_{210} cp	E °R	π_3	T_2 °F re 2000 psi	$T_{1\,max}$ °F Adiabatic Wall Conditions	τ re 1 μinch and Adiabatic Wall Conditions	T_1 actual °F	τ_{actual} re 1 μin. psi	h μinch	τ_{actual} psi
1	75	4×10^6	$.055\times10^5$	1743	2.25	105	238	5.4×10^4	235	5.6×10^4	33	1700
2	104									6.9×10^4*	30	2300 *
3	122	11×10^6	$.47\times10^5$	1893	2.29	116	307	7.2×10^4	304	7.5×10^4	29	2580
4	134									7.8×10^4	30	2600 *
5	142	40×10^6	1.12×10^5	1964	2.28	123	332	7.9×10^4	329	8.1×10^4	31	2610
6	147									8.2×10^4*	31	2650 *
7	150	66×10^6	1.6×10^5	2000	2.27	129	342	8.0×10^4	340	8.3×10^4	30	2770
8	147									8.1×10^4*	29	2790 *
9	142	40×10^6	1.12×10^5	1964	2.28	135	332	7.5×10^4	329	7.7×10^4	29	2650
10	134									7.3×10^4*	29	2540 *
11	122	11×10^6	$.47\times10^5$	1893	2.29	139	306	6.5×10^4	306	6.8×10^4	27	2520
12	104									5.9×10^4*	20	2950 *
13	75	4×10^6	$.055\times10^5$	1743	2.25	144	239	4.2×10^4	235	4.4×10^4	19	2320
14	0											

*Interpolated values.

Evaluation of the Adiabatic Wall Criteria

The temperature profile, Table 31, $T_{1\ max}$, at the surface of the stationary wall is derived under the assumption that adiabatic conditions prevail pointwise. The temperature profile cannot, however, be maintained on the surface of a heat conducting material (sapphire) if $T,_3(0) = 0$ as assumed. The gradient $T,_3(0)$ is therefore > 0 and non-adiabatic conditions are present. The extent to which the actual situation deviates from the adiabatic case can be investigated directly and expressed in terms of a heat flux into the sapphire.

It is found that the temperature distribution of the sapphire surface very closely resembles the temperature profile obtained for constant heat flux over a circular area however with a radius somewhat smaller than the contact radius. Thomas (74) gives the solution for this case as

$$\Delta T = (2/\pi)(q_o/k_t)R_q E(r/R_q) \qquad (A\text{-}2)$$

where ΔT is the temperature difference over the environment, q_o is the heat flux, k_t is the coefficient of heat conduction in the material, R_q is the radius of the circular heat source with constant heat flux and E is the complete elliptic integral of second kind.

The environmental temperature is assumed as before to be 90°F ($\simeq$ 32°C) ΔT_{max} is therefore 252°F where $r = 0$ $E(r/R) = E(0) = \pi/2 \simeq$ 1.57. When $r = R_q$ $E(r/R_q) = 1$. The radius R_q is therefore the location where the temperature difference over the environment is 252/1.57 $\simeq$ 161°F. This location is found at 5.7×10^{-3} inch. The temperature

distribution T_s from a circular heat source with constant flux within a radius of 5.7×10^{-3} inch is summarized in Table 32 and compared to the temperatures of the sapphire surface, $T_{1\ max}$, Table 31. Table 32 shows that the difference between these two temperatures is of the same magnitude as the inaccuracy of the temperatures. The temperature distribution $T_{1\ max}$ as shown in Figure 54 can therefore be regarded as being created by a constant heat flux over a circular area with radius $R_q = 5.7 \times 10^{-3}$ in. The magnitude of the constant heat flux over the area can conveniently be calculated for the center. At the center

$$\Delta T = (q_o/k_t)\, R_q = T,_3\, R_q \qquad \text{(A-3)}$$

which gives $T,_3 = 44300°F/in.$ over the area of $R_q = 5.7 \times 10^{-3}$ inch. This assumes that the heat flux at the surface is directed entirely perpendicular to the wall. The heat flux is the same in the lubricant as in the sapphire material and is also directed perpendicular to the wall in the lubricant side of the surface. The temperature gradient is thus $44300\ (3.14/0.0167) = 8.35 \times 10^{6}°F/in.$ in the lubricant. From Figure 53 it is then seen that the actual wall temperature is then 340°F and τ(re 1 μinch) $= 8 \times 10^{4}$ psi. The temperature gradient $T,_3(h)$ and the average radiation temperature are hardly changed.

Table 31 shows the actual temperatures $T_{1\ actual}$ of the stationary wall in the non-adiabatic case. The corresponding shear stress (re 1μinch) is also tabulated. Table 31 shows further the film thickness measured in the actual experiment and the shear stress of the film τ_{actual}.

Table 32. Comparison of Temperatures T_s Generated by a Constant Heat Flux Source ($R_q = 5.7 \times 10^{-3}$ in) and the Maximum Temperatures of the Stationary Wall $T_{wall}(0)_{max}$

Position	$\frac{T_s}{^oF}$	$\frac{T_{wall}(0)_{max}}{^oF}$	$\frac{T_s - T_{wall}(0)_{max}}{^oF}$
7	342	342	0
8-6	340	339	1
9-5	335	332	3
10-4	324	322	2
11-3	307	306	1
12-2	283	282	1

Figure 54 shows the actual wall temperatures and film shear stress along the center line. The film thickness and the temperature of the moving surface is also shown. The figure shows the symmetry of the temperature profile, T_1, of the stationary wall and the steadily increasing temperatures, T_2, of the moving wall. This shows that T_1 is a weak function of T_2 at least in the assumed ranges of parameters. The actual shear stress is very nearly constant over about 11 x 10^{-3} inch of the total magnitude of the diameter of 14 x 10^{-3} inch with an estimated average value of approximately 2700 psi. The average value over the total diameter, along the centerline, is found to be about 2450 psi. The shear stress (re 1 μinch) at the center, position 7, is 8 x 10^4 psi. Tau is therefore 8 x $10^4/30$ = 2670 psi. This compares well with the shear stress of 2790 psi

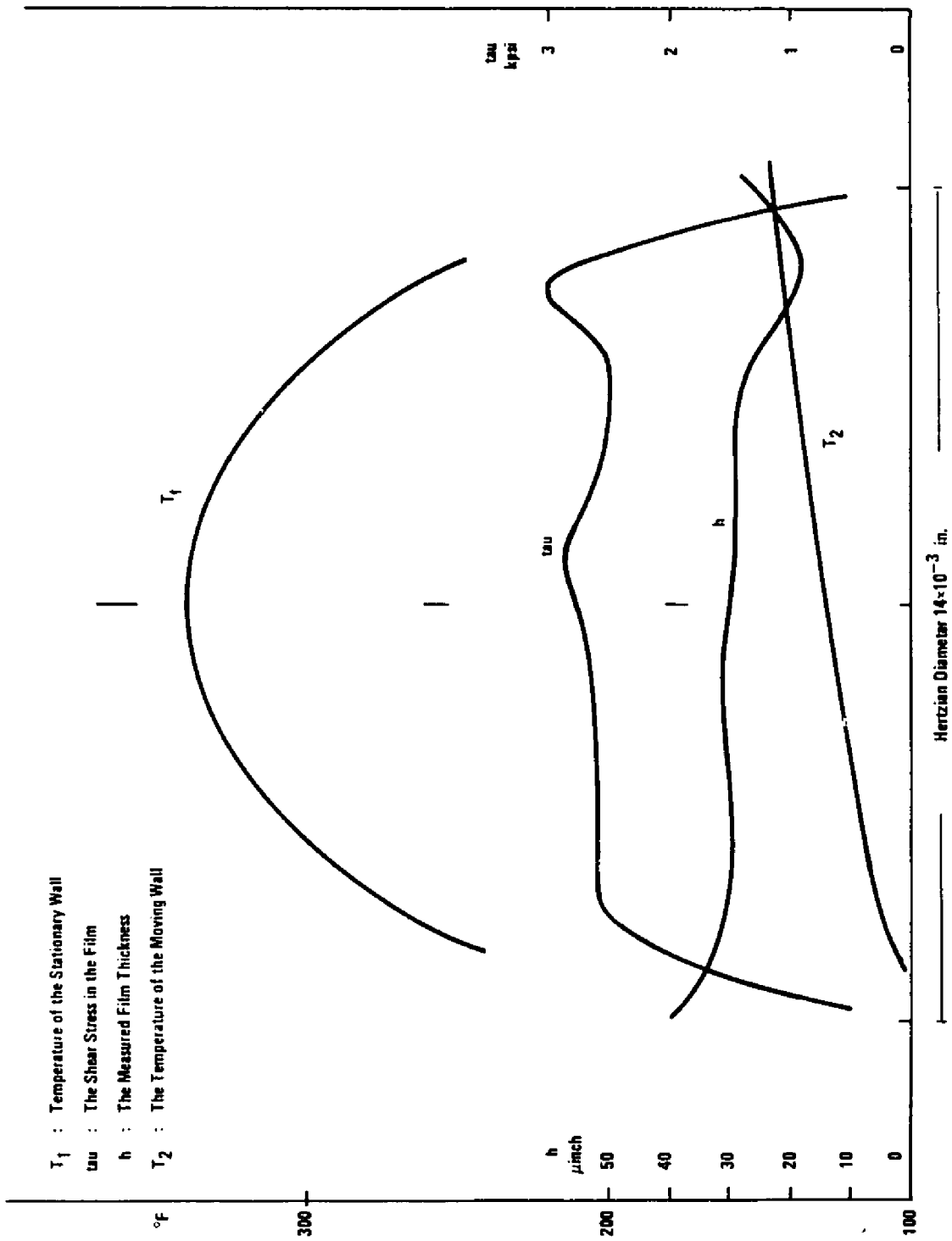

Figure 54. Results of a Film Calculation.

predicted through linear interpolation on the dimensionless diagrams, although the temperature T_2 was 137°F, slightly higher than the actual 129°F found in Table 31. The calculation of film properties can also be performed along lines parallel to the centerline but offset in the x_2 direction and thereby achieve a more nearly accurate estimate of the local shear stress. The cold wall temperatures will be lower when $x_2 \neq 0$ than the temperatures along the centerline, $x_2 = 0$. This will tend to give slightly increased shear stress.

An iteration can be performed in order to increase accuracy. The temperature T_2 of the moving surface can be estimated more accurately when the shear stress curve of Figure 54 is applied. The shear stress curve can furthermore be approximated in the calculations with shear stress distributions consisting of stepwise changes of constant shear stress. The resulting temperature profiles can then be summed up to a resulting T_2-distribution. This will yield some increase in local accuracy.

The average shear stress over the high pressure area of the contact has been estimated also for the sliding velocities 27.4 inch/sec and 13.7 inch/sec. Figure 55 shows the results. The measured traction coefficient for the total contact is also plotted for comparison. The ratio's of measured to calculated traction coefficients are .8 - 1.1 - 1.4 for the velocities 13.7 - 27.4 - 54.8 inch/sec. The estimated accuracy is .1. The calculations are based on viscosities which are extrapolated more than twice the experimentally investigated range. The calculations are based on the assumption that the lubricant

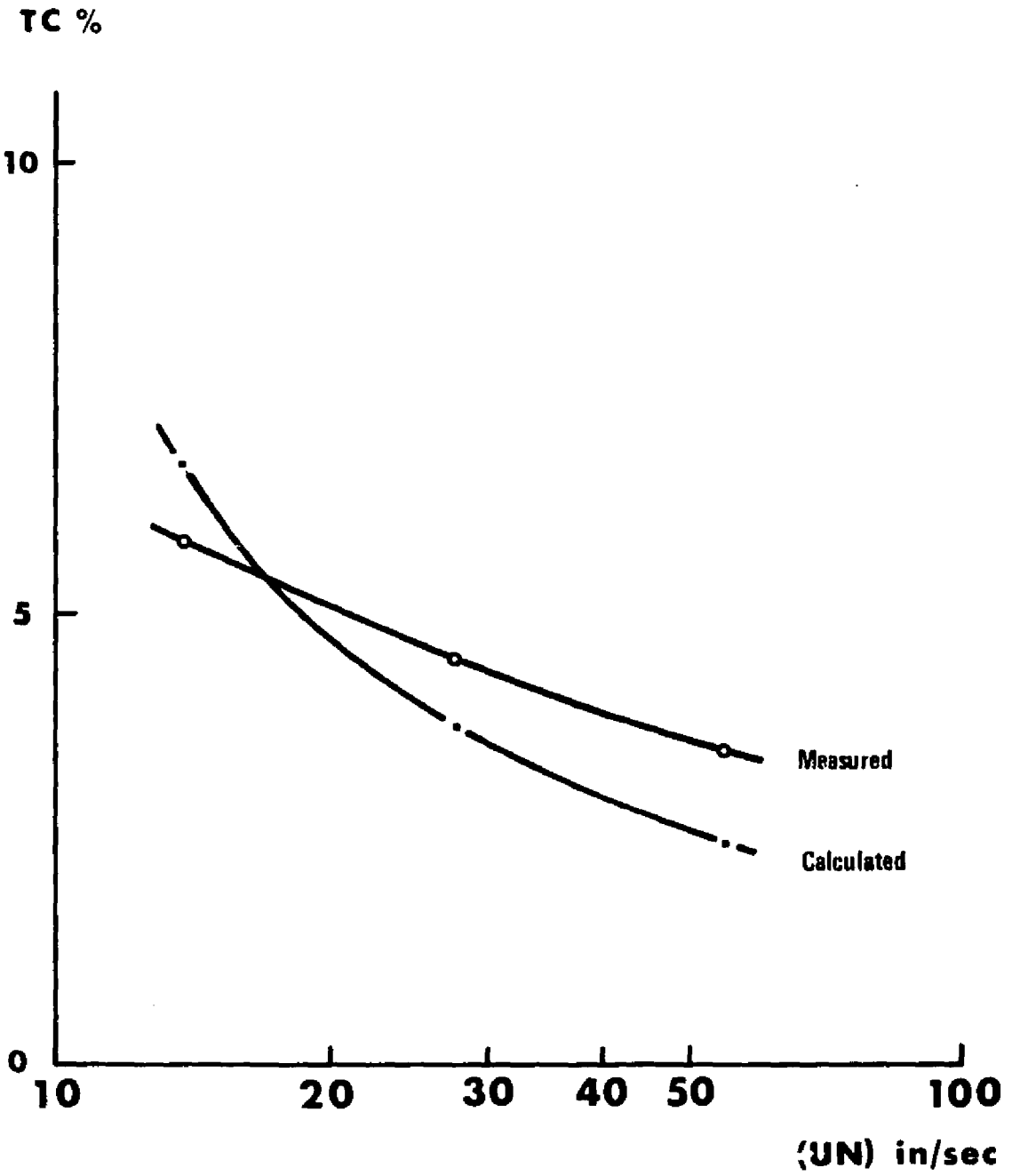

Figure 55. Measured Total Traction Coefficient Compared with Traction Coefficient from the High Pressure Area of the Contact.

behaves as a liquid. Solidification or other non-liquid behavior of lubricants are not investigated yet for the short time duration of interest of an elastohydrodynamic lubrication situation and are thus unknown. A realistic approach has thus been developed to estimate the traction coefficient from the high pressure area of an elastohydrodynamic contact based on existing viscometric data. The result, however, also emphasizes the need for further viscometric investigations into the elastohydrodynamic conditions the lubricant is subjected to during passage of a contact.

APPENDIX H

PROGRAM TO DETERMINE DIMENSIONLESS TEMPERATURES IN THE FILM

```
JJ.A3
      DIMENSION DT(305),DREYH(305),DDSU(305),DSU(305)
      READ(5,350)PI3,PI0,PI
      JJ=1
C      DDEL=(PI-PI0)/12.
C      WRITE(6,350)DDEL
      DDEL=.0025
      DT(1)=PI0
      DSU(1)=0.0
      DREYH(JJ)=EXP((1/DT(JJ))**(PI3))
 50   WRITE(6,350)JJ,DT(JJ),DREYH(JJ),DDSU(JJ-1),DSU(JJ)
 350  FORMAT()
      JJ=JJ+1
      IF((JJ).GT.41.)DDEL=.005
      IF((JJ).GT.81.)DDEL=.01
      DT(JJ)=DT(JJ-1)+DDEL
      DREYH(JJ)=EXP((1/DT(JJ))**(PI3))
      DDSU(JJ-1)=(2*DDEL)/(DREYH(JJ)+DREYH(JJ-1))
      DSU(JJ)=DDSU(JJ-1)+DSU(JJ-1)
      IF((JJ).GT.300.)GO TO 150
      IF(DT(JJ).GT.(PI))GO TO 150
      GO TO 50
150   STOP
      END
```

APPENDIX I

PROGRAM TO DETERMINE DIMENSIONLESS SHEAR STRESS IN THE FILM

The accompanying program calculates the π_5 values in accordance with the rewritten expression for π_5:

$$\pi_5 = 1/2\ \pi_4^{-1/2} \int_{\pi_2}^{\pi_1} \left(\pi_4 - \int_{\pi_2}^{\theta} \mu(\xi,\pi_3)^{-1} d\xi\right)^{-1/2} d\theta \quad \pi_2 < \pi_1 \qquad (I\text{-}1)$$

This formulation is chosen because summation difficulties is encountered when the integration starts from π_1. π_4 is calculated according to equation (62)* in the first part of the program. π_5 is then summed up of product terms of the integrand times delta θ. The integrand increases without bound as θ approaches π_1. Delta θ starts off as .01 $(\pi_1 - \pi_2)$ at the lower end (at π_2) of the integration interval. Delta θ is decreased in two steps, as the integrand grows bigger, to a final value of .0001 $(\pi_1 - \pi_2)$ in order to obtain satisfactory accuracy. Only the last few results of the summation are printed out. Exit is via error termination. Run time of the program is about 300 msec.

---

* Chapter IV.

```
'JJ.A;3
      DIMENSION D4T(105),D4REYH(105),DD4SU(105),D4SU(105)
      DIMENSION DT(305),DREYH(305),DDSU(305),DSU(305),PI5(20)
      DIMENSION VRDSU(305),DDSSU(305),DSSU(305),RTOV(305),TVOV(305)
      INTEGER PP
      READ(5,350)PI3,PI2,PI1
C      WRITE(6,350)PI3,PI2,PI1
      JJ=1
      PP=1
      DDELTA=(PI2-PI1)/100.
      DDEL=DDELTA
      DT(1)=PI1
      D4T(1)=PI1
      DSU(1)=0.0
      D4SU(1)=0.0
      D4REYH(PP)=EXP((1/D4T(PP))**(PI3))
 40   PP=PP+1
      D4T(PP)=D4T(PP-1)+DDEL
      D4REYH(PP)=EXP((1/D4T(PP))**(PI3))
      DD4SU(PP-1)=(2*DDEL)/(D4REYH(PP)+D4REYH(PP-1))
      D4SU(PP)=DD4SU(PP-1)+D4SU(PP-1)
      IF((PP).LT.102.)GO TO 40
C      WRITE(6,350)(PP),D4T(PP-1),D4REYH(PP-1),DD4SU(PP-2),D4SU(PP-1)
      VRDSU(JJ)=1/((D4SU(101)-(DSU(JJ)))**(.5))
C      WRITE(6,400)
400   FORMAT(//2X,'JJ',2X,'DT(JJ)',1X,'DREYH(JJ)',1X,
     1 'DDSU(JJ-1)',1X,'DSU(JJ)',1X,'VRDSU(JJ)',1X,'DDSSU(JJ-1)',
     2 1X,'DSSU(JJ)'/)
```

```
      DSSU(1)=0.0
      DREYH(JJ)=EXP((1/DT(JJ))**(PI3))
350   FORMAT()
360   FORMAT(1X,I3,2X,1F5.4,1X,10(E10.4),0X,1(E10.4),3X,8(E10.4))
 50   JJ=JJ+1
      DT(JJ)=DT(JJ-1)+DDEL
      DREYH(JJ)=EXP((1/DT(JJ))**(PI3))
      DDSU(JJ-1)=(2*DDEL)/(DREYH(JJ)+DREYH(JJ-1))
      DSU(JJ)=DDSU(JJ-1)+DSU(JJ-1)
      VRDSU(JJ)=1/((D4SU(101)-(DSU(JJ)))**(.5))
      DDSSU(JJ-1)=(DDEL/2.)*(VRDSU(JJ)+VRDSU(JJ-1))
      DSSU(JJ)=DDSSU(JJ-1)+DSSU(JJ-1)
      RIOV(JJ)=(VRDSU(JJ)-VRDSU(JJ-1))
      TVOV(JJ)=.05*VRDSU(JJ-1)
      DDELT=.05*DDELTA
      DDELTT=.01*DDELTA
      IF(DT(JJ).GT.(PI2-2.*DDEL))GO TO 250
      IF(DDEL.LT.(.5*DDELT))GO TO 251
      IF(RIOV(JJ).GT.TVOV(JJ))DDEL=DDELT
      IF(RIOV(JJ).GT.(2*TVOV(JJ)))DDEL=DDELTT
251   IF(DT(JJ).GT.(PI2))GO TO 150
      IF((JJ).GT.300.)GO TO 150
      GO TO 50
250   WRITE(6,360)JJ,DT(JJ),DREYH(JJ),DDSU(JJ-1),DSU(JJ),VRDSU(JJ),
     1 DDSSU(JJ-1),DSSU(JJ)
      PI5(JJ)=(DSSU(JJ))/(2.*((DSU(JJ))**.5))
      WRITE(6,350)PI5(JJ)
      GO TO 50
150   STOP
```

APPENDIX J

NOMENCLATURE

Symbol	Description
a	Hertzian contact radius
a_c	Constant of proportionality
$a_1 \ldots a_{\bar{n}}$	Constant coefficients in series solution $\bar{n}$ positive integer
c	Specific heat per unit volume $c = c_v\rho$
c_o	Diagram constant $c_o = .6\ cs$
c_v	Specific heat per unit mass
c_1	Dimensioned constant $c_1 = n/\lvert n\rvert$
$c_2 \ldots c_m$	Constants of integration
e	Base number of the natural logarithm
h	Film thickness
k	Constant
$k_o k_1$	Constants of the Hausenblas temperature viscosity relation
k_t	Coefficient of heat conduction
h_c	Film thickness along the centerline of a point contact
h_m	Minimum film thickness in a point contact
ℓ	Half side length of a moving square heat source
$\bar{n}$	Positive integer
n	Variable
p	Pressure

p_1	Pressure before capillary (or orifice)
p_2	Pressure after capillary (or orifice)
p_3	Pressure level in test section
p_m	Maximum Hertzian pressure
p,	Index referring to pressure gradient
$\bar{p}$	$= p/p_m$
q	Characteristic pressure in $\eta(p,T)$ relation ($q = p/Q$)
q_o	Heat flux
q_1	Temperature gradient $\perp$ a sliding surface $\tau \times (UN)/k_{t_{ball}}$
r	Radius
r	Radial coordinate in cylindrical coordinate systems
s	Constant
sl	Index referring to sliding
t	Time
t_r	Time of exposure to a heat flux
$x_1x_2x_3$	Coordinates in Cartesian coordinate systems
$u_1u_2u_3$	Velocities in the $x_1x_2x_3$ directions
xyz	Dimensionless coordinates in Cartesian coordinate systems
uvw	Dimensionless velocities in the xyz directions
$r\ \bar{\theta}\ \bar{z}$	Coordinates in cylindrical coordinate systems
$u\ u_{\bar{\theta}}u_{\bar{z}}$	Velocities in the $r\bar{\theta}\bar{z}$ directions
$\bar{\rho}\ \bar{\theta}\ \omega$	Dimensionless coordinates in cylindrical coordinate systems
$u_{\bar{\rho}}u_{\bar{\theta}}u_{\omega}$	Dimensionless velocities in cylindrical coordinate systems
u_H	Film velocities when convection in the x_1-direction is disregarded
u_L	Film velocities defined as $((1/\pi_4)\int_{\pi_{10}}^{\theta} -\mu(\xi,\pi_3)^{-1}d\xi)^{1/2}$

z_1	z-ordinate of adiabatic plane in film
A	Material parameter for a viscous liquid. $A = \ln \eta \mid T = 1^{\circ}R$ (η in cp)
A_1^*	A of fluid 1
A_2^*	A of fluid 2
$\bar{D}$	Dimensionless convection parameter $= \pi_\beta \theta_{,xM} / \pi_4 \pi_5 \cdot 2$
D	Diameter of capillary
E	Material parameter $E = A^{1/Q}$. E is the temperature ($^{\circ}R$) at which the viscosity of the lubricant is $\eta = e \simeq 2.718$ cp.
E_i	Moduli of elasticity for solids
E'	Reduced elastic modulus $= 2\left(\frac{1 - \sigma_1^2}{E_1} + \frac{1 - \sigma_2^2}{E_2}\right)^{-1}$
E_n	Internal energy per unit mass
$ER(x_3)$	Deviation from the solution to the dimensional counterpart to equation (25) Chapter IV
G	Thermal function containing viscosity
H	Dimensionless film thickness $H = h/R_b$
$H_1 \cdots H_n$	Symbols for functions
$I_1 \cdots I_n$	Symbols for integrals
L	Length of capillary
MW	Molecular weight
Q	Temperature viscosity coefficient in $\ln\ln\eta$-$\ln T$ presentation. A rectifying diagram of ASTM D 341-43 type ($Q = \pi_3$)
$\bar{Q}$	Volume flow rate
$\hat{Q}$	Heat flux
Q_1^*	Q of fluid 1
Q_2^*	Q of fluid 2
R	Radius of capillary
Rl	Dimensionless parameter $= -p_{,z} R^4 / 4L\eta\kappa$

R2	Dimensionless parameter = $-p_{,z}L/c_v\rho E$
R_b	Effective radius of contacting surfaces (1,2) $(\frac{1}{R_1} + \frac{1}{R_2})^{-1}$
R_q	Radius of circular heat source with constant heat flux, in the contact
Re	Reynolds number
$R_o\Theta_o Z_o$	Body forces per unit volume of liquid in the $r\bar{\theta}z$ directions Cylindrical coordinates
T	Temperature
T_1	Temperature of the stationary wall
T_2	Temperature of the moving wall
T_s	Temperature distribution from a circular heat source ($r = R_q$) with constant heat flux, in the contact.
T_1^*	Temperature of fluid 1
T_2^*	Temperature of fluid 2
TC	Traction coefficient
(UN)	Velocity, in the x_1-direction, of the moving surface in a plane parallel bearing surface configuration
U	Dimensionless velocity parameter $c_1(UN)/R_bE'$
V	Dimensionless velocity for moving heat sources $(UN)\ell/4\kappa$
W	Total normal load in a Hertzian point contact
X_i	Body forces per unit volume of liquid in the i directions. Cartesian coordinates
Z	Pressure viscosity coefficient in lnlnη-lnp presentation. A rectifying diagram of Roeland's type

α Pressure viscosity exponent

α_{OT} Pressure viscosity coefficient defined as follows:

$$\alpha_{OT} = \left.\frac{d \ln \eta}{dp}\right|_{p=atm}$$

α^* Pressure viscosity coefficient defined as follows:

$$\alpha^* = \int_0^\infty \frac{\eta(0)}{\eta(p)}\, dp^{-1}$$

β Exponential temperature viscosity coefficient

$\dot{\gamma}$ Shear rate

Δp $= p_1 - p_2$ over a capillary

Δp_o $= p_1 - p_2$ over an orifice

Δp_t $= \Delta p + \Delta p_o$ (Total pressure drop)

ΔT Temperature change

ΔT_1 $= \Delta \pi_1 \times E$

ΔT_1^* Change of T_1^*

ΔT_2^* Change of T_2^*

$\Delta \eta$ Viscosity change

$\Delta \eta_1^*$ Change of η_1^*

$\Delta \eta_2^*$ Change of η_2^*

$\Delta \pi_1$ $\pi_1 - \pi_{10}$

ζ Dummy variable for dimensionless velocity or for z

η Viscosity cp or Reyn (lbf sec/in^2)

η_{100} Viscosity cp at 100°F (559.67°R) 37.8°C

η_{210} Viscosity cp at 210°F (669.67°R) 98.9°C

η_1 First Newtonian viscosity of a shear thinning lubricant

η_2 Second Newtonian viscosity of a shear thinning lubricant

η_b Viscosity of base oil in polymer blends

η_o Base viscosity in the temperature viscosity relation $\eta = \eta_o \exp(\beta\Delta T)$ or in the pressure viscosity relation $\eta = \eta_o \exp(\alpha p)$

η_1^* η of fluid 1

η_2^* η of fluid 2

θ Dimensionless temperature $\theta = T/E$

$\theta_{,xM}$ Maximum dimensionless temperature gradient in the x-direction

θ^* Dummy variable for the temperature θ

$\hat{\theta}$ Dummy variable for the temperature θ

λ $= -2\eta/3$

$\lambda(z)$ Function of z $\lambda(z) = \int_0^z u(\zeta)d\zeta$ = volume flow

$\lambda_m(z)$ Function of z $\lambda_m(z) = (1/u(z)) \int_0^z u_{,\zeta}\lambda(\zeta)d\zeta$

κ Heat diffusivity $= k_t/c$

μ Dimensionless viscosity $= \eta/c_1$ $\mu = |\eta|$ η in cp

μ_{100}(cp) $= |\eta_{100}|$ η in cp

μ_{210}(cp) $= |\eta_{210}|$ η in cp

ν Kinematic viscosity

ξ Dummy variable for dimensionless temperature or for z

π_1 Dimensionless parameter, temperature at wall 1 (T_1/E)

π_{10} π_1 $(\bar{D} \neq 0)$

π_2 Dimensionless parameter, temperature at wall 2(T_2/E)

π_3 Dimensionless parameter, temperature viscosity exponent p/q $(\pi_3 = Q)$

π_4 Dimensionless parameter velocity. $c_1(UN)^2/2k_tE$

π_5 Dimensionless parameter, shear stress $\tau h/c_1(UN) = \mu u_{,z}$

π_α Dimensionless parameter, pressure gradient in the 1 or the 2 direction in an elastohydrodynamic contact.

$$\pi_\alpha = (H^2/\pi_5 U)(\bar{p}_{,\bar{\rho}})(z - 1/2)/\pi$$

$\pi_{\alpha.9}$ $|\pi_\alpha|_{\bar{\rho}} \geq .9$

π_β Dimensionless parameter, temperature gradient in the 1 or the 2 direction in an elastohydrodynamic contact.

$$\pi_\beta = h^2(UN)/\kappa a$$

ρ Density (mass per unit volume)

$\bar{\rho}$ Dimensionless radius

σ Poisson's ratio

τ Shear stress

ψ Half of cone angle in sapphire capillary

ω Dimensionless axial length of capillary ($\omega = \bar{z}/L$)

Γ Auxiliary parameter = $\theta_{,z}(1)/2\pi_4\pi_5$

Δ Auxiliary parameter = $(1 - \sigma_i^2)/E_i$ $i = 1,2$

Φ Dissipation function in Cartesian coordinates

Φ_c Dissipation function in cylindrical coordinates

Ω Symbol for a function

ln Natural logarithm, base number e

log Briggs logarithm, base number 10

, Index denoting differentiation with respect to the following symbol.

exp( ) $= e^{( )}$

O( ) = The order of magnitude of ( )

E( ) Complete elliptic integral of second kind

$\frac{D}{Dt}$ $= ,_t + ,_1(u_1) + ,_2(u_2) + ,_3(u_3)$ in cartesian coordinates

$\frac{D}{Dt}$ $= ,_t + ,_r(u_r) + ,_{\bar{\theta}}(u_{\bar{\theta}}/r) + ,_z(u_{\bar{z}})$ in cylindrical coordinates

∇^2 $= ,_r,_r + ,_r(1/r) + ,_{\bar{\theta}},_{\bar{\theta}}\ (1/r^2) + ,_{\bar{z}},_{\bar{z}}$ in cylindrical coordinates.

BIBLIOGRAPHY

1. Nowak, J. D., An Experimental Investigation of the Combined Effects of Pressure, Temperature and Shear Stress Upon Viscosity, Doctoral Thesis, Univ. of Mich., 1968.

2. Pressure-Viscosity Report, Vols. I and II, a report prepared by the ASME Research Committee on Lubrication, ASME, New York, 1953.

3. Hersey, M. D., and Snyder, G. H. S., High-Pressure Capillary Flow, Journal of Rheology, 3, No. 3, 1932.

4. Hersey, M. D., and Zimmer, J. C., Heat Effects in Capillary Flow at High Rates of Shear, Journal of Applied Physics, Vol. 8, May, 1937.

5. Norton, A. E., Knott, M. J., and Muenger, J. R., Flow Properties of Lubricants under High Pressure, ASME Trans., 63, No. 7, 1941.

6. Philippoff, W., Über das Fliessen in Kapillaren bei extrem hohen Schubspannungen, Physikalische Zeitschrift, 43. Jahrgang, Nr. 19/20, 1942.

7. Fritz, W., and Hennenhöfer, J., Strömung zäher Öle in Kapillaren bei hohen Schergeschwindigkeiten und hohen Reibungsleistungen, Angew. Chem. B. 19 Jahrg. Nr. 5/6, 1947.

8. Schnurmann, R., Das Verhalten von Schmiermitteln bei hohen Schergefällen. Erdöl und Kohle, Erdgas, Petrochemie. Nr. 6. Juni 1962. 15 JAHRG.

9. Gerrard, J. E., and Philippoff, W., Viscous Heating and Capillary Flow, 4th International Congress of Rheology, 1963, Paper 51.

10. Gerrard, J. E., Steidler, F. E., and Appeldoorn, J. K., Viscous Heating in Capillaries: The Adiabatic Case. ACS Petroleum Division Meeting, Chicago, Ill., Sept. 1964.

11. Gerrard, J. E., Steidler, F. E., and Appeldoorn, J. K., Viscous Heating in Capillaries: The Isothermal-Wall Case, ACS Petroleum Division Meeting, Atlantic City, N. J., Sept. 1965.

12. Winer, W. O., and Novak, J. D. Some Measurements of High Pressure Lubricant Rheology. Trans. ASME, Series F, Journal of Lubrication Technology, Vol. 90, No. 3, July 1968, 580 - 591.

13. Novak, J. D., and Winer, W. O., The Effect of Pressure on the Non-Newtonian Behavior of Polymer Blended Oils, Trans. ASME, Series F, Journal of Lubrication Technology, 91, July 1969, p. 459-464.

14. Winer, W. O., A Viscometer for High Pressure Use, and Some Results. Trans. ASME, Journal of Basic Engineering, September 1972, 586-588.

15. Bondi, A., Flow Orientation in Isotropic Fluids, Journal of Applied Physics, Vol. 16, September 1945.

16. Smith, F. W., Some Aspects of Nonlinear Behavior in Lubricants under Extreme Stress. ASME Trans. Journal of Lubrication Technology, 90, July 1968, p. 549-552.

17. Grubin, A. N. and Vinogradova, I. E., Central Scientific Research Institute for Technology and Mechanical Engineering, Book No. 30, Moscow (DSIR Translation No. 337).

18. Dowson, D. and Higginson, G. R., A Numerical Solution to the Elastohydrodynamic Problem, J. Mech. Engr. Sci., 1, No. 1, 6, 1959.

19. Dowson, D. and Higginson, G. R., The Effect of Material Properties on the Lubrication of Elastic Rollers, J. Mech. Eng. Sci., 2, No. 3, 188, 1960.

20. Dowson, D., Higginson, G. R., and Whitaker, A. W., Elastohydrodynamic Lubrication: A Survey of Isothermal Solutions, J. Mech. Engr. Sci., 4, No. 2, 121, 1962.

21. Cheng, H. S. and Sternlicht, B., A Numerical Solution for the Pressure, Temperature, and Film Thickness between Two Infinite Long, Lubricated Rolling and Sliding Cylinders, under Heavy Loads, Journal of Basic Engineering, Trans. ASME, Series D. Vol. 87, No. 3, 695, 1965.

22. Dowson, D. and Whitaker, A. V., A Numerical Procedure for the Solution of the Elastohydrodynamic Problem of Rolling and Sliding Contacts Lubricated by a Newtonian fluid. Symp. on Elastohydrodynamic Lubrication Proc. Instn. Mech. Engrs., 1965-66, 180, Pt. 3B, 57.

23. Cheng, H. S., A Refined Solution to the Thermal-Elastohydrodynamic Lubrication of Rolling and Sliding Cylinders. ASLE Trans., Vol. 8, No. 4, 397, 1965.

24. Cheng, H. S., Calculation of Elastohydrodynamic Film Thickness in High Speed Rolling and Sliding Contacts. Technical Report, Mechanical Technology Incorporated, MTI-67TR24.

25. Mason, W. P., Measurements of the Viscosity and Shear Elasticity of Liquids by Means of a Torsionally Vibrating Crystal, Trans. ASME, May 1947.

26. O'Neil, H. T., Reflection and Refraction of Plane Shear Waves in Viscoelastic Media, Physical Review, Vol. 75, No. 6, 928-935, 1949.

27. Barlow, A. J., and Lamb, J., The Visco-Elastic Behaviour of Lubricating Oils under Cyclic Shearing Stress, Proc. Roy. Soc. A 253, 1959.

28. Barlow, A. J., Harrison, G., and Lamb, J., Viscoelastic Relaxation of Polydimethylsiloxane Liquids, Proc. Roy. Soc. A 282, 1964.

29. Lamb, J., Viscoelastic Behaviour and the Lubricating Properties of Liquids, Am. Soc. Mech. Engrs. Symposium on Rheology (Washington) 1965 (Marris, A. W., and Wang, J. T. S., eds).

30. Lamb, J. Physical Properties of Fluid Lubricants: Rheological and Viscoelastic Behaviour. Paper 18, Proc. Instn. Mech. Engrs., 1967-68, 182, Pt 3A, 293.

31. Barlow, A. J., Harrison, G., Irving, J. B., Kim, M. G., Lamb, J., and Pursley, W. C., The Effect of Pressure on the Viscoelastic Properties of Liquids, Proc. Roy. Soc. Lond. A 327, 403-413, 1972.

32. Appeldoorn, J. K., Okrent, E. H., and Philippoff, W., Viscosity and Elasticity at High Pressures and High Shear Rates, 27th Midyear Meeting API Division of Refining, San Francisco, Calif., May 14, 1962.

33. Private communication from J. F. Hutton, Shell Thornton Research Center, Thornton, England.

34. Wurst, W., Strömung durch Schlitz- und Lochblenden bei kleinen Reynolds-Zahlen, Ingenieur-Archiv, XXII Band, Sechstes (Schluss-) Heft, 1954.

35. Rouse, H., Ed. Advanced Mechanics of Fluids, John Wiley and Sons, Inc., New York, 1959.

36. Goldstein, S., Ed. Modern Developments in Fluid Dynamics, Vol. I. Oxford, at The Clarendon Press, 1957.

37. Hersey, M. D., Theory and Research in Lubrication, New York, Wiley and Sons, Inc. 1966.

38. Appeldoorn, J. K., Physical Properties of Lubricants, Chapter 8, Boundary Lubrication, An Appraisal of World Literature, The ASME Committee on Lubrication, New York, 1969.

39. Winer, W. O., Fluid Measurements, NASA Report No. NAS3-15383, Georgia Institute of Technology, Atlanta, January 1972.

40. Winer, W. O., Sanborn, D. M., Lee, D., Jakobsen, J., Carlson, S., and Bohn, M., Investigations of Lubricant Rheology as Applied to Elastohydrodynamic Lubrication, NASA Report No. 11-002-133, Georgia Institute of Technology, Atlanta, June 1972.

41. Winer, W. O., High Pressure Rheology of XRM 109F and Krytox 143-AB, NASA Report No. C-57357-B, University of Michigan, Ann Arbor, Michigan, July 1969.

42. Hersey, M. D., Note on Heat Effects in Capillary Flow, Physics, Vol. 7, November 1936.

43. Grigull, U., Wärmeübergang in Laminarer Strömung mit Reibungswärme, Chemie-Ing.-Techn. 27 Jahrg. Nr. 8/9, 1955.

44. Schlichting, H., Einige exakte Lösungen fur die Temperaturverteilung in einer Laminaren Strömung. Z. angew. Math. Mech. Bd. 31, Nr. 3 März 1951.

45. Nahme, R. Beiträge zur Hydrodynamischen Theorie der Lagerriebung, Ingenieur-Archiv, Vol. XI, 1940.

46. Hausenblas, H., Die Nichtisotherme Laminare Strömung einer Zähen Flüssigkeit durch enge Spalte und Kapillarröhren, Ingenieur-Archiv, XVIII, Band 1950.

47. Brinkman, H. C., Heat Effects in Capillary Flow I., Appl. Sci. Res., A2, 120-124, 1951.

48. Millsaps, K., and Pohlhausen, K. Thermal Distributions in Jeffery-Hamel Flows Between Nonparallel Plane Walls. Journal of the Aeronautical Sciences, March 1953, 187 - 196.

49. Toor, H. L., The Energy Equation for Viscous Flow. Effect of Expansion on Temperature Profiles, Industrial and Engineering Chemistry, Vol. 48, No. 5, May 1956.

50. Toor, H. L., Heat Generation and Conduction in the Flow of a Viscous Compressible Liquid, Trans. Soc. Rheology, Vol. I, 177-190, 1957.

51. Gee, R. E., and Lyon, J. B., Nonisothermal Flow of Viscous Non-Newtonian Fluids, Industrial and Engineering Chemistry, Vol. 49, No. 6, June 1957.

52. Kearsley, E. A., The Viscous Heating Correction for Viscometer Flows, Trans. Soc. Rheology, Vol. VI, 253-261, 1962.

53. Pai, S.I., Viscous Flow Theory I - Laminar Flow, Van Nostrand, New York, 1956.

54. Kingsbury, A., Heat Effects in Lubricating Films, Mech. Eng., Vol. 56, 120-121, 1934.

55. Hagg, A. C., Heat Effects in Lubricating Films. Trans. ASME Journal of Basic Engineering, 1944.

56. Regirer, S. A., The Influence of Thermal Effects on the Viscous Resistance of a Steady Uniform Flow of Liquid, PMM vol. 22, No. 3 414 - 418, 1958.

57. Crook, A. W., The Lubrication of Rollers III. A Theoretical Discussion of Friction and the Temperatures in the Film, Proc. Roy. Soc. Lond. A 254, 1961.

58. Bostandzhyan, S. A., Merzhanov, A. G., and Khudyaev, S. I., Some Problems of Nonisothermal Steady Flow of a Viscous Fluid, Zhurnal Prikladnoi Mekhaniki i Tekhnicheskoi Fiziki, No. 5, 45 - 50, 1965.

59. Hunter, W. B., and Zienkiewicz, O. C., Effect of Temperature Variations across the Lubricant Films in the Theory of Hydrodynamic Lubrication, J. Mech. Eng. Sci. Vol. 2, No. 1, 1960.

60. Gohar, R. and Cameron, A., The Mapping of Elastohydrodynamic Contacts. ASLE Paper No. 66LC-21, Presented at the ASLE/ASME Lubrication Conference, Minneapolis, Minnesota 18-20 Oct. 1966.

61. Sanborn, D. M., An Experimental Investigation of the Elastohydrodynamic Lubrication of Point Contacts in Pure Sliding, Ph.D. Thesis, University of Michigan, 1969.

62. Sanborn, D. M. and Winer, W. O., Fluid Rheological Effects in Sliding Elastohydrodynamic Point Contacts with Transient Loading. Trans. ASME, J. Lubrication Technology, 93, April 1973, July 1973.

63. Cheng, H. S., and Orcutt, F. K., A Correlation between the Theoretical and Experimental Results on the Elastohydrodynamic Lubrication of Rolling and Sliding Contacts, Proc. Inst. Mech. Engrs., Vol. 180, Pt. 3B, 1965-66.

64. Kannel, J. W., Measurements of Pressures in Rolling Contact, Paper 11, Proc. Inst. Mech. Engrs. Vol. 180, Pt. 3B, 1965-66.

65. Hamilton, G. M., and Moore, S. L., Deformation and Pressure in an Elastohydrodynamic Contact, Proc. Roy. Soc. Lond., A 322, 313-330, 1971.

66. Winer, W. O., Fluid Measurements, NASA Report No. NAS 3-14546. Georgia Institute of Technology, Atlanta, Sept. 24, 1970.

67. Winer, W. O., Sanborn, D. M., and Jakobsen, J., Investigations of the Rheology of a Series of Silicones as Related to Elastohydrodynamic Lubrication, a Report Prepared for Dow Corning Corporation, Midland, Cleveland, Georgia Institute of Technology, Atlanta, Georgia, November 1972.

68. Turchina, V. A., Pressure and Temperature Measurement Techniques in Elastohydrodynamic Contacts, Master of Science Thesis, Georgia Institute of Technology, Atlanta, Georgia, June, 1973.

69. Turchina, V. A., Sanborn, D. M., and Winer, W. O., Temperature Measurements in Sliding Elastohydrodynamic Contacts, To be Presented at the ASME/ASLE Joint Lubrication Conference, Atlanta, Georgia, October 15-17, 1973.

70. Blok, H., Theoretical Study of Temperature Rise at Surfaces of Actual Contact under Oiliness Lubrication Conditions, Inst. Mech. Eng., 2, p. 222 (General Discussion on Lubrication).

71. Jaeger, J. C., Moving Sources of Heat and the Temperature at Sliding Contacts, J. Proc. Roy. Soc. N. S. W. 76, 203-24, 1942.

72. Carslaw, H. S., and Jaeger, J. C., Conduction of Heat in Solids, Oxford at the Clarendon Press, 1962.

73. Jakob, M., Heat Transfer, John Wiley and Sons, Inc., New York, 1964.

74. Thomas, P. H., Some Conduction Problems in the Heating of Small Areas on Large Solids, Quart. J. Mech. Appl. Math. 10, 482, 1957.

VITA

Jørgen Jakobsen was born in Aarhus, Denmark, on October 23, 1930.

1936-42 Attended elementary school in Aarhus

1942-49 Attended preparatory school and high school in Aarhus

1949 General Certificate: Aarhus Kathedralskole

1949-55 Attended the Technical University of Denmark, Copenhagen, Denmark
Workshop practice: Sweden, Denmark, Great Britain
Civilingeniør-eksamen (M.Sc.), Department of Combustion Engines and Air Compressors with study-project in design of free piston gasifiers

1955 Member of The Institution of Danish Civil Engineers, Copenhagen

1955-57 Conscript service, Royal Danish Air Force, Lieutenant 1956

1957-59 Civil appointment, Air Material Command, RDAF
Responsible for Aircraft Engines RR-Derwent 8, DH-Gipsy, and GE-J 47

1959 Appointment as laboratorieingeniør, Department of Machine Design, The Technical University of Denmark

1966 Appointment as afdelingsleder, Department of Machine Design, The Technical University of Denmark

1969 Graduate Study at School of Mechanical Engineering
Georgia Institute of Technology
Field of Study: Lubrication Technology
Adviser: Professor Ward O. Winer, Ph.D.

1972 Appointment as Lektor, The Technical University of Denmark

The position as laboratorieingeniør/afdelingsleder involved:

1. Administration, establishing, and supervising the laboratory.

2. Directing research-, non-routine projects or investigations for the industry.

3. 1967-69 Lecturing for the last-term students. Directing their study-project (theses).

4. 1966-69 Mechanical Engineering Development mainly in the field of hydrostatic transmissions.

   Design, building and testing of a high efficiency, low noise-level, axial piston pump (in experimental design, 250 HP at 3000 rpm and 250 kp/cm^2).

   Preliminary investigations: Design of a Free Piston Dieseldriven hydraulic pump.

   Outside the hydrostatic field: Design, building and testing of a Light-weight Pile-driver (in model, force amplitude: 2 tons).

Besides the employment at The Technical University:

1966-68 Consulting engineer: Leif Sørensen, Mechanical Engineering Development, Farum, Denmark.

The work as consulting engineer concerned:

Design, building, and testing of an Electronic Servo-control System for Hydraulic Excavators.

Design-study in High-efficiency Flexible Power Transmission System cooperating with the above mentioned control-system.

Preliminary study in hydraulic-electronic governors for Diesel engine use.

1968-69 Member of the Organizing Committee for the Danish Conference on Hydrostatic Transmissions, Copenhagen 1969

1973 Associate member of the Society of Sigma Xi.

Publications:

Afvejning af rotorer for heliumanlaegget på forsøgsstation RISØ
Ingeniøren, nr. 20, 15. oktober 1962

21 reports on industrial investigations:

Optical measurements of surfaces of machine elements
Failures in manufacturing of plastfoils
Vibration- and noise-investigations

Coauthor: Two papers:

Jakobsen, J., Sanborn, D. M., and Winer, W. O., "Simulations of Severe Shear Conditions in Lubrication," The ASTM-SAE symposium on Viscometry, Detroit, Michigan, May 1973.

Jakobsen, J., Sanborn, D. M., and Winer, W. O., "Pressure Viscosity Characteristics of a Series of Siloxane Fluids," to be presented at the ASME/ASLE Joint Conference, Atlanta, Georgia, October 1973.